Virus-host interactions in an ovine model of lung cancer

Submitted in fulfilment of the requirements of the degree of
DOCTOR OF PHILOSOPHY

by Bartosz Szafran, B.Sc., M.Sc.

College of Veterinary, Medical and Life Sciences
University of Glasgow

October 2014

Declaration

I declare that all of the work submitted herewith is my own.
Collaborative work is acknowledged where appropriate.

Bartosz Szafran
October 2014

Acknowledgements

I much appreciate the opportunity that the University of Glasgow has given me to pursue my dream PhD project in the Moredun Research Institute, an excellent research facility located in the charming city of Edinburgh, which is a world-renowned centre of science and art. I am thankful to my supervisors David Griffiths, Chris Cousens, and Massimo Palmarini for their outstanding expertise, patience and mentoring.

I am grateful to many members and former staff of the Moredun Research Institute. I acknowledge Patricia Dewar, Ann Wood, Mara Rocchi, Maira Connelly and Tom McNeilly for teaching me lab techniques and their help at various steps during my project. I thank to Jeanie Finlayson for performing the immunohistochemistry. I am grateful to many people who provided me with samples and reagents; Kim Willoughby, Keith Ballingall, Craig Watkins and all members of my team and Glasgow Veterinary Medicine group members who contributed to progress in the area of jaagsiekte sheep retrovirus biology.

During my project I got an opportunity to relax by playing table tennis with Yvonne, Charline, German, Thomas, Edward, Allen, Rob, Colin, Manus, David and Peter Nettleton, an exceptional ping pong player and provider of the excellent writing for publication course.

I am very grateful to my family for their support and faith in me. I would like to thank Dorota for her love and care.

This thesis is dedicated to my great grandmother Zofia.

Table of Contents

List of figures

List of tables

List of most commonly used abbreviations

A3	APOBEC3
AID	Activation-induced cytidine deaminase
AmpR	Beta-lactamase
APOBEC	Apolipoprotein B mRNA editing enzyme, catalytic polypeptide-like
BAC	Bronchioloalveolar carcinoma
BST-2	Tetherin
C/EBPα	CCAAT enhancer binding protein alpha
CA	Capsid
CAEV	Caprine Arthritis Encephalitis Virus
CC	Coiled coil domain
CCSP	Clara cell-specific protein
CMV	Cytomegalovirus
cPPT	Central polypurine tract
CTE	Cytoplasmic transport element
CypA	Cyclophilin A
DC	Dendritic cell
DMEM	Dulbecco's Modified Eagle's Medium
EGFP	Enhanced green fluorescent protein
EIAV	Equine infectious anemia virus
enJSRV	Endogenous JSRV
ENTV-1and -2	Enzootic nasal tumour viruses -1 and-2
ERV	Endogenous retrovirus
FCS	Foetal Calf Serum
FeLV	Feline leukaemia virus
FITC	Fluorescein isothiocyanate
FIV	Feline immunodeficiency virus
GFP	green fluorescent protein
GPI	Glycosylphosphatidylinositol
GvHD	Graft versus host disease
HA	Haemagglutinin tag
HERV-K	Human endogenous retrovirus-K
HIV-1	Human Immunodeficiency Virus type 1
HNF-3	Hepatocyte nuclear factor-3
HRP	Horseradish peroxidise
Hsp	Heat shock protein
HTLV-1 and -2	Human T-lymphotropic virus type 1 and type 2
hu	Human
Hyal2	Hyaluronidase type 2 receptor
Hyg or HygR	Hygromycin resistance gene
Ig	Immunoglobulin
IHC	Immunohistochemistry
IL	Interleukin

IMDM	Iscove's Modified Dulbecco's Medium
IN	Integrase
IFN	Interferon
IRES	Internal ribosomal entry site
JSRV	Jaagsiekte sheep retrovirus
lacZ	β-galactosidase encoding gene
LB	Luria Bertani Broth
LDL	Low-Density lipoprotein
LF	Lung fluid
LPS	Lipopolysaccharide
LTR	Long terminal repeats
MA	Matrix
MCS	Multiple cloning site
MEME	Minimum Essential Medium Eagle
miRNA	micro RNA
MLV	Murine leukaemia virus
MMTV	Mouse mammary tumour virus
MOI	Multiplicity of infection
MPMV	Mason-Pfizer monkey virus
MRI	Moredun Research Institute
mu	Murine
VMV	Visna-Maedi Virus
NC	Nucleocapsid
Neo, NeoR	Neomycin transferase
NFκB	Nuclear factor kappa-light-chain-enhancer of activated B cells
OPA	Ovine pulmonary adenocarcinoma
ORF	Open reading frame
orf-x	Open reading frame X
PBMC	Peripheral blood mononucleated cell
PBS	Primer binding site
PFV	Primate foamy virus
PI3K	phosphatidyl inositol 3-kinase
PIC	pre-integration complex
PPT	Polypurine tract
PR	Protease
qPCR	Quantitative PCR
RT-qPCR	Quantitative reverse transcriptase PCR
rh	Rhesus macaque
RING	Really Interesting New Gene
rpm	Revolutions per minute
RRE	Rev Responsive Element
RSV	Rous sarcoma virus
RT	Reverse transcriptase
RTC	reverse transcription complex

RT-PCR	Reverse transcriptase PCR
SA	Splice acceptor
SAMHD1	SAM domain and HD domain-containing protein 1
SCID	Severe combined immunodeficiency
SD	Splice donor
SDS	Sodium dodecyl sulphate
siRNA	Small interfering RNA
SIV	Simian immunodeficiency virus
SN	Supernatant
SP	Signal peptide
SPA	Sheep Pulmonary Adenomatosis
SP-C	Surfactant protein-C
SU	Surface domain of envelope protein
SV40	Simian vacuolating virus 40
T5	TRIM5
TLR	Toll-like receptor
TM	Transmembrane domain of envelope protein
TRIM	Tripartite motif protein
V5	V5 epitope tag
VSV-G	Vesicular stomatitis virus G protein
WB	Western blot
wt	Wild type

Abstract

Ovine pulmonary adenocarcinoma (OPA) is a respiratory disease caused by jaagsiekte sheep retrovirus (JSRV). This virus induces the growth of large lung tumours in affected sheep and is a significant problem for the sheep industry. An interesting feature of OPA is that it occurs only in sheep. Goats may also be infected by JSRV but disease progression is limited to the early stages so that clinical signs do not develop. The ability of a virus to replicate in its host is dependent on a wide range of cellular proteins, including essential, required ('dependency') factors, and proteins that act to inhibit replication, referred to as restriction factors. Greater understanding of the roles of dependency and restriction factors can provide insights into pathogenesis and the species-specificity of infection.

The aim of this study was to investigate the potential role of previously identified restriction factors on the replication of JSRV, and specifically whether APOBEC3 or TRIM5 proteins are responsible for the specificity of OPA for sheep. To examine this question, ruminant genes for APOBEC3 were cloned and their activity against JSRV was tested using a replication-defective reporter virus that expresses GFP. This system allows the activity of putative restriction factors to be measured quantitatively by flow cytometry. These experiments revealed that ruminant APOBEC3 proteins, including those from sheep, inhibit JSRV infection *in vitro*. Further analysis of the mechanism of restriction of JSRV by sheep APOBEC3 provided evidence for cytidine deaminase-dependent and independent mechanisms against this virus. Analysis of virus purified from lung fluid from natural cases of OPA found that APOBEC3 is not encapsidated by JSRV *in vivo*, suggesting that JSRV somehow evades this restriction factor in infected sheep. Further studies using immunohistochemistry suggested that the

pulmonary epithelial cells targeted for infection by JSRV do not express APOBEC3. Collectively, these results indicate that JSRV is susceptible to ruminant APOBEC3 proteins but evades restriction *in vivo* by having tropism for cells that do not express APOBEC3. The data also suggest that APOBEC3 is not responsible for the species tropism of JSRV, at least among ruminants.

In order to extend the studies on the species-specificity of APOBEC, several human and mouse APOBEC proteins were analysed for their activity against JSRV. Murine APOBEC3 and human APOBEC3F were both able to restrict JSRV *in vitro*, while other human APOBECs tested were not. These results have impact for the development of murine model of OPA and for the development of JSRV as a gene delivery vector.

To assess the impact of TRIM5 on JSRV replication, derivatives of the permissive cell line CRFK were created that stably express TRIM5 from a range of ruminant and primate species. Infection studies performed in cell culture indicated that none of the TRIM5 proteins tested restrict JSRV, at least during the early stages of virus infection. Further studies are needed to examine other potential mechanisms of activity of TRIM5 against JSRV.

This thesis has revealed new insights into host-pathogen interactions in OPA that may contribute to the development of control strategies against this disease. In addition, these data provide a background for the future development of JSRV as a gene delivery vector.

Chapter 1 – Introduction

1.1 Overview of Ovine Pulmonary Adenocarcinoma

Ovine Pulmonary Adenocarcinoma (OPA) is a transmissible lung cancer of sheep first reported at the end of the 19th century (Dykes, 1888). Jaagsiekte sheep retrovirus (JSRV) is the causative agent of OPA, which is distributed worldwide with the exception of Iceland, Australia and New Zealand (Fan et al., 2003). OPA is also called SPA (Sheep Pulmonary Adenomatosis) or Jaagsiekte, in Afrikaans the word Jaag means chase and siekte means sickness, which refers to the laboured breathing of affected animals after herding (Tustin, 1969). Apart from sheep, JSRV may also infect goats although almost without any clinical signs (De las Heras et al., 2003a). Sheep are the only species that develops OPA. The aim of this project is to investigate host factors responsible for the species-specificity of JSRV infection.

1.1.1 Epidemiology and clinical signs of OPA

The clinical signs of OPA are "harsh breathing" and over-production of lung fluid (Griffiths et al., 2010). Lung fluid is thought to be responsible for disease transmission, which occurs mainly via the respiratory route (Dungal, 1938). An alternative route of transmission affects newborn lambs by suckling, because virus is present in milk and colostrum of JSRV positive ewes (Grego et al., 2008). Other clinical signs include progressive loss of weight, decreased milk production, dyspnoea, coughing and increased susceptibility to opportunistic respiratory infections (De las Heras et al., 2003a). A simple diagnostic test for OPA is called the wheelbarrow test which, after lowering the sheep's head, may release up to 500 ml of lung fluid through the nose. This fluid contains 10^7 to 10^{10} of JSRV RNA copies per ml (Cousens et al., 2009). The virus is able to survive for several weeks in conditions of low temperature and high humidity (Cousens et al., 2009).

The development of OPA occurs from several months to years after infection. Some JSRV infected sheep do not show clinical signs even though they may have tumours in their lungs and will not be recognized by farmers. Therefore, this long asymptomatic period enhances the spread of the disease. Currently, there is no effective control for

OPA and no accurate diagnostic test suitable for detecting the disease in individual animals during the early stages of infection (Griffiths et al., 2010).

In natural infection it takes several months until the clinical signs of OPA are visible, but in experimental settings even 10 days after intra-tracheal inoculation of lambs some early tumour lesions may be visualised by immunohistochemistry (Griffiths et al., 2010, Martineau et al., 2011, Murgia et al., 2011). Usually adult sheep aged 1-4 years are affected by the disease. However, sheep of all ages are susceptible to OPA (Gonzalez et al., 1993). In comparison to older animals the progress of the disease amongst lambs is faster due to the more rapid cell division, which enhances integration of the provirus and spread of the tumour (Murgia et al., 2011). After the onset of clinical signs the animal dies a few months later (Dungal, 1938). The mortality within an infected flock is the highest (up to 50% per year) during the first years of an outbreak and then decreases to around 5% per year (Griffiths et al., 2010, De las Heras et al., 2003a).

1.1.2 Pathology of OPA

OPA lesions are located in the lungs, although thoracic lymph nodes may also be affected (Rosadio et al., 1988). The size of the tumour ranges from 0.5 to 2 cm nodules to large half-lobe sized lesions in both lungs. Two pathological forms of OPA are recognised; classical OPA (see Fig. 1.1), which is the most common, and atypical OPA (Garcia-Goti et al., 2000). During post-mortem examination of classical OPA, the lungs are enlarged and may weigh three times more than normal. In contrast to the surrounding healthy pink coloured tissue the neoplastic regions are greyish and form "hard" tumours located usually in cranioventral parts of the lungs (Griffiths et al., 2010, De las Heras et al., 2003a). In the advanced stages of disease the affected areas are white and very solid due to fibrosis. Opportunistic bacterial infections, principally *Mannheimia haemolytica* pneumonia, are common in OPA. The atypical form of OPA is characterised by white granular structures that are easy to differentiate from healthy tissue and are usually present in the diaphragmatic lobe (De las Heras et al., 2003a).

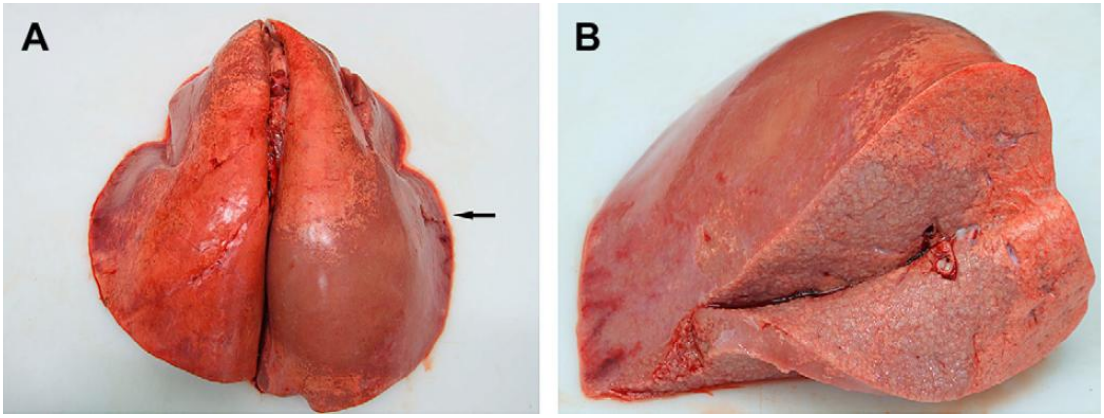

Fig. 1.1 Gross pathology of a natural OPA case
Reproduced with permission from Griffiths et al. 2010. Panel A shows appearance of the classical form of OPA in an adult sheep is shown. The tumour-affected, enlarged part of the right lung is marked by an arrow. Affected areas are darker than normal tissue. Panel B displays lung section at the level of the arrow in (A). Dense and greyish tumour is located adjacent to normal healthy pink lung in the dorsal region of the lobe.

Until recently, no antibody or T cell responses specific to JSRV antigens had been detected in sheep (DeMartini et al., 2003). The expression of enJSRV and its similarity with exogenous JSRV is thought to cause immune tolerance to viral antigens (see Section 1.3.) (Spencer et al., 2003, Summers et al., 2006). However, there are indications for the occurrence of other immunosuppressive mechanisms involved in OPA pathogenesis. It was suggested that the presence of surfactant proteins in lung fluid could suppress the activity of macrophages (Summers et al., 2005). However, OPA-specific immune responses were detected and tumour regression was reported in sheep co-infected with JSRV and ovine lentivirus (Hudachek et al., 2010). Surprisingly, in this experimental setting neutralising antibodies against JSRV Env were detected, which correlated with regression (Hudachek et al., 2010). Moreover, CD3+ T cells infiltrated the lung tissue, although there was no evidence that these cells were specific to JSRV (Hudachek et al., 2010).

1.1.3 Histopathology

The histopathological features of OPA are non-encapsulated neoplastic foci originating from the alveolar and bronchiolar epithelia (Platt et al., 2002, De las Heras et al., 2003a). The tumour nodule structure consists of acinar and papillary proliferations towards the neighbouring structures, which is shown in Fig. 1.2.

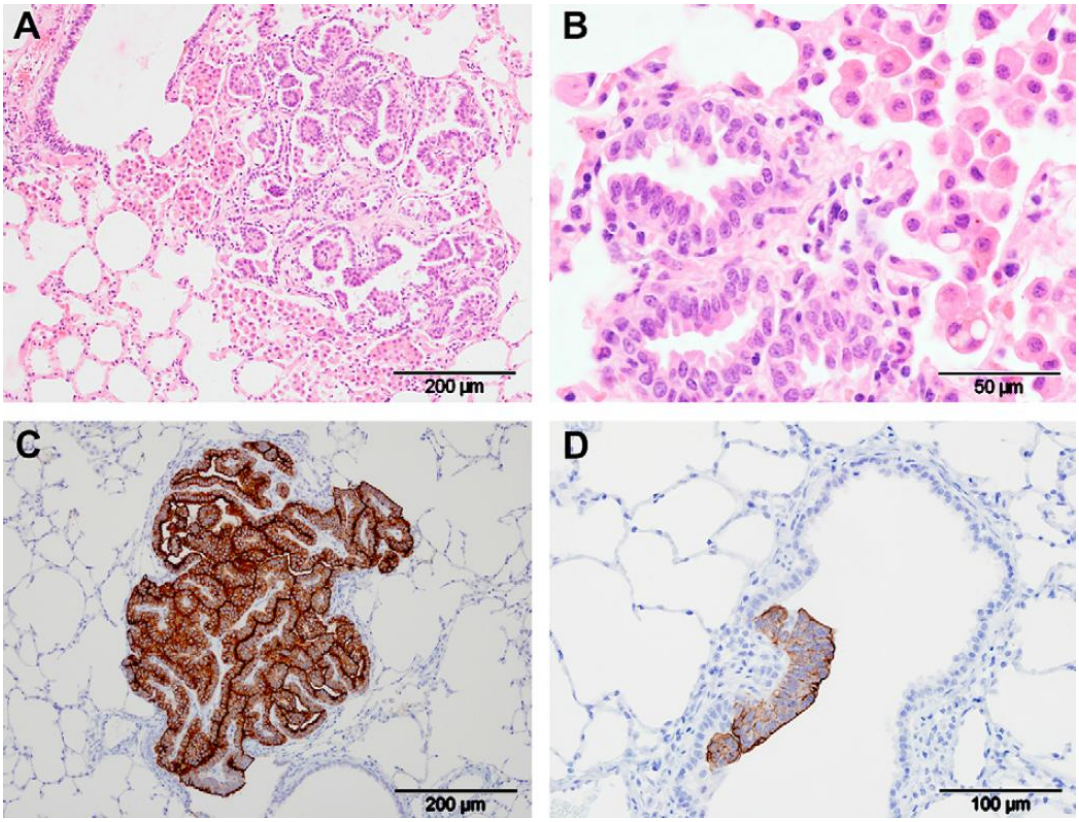

Fig. 1.2 Histological analysis of transformed lung tissue

Copied with permission from (Griffiths et al., 2010). Panels A and B – haematoxylin and eosin staining of OPA-affected lung; Panels C and D – immunohistochemical detection of Env using anti-Env (SU) antibody.

The fibrovascular connective tissue supports the structure and usually forms the centre of advanced tumour nodules. The classical form of OPA has a higher proportion of JSRV-positive cells than the atypical form. Another difference between the two forms of OPA is based on the prevalence of leukocytes in the surrounding stroma. In both cases the nodule may be infiltrated by macrophages but in case of the atypical form also by CD4 and CD8 lymphocytes and B cells (De las Heras et al., 2003a, Summers et al., 2012). The presence of leukocytes is enhanced by the presence of secondary bacterial infections (Garcia-Goti et al., 2000, Wootton et al., 2006a, Martineau et al., 2011).

Clara cells and type II pneumocytes are suspected to be the cell types of origin of the OPA tumour, although the occurrence of undifferentiated cells suggests that progenitor or stem cells may be the first that become infected and transformed

(Martineau et al., 2011, Wootton et al., 2006b, Griffiths et al., 2010, Platt et al., 2002, Murgia et al., 2011). Developed OPA tumours express surfactant protein-C (SP-C), which is a characteristic marker of type II pneumocytes. In contrast, Clara cell-specific protein (CCSP), which is a Clara cell marker was detected only in a fraction of tumours analysed (Murgia et al. 2011). In order to determine early targets of JSRV infection experimental inoculation was performed (Martineau et al., 2011). Ten days later, single JSRV-infected cells were identified in alveolar and bronchiolar regions. Immunohistochemistry showed that those cells were expressing SP-C or CCSP, implying that primary differentiated epithelial cells are infected by JSRV. Additionally, cells were detected that expressed the JSRV Env protein, but did not express either SP-C or CCSP (Martineau et al. 2011). This observation was confirmed in the other study (De las Heras et al., 2014)

In order to investigate the species specificity barriers of OPA, Caporale and colleagues performed experimental infection of goat kids, which resulted in a different macroscopic and histopathological tumour pattern compared to tumour in infected lambs (Caporale et al., 2013b). Interestingly, the tumour appeared to originate in similar cell types in both species. However, the number of infected goat cells was significantly lower and the tumour nodules in goats were significantly smaller and less abundant than those in lambs. This suggests that caprine cells are vulnerable to viral infection and transformation, but also implies that goat cells restrict viral replication, most likely at a late stage in replication, enabling fewer rounds of infection within the lung (Caporale et al., 2013b). Infected lambs have multiple tumour foci of polyclonal origin and the tumour spread is expected to be enhanced by a viral progeny from primary infected and transformed cells.

1.1.4 OPA as a model for human lung cancer

The histological features of OPA resemble human bronchioloalveolar carcinoma (BAC). Human BAC is a rare type of lung cancer, which on the basis of histopathology, has been classified as an adenocarcinoma with a pure bronchioloalveolar growth pattern (Mornex et al., 2003). Smoking is the major risk factor of most lung cancers. However, the prevalence of BAC has a weak association

with smoking, which suggests other risk factors, such as genetic factors or infectious agents (Sun et al., 2007).

From 30 to 40% of human lung adenocarcinomas contain an antigen that is detected by immunohistochemistry using antibodies to JSRV Gag (De las Heras et al., 2000a, De las Heras et al., 2007, Hopwood et al., 2010). A recent study showed an increased prevalence of an antigen detected by antibodies to JSRV Env in advanced stages of some types of human lung tumours (Linnerth-Petrik et al., 2014). PCR amplification using enJSRV specific primers was positive in the majority of BAC samples among Sardinian patients, while only one out of ten non-Sardinian patients was found to be positive (Rocca et al., 2008). However, those results contradict other studies where no JSRV was detected by PCR in lung tumour samples (Yousem et al., 2001, Hopwood et al., 2010). To date, no solid proof of association of BAC and JSRV has been found, although research on OPA has contributed to a better understanding of the process of carcinogenesis (Griffiths et al., 2010).

1.2 JSRV classification, structure and replication

Retroviruses are a large family of viruses that are responsible for a variety of diseases. They are classified into two subfamilies (*orthoretrovirinae* and *spumavirinae*) and seven genera based on their sequence similarity in the reverse transcriptase (RT) protein (Linial et al. 2005) (see Fig. 1.3).

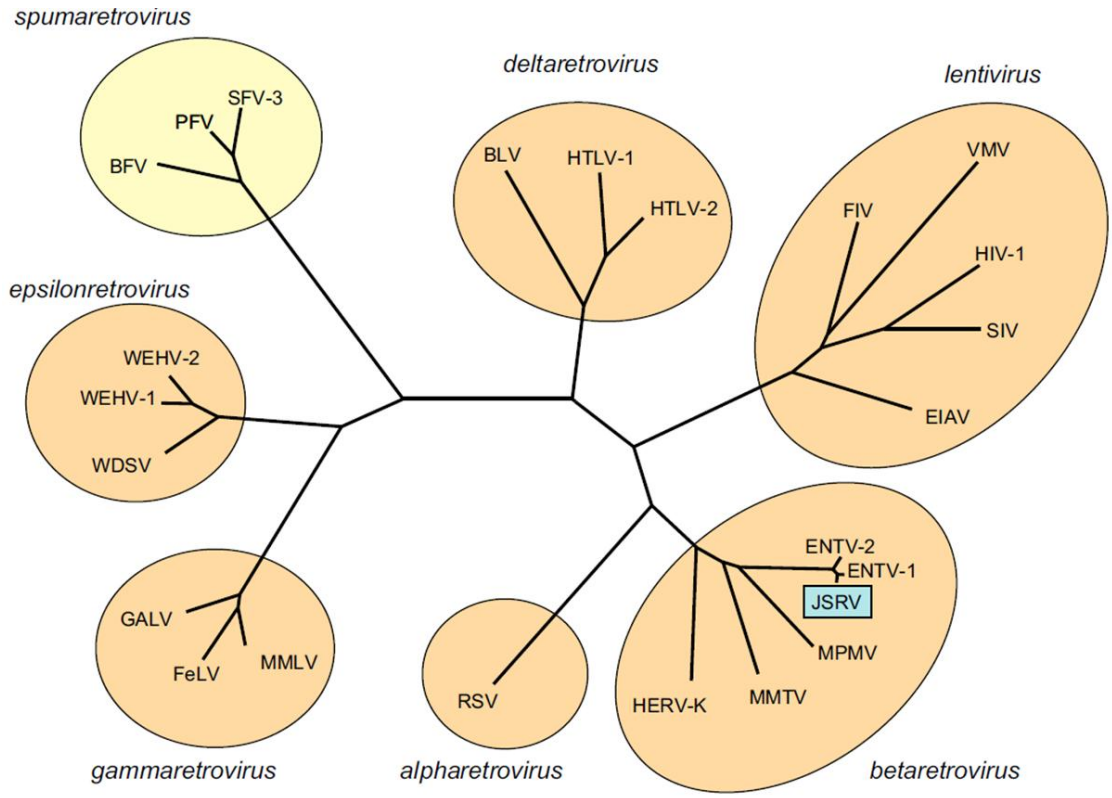

Fig. 1.3 Phylogenetic relationship between different retroviruses based on amino acid sequence similarity in the reverse transcriptase (RT) protein.
Classification of retroviruses divides them into two subfamilies: spumaretrovirinae (yellow) and orthoretrovirinae (orange), which includes seven genera (Linial, M. et al 2005). JSRV (boxed in blue) belongs to the betaretrovirus genus. MMTV, (mouse mammary tumour virus); MPMV (Mason-Pfizer monkey virus); HERV-K (human endogenous retrovirus-K); ENTV-1and ENTV-2, (Enzootic nazal tumour virus type -1 and -2); SIV (simian immunodeficiency virus); FIV, (feline immunodeficiency virus); EIAV, (equine infectious anaemia virus); VMV, (Visna-Maedi virus); HTLV-1 and -2, (human T-lymphotropic virus type 1 and type 2); BLV, (bovine leukaemia virus); RSV, (Rous sarcoma virus); FeLV, (feline leukaemia virus); GALV, (gibbon ape leukaemia virus); MMLV, (Moloney murine leukaemia virus); PFV, (primate foamy virus); SFV-3, (simian foamy virus type 3); BFV, (bovine foamy virus); WDSV, (walleye dermal sarcoma virus); WEHV-1 and -2, (walleye epithelial hyperplasia virus type 1 and type 2). Reproduced with permission from (Griffiths et al., 2010).

1.2.1 JSRV structure

The retroviral genome consists of at least four structural genes *gag, pro, pol* and *env*. In the case of more complex retroviruses additional regulatory and accessory genes are present. The *gag* gene encodes at least three proteins: matrix (MA), capsid (CA), and nucleocapsid (NC) (see Fig. 1.4 and Fig. 1.5). These proteins are formed by the cleavage of a Gag precursor polyprotein by the protease (PR), which may be encoded by a separate open reading frame gene, *pro,* or in the same open reading frame as *gag*

(alpharetroviruses) or *pol* (gammaretroviruses and lentiviruses). The *pol* gene encodes the viral enzymes reverse transcriptase (RT) and integrase (IN). The *env* gene encodes the envelope glycoproteins: surface (SU) and transmembrane (TM) (Engelman, 2010) (see Fig. 1.5). JSRV additionally has a unique highly conserved reading frame named *orf-x* that overlaps the *pol* gene region, although its function is unknown (Griffiths et al., 2010, Palmarini et al., 2002).

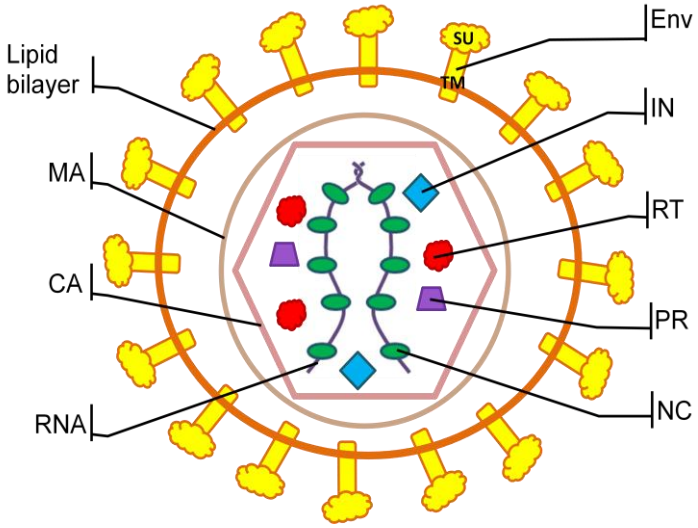

Fig. 1.4 The retroviral virion structure

Two positive-sense ssRNA molecules together with MA, CA, NC, RT, IN and PR proteins are associated with the retroviral core. The viral capsid is enveloped by a lipid bilayer in which the envelope Env glycoprotein surface SU domain is anchored by the transmembrane TM domain.

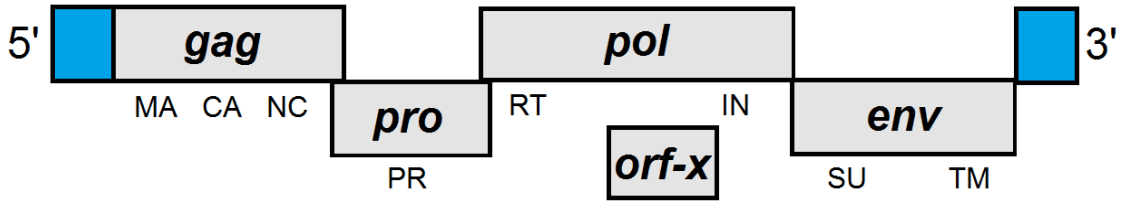

Fig. 1.5 The JSRV genome

The JSRV RNA genome contains *gag*, *pro*, *pol*, *env* genes and an additional *orf-x* reading frame (grey boxes). The products encoded by these genes are displayed below the boxes. The retroviral RNA is flanked by two 5' and 3' long terminal repeats (blue boxes). Figure not to scale.

Betaretrovirus genomes are highly conserved among different isolates. For example mouse mammary tumour virus (MMTV) genomes show 96% sequence similarity (Walsh et al., 2010). Three genomes of JSRV from viruses isolated over a 13-year period, including 2 British isolates $JSRV_{21}$ (Palmarini et al., 1999a), $JSRV_{JS7}$ (DeMartini et al., 2001) and one South-African isolate $JSRV_{SA}$ (York et al., 1991) share 93% or greater sequence similarity. Similarly, there is 96% identity between ENTV-1 isolated from Europe in 1999 and a recent ENTV-1 isolate from North America (Walsh et al., 2010), with the highest polymorphism in LTR and *Orf-x* (Walsh et al., 2010). In contrast, some other retroviral genomes are characterised by high variability, for example quasi-species of VMV (Visna-Maedi virus) and CAEV (Caprine Arthritis Encephalitis Virus) show 84% sequence similarity in *gag* and *pol* and less than 78% in *env* (Overbaugh and Bangham, 2001).

It is likely that sequence variation is constrained in some viruses by the fact that some coding and non-coding RNA sequence elements may be overlapping. Sequence variability occurs due to the pressure of the host immune system and the error prone process of reverse transcription and RNA transcription. However, mutated viral progeny may often be defective. For example, the majority of even single mutations affecting the CA (capsid) encoding region can result in virus attenuation (Rihn et al., 2013).

1.2.2 Replication of JSRV

The replication cycle of JSRV can be divided into early and late events. Early events include viral entry, uncoating, reverse transcription and integration. The late events are transcription, translation, virion assembly, budding and maturation (see Fig. 1.6). Retroviral replication depends on the interplay between both dependency and restrictive factors which determine the species specificity and cellular tropism of the virus (Engelman, 2010, Goff, 2007, Martin-Serrano and Neil, 2011, Maillot et al., 2013).

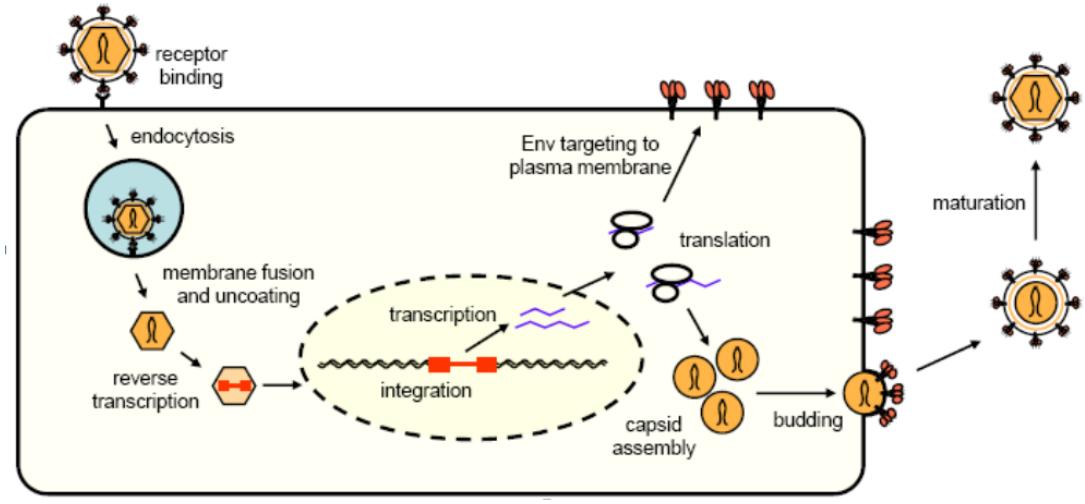

Fig. 1.6 Replication cycle of JSRV
The virus enters the cell by receptor binding and endocytosis. After membrane fusion and uncoating, reverse transcription is initiated. Newly synthesised viral DNA is imported into the nucleus where it integrates into the host genome as a provirus. Transcribed viral RNA is a template for translation of the viral structural proteins which form new virions. Fully transcribed viral RNA is packaged into the assembling virion as genomic RNA. Once the virion is released by budding, the maturation occurs which is required for infectivity. Copied with permission from (Griffiths et al., 2010).

1.2.3 Early phase of JSRV replication cycle

Initially, the SU domain of the Env glycoprotein binds to the cellular receptor, which for JSRV has been identified as hyaluronidase-2 (Hyal-2) (Rai et al., 2001). Rabbit, goat, cow and human but not mouse Hyal-2 are able to support infection mediated by JSRV Env (Miller, 2008). Rat Hyal-2 can also function as a JSRV receptor but only if overexpressed in target cells in culture (Miller, 2008). The fact that heterologous Hyal-2 proteins interact with JSRV Env indicates that the cellular receptor is not a major species determinant of infection. Endocytosis of JSRV is mediated by cellular dynein. The entry of JSRV into the cytoplasm is a pH-dependent process, the virus particle fuses with endosomal membranes allowing the release of the viral core into the cytoplasm (Bertrand et al., 2008, Cote et al., 2012).

Reverse transcription is initiated when the JSRV core enters the cytoplasm. The viral ssRNA is converted into a dsDNA form within a structure referred to as the reverse transcription complex (RTC). The reverse transcription reaction is initiated by annealing of primer to the primer binding site (PBS) located at the 5'end of the viral

RNA (see Fig. 1.7). This reaction utilises a Lys-3 tRNA molecule as a primer which is encapsidated into the virion during assembly.

Once reverse transcription is complete, this structure becomes the pre-integration complex (PIC). Newly synthesised DNA is trafficked in the PIC towards the nucleus utilising cytoskeletal components, finally reaching the microtubule organising centre (MTOC) located on the external nuclear membrane (McDonald et al., 2002, Gaudin et al., 2013).

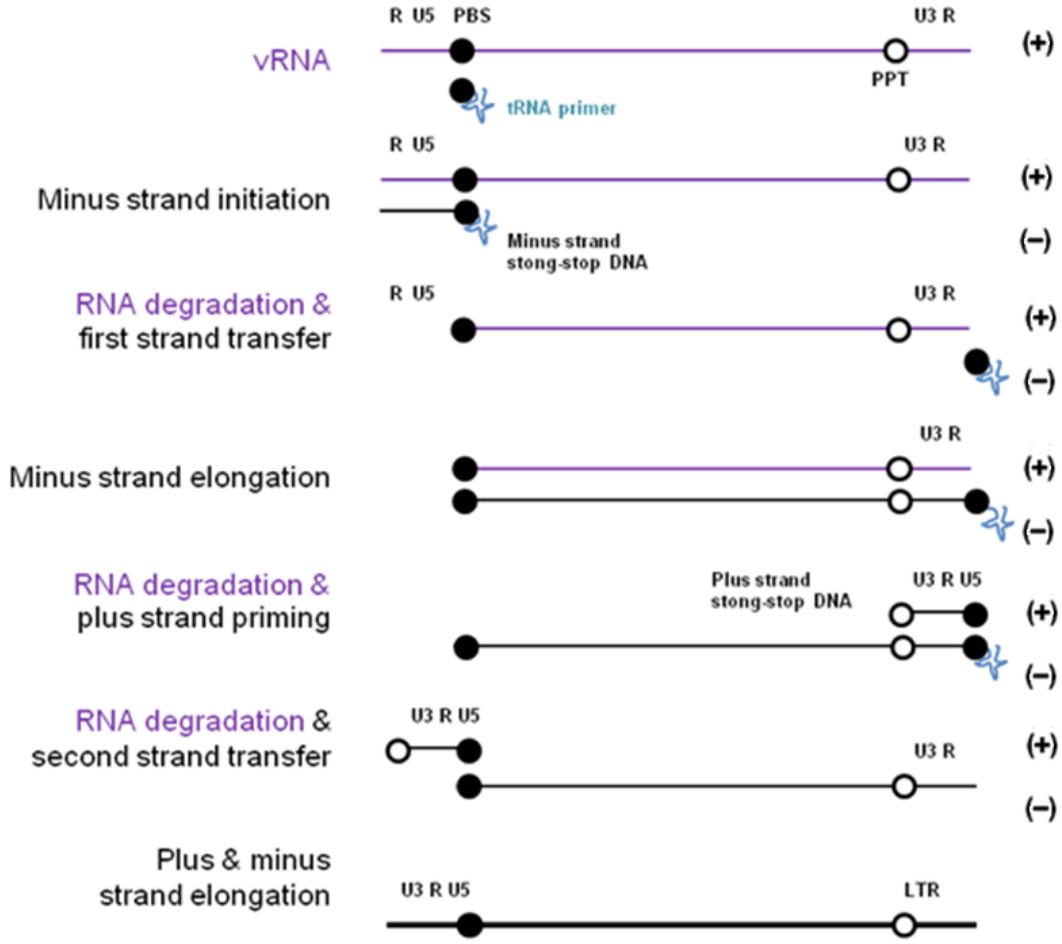

Fig. 1.7 Mechanism of reverse transcription

Reverse transcription is initiated by a tRNA molecule acting as a primer which anneals to the primer binding site (PBS) on the viral genomic RNA. This results in the synthesis of minus strand strong-stop DNA containing R and U5 sequences. Due to the RNAse H activity of RT, the 5' end of the viral RNA is then degraded and the newly synthesized DNA anneals to the 3' end of viral RNA (first strand transfer). The minus strand DNA is then further elongated. The copied RNA is degraded by RNAse H with the exception of a short region of adenosine and guanidine nucleotides, the polypurine tract (PPT), which promotes the initiation of plus DNA strand priming and its elongation after second strand transfer. Reverse transcription is completed when viral dsDNA is flanked on both sides by long terminal repeats (LTR). Figure based on (Engelman, 2010).

For most retroviruses, including JSRV, entry of viral DNA into the nucleus is dependent on cellular division as it requires the destabilisation of the nuclear membrane during mitosis, because the PIC cannot get through nuclear pores. However, lentiviruses are an exception as may be actively transported into the nucleus regardless of the cell cycle by the utilisation of the nucleopore complex (NPC) (Patton et al., 2004). Nuclear import is enabled by the interaction of the central poly purine tract (cPPT) sequence which is a triple stranded DNA structure (Zennou et al., 2000).

When the viral DNA reaches a suitable site in chromatin, integrase (IN) catalyses its insertion into the host genome. Initially, the active IN multimer processes the 3' ends of viral DNA near conserved CA/GT dimers, which enables hydrolysis of target DNA and insertion of viral DNA (Panganiban and Temin, 1983). Once inserted in the host cell genome the virus DNA is referred to as a provirus (Coffin, 1997). Cousens, et. al. analysed the integration sites in a number of different OPA tumours and showed that there may be a common JSRV integration site located on sheep chromosome 16 (Cousens et al., 2004).

1.2.4 Late phase of infection

Transcription of viral genes is under the control of the viral promoter and enhancer elements located in the U3 region of the LTR (Fig. 1.8). In the case of JSRV, this process depends on tissue-specific transcription factors such as lung and liver specific hepatocyte nuclear factor-3 (HNF-3) and the ubiquitous CCAAT enhancer binding protein alpha C/EBPα (McGee-Estrada and Fan, 2007). These transcription factors play an important role in virus tropism and in consequence its pathogenesis which results in cancer.

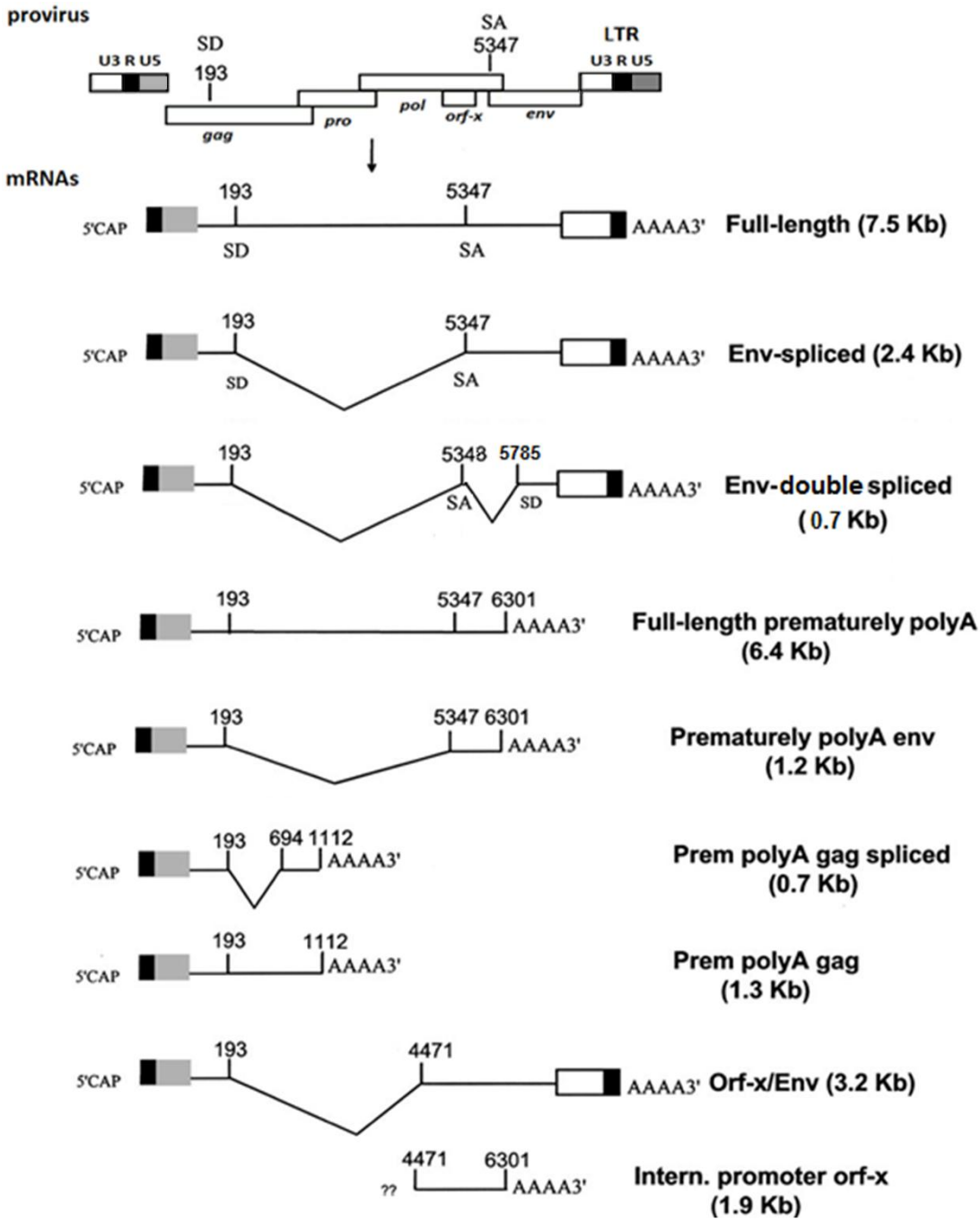

Fig. 1.8 JSRV provirus and its transcripts

The organisation of the JSRV proviral genome and its RNA transcripts are shown. The positions of the splice donors (SD), splice acceptors (SA), and premature termination sites are highlighted. The function of many transcripts is still unknown. Figure adapted from (Palmarini et al., 2002, Palmarini and Fan, 2003, Caporale et al., 2009).

There are two main transcripts generated by alternative splicing: full length viral RNA, and an Env coding transcript (see Fig. 1.5.3). The full-length RNA is utilised in translation to produce Gag, Pro and Pol proteins, but also may be packaged in newly synthesised virions. Expression of Gag, Pro and Pol takes place in the cytoplasm, where capsid assembly also occurs. Env is co-translationally targeted to the ER where it undergoes cleavage to obtain SU, TM and SP (Caporale et al., 2009). Processed envelope glycoprotein is targeted to the plasma membrane where budding of viral progeny occurs. Maturation of newly synthesized viral particles is mediated by PR (Caporale et al., 2009).

Recently, the Rej regulatory protein has been identified as a factor upregulating export of the full viral RNA and enhancing new viral particle formation (Caporale et al., 2009). Rej is encoded by the 5' end of *env* and is either a product of multiply spliced *env* gene (Hofacre et al., 2009) or a post-translationally cleaved Env SP (Caporale et al., 2009). Rej function corresponds to its retroviral homologues Rem and Rec of MMTV and HERV-K respectively as well as Rev of HIV-1 (Mertz et al., 2009, Hofacre et al., 2009).

1.3 Other Retroviruses

1.3.1 Enzootic nasal tumour viruses (ENTV-1 and ENTV-2)

Enzootic nasal tumour viruses are the aetiological causes of enzootic nasal adenocarcinoma in sheep (ENTV-1) (De las Heras et al., 1993) and goats (ENTV-2) (De las Heras et al., 1991). These viruses are the closest known relatives to JSRV (92% sequence similarity) and, as for JSRV, their genome appears to be extremely stable among different isolates (Bai et al., 1996, Walsh et al., 2010, Garcia-Goti et al., 2000). The majority of sequence differences between JSRV and ENTV are present in the LTR (Cousens et al., 1999, Ortin et al., 2003). The sequence of the TM region of Env isolated from infected sheep and goats suggests that ENTV-1 and ENTV-2 are different viruses and not geographical variants (Cousens et al., 1999, Ortin et al., 2003).

ENTV-affected flocks are characterised by a low level of cases over many years (0.1 to 6.6% per annum) (Charray et al., 1985). Respiratory malfunction, skull deformation and bulging eyes may be a clinical sign of a tumour growing in the nasal cavity (Charray et al., 1985). The disease has been reported in Africa, Europe, Asia and North and South America (De las Heras et al., 2003b), but has not been described in New Zealand or the UK (Griffiths et al., 2010). Diseases with similar pathology were reported among cattle in India (Rajan, 1987) and in moose and deer in Sweden (Borg and Nilsson, 1985), but their cause is unknown.

Although ENTV-1 and ENTV-2 are different viruses, the pathology of the disease they cause is similar in the two host species. Both viruses are able to transform secretory epithelial cells of the ethmoid turbinate but analysis of their tissue distribution by the specific PCR, demonstrated that ENTV-1 is present only in the tumour, while ENTV-2 causes a more disseminated lymphoid infection (Ortin et al., 2003). Similarly to OPA, tumours in ENT cause fluid production and there is no antibody response to ENTV in infected animals (Ortin et al., 1998).

JSRV and ENTV enter the cell via the Hyal-2 receptor and replicate in the airway epithelial cells (Dirks et al., 2002, Miller, 2003). ENTV transforms secretory epithelial cells of the nasal gland in their ruminant hosts (Miller, 2003, De las Heras et al., 2003b). Surprisingly, in mice the expression of the ENTV Env in airway epithelia caused similar lung tumour lesions to JSRV Env (Wootton et al., 2006a). ENTV uses the same receptor as JSRV, although it requires a slightly more acidic pH for optimal infection (Cote et al., 2011).

1.3.2 Mouse mammary tumour virus (MMTV)

MMTV is a betaretrovirus which is transmitted to offspring through milk. The first report of transmission of mouse mammary carcinoma by a cell free agent from milk was by Joseph Bittner in 1942 (Bittner, 1942). MMTV can be transmitted in two ways, either by exogenous virus present in milk of affected animal or by an endogenous virus via the germ line (Bentvelzen and Daams, 1969).

During virus transmission, gut-associated B cells and dendritic cells are the primary targets of infection (Held et al., 1993). They express virus encoded superantigen (SAG) and present it in association with class II major histocompatibility complex to cognate CD4 T cells containing a particular class of Vβ chains as part of their alpha/beta receptors (Ross, 2000, Golovkina et al., 1994). This process causes constant proliferative stimulation of a large subset of T cells and in consequence the enhancement of proliferation of infected B cells, thereby increasing the virus reservoir (Choi et al., 1991). MMTV replication in activated lymphocytes leads ultimately to virus transmission to mammary epithelial cells. During puberty, gonadotrophin hormone levels increase, resulting in high levels of MMTV transcription in the dividing mammary cells. The ubiquitous viral expression in lymphoid cells causes impairment of the immune response to MMTV and enables it to persist in its host (Ross, 1998). Virus expression in mammary epithelium is further enhanced by proliferation during pregnancy and upregulated level of glucocorticoids during this period (Ross, 1998).

Three stages of tumourigenesis have been identified in infected MMTV mice: preneoplastic hyperplastic nodules, malignant tumour and finally distant metastatic lesions (often in the lung) (Callahan, 1996). Every stage of mammary carcinogenesis results from the clonal outgrowth of cells containing increased numbers of MMTV provirus (Callahan, 1996).

MMTV induces tumours through insertional activation of cellular oncogenes (see Section 1.7.2). Some of the mutations present in transformed cells as a result of integration of MMTV are relevant to the development of human breast cancer. A high throughput analysis of MMTV-induced mammary tumours has been performed (Theodorou et al., 2007), which identified 33 common insertion sites in potential candidate oncogenes. The expression of human orthologs of those genes was often deregulated in human breast cancers and was associated with a number of tumour parameters, which determined their malignancy. The computational analysis showed that those genes were often connected with signalling pathways mainly associated with development and growth factor signalling (Theodorou et al., 2007). The study of MMTV cis-interactions resulting from virus integration enabled the discovery of oncogenes and pathways present in human cancers such as members of the Wnt family

(Ross et al., 2006) and ITAM-mediated signaling, which contribute to the novel mechanism of transformation (Katz et al., 2010). The use of the MMTV LTR to direct expression to murine epithelial cells enabled the creation of many transgenic mouse strains which are critical models for research on human breast cancer (Ross, 2010).

1.3.3 Endogenous retroviruses

Endogenous retroviruses (ERVs) originate from ancient exogenous retrovirus infections. When a retrovirus infects germ line cells it can result in integrated proviral sequences which are vertically transmitted to subsequent generations. ERVs are present in every vertebrate genome sequenced so far and represent approximately 8% of the human genome (Li et al., 2001). Initially, simple endogenous retroviruses related to alpha-, beta- and gamma- retroviruses were discovered, although more recently complex endogenous retroviruses have been identified, e.g. rabbit endogenous lentivirus (Katzourakis et al., 2007).

The sheep genome contains at least 27 copies of endogenous betaretroviruses related to JSRV (enJSRV), and is an excellent example of virus-host coevolution (Arnaud et al., 2007a). The Env protein of enJSRV plays a role in sheep placental development (Palmarini et al., 2001a, Spencer et al., 2010). Other mammalian species have similar interactions with their ERVs (Dunlap et al., 2006a, Black et al., 2010b, Black et al., 2010a, Spencer et al., 2010).

The ERV genome is usually modified so that it loses its replication ability. However, it is common that some open reading frames (ORFs) are transcribed and viral proteins are expressed. *In vitro* experiments have demonstrated the potential protective role of ERV genes, which compete with their homologous genes during exogenous retrovirus infection. For example, enJSRV Env lacks transformation potential. However its similarity with the exogenous JSRV homologue results in the receptor interference by competition for binding to Hyal-2 (Spencer et al., 2003). The expression of enJS56A1 Gag may interfere with trafficking of exJSRV Gag and in consequence restrict replication (Murcia et al., 2007, Arnaud et al., 2007b). The observation that enJSRVs

are not expressed significantly in type II pneumocytes and Clara cells, may explain the lack of those restrictions in target cells for exJSRV infection (Palmarini et al., 2000b).

1.4 Oncogenesis by retroviruses

Carcinogenesis is one of the possible outcomes of retroviral infection. The first report of transmission of cancer by cell-free filtrates was published in 1908. Ellermann and Bang studied erythro-myeloblastic leukaemia in chickens caused by what was later identified as myeloblastosis virus (AMV) (Maeda et al., 2008, Ellermann, 1908). In the 1980s research on human T-lymphotropic virus type-1 (HTLV-1) provided the first evidence of retrovirus mediated cancer among humans (Yoshida et al., 1982). Retroviruses can be divided into acute transforming viruses and non-acute transforming retroviruses, depending on the mechanism of tumourigenesis, as described below.

Moreover, some retroviruses cause immunosuppression which supports the development of cancer through various mechanisms. For example HTLV-1 Tax impairs the immune system by upregulation of the NFκB pathway and destabilisation of interleukin expression including upregulation of immunosuppressive IL-13 (Currer et al., 2012). MMTV is able to induce the expression of immunosuppressive IL-10 in B-cells by signalling through Toll-like receptor 4 (Jude et al., 2003). A significant portion of the AIDS-affected population develops some kind of cancer due to depletion of CD4+ cells and chronic immune system activation. Moreover, AIDS patients are extremely prone to other oncogenic viruses such as Kaposi's sarcoma herpes virus (Bellan et al., 2003, Dalgleish and O'Byrne, 2002).

1.4.1 Acute transforming viruses

Acute transforming viruses cause transformation due to the presence of host-derived oncogenes captured in their genome. Animals infected with acute-transforming viruses are affected by transformation within days to weeks after infection (Maeda et al., 2008). Acute transforming viruses are often replication defective unless the same cell becomes superinfected by a replication competent helper virus.

The first viral oncogene to be described was *V-Src* which is responsible for inducing cancer by Rous Sarcoma Virus (RSV) (Stehelin et al., 1976). The homology between *V-Src* and cellular *Src* led to the definition of proto-oncogenes (Stehelin et al., 1976). Depending on their mechanism of interaction, proto-oncogenes are classified into the following groups: receptor tyrosine kinase, non-receptor tyrosine kinase, serine/threonine kinase, transcription factor, cyclins, G-protein and growth factor (Rosenberg, 1997; Maeda et al. 2008). Proto-oncogenes can be any protein involved in the control of cell growth and differentiation. Their capture into the viral genome is caused by cross packaging of an expressed cellular host-gene, which later during reverse transcription recombines and leads to the emergence of a hybrid RNA. This process often results in creation of a replication-defective virus, which needs a helper virus for its replication. The helper virus is responsible for provision of viral proteins in order to form the virion, which packages RNA of the replication-defective virus (Muriaux and Rein, 2003).

1.4.2 Non acute transforming retroviruses

These viruses are carcinogenic due to insertional mutagenesis (see Fig. 1.9). The integration of provirus into the host genome may alter the expression of cellular genes. In cases when the genes affected are responsible for cellular growth and proliferation control, this may result in oncogenic transformation several months or years post-infection (Pedersen, 2010).

Proviral integration may impact on the expression of genes defined as cellular proto-oncogenes (Fig. 1.9). This is the mechanism of oncogenesis exhibited by non-acute transforming retroviruses. This process may affect loci present a long distance from the provirus (Singhal et al., 2011, Uren et al., 2005). The *in vivo* transformation is a rare event and often requires multiple infection events, which is why non-acute transforming viruses in general do not promote transformation *in vitro* (Pedersen, 2010).

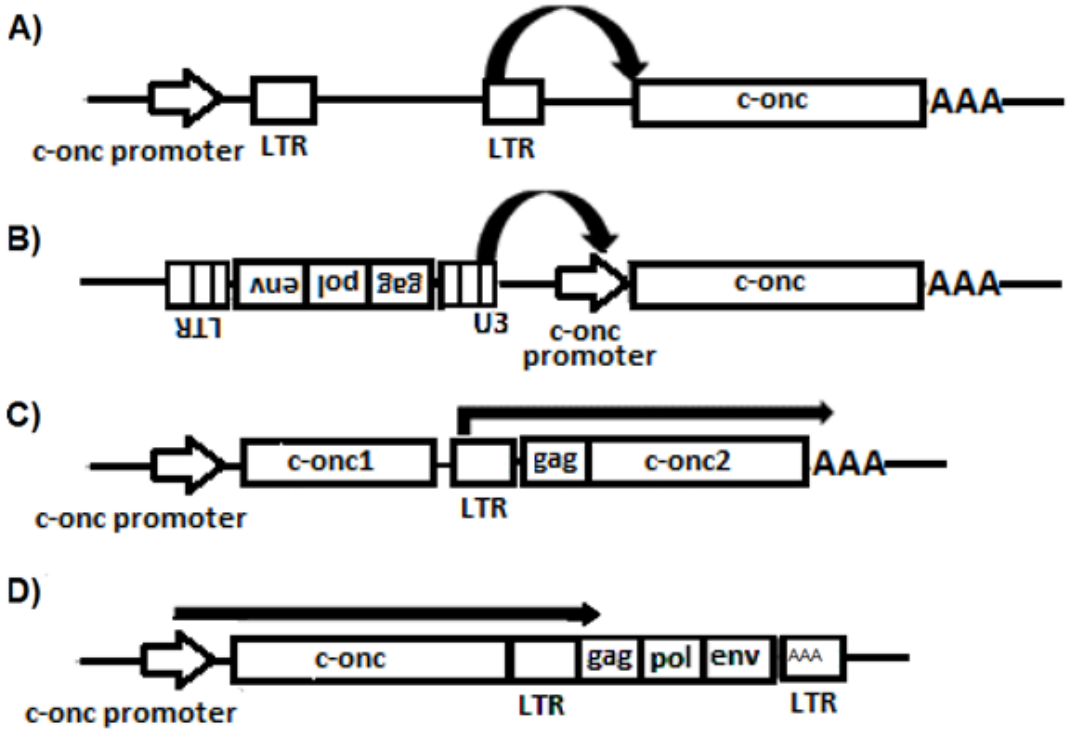

Fig. 1.9 Mechanisms of activation of cellular proto-oncogenes
(A) Insertion of promoter (B) U3 enhancer activation (C) Read-through transcription resulting in chimeric transcripts causing expression of proto-oncogenes fused with viral genes (D) Disruption of the 3' end of a cellular oncogene results in upregulated expression due to the presence of a polyadenylation signal located in the viral LTR. Figure adapted from (Maeda et al., 2008).

1.4.3 Mechanism of transformation induced by JSRV

JSRV represents a group of acutely transforming trans-activating retroviruses, whose main feature is the presence of viral oncogenes unrelated to cellular sequences. In the case of JSRV, Env is responsible for oncogenesis and it was demonstrated that expression of this glycoprotein alone causes transformation *in vitro* (Maeda et al., 2001, Rai et al., 2001) and *in vivo* (Caporale et al., 2006, Wootton et al., 2005). Various cell lines and tissues from different species can be transformed by JSRV Env expression (Maeda et al., 2001, Wootton et al., 2006a, Rai et al., 2001, Maeda et al., 2005). The transformation mechanism is based on the triggering of protein kinase signalling cascades involved in cellular proliferation.

The VR3 region located in the cytoplasmic tail domain of TM is a major determinant of the transformation potential of Env (Palmarini et al., 2001b, Fan et al., 2003). The YXXM motif present in VR3 interacts with a signalling pathway mediated by PI3K

(phosphatidyl inositol 3-kinase) - Akt. Disruption of this motif by mutation of tyrosine (Y590D) abolished the transformation potential. The exJSRV Env shares high similarity to enJSRV Env, except in the VR3 domain of TM where the YXXM motif is not present in enJSRV, which explains the lack of transformation potential of enJSRV (Fan et al., 2003).

It has been suggested that the SU domain of JSRV Env also plays a role in tumourigenesis by binding with Hyal-2 (Danilkovitch-Miagkova et al., 2003). The deletion of the Hyal-2 gene is often observed in human lung cancer (Rai et al., 2000, Rai et al., 2001). Experiments on the human epithelial cell line BEAS-2B showed JSRV Env mediated downregulation of Hyal-2 control on RON tyrosine kinase signalling (Danilkovitch-Miagkova et al., 2003).

The activation of the mitogen-activated protein kinase ERK signalling pathway was demonstrated as an alternative JSRV transformation mechanism (De Las Heras et al., 2006). The alternative cellular signalling pathways proposed to have a role in JSRV transformation are presented in Fig. 1.10.

Since JSRV Env is a powerful oncogene, the mechanism of OPA carcinogenesis is unlikely to be connected with insertional mutagenesis or oncogene transduction (Cousens et al., 2004). However, the analysis of natural OPA cases, revealed the occurrence of a common JSRV integration site on chromosome 16, which may suggest a role for insertional mutagenesis in some cases of OPA (Cousens et al., 2004, Philbey et al., 2006).

Sprouty2 has been described as a tumour suppressor because its overproduction decreases nodule growth and motility of transformed cells (Chitra et al., 2010). While the direct interaction of Sprouty2 with JSRV Env has not been described, it is suggested that the oncostatic mechanism is based on the interference with the same signalling pathway that is utilised by Env (Chitra et al., 2010).

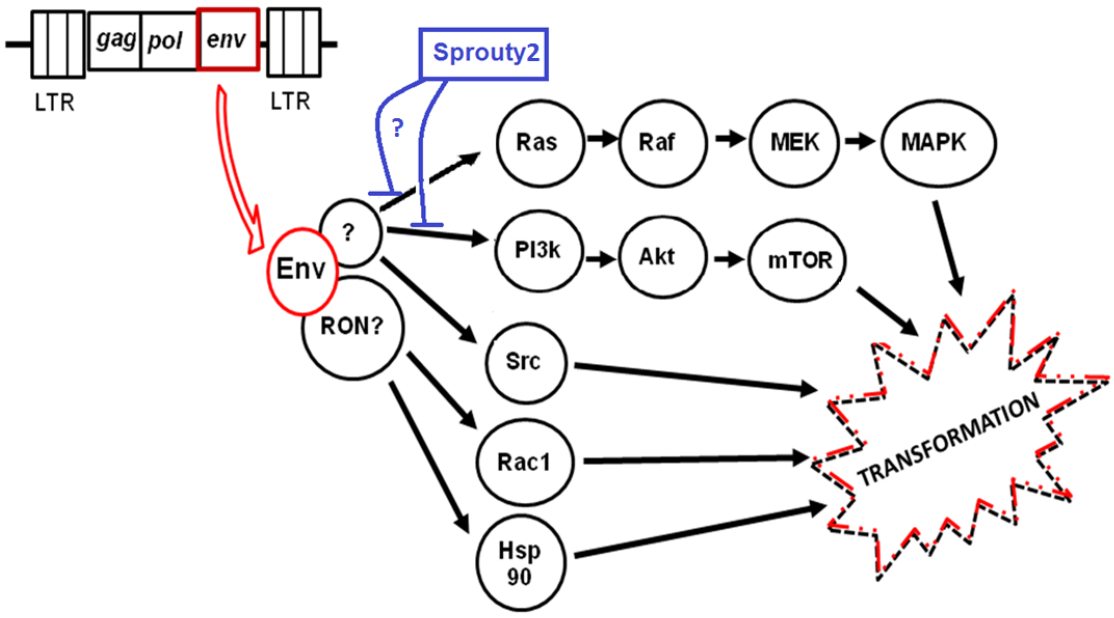

Fig. 1.10 Mechanisms of JSRV/ENTV transformation
The Ras-MAPK and PI3k transformation pathways have been shown to play a role in JSRV Env mediated transformation (Maeda et al., 2005, Hull and Fan, 2006). Hsp90 and Src may play a role in JSRV transformation (Varela et al., 2008). Rac1 has been identified to play role in both JSRV-1 and ENTV-1 transformation (Maeda and Fan, 2008). Sprouty2 has been reported to interfere with some of the transformation pathways (Chitra et al., 2010). Figure adapted from (Maeda et al. 2008).

1.5 Restriction factors

Cellular resistance to retroviral infection is determined by host proteins known as restriction factors. Many sophisticated intracellular mechanisms that inhibit retroviruses at various stages of their replication have been described. Several restriction factors have been identified and include APOBEC3 (Harris et al., 2003), TRIM5α (Stremlau et al., 2004), tetherin (Neil et al., 2008), SAMHD1 (Hrecka et al., 2011, Laguette et al., 2011) and others (Liu et al., 2011, Marno et al., 2014), which were initially identified during studies on HIV-1 and SIV. They have been described as a part of innate immunity and determine the specificity of viral infection at the cellular level. A high throughput screen has been performed to identify potential HIV-1 restriction factors using small-interfering RNA (siRNA), which has identified 114 genes with significant capability to inhibit infection (Liu et al., 2011). Therefore it is possible that additional retroviral restriction factors may yet be discovered.

In response, retroviruses have developed evasion strategies to counteract cellular restriction factors in a similar way as escape mutants evading the host immune response (Sawyer et al., 2005). In the process of co-evolution, retroviruses, as well as their hosts, are continuously developing and improving these mechanisms. The study of these viral-host interactions may enable the creation of vaccines and drugs against persistent retroviral infections (Huthoff and Towers, 2008).

1.5.1 APOBEC

APOBEC (apolipoprotein B mRNA editing enzyme, catalytic polypeptide-like) proteins belong to a family of activation-induced cytidine deaminase (AID) molecules, which are able to edit nucleic acids by changing cytosine to uracil. This family consists of activation-induced cytidine deaminase (AID) and APOBEC1 (A1); APOBEC2 (A2), APOBEC3 (A3), APOBEC4 (A4) molecules. AID activity has been described to be responsible for generating antibody diversity in activated B-cells (Muramatsu et al., 1999). The cytidine deamination activity of APOBEC was initially discovered in A1, which edits apoB mRNA at a specific site in gastrointestinal tissues (Chester et al., 2000). Subsequently, A1 and A3 family members were shown to inhibit replication of various viruses in contrast to AID and A2 whose antiviral activity has not been documented (Ikeda et al., 2011, Koito and Ikeda, 2013).

1.5.1.1 Apobec3 restriction

Mammalian *A3* genes are located between conserved flanking genes *CBX6* and *CBX7* (see Fig. 1.11). Each *A3* gene encodes a protein which includes one or two zinc-coordinating motifs denoted Z1, Z2 or Z3, which are responsible for cytidine deaminase activity. The number of *A3* proteins varies between species from one in mice to seven in primates (Harris and Liddament, 2004, Jonsson et al., 2006). There are three *A3* genes present in the ovine genome and these encode four proteins: A3-Z1, A3-Z2, A3-Z3 and A3-Z2Z3, which is a fusion protein formed by alternative splicing of the *Z2* and *Z3* genes (LaRue et al., 2008).

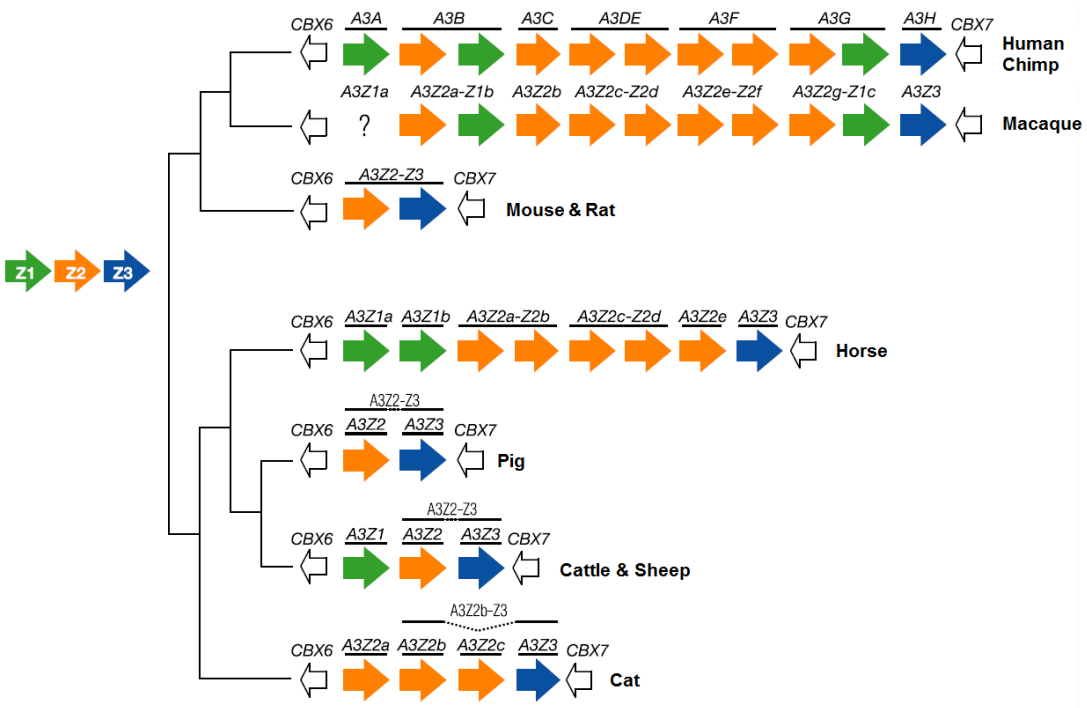

Fig. 1.11 Schematic representation of mammalian APOBEC3 loci
Adapted from (LaRue et al., 2008, LaRue et al., 2009). Mammalian *APOBEC* genes are flanked by genes *CBX6* and *CBX7*. Each *APOBEC3* gene encodes a protein including one or two zinc-Coordinating motifs Z1 (green), Z2 (yellow) or Z3(blue).

The deamination of cytidines during reverse transcription converts these nucleotides to uracil, which results in G to A mutations on the positive sense retroviral DNA and in consequence leads to integration of a defective provirus or to degradation of viral DNA (Harris and Liddament, 2004, Bishop et al., 2008). The degradation of DNA is based on the detection and removal of uracils by UNG2 (Uracil DNA Glycosylase), resulting in the emergence of abasic sites which render the DNA molecule prone to other nucleases such as APEX1, TREX1, DNAse 1 and 2 (Stenglein et al., 2010).

In addition to the cytidine deaminase-mediated hypermutation, A3 family proteins inhibit viral replication through additional mechanisms. Some A3 proteins act to inhibit reverse transcription in a dose dependent manner regardless of the cell type (Bishop et al., 2008). Those mechanisms of A3 mediated restriction are shown in Fig. 1.12.

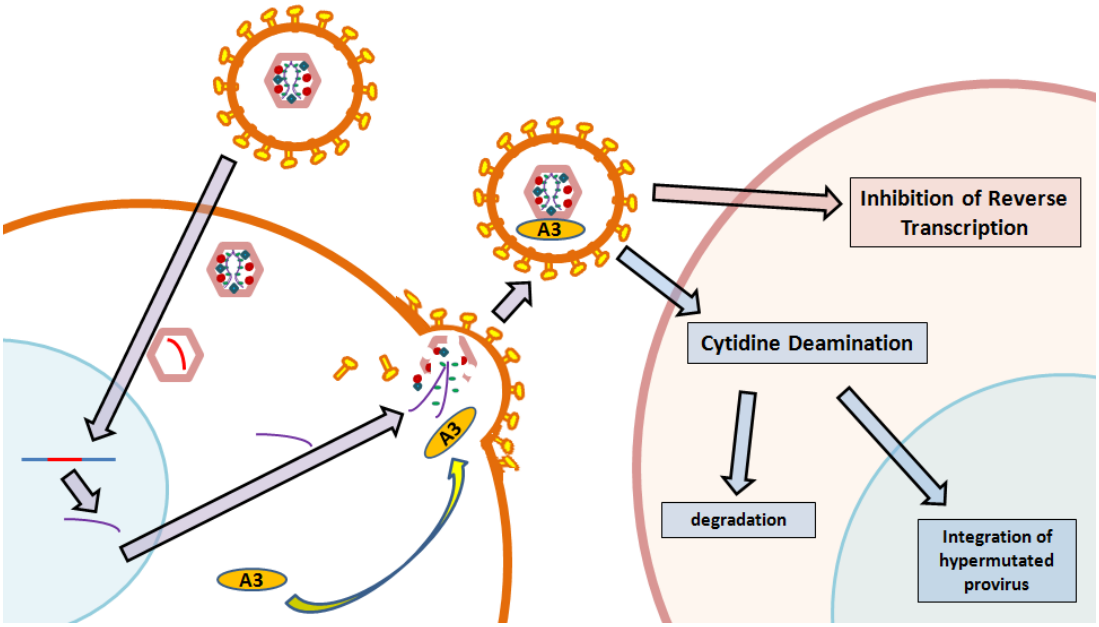

Fig. 1.12 Restriction mechanism of APOBEC3
A primary infected cell (left) packages A3 into virion progeny. A3 activity is exhibited during the next round of infection (right). The antiviral mechanism of A3 is based on the enzymatic inhibition of reverse transcription or cytidine deamination which leads to editing of newly synthesized DNA (hypermutation). In consequence it may lead to degradation of viral DNA or integration of attenuated provirus.

A3 is packaged into retrovirus virions during assembly and its activity is exhibited during infection of the next target cell at the reverse transcription step (Huthoff and Towers, 2008). In addition to retroviruses, A3 proteins are able to edit the genetic material of other parasitic elements including hepadnaviruses (Turelli et al., 2004), retrotransposons (Koito and Ikeda, 2013), parvovirus, adeno-associated virus (Narvaiza et al., 2009), herpesviruses (Suspene et al., 2011) and human papillomavirus (Vartanian et al., 2008).

There are many unresolved questions about the biology of A3 proteins and it is still not known how A3s distinguish host from non-self ssDNA. It has been suggested that human A3 proteins may be oncogenic; for example, C to T mutations in breast cancer cells are likely to be caused by A3B (Burns et al., 2013, Nik-Zainal et al., 2012, Taylor et al., 2013, Nowarski and Kotler, 2013, Demorest et al., 2011).

1.5.1.2 Structural features of APOBEC3

All APOBEC3 proteins include one or two cytidine deaminase domains, which coordinate a zinc ion by a histidine and two cysteines, while a glutamate is predicted to promote the formation of a hydroxide ion that is essential for deamination (Harris and Liddament, 2004, Navarro et al., 2005). A3 proteins are classified into A3-Z1, A3-Z2 and A3-Z3 depending on their cytidine deaminase domain amino acid specificity. All A3 proteins are characterized by the specific consensus amino acid sequence in their Z-motifs which is HxEx(24-31)Cx(2-4)C (where x can be any residue) (LaRue et al., 2008, LaRue et al., 2009). A unique feature of Z1 domains is the isoleucine adjacent to a conserved arginine which is present in all DNA deaminases (Chen et al., 2008).

Z2 domains possess a unique tryptophan-phenylalanine motif located five residues after the (pseudo)catalytic glutamate. Z3 domains contain the unique TWSPCx(2-4)C zinc-coordinating motif, while the Z1 and Z2 domains include a SWS/TPCx(2-4)C motif (LaRue et al., 2009).

Recently high resolution structures have been published of the cytidine deaminase domains of human A3A (Byeon et al., 2013), A3C (Kitamura et al., 2012), A3F (Bohn et al., 2013) and A3G (Chen et al., 2008, Li et al., 2012). The crystal structures analysed by X-ray and NMR revealed globular proteins containing six α-helices and five β-sheets forming a specific motif (α1-β1-β2/2'-α2-β3-α3-β4-α4-β5-α5-α6) (Chen et al., 2008, Vasudevan et al., 2013, Li et al., 2012).

1.5.1.3 Evasion of APOBEC3 by retroviruses

Many retroelements have developed strategies to inhibit restriction of their host's A3 factors. Notably, these evasive mechanisms may not work in the presence of A3 proteins from other species, even if they are closely related. For example, the study of *vif* deletion mutants revealed that HIV and SIV Vif acts as an adaptor protein and directs A3G to ubiquitin-dependent proteasomal degradation (Yu et al., 2003). Similarly, the Bet protein of primate foamy virus is responsible for escape from A3

restriction (Perkovic et al., 2009). Simple retroviruses such as MLV and MPMV do not encode a Vif protein, although they are resistant to their host's A3. MLV encodes a glycosylated Gag protein that enhances capsid integrity and in consequence protects the reverse transcription complex from A3 (Stavrou et al., 2013). MPMV poorly incorporates A3 of rhesus monkey into virions. However, murine A3 binds to MPMV Gag efficiently, and restricts its replication (Doehle et al., 2006).

Recent findings indicate that the species-specificity of the antiviral activity of A3 needs to be revaluated since there are some reports of the natural host A3 inhibiting viral replication. A3 proteins of the natural host have been shown to restrict equine infectious anemia virus (EIAV) (Zielonka et al., 2009) and MLV (Takeda et al., 2008, Stieler and Fischer, 2010). The restriction of MMTV by mouse A3 was demonstrated by challenge of animals with knockdown of this gene (Okeoma et al., 2007, Ross, 2009). Moreover, it was proven that various A3 alleles present in the different murine strains influence MMTV resistance (Okeoma et al., 2009b). Also, in humans an A3G haplotype has been reported that correlates with increased probability of HIV-1 infection (Valcke et al., 2006).

Much of the data on A3 activity against retroviruses comes from *in vitro* overexpression studies. However, it is possible that such experimental systems can produce artefactual results. Therefore, there is a need for further investigation to determine whether restriction factors are expressed *in vivo* at a level that is required for effective restriction. In addition, the differential cell and tissue expression patterns play a role in the significance of restriction by the different kinds of A3 proteins (Stavrou et al., 2014). It has been demonstrated that the distribution of expression and the activity function of human A3G and A3F varies between cell subsets and tissues, and may be induced by cytokines such as interferon-α (IFNα) in dendritic cells (DC) and macrophages (Koning et al., 2009). Administration of LPS (lipopolysaccharide) to mice increased the level of IFNα, which resulted in the upregulation of A3, TRIM and tetherin expression and in consequence enhanced resistance to MMTV (Okeoma et al. 2009b). In the same experiment an increased ratio of MMTV-restrictive mature dendritic cells (mDC) to immature DCs (iDC) was detected. This is significant since DC are the primary cells infected by MMTV (Okeoma et al., 2009a).

1.5.2 Tetherin

Research conducted on HIV carrying a deletion of the regulatory gene *vpu* (HIVΔ*vpu*) revealed the presence of a restriction factor that prevents viral particle release. Due to the mechanism of its action this factor was called tetherin (Neil et al., 2008, McNatt et al., 2013). Tetherin has subsequently been shown to restrict numerous enveloped viruses including retroviruses, filoviruses, influenza virus (Jouvenet et al., 2009), flaviviruses, rhabdoviruses (Weidner et al., 2010), arenavirus and herpesvirus families (Evans et al., 2010).

1.5.2.1 Tetherin restriction mechanism and its structure

Tetherin, also called BST-2, CD317 or HM1.24, is a type II transmembrane protein (Neil et al., 2008, Hammonds et al., 2012a). Its N-terminus is in the cytoplasm, and its internal ectodomain is attached to the membrane by a C-terminal glycosylphosphatidylinositol (GPI) membrane anchor (see Fig. 1.13) (Hammonds et al., 2012b).

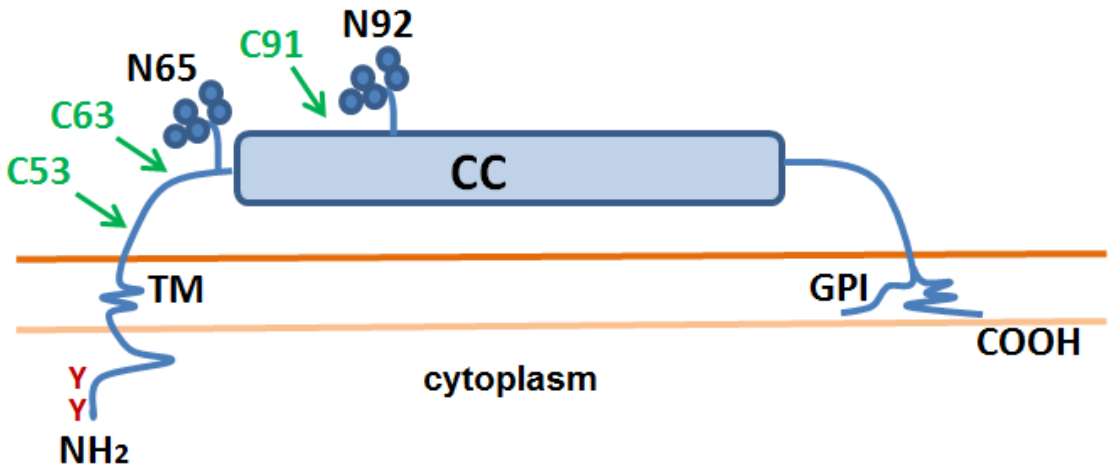

Fig. 1.13 The structure of tetherin
Tetherin contains transmembrane (TM) and glycophosphatidylinositol (GPI) membrane anchors placed within the membrane. Extracellular CC - coiled coil domain; potential N-linked glycosylation sites are marked; Y - tyrosine residues present in endocytic motif are highlighted in red. Highlighted cysteines (green) are involved in the creation of disulfide links which permit dimerization. Numbers represent the residue location in human tetherin. Model based on (Hammonds et al., 2012b).

The cytoplasmic domain is responsible for interaction with cytoskeletal actin. The internal domain's cysteine and α-helical structures enable dimerisation of tetherin. Potentially, the inhibition of viral release by tetherin occurs by holding of fully formed virions to the cell surface which prevents their release and spread (Neil et al., 2008). Virions can also be internalized by endocytosis and undergo degradation mediated by RING-type 3 ubiquitin ligase (Evans et al., 2010).

1.5.2.2 Restriction of JSRV by tetherin

Two forms of tetherin are expressed by sheep, denoted BST-2A and BST-2B, both restrict exJSRV, enJSRV and Δ*vpu*HIV (Arnaud et al., 2010). The ovBST-2B is less restrictive than ovBST-2a and this may be explained by the lack of a GPI anchor in ovBST-2B (Arnaud et al., 2010). The interaction between enJSRV and tetherin may be relevant to the function of the sheep placenta. Placental morphogenesis of the sheep embryo is dependent on enJSRV expression (Dunlap et al., 2006b). During early pregnancy, enJSRV expression is regulated by interferon tau production. Interferon tau elevates the production of tetherin in the ovine trophoblast, mainly in the endometrial stromal cells. However, in luminal and glandular epithelial cells, the lack of tetherin may explain high enJSRV expression. These results correlate with the finding that the cells responsible for exJSRV replication lack tetherin expression (Arnaud et al., 2010).

Several mechanisms for evading tetherin activity have been described (Neil et al., 2008, Evans et al., 2010, McNatt et al., 2013). HIV-1 Vpu was identified as a factor responsible for escape from tetherin restriction by the interaction between the transmembrane domains of these two proteins (Neil et al., 2008). This leads to cellular internalisation, resulting in abrogation of tetherin's antiviral properties by the downregulation of its levels on the cell surface (Neil et al., 2008, Evans et al., 2010, McNatt et al., 2013). Both SIV and HIV-2 Env reduce the BST-2 activity by binding to its exodomain, which causes endocytosis of the Env-BST-2 complex and its degradation (Douglas et al., 2010). SIV_{mac} Nef inhibits BST-2 by interaction with a GDIWK motif present in the cytoplasmic domain of BST-2. Human BST-2 does not include this five amino acid fragment which may explain its restrictive character towards SIV_{mac} (Douglas et al., 2010). FIV Env shields the budding virus from a

potentially restrictive tetherin; however in this case the tetherin also is a cofactor required for optimal particle release during budding (Morrison et al., 2014).

1.5.3 TRIM5

Tripartite motif protein 5α (TRIM5α or T5α) is a major post-entry determinant for the host range of retroviral infection (Huthoff and Towers, 2008). Its antiretroviral properties were discovered during a study on the orthologue from rhesus macaque, which potently inhibited HIV replication (Stremlau et al., 2004, Sodroski, 2004). MPMV, which naturally infects old world monkeys, has been shown to be restricted by T5α of new world primates including squirrel monkey and tamarin monkey (Diehl et al., 2008).

1.5.3.1 TRIM5 structure

T5 proteins have a number of conserved domains collectively denoted (RBCC): a RING domain, 1 or 2 B-boxes and a coiled coil. Because of alternative splicing, several isoforms of T5 may be expressed, but only T5α exhibits antiretroviral activity, due to the presence of a C-terminal PRY/SPRY, or B30.2 domain. Features of T5α structure are shown in Fig. 1.14.

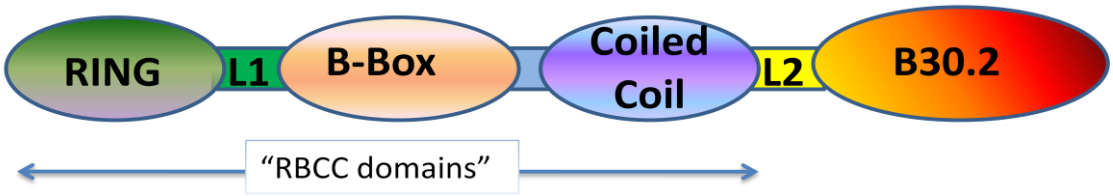

Fig. 1.14 Composition of TRIM5α domains
N terminal RBBC domains are fused to the C-terminal B30.2 domain by the L2 (linker 2 peptide).

The RING (Really Interesting New Gene) domain contains from 40 to 60 amino acids and is present in approximately 600 human genes (Deshaies and Joazeiro, 2009, Francis et al., 2013). The RING domain located at the N-terminus of T5 proteins has a zinc-coordinating motif and possesses E3 ubiquitin ligase activity, which mediates the proteasomal degradation of viral capsids (Stremlau et al., 2004). This is the main, but not the only, mechanism of T5α restriction because deletion of the RING domain significantly decreases but does not abolish huT5α activity against N-MLV (Perez-Caballero et al., 2005).

The B-Box domain of T5 is involved in the multi-oligomerisation of the molecule and subsequently, the creation of cellular bodies (Li and Sodroski, 2008). Mutations of the B-Box domain that prevent formation of multimerised organised structures decrease the restrictive character of rhT5 although not to the same degree for all retroviruses (Li and Sodroski, 2008). The coiled coil and linker peptide 2 domains enable dimerisation of T5α, which enhances its ability to bind CA and to restrict replication (Langelier et al., 2008).

The B30.2 domain binds viral capsids and in this sense it acts as a pattern recognition receptor for retroviral capsids (Huthoff and Towers, 2008). Notably, this interaction is highly species and virus specific and even a single amino acid substitution in the viral capsid protein may significantly change its susceptibility to T5α inhibition. Similarly, often the mutation of one residue in the B30.2 PRY/SPRY v1 variable region can cause a switch in the specificity of T5α restriction (Diaz-Griffero et al., 2008).

It has been demonstrated that various T5α alleles may have different antiviral functions (Goldschmidt et al., 2006, Rahm et al., 2013). The most common human T5α alleles are not protective against HIV, although haplotypes associated with the slower progression of the disease have been identified (Goldschmidt et al., 2006, Rahm et al., 2013).

1.5.3.2 TRIM5 restriction mechanism

T5α function is not yet fully understood although it appears to induce premature dissociation of viral cores by promoting their proteasomal degradation (Diehl et al., 2008). However, inhibition of proteasomal degradation does not completely abolish the antiretroviral activity of T5α, which suggest the presence of additional restriction mechanisms (Diaz-Griffero et al., 2008).

The owl monkey is the only New World Primate that restricts HIV-1 infection (LaBonte et al., 2002, Stremlau et al., 2004); (Sayah et al., 2004), It appears that this resistance is caused by the unique Cyclophilin A which is a part of T5 and CyclophilinA (TRIMCyp) fusion protein, which is responsible for HIV-1 CA binding. The structural difference between T5α and TRIMCypA is based on the substitution of the B30.2 domain with CypA (Sayah et al., 2004). Feline T5 does not contain PRY-SPRY capsid-binding domain and therefore has no restriction potential against retroviruses (McEwan et al., 2009, Koba et al., 2013).

In addition to its direct antiviral effects, T5α can also trigger innate immune responses in infected cells. In this way it may act additionally as a pattern recognition receptor, responsible for sensing of viral infection (Pertel et al., 2011, de Silva and Wu, 2011). By its connection with the E2 ubiquitin-conjugating enzyme complex UBC13-UEV1A, T5α has the potential to activate the TAK1 kinase complex, which mediates the immune response by stimulation of expression of *NF-κB* and *MAPK* inflammatory genes (Pertel et al., 2011, de Silva and Wu, 2011).

In addition to the well-characterised post-entry activity of TRIM5, there is some evidence that T5α may also inhibit late steps of retroviral replication. Both the rhesus monkey T5α and African green monkey TRIM5α can inhibit HIV-1 Gag production by targeting this polyprotein precursor to degradation (Sakuma et al., 2007). Moreover, a cleaved form of rhT5α is encapsidated in HIV-1 viral particles suggesting the possibility that it has additional antiviral functions (Sakuma et al., 2007).

1.5.3.4 TRIM5 proteins among ruminants

T5 has been extensively studied in primates, but relatively little is known in other species. Due to their number and the rapid evolution of TRIM genes it is difficult to define which genes are actually the true homologues (Si et al., 2006, Han et al., 2011, Malfavon-Borja et al., 2013).

One of the bovine T5 proteins has been shown to restrict HIV-1 and N-tropic MLV (Si et al., 2006). Recently a number of goat and sheep T5 alleles have been described (Jauregui et al., 2012). The Ov1 and Ov2 variants of sheep T5α exhibited inhibition of MVV in contrast to the Ov4 allele which did not restrict MVV (Jauregui et al., 2012).

1.5.3.5 Properties of other TRIM family proteins

There are nearly 100 *TRIM* genes present in the human genome and a significant proportion of these are synthesised as multiple isoforms (Reymond et al., 2001, Han et al., 2011). The representatives of this family of proteins take part in various cellular processes, including cellular differentiation, apoptosis, oncogenesis, proliferation and innate immunity (Grutter and Luban, 2012).

In addition to T5α, there are several other TRIM proteins that restrict retroviruses. Extensive analysis of the human and mouse TRIM families of proteins has identified inhibitors of HIV, N-MLV and B-MLV (Uchil et al., 2008). The expression patterns of feline TRIM proteins and their IFN-mediated upregulation has been reported (Koba et al., 2013). These studies showed that TRIM11, TRIM15 and TRIM31 inhibited retroviral entry. However, interestingly gene silencing of TRIM25, TRIM31 and TRIM62 interfered with viral release, suggesting their role in virus replication (Uchil et al., 2008). TRIM1 was shown to restrict N-MLV but not as effectively as T5α (Yap et al., 2004).

TRIM28 is able to acetylate HIV-1 integrase within the PIC and subsequently inhibits the integration of provirus (Allouch et al., 2011). Moreover, it has been shown that TRIM28 protects mouse embryonic stem cells by binding to the MLV PBS, thereby preventing transcription from the proviral LTR (Wolf and Goff, 2007). TRIM22

localised in the nucleus acts as an inhibitor of HIV-1 transcription suppressing the HIV-1 LTR promoter mediated gene expression (Kajaste-Rudnitski et al., 2011, Barr et al., 2008).

1.5.4 Restriction of retroviruses by SAMHD-1

SAMHD1 (SAM domain and HD domain-containing protein 1) is a recently discovered restriction factor that inhibits retroviral replication in myeloid cells and macrophages (Laguette et al., 2011). Its antiviral activity is based on the reduction of the total pool of dNTPs that are present in the cytoplasm, which in consequence may interfere with the process of reverse transcription. SAMHD1 is an enzyme that exhibits phosphohydrolase activity, converting nucleotide triphosphates to a nucleoside and triphosphate. In doing so, SAMHD1 depletes the pool of nucleotides available to reverse transcriptase for viral cDNA synthesis and thus prevents viral replication (Lahoussa 2012). The Vpx proteins of HIV-2 and SIV_{agm} enable the successful evasion of SAMHD1 activity (DeLucia et al., 2013). SAMHD1 is involved in HTLV-1 restriction by the emergence of transcription intermediates, which direct primary human monocytes to IRF3-mediated antiviral responses and apoptosis (Sze et al., 2013a). Moreover, it has been suggested that SAMHD1 plays a role in the immune sensing of retroviral infection (Sze et al., 2013b).

1.6 Retroviral vectors

Retroviral vectors can also be used to investigate infection mechanisms and various steps of viral replication. For example, there is no permissive cell culture system available for JSRV, partially because the JSRV LTR has low activity in the cultured cell lines tried to date (Palmarini et al., 2000a, Griffiths et al., 2010). Retroviral vectors based on JSRV are a powerful tool in the investigation of viral host-cell interactions that are present in OPA. Many aspects of OPA biology and pathogenesis have been revealed by utilisation of an infectious molecular clone of JSRV denoted $pCMV2JS_{21}$ (Fig. 1.15) (Palmarini et al., 1999).

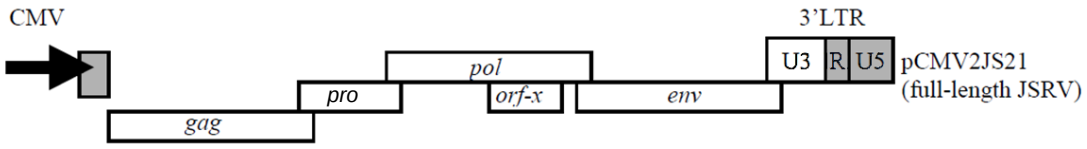

Fig. 1.15 Features of pCMV2JS$_{21}$

The plasmid pCMV2JS$_{21}$ contains an infectious molecular clone of the exogenous JSRV$_{21}$ isolate (Palmarini et al., 1999). Figure adapted from (Maeda et al., 2001, Hofacre and Fan, 2010).

When pCMV2JS21 JSRV is introduced into producer cells by transfection, JSRV expression is under the control of the CMV immediate early promoter and results in the production of viral particles with the same structure and genome as wild-type JSRV (Palmarini et al., 1999).

Retroviruses may be used to efficiently transduce target cell lines providing long-term and stable gene transfer even after several rounds of cell division (Durand and Cimarelli, 2011). Retroviral vectors are able to carry inserted genes up to 20kb (Shin et al., 2000). However, in practice the capability of retroviral vector RNA is limited to 8kb because of the errors that occur during viral replication. In addition to their application in cell culture, retroviral vectors allow transduction of genes *in vivo*; for example, for use in gene therapy or in the creation of transgenic animals (Pages and Bru, 2004).

Potential applications of retroviral vectors include expression of therapeutic recombinant proteins or siRNA molecules, targeted gene repair by homologous recombination, and vaccination either by antigens displayed in the vector virus or by expression of an immunogenic transgene (Mühlebach, 2010). Up to June 2014 retroviruses had been used in approximately 406 clinical gene therapy trials (wiley.co.uk/genmed/clinical), which accounts for a significant part of the total number of gene therapy trials and is one of the most common methods of gene transfer to patients. Retroviral vectors' advantage is their relatively low immunogenic character of the vector component compared to the more widely used adenovirus vectors which are more immunogenic due to pre-existing immunity (Mingozzi and High, 2013).

1.6.1 Safety of retroviral vectors

Retroviral gene therapy has been successfully used as a treatment for a number of diseases including SCID (severe combined immunodeficiency) (Fischer et al., 2013) and GvHD (graft versus host disease) (Taflin et al., 2013). However, some trials have revealed the risk of cellular transformation induced by vector integration (Mühlebach, 2010, Hacein-Bey-Abina et al., 2003). Due to the sequence similarity with endogenous retroviruses there is also a potential risk of recombination events leading to the emergence of replication competent virus (Donahue and Clark, 1992). There is also a possibility that vector particles might cross-package RNA from other retroviruses, which was documented as MPMV encapsidating HIV and SIV RNA (Al Shamsi et al., 2010). This observation raises the question of whether there is a risk of creating recombinant replication-competent virus with pathogenic potential (Al Shamsi et al., 2010). In order to improve vector safety, viral structural genes are provided *in trans* on a separate plasmid from the vector construct that carries the packaging signal and the transgene (Pages and Bru, 2004, Ismail et al., 2000). The further separation of *env* from *gag-pol* also increases the safety of a vector.

Retroviral vector production may be based on transient transfection or stable gene expression in a producer cell line or a combination of both systems (Pages and Bru, 2004). In order to maximize vector titre and safety, several systems have been developed. The development of self-inactivating vectors minimises the risk of insertional interference as in these constructs the enhancer elements in the U3 of the viral 3'LTR are deleted and transgene expression is driven by an internal promoter. The inclusion of splice sites in the vector greatly improves the level of transgene expression (Krall et al., 1996) and enables the removal of the packaging signal Ψ (Ismail et al., 2000). Localisation of the splice donor site in the 3' LTR region and the splice acceptor site downstream of Ψ causes its removal in the target cell line during reverse transcription (Ismail et al., 2000).

Vectors that remove all their genetic information other than the transgene may be created by the utilisation of site specific Cre recombinase which removes the sequence between LoxP sites (Pages and Bru, 2004). Furthermore, the utilisation of site specific

recombinases may enable insertion of the transgene in a precise locus (Artegiani and Calegari, 2013).

Integration-defective lentiviral vectors have been developed in order to increase their safety by avoiding the potential risk of transformation. In addition integration-defective lentiviral vectors, have reduced potential of silencing of the integrated transgene (Wanisch and Yanez-Munoz, 2009). Recently an integrase-deficient retroviral vector has been developed whose transgene insertion could only be achieved by locus targeted recombination (Huang et al., 2010).

1.6.2 Features of retroviral vectors that enhance the efficiency of production and transduction

There are several optional parts of a retroviral vector that enhance its production and the level of transgene expression (see Fig. 1.16). The addition of a lentiviral central polypurine tract (cPPT) greatly increases their transducing potential (Logan et al., 2004). The presence of a cPPT enhances the efficient nuclear import of genetic material in non-dividing cells. The MPMV-derived cytoplasmic transport element (CTE) significantly enhances the export and stability of transcripts and allows the omission of Rev-like regulatory proteins from the vector production system (Pages and Bru, 2004).

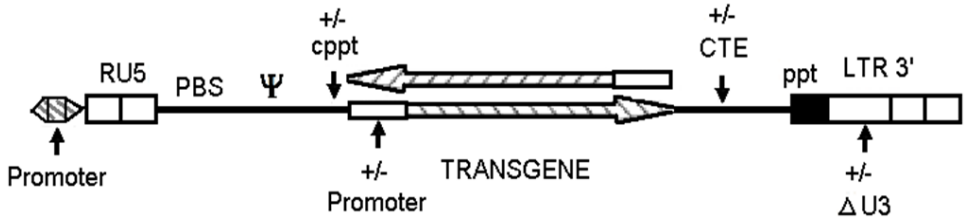

Fig. 1.16 Potential features present in a retroviral vector
PBS - primer binding site; cppt – central polypurine tract; ppt - polypurine tract; +/- indicate features that are optional; ΔU3: deletion of transcriptional sequences within 3' LTR. Reproduced from (Pages and Bru, 2004).

The inclusion of picornaviral internal ribosomal entry site (IRES) mediating 5' cap-independent translation, enables the expression of two genes from a single RNA molecule (Martinez-Salas, 1999).

1.6.3 Retroviral vector pseudotyping

Retroviral vector design enables the creation of viral particles containing structural proteins from the various kinds of retroviruses and a variety of envelope glycoproteins including those which originate from other viral families. Such utilisation of proteins from other viruses in a vector is referred to as pseudotyping. Such manipulations may enable gene transfer to be targeted to specific subsets of cells. Vesicular stomatitis virus envelope protein (VSV-G) is widely used in viral vector production due to the broad range of cell lines and organisms that allow its entry. Moreover, VSV-G is considerably more stable than some retrovirus Env proteins during ultracentrifugation and freezing (Burns et al., 1993). However, there are some disadvantages associated with VSV-G pseudotyping, such as cytotoxicity in the vector-producing cells. In addition, experiments with VSV-G pseudotyped vectors may result in the formation of tubulovesicular structures (TVS) during the preparation of viral stocks (Pichlmair et al., 2007). TVS may cause the carryover of DNA or induce immunomodulaion due to interaction with Toll like receptor 9 (Pichlmair et al., 2007). The Low-Density lipoprotein (LDL) receptor has been shown to mediate entry of VSV-G pseudotyped vectors (Finkelshtein et al., 2013). This explains the broad range of cell lines that are permissive for VSV-G pseudotyped virus entry, as the LDL receptor is ubiquitously expressed in various tissues and species (Finkelshtein et al., 2013). Additionally, a role for the endoplasmic reticulum chaperone protein gp96 in mediation of VSV-G enveloped virus entry had been described (Bloor et al., 2010). It should be noted that VSV-G pseudotyped vectors may enter the cell via a different pathway than the one mediated by Env, and this may influence early infection events. Therefore, it is worth conducting parallel experiments using natural envelope glycoprotein.

1.7 Aim of the project

JSRV is primarily a sheep pathogen. Although it is also able to occasionally infect goats, it rarely results in clinical disease in this species. Recent data has provided evidence for restriction to JSRV in lung epithelial cells of goats although the precise mechanism is still unknown (Caporale et al., 2013b). Moreover, some cells are able to be infected by JSRV Env pseudotyped vectors (Rai et al., 2000) and a variety of cell lines from different species can be transformed by JSRV Env (Maeda et al., 2001, Alberti et al., 2002, Johnson et al., 2010). In order to examine the species specificity barriers of OPA, I studied the significance of A3 and TRIM5α in JSRV restriction.

In this project I have investigated the impact of ruminant A3 proteins on JSRV replication (Chapter 3). Flow cytometry analysis of infected cells, sequencing of proviral sequences and reverse transcriptase assays provided insights into the mechanisms of A3 restriction of JSRV *in vitro*. Western blot assays on lung fluid from natural cases provided a significant contribution to understanding the role of A3 in the pathogenesis and epidemiology of OPA. In addition, I analysed the activity of human and murine A3 to investigate the possibility of using the mouse as an animal model for OPA (Chapter 4).

TRIM5α was the second restriction factor investigated (Chapter 5). I made cell lines that stably express ruminant, rhesus macaque and human TRIM5α. Infectivity assays performed on these cells analysed the activity of various TRIM5α homologues against JSRV and HIV-1. These studies have extended the understanding of species specificity barriers of OPA and are relevant to speculation about connections between JSRV and human bronchioloalveolar carcinoma. The results obtained could contribute to the development of disease control strategies such as the creation of sheep that are resistant to OPA and provide important information for the potential utilisation of JSRV based vectors in gene therapy.

Chapter 2 – Materials and Methods

2.1 DNA plasmids

2.1.1 pGEM-T Easy [Promega]

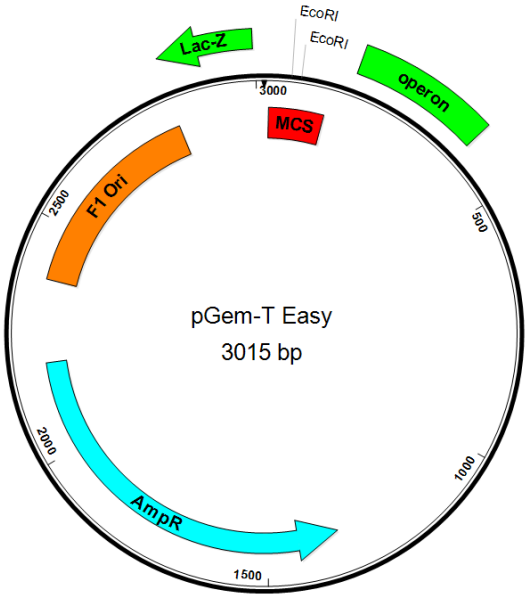

Fig. 2.1 pGEM-T Easy plasmid map
Red – MCS; green – *LacZ* ORF; blue – Beta-lactamase (AmpR); orange – Phage F1 region.

2.1.2 pCI-Neo [Promega]

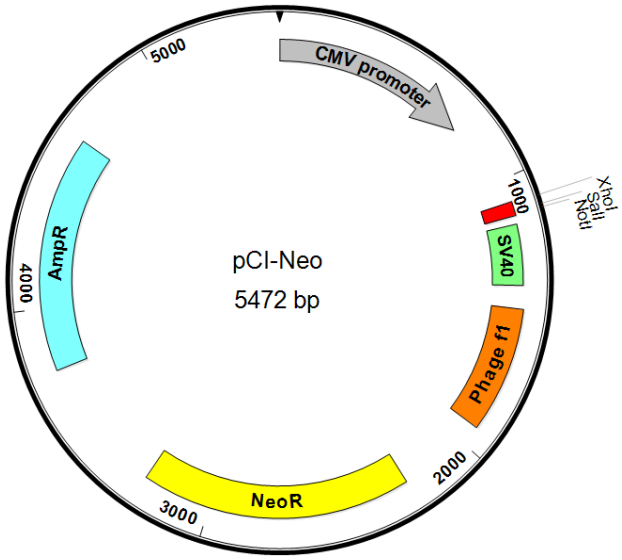

Fig. 2.2 pCI-Neo vector map
Grey – CMV promoter; red – MCS; green – SV40 polyadenylation signal; orange – Phage F1 region; yellow – neomycin transferase (NeoR); blue – Beta-lactamase (AmpR).

2.1.3 pCMV2JS$_{21}$

Features of pCMV2JS$_{21}$ are presented in Fig. 1.15. The rest of the plasmid is pBluescript which contains some sheep genomic DNA at 3' end of provirus.

2.1.4 pLNCX-2 [Clontech]

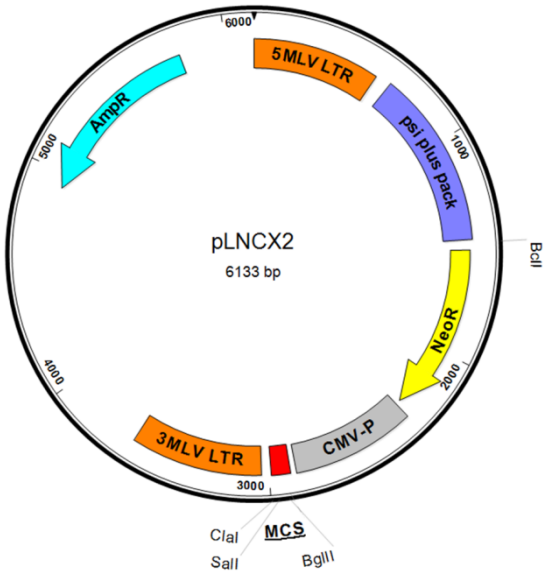

Fig. 2.3 pLNCX-2 vector map
orange – MLV 5' and 3' LTR; violet – psi plus packaging element; yellow – neomycin transferase gene (NeoR); grey – CMV promoter; red – MCS; blue – beta-lactamase (AmpR).

2.1.5 pLPCX [Clontech]

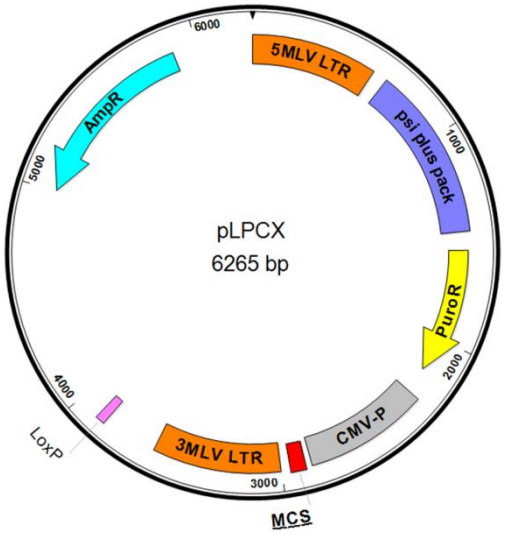

Fig. 2.4 pLPCX vector map
Orange – MLV 5' and 3' LTR; violet – psi plus packaging element; yellow – puromycin resistance gene (PuroR); grey – CMV promoter; pink – LoxP site; red – MCS; blue – Beta-lactamase (AmpR).

2.1.6 pEGFP-FLAG

pEGFP-FLAG (made by David Griffiths) is a derivative of pEGFP-C1 [Clontech], produced by inserting a linker encoding a FLAG epitope tag and additional unique restriction sites immediately downstream of the Enhanced Green Fluoresent Protein (EGFP) ORF.

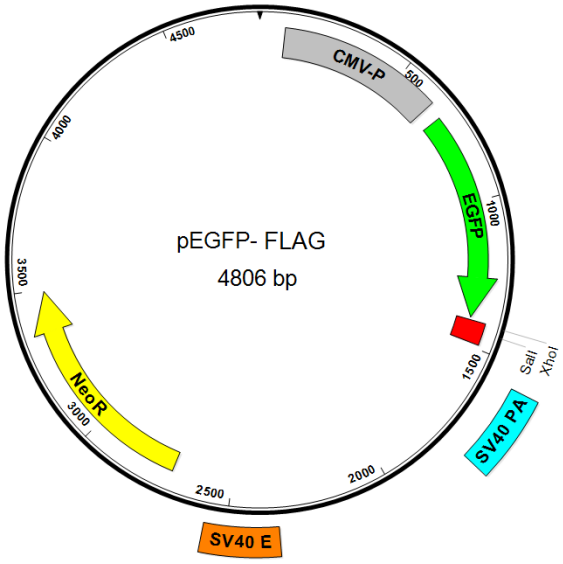

Fig. 2.5 pEGFP-FLAG vector map
Grey – CMV promoter; green - EGFP; red – MCS; blue – SV40 poly adenylation termination signal; orange – SV40 enchancer; yellow – neomycin transferase gene (NeoR).

2.1.7 pVSV-G

The pVSV-G contains the VSV envelope ORF inserted into pMDG [Addgene].

2.1.8 pCAG-JSEnv

The pCAG plasmid [Addgene] modified by insertion of JSRV Env under the control of CAG promoter.

2.1.9 pCMVJS-ΔE-CG

pCMVJS-ΔE-CG (made by David Griffiths) is derived from pCMV2JS[21], where the *env* gene was substituted by EGFP under the control of an internal CMV promoter.

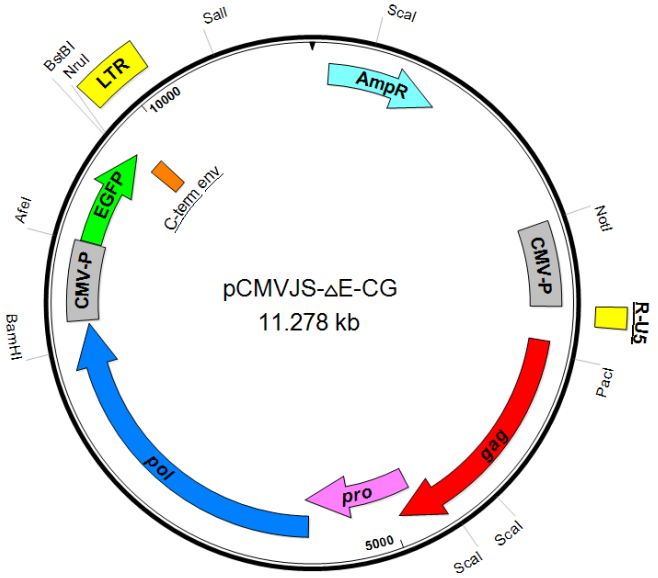

Fig. 2.6 pCMVJS-ΔE-CG vector map

Bright blue – beta-lactamase (AmpR); grey – CMV promoter; yellow – JSRV 5' and 3' LTR; red – JSRV *gag*; pink – JSRV *pro;* dark blue – JSRV *pol*; green – EGFP; orange – C terminal fragment of JSRV *env*.

2.1.10 pCMV JSE SP-FLAG

The pCMV JSE SP-FLAG is a derivative of pCMV3ΔGPJS$_{21}$, which expresses only the SP peptide (encoded by the 5' region of env) fused to a C-terminal FLAG epitope tag (Caporale et al., 2009).

2.1.11 pIREShyg3 [Clontech]

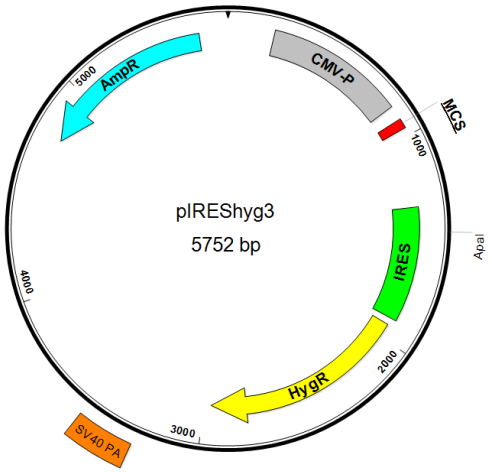

Fig. 2.7 pIREShyg3 vector map

Pink – CMV promoter; green – EGFP; red – MCS; green – IRES (Internal Ribosome Entry Site); yellow – hygromycin resistance gene (HygR); orange – SV40 poly adenylation termination; blue – beta-lactamase (AmpR).

2.1.12 pCS-CG [Addgene]

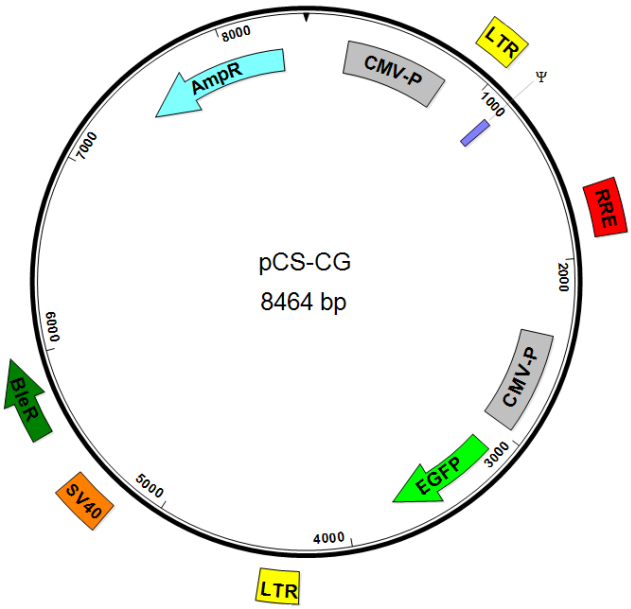

Fig. 2.8 pCS-CG vector map
Grey – CMV promoter; yellow - HIV-1 LTR; violet – packaging signal (Ψ); red – Rev Responsive Element (RRE); green – EGFP; grey – SV40 promoter; dark green – bleomycin resistance gene (BleR) blue – Beta-lactamase (AmpR).

2.1.13 pMDLg/pRRE

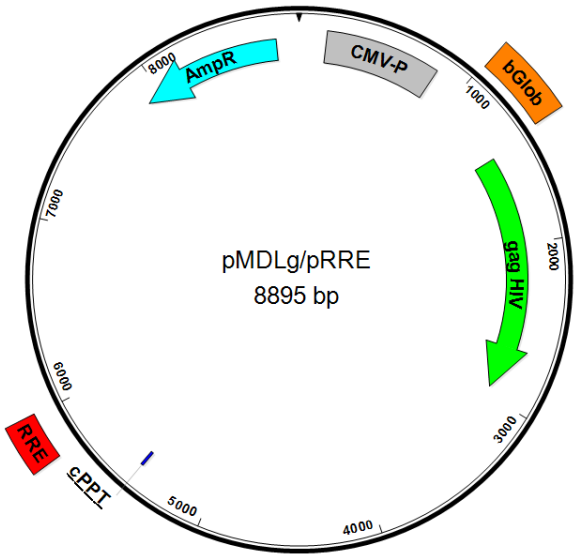

Fig. 2.9 MDLg/pRRE
Grey – CMV promoter; orange – beta globin intron; green – HIV *gag*; blue – central polypurine tract (CPPT); red – RRE (Rev Responsive Element); blue – Beta-lactamase (AmpR).

2.1.14 pCNC-Rev

The pCNC-Rev plasmid provides the expression of Rev in mammalian cells (Ikeda et al., 2003). The expression of Rev from a separate plasmid enhances the safety of vector system.

2.1.15 pHIT60

The pHIT60 plasmid provides the expression of MLV Gag and Pol in mammalian cells (Markowitz et al., 1988). The expression of structural proteins from a separate plasmid enhances the safety of the vector system.

2.2 Primers

Table 2.1 Oligonucleotide primers used in this project

(F-forward; R-reverse)

Primer	Sequence
A3Z1-F	CTGCCGCTTGAACAACTTCAAGGAG (25)
A3Z1-R	TTGRATCAGTCTGGAGACAGTAGC (24)
A3Z1-OA_Ex_F	GATCGATCCTCGAGGCCACCATGGATGAAAACACCTTCACT GAG (44)
A3Z1-OA_ExHA_R	GATCGATCGCGGCCGCTCAAGCGTAGTCTGGGACGTCGTA TGGGTAGTTTTGCTGAGCCCTGAGAATG (68)
A3Z1-BT_Ex_F	GATCGATCGTCGACGCCACCATGGACGAATATACCTTCACT GAG (44)
A3Z1-BT_Ex_R	GATCGATCGCGGCCGCTCAGTTTTGCTGAGTCTTGAGAAT G (41)
A3Z1-BT_ExHA_R	GATCGATCGCGGCCGCTCAAGCGTAGTCTGGGACGTCGTA TGGGTAGTTTTGCTGAGTCTTGAGAATG (68)
A3Z2Z3-F	ACAAAGGCCAGGGATGCAACCAGC (24)
A3Z2Z3-R	GGGATGAGAGTCTGATGCTCAAGC (24)
A3Z2-F	AGAGCCGGCCTGGGAGGTCACTC (23)
A3Z2-R	AGGCTGAGAAGGGAGGTAACRGTGG (25)
A3Z3-Oa_ExF	GATCGATCGTCGACGCCACCATGACGGAGGGCTGGGCTG GATCAG (45)
A3Z3-BT_Ex_F	GATCGATCGTCGACGCCACCATGACCGAGGGCTGGGCTG GGTCAG (45)
A3Z2Z3-Ov-Exp-F	GATCGATCGTCGACGCCACCATGCCCTGGATCAGCGACCA CG (42)
A3Z2-OA_Ex_R	GATCGATCGCGGCCGCTCACCCGAGAATGTCCTCAAGCTC (40)
A3Z2-Oa_ExHA_R	GATCGATCGCGGCCGCTCAAGCGTAGTCTGGGACGTCGTA TGGGTACCCGAGAATGTCCTCAAGCTC (67)
A3Z2-OaBT_ExHA_R	GATCGATCGCGGCCGCTCAAGCGTAGTCTGGGACGTCGTA TGGGTACCCGAGAATGTCCTCAAGCTC (67)
A3Z2-BT_Ex_F	GATCGATCGTCGACGCCACCATGCCCTGGACCAGAGACTC CAG (43)
A3Z3-Oa_ExF	GATCGATCGTCGACGCCACCATGACGGAGGGCTGGGCTG GATCAG (45)
A3Z3-BT_Ex_F	GATCGATCGTCGACGCCACCATGACCGAGGGCTGGGCTG GGTCAG (45)
A3Z3-BT_Ex_R	GATCGATCGCGGCCGCCTAAATTGGGGCCGTTAGGATCC (39)
A3Z3-BT_ExHA_R	GATCGATCGCGGCCGCTCAAGCGTAGTCTGGGACGTCGTA TGGGTAAATTGGGGCCGTTAGGATCC (66)
A3Z3-CAP_Ex_R	GATCGATCGCGGCCGCCTAAGTTGGCGCTGTCAGGATCCT (40)
A3Z3HA-CAP_Ex_R	GATCGATCGCGGCCGCTAAGCGTAGTCTGGGACGTCGTAT GGGTAAGTTGGCGCT (55)
A3Z2Z3-Ov-Exp-R	GATCGATCGCGGCCGCTCACTAAGTCGGCGCCGTCAGGAT CCTCTG (46)
A3Z2Z3HA-Ov-ExpR	GATCGATCGCGGCCGCTCACTAAGCGTAGTCTGGGACGTC

	GTATGGGTAAGTCGGCGCCGTCAGGATCCTCTG (73)
Z3xtF1	GGCTCTGCCAAGAGGGAGGGC (21bp)
Z3xtR1	GTCCCTTATCTGAGAATGTTC (21bp)
Z3xtF2	AGTCTTGCCAGGGYACTAAATGAC (24bp)
Z3xtR2	AGAACTGGCATCGATACCTGGTC (23bp)
TRIM-F1	GGCAGAATTTGAAAGATACACAAG (24bp)
TRIM-R1	GTGTGTCAGATGTACTTACAGTAAG (25bp)
Oa-TRIM-F-BCL	GATCGATCTGATCAGCCACCATGGCTTCAGGAATCCTGATG AAC (44bp)
BtOa-TRIM-R	GATCGATCGTCGACTCAACAGCTTGGTGAGCACATGTGCT CACCAAGCTGTTGA (34bp)
BtOa-TRIM-HA-R	GATCGATCGTCGACTCAAGCGTAGTCTGGGACGTCGTATG GGTAACAGCTTGGTGAGCACA (61bp)
IRES-Hyg F	GATCGATCGTCGACGGCGGTCGCACTAGAGGAATTC (36bp)
IRES-Hyg R	GATCGATCCTCGAGCTCTTGTTCGGTCGGCATCTACTC (38bp)
Oa-TRIM-F-BCL	GATCGATCTGATCAGCCACCATGGCTTCAGGAATCCTGATG AAC (44bp)
BtOa-TRIM-R	GATCGATCGTCGACTCAACAGCTTGGTGAGCACA (34bp)
IREShyg-F-Cla	GATGGATCATCGATGGGCGGCCGCACTAGAGGAATTC (37)
IREShyg-R-Bst	GATCGATCTTCGAACTCTTGTTCGGTCGGCATCTACTC (38)
1164 GFP F	GTACGGTGGGAGGTCTATATAAGC (24)
1164 GFP R	AGCTCCCAGGACTTAACCCTTCAC (24)
JS21EnvF	GAATGAGGCACATGTACAACCTCC (24)
JS21EnvR	GCTGAGAGCCGTATTAATGCGTTG (24)
CX-R	TCTTTCATTCCCCCCTTTTTCTGG (24)
LN-F	GGTAGGCGTGTACGGTGGGAGGTC (24)
IH-5-R	AAGCGGCTTCGGCCAGTAACGTTA (25)
TRIM-R6	CCAAGTAGACATCTCTTCTCTGAC (24)
TRIM-F3	GGTTCAGGTGACCCTGAATTCTC (23)
TRIM-R3	TTCTYTGACACGTCTACCTCCCAG (24)
TRIM-F2	CTCCAATCATGTCTGCAGAGGCTG (24)
Primers and probes used for quantitative PCR	
P1	TGGGAGCTCTTTGGCAAAAGCC (22)
P6	TGATATTTCTGTGAAGCAGTGCC (23)
JSRV-T-FAM probe	FAM-AGCAAACATCCGARCCTTAAGAGCTTTCAAAA-BHQ

The alignments of primers which were used in cloning are shown (see Fig 3.3 to 3.6 and Fig 3.4). The accession numbers of published TRIM5 and APOBEC3 sequences are shown in Table 3.1 and Table 5.1.

2.3 Molecular Cloning

2.3.1 Preparation of competent cells

A stationary phase culture of JM109 [Promega] was diluted 1:100 with 500 ml LB (Luria Bertani Broth) [Moredun Services], cultured until the optical density (OD) ($\lambda = 600$ nm) was 0.4-0.6 (typically 2-3 h), then incubated on ice for 10 min and centrifuged at 1800 × *g* for 10 min at 4°C. The cells were suspended in 20 ml ice cold 100 mM $CaCl_2$, incubated on ice for 30 min, centrifuged at 1800 × *g* for 10 min at 4°C and resuspended in 8 ml of ice cold 100 mM $CaCl_2$ 15% glycerol [Fisher Scientific]. Cells were then aliquoted to tubes, snap frozen and stored at -80°C for later use. In some cases commercial competent JM109 cells [Promega] were utilised.

2.3.2 Transformation

In order to transform bacteria, 50 µl of competent JM109 were mixed with 1 µl of plasmid DNA or ligation complexes and incubated on ice for 30 min. The cells were then incubated at 42°C for 50 s before placing on ice for 2 min. SOC medium (0.5 ml) [Sigma] was added and the cells incubated at 37°C for 30 min with shaking. Between 50 µl to 200 µl of transformed bacteria were plated on LB-agar plates containing 100 µg/ml ampicillin.

2.3.3 Bacterial glycerol stocks

Bacterial glycerol stocks were prepared for long term storage of desired transformed clones. Between 200 to 600 µl of overnight bacterial culture was mixed with glycerol to a final concentration of 15% Glycerol and stored at -80°C.

2.3.4 Small scale DNA purification – Qiagen Miniprep kit

DNA was purified from 5 ml of overnight culture using the Plasmid Mini kit [Qiagen] according to the supplier's instructions. The DNA was eluted in 50 µl of water. This

kit is based on ion exchange chromatography where DNA binds to a silica column and after washes is eluted with water.

2.3.5 Large scale DNA purification – Maxiprep plasmid purification

For large scale purification of transfection grade plasmid DNA, the Endofree Maxi kit [Qiagen] was utilised, starting with 100 ml to 500 ml of stationary phase culture. The procedure was conducted according to the supplier's manual. DNA was eluted using 1 ml of water.

2.3.6 Agarose gel DNA electrophoresis

Agarose gel DNA electrophoresis was used to separate DNA by size. Agarose gels were prepared by solubilisation of agarose to a final concentration of 1% to 1.5% in TAE buffer (40 mM Tris acetate [Sigma] 1 mM EDTA [Sigma]. Ethidium bromide [Promega] was added to a concentration of 0.5 µM. Once set, the gel was put in an electrophoresis tank containing TAE buffer. Samples were prepared by adding 1/6 volume of loading buffer (40% glycerol, orange-G [Sigma]) and were loaded and run on the gel alongside DNA size markers (Hyperladder I or Hyperladder IV [Bioline]). The DNA in the gels was visualised using a UV transilluminator [Uvi Tec].

2.3.7 Purification of DNA from agarose gels

DNA was purified from agarose gel slices using a Qiagen Gel extraction kit, according to the manufacturer's protocol with minor changes. In order to improve the yield of DNA, QG buffer was modified by addition of 500 µl 3 M sodium acetate per 20 ml QG. Agarose gel slices were dissolved by 30 min incubation at 50°C. After the DNA binding and washing steps, columns were centrifuged 40 s at 2000 × g. DNA was eluted using water.

2.3.8 Restriction enzyme digestion of DNA

Digestion of DNA was conducted in a reaction mixture containing the appropriate 10× buffer [Roche or Promega] and restriction enzyme [Roche or Promega], which was incubated for 1 to 4 h at 37°C, with the exception of SwaI, which was incubated for at least one hour at 25°C.

2.3.9 DNA ligation

DNA was ligated using 3U of T4 DNA ligase [Promega] and the supplied buffer [Promega] in a reaction volume of 20 µl. DNA was added in a molar ratio of 3:1 (insert to vector), the amount of vector used in a single reaction varied from 5 to 50 ng. Ligation reactions were incubated overnight at room temperature.

Alternatively, some ligations were performed using the Clonables 2× reagent [Merck], which was mixed with water and DNA. Those ligation reactions were incubated at 4°C to 12°C for 2 h. Prior to ligation, all digested plasmids were treated with shrimp alkaline phosphatase [Promega], in order to eliminate 5' terminal phosphates, which minimised the probability of plasmid re-ligation and occurrence of vectors lacking the insert. Two units of shrimp alkaline phosphatase [Promega] was added at the end of digestion reaction and incubated at room temperature for 30 min, afterwards alkaline phosphatase was inactivated by 15 min incubation at 70°C.

2.3.10 RNA extraction

RNA was extracted from tissues or cultured cells using an RNAeasy kit [Qiagen] according to the supplier's protocol. Prior to RNA extraction, cells were homogenized using a Qiashredder column [Qiagen]. For homogenization of tissue, samples were added to lysing matrix D tubes [MP Biomedicals] containing ceramic beads and processed in a Precellys 24 [Precellys] tissue homogenizer set to two rounds of 30 s at 5000-6000 rpm separated by 2 min pause for 30 s.

2.3.11 DNA extraction from cells

DNA was extracted from cells using the DNA Blood and Tissue kit [Qiagen] as recommended. DNA was eluted in AE buffer.

2.3.12 Reverse transcriptase PCR (RT-PCR)

One-step Superscript 2 Platinum Taq polymerase [Invitrogen] was used to amplify various genes from RNA. The volume of RT-PCR reaction was 25 µl, which contained 12.5 µl 2× supplied buffer, 100 U RT/Taq and a pair of primers, each in a concentration of 200 nM. Each reaction used as a template 50-400 ng RNA. Water [Sigma] was added to make the final volume of reaction mixture up to 25 µl.

2.3.13 High fidelity DNA PCR

KOD Polymerase [Novagen] was used to amplify DNA. Reactions were carried out in a volume of 50 µl, which contained 5 µl of the supplied KOD Polymerase 10× buffer, 0.2 mM dNTPs [Novagen], 1 U KOD polymerase, 1-4 mM $MgSO_4$ [Novagen] and a pair of primers, each at a concentration of 300 nM. As template either 1 ng of plasmid DNA or between 50-200 ng DNA purified from tissue or cells was used.

2.3.14 Addition of 'A' overhangs

KOD polymerase has a proofreading ability, therefore it produces blunt ended amplicons. In order to enable the ligation of KOD PCR products into pGEM-T Easy, adenosine overhangs were added using Flexi Taq Polymerase [Promega]. The reaction mixture contained gel-purified DNA and 0.2 mM dNTPs [Novagen], 5 U Flexi Taq Polymerase [Promega], 2.5 mM $MgCl_2$ in a total volume of 100 µl and was incubated for 2 h at 72°C.

2.4 Mammalian cell culture

All mammalian cell lines (listed in Table 2.2) were cultured in T-75 flasks (vent-cap; Corning) at 37°C in a humidified incubator, with 5% CO_2. In order to passage cells

they were washed using PBS and dispersed using 0.0125% trypsin [Moredun services] and Versene (3.2 mM EDTA) [Moredun services]. Since 293T cells are sensitive to digestion and relatively easy to disperse, the trypsin/versene mixture was diluted tenfold in PBS before use.

2.4.1 Cell lines used in this project

Table 2.2 Cell lines used in this project

Cell line	Species, cell type	Medium	Reference
293T	Human, fetal kidney cells,	A	(Graham et al., 1977)
CPT-Tert	Sheep, fibroblasts,	A	(Arnaud et al., 2010)
CRFK	Cat, kidney;	A	(Crandell et al., 1973)
CRFKovH2	Cat, kidney, stably expressing sheep Hyal-2	A	This study
BOMAC	Cow, macrophages	A	(Stabel and Stabel, 1995)
RK13C	Rabbit, epithelial renal	B	(Beale, 1963)
MDBK	Cow, epithelial like	A	(Madin and Darby, 1958)
TIGEF	Goat, fibroblasts	C	(Da Silva Teixeira et al., 1997)

A - Iscove's Modified Dulbecco's Medium (IMDM) [Sigma],
supplemented with 4 mM Glutamine and 9% FCS [Biosera]

B - Minimum Essential Medium Eagle (MEME) [Sigma],
supplemented with 1% non essential amino acids [Sigma],
2 mM Glutamine [Moredun Services] and 9% FCS

C - Dulbecco's Modified Eagle Medium (DMEM) [Sigma],
2 mM Glutamine and 9% FCS

2.4.2 Transfection of mammalian cells

Transfection was performed using Fugene-HD [Roche] as recommended. Briefly OptiMEM [GIBCO] was added to DNA (100 µl per 2 µg of DNA). Then Fugene-HD [Roche] was added (3 µl per 1 µg of DNA). Transfection complexes were formed during 20 min incubation at room temperature and then added to approximately 90%

confluent cells in T-75 flasks containing 5 ml medium or 6 well plates containing from 0.5 ml to 1 ml medium per well. Cells were incubated with transfection complexes for 16-18 h before medium was replaced with fresh.

2.4.3 Creation of CRFK cells which stably express ovine Hyal-2

CRFKoH2 cells were generated by transduction of parent CRFK cells with a murine leukaemia virus (MLV) vector pLNCX2 expressing ovine Hyal-2, the cellular receptor for JSRV. Stably transduced cells were selected in 500 μg/ml G418 (Sigma) and used as a polyclonal population.

2.5 Production of retroviral vectors

Production of virus stocks was initiated by transfection of producer cell line (see Section 2.4.2).

2.5.1 Virus harvest and concentration

Culture supernatant (SN) was replaced with 10 ml fresh medium 16 h after transfection complexes were first added. On the following day SN was harvested, centrifuged at $1800 \times g$ for 10 min at 4°C and filtered through a 0.45 μm filter [Sartorius], then frozen at -80°C. Supernatants from 42 h and 66 h were optionally pooled and concentrated from 5 to 200 times (usually 25 ×) by ultracentrifugation at $100{,}000 \times g$ for 2 h at 4°C and resuspended in serum-free IMDM [Sigma].

2.5.2 Cell lysate preparation

Cells were harvested and washed in 10 ml cold PBS per T75 flask, centrifuged at $430 \times g$ for 10 min at 4°C. The cell pellet was resuspended and lysed using 1 ml RIPA buffer containing 50 U of benzonase [Novagen], incubated on ice for 2h, inverting tubes occasionally. RIPA buffer contains 150 mM NaCl, 1% Igepal [Sigma], 0.5% Sodium deoxycholate, 0.1% SDS [Sigma] and 50 mM Tris pH 8.0.

2.6 Western blotting

2.6.1 Sample preparation

Each sample was mixed with Laemmli sample buffer (4×) and then boiled for 2 min.

Laemmli sample buffer 4× contains 0.26 M SDS [Sigma], 0.25 M Tris pH 6.8, 10% ß-mercaptoethanol [BDH chemicals], 40% glycerol and 0.01% bromophenol blue.

2.6.2 SDS- PAGE electrophoresis

SDS PAGE was performed using the Laemmli method (Laemmli, 1970) and utilised a 10-15% resolving gel and a 3% stacking gel.

Laemmli Resolving Gel Buffer (4×) contains 1.5 M Tris (base), 13 mM SDS (pH 8.8).

Laemmli stacking buffer (2×) was made by solubilising 0.5 M Tris (base) and 13 mM SDS in water up to final volume. Afterwards the pH was adjusted to pH 6.8.

Electrode buffer (5×) contains 127 mM Tris (7.9), 0.96 M Glycyine, 13 mM SDS.

Stacking gel was made by mixing 3 ml Laemmli stacking buffer (2×), 4 ml water, 1 ml acrylamide (30%) [Severn Biotech], 50 µl 10% ammonium persulphate [Sigma] and 10 µl TEMED [Sigma].

Resolving gel was made by solubilising 0.6 g sucrose [Fisher] in 4 ml water and then adding 3 ml Laemmli gel buffer (4×), 5 ml acrylamide (30%) [Severn Biotech], 50 µl 10% ammonium persulphate [Sigma], 10 µl TEMED [Sigma].

2.6.3 Protein transfer

Semi-dry transfer was performed using a BioRad transfer apparatus applying 15V for 48 min. Protein was transferred to Hybond ECL nitrocellulose [GE Healthcare].

Transfer buffer 10× contains 0.2 M Tris (7.9), 1.53 M glycine solubilised in water up to a final volume.

Transfer buffer 1× was made by diluting 100 ml transfer buffer 10× in 200 ml methanol and 700 ml H_2O.

2.6.4 Antibody – binding

The nitrocellulose membrane with transferred proteins was incubated overnight at 4°C in blocking solution (PBS, 5% dried skimmed milk [Marvel], 0.2% Tween-20). On the next day blocking solution was removed, and the membrane was incubated for 1 h with primary antibody in PBS, 5% Marvel.

For detection of HA-tagged proteins 1:1000 diluted Mouse HA.II Clone 16B12 monoclonal antibody IgG [Covance] was used. For JSRV Gag detection 1:1000 diluted Rabbit anti-Gag polyclonal serum (Salvatori et al., 2004) was used. For detection of ovine A3-Z2 and A3-Z3, custom rabbit polyclonal antibodies [Proteintech] were employed (1:1000 dilution).

Afterwards, blots were washed in PBS 0.1% Tween20 [Fisher Scientific] three times for 10 min each. Then incubated with horseradish peroxidise [HRP] conjugate secondary antibody, 1:1000 diluted Goat anti-rabbit [Dako] or Rabbit anti mouse [Dako] in (PBS 5% Marvel). Subsequently, blots were washed three times for 10 min using PBS, 0.1% Tween20. After a final wash in PBS, blots were developed using Amersham ECL Western Blotting Detection Reagents [GE Healthcare]. The OPTIMAX 2100 X-Ray film processor [PROTEC] or ImageQuant imager [GE Healthcare], were used to develop or capture the western blot image.

2.7 *In vitro* infections

2.7.1 Infection protocol (12 well plate)

1×10^5 cells were plated in each well of a twelve well plate on the day prior to infection. Before infection cells were washed using PBS and medium was replaced with 0.5 ml fresh medium containing 8 µg/ml polybrene (1,5-dimethyl-1,5-diazaundecamethylene polymethobromide) [Sigma]. Then virus was added to the cells and incubated for 16 h and before replacing with fresh medium. As a negative control, uninfected cells and cells infected by heat inactivated virus were used. Virus was heat-inactivated by incubation at 70°C for 20 min.

2.7.2 Preparation of cells for flow cytometry analysis

Three days post-infection cells were examined by UV microscopy. Then cells were harvested by dispersion using 0.5 ml trypsin/versene mix per well. After 10 min 0.5 ml of serum-containing media was added to stop digestion. Cells were washed using 10 ml PBS and centrifuged at 430 × *g* for 5 min. Cells were fixed by 15 min incubation in 1 ml of 1% paraformaldehyde [Fisher] diluted in PBS. Then, the cells were centrifuged at 430 × *g* for 5 min and suspended in 1% sodium azide [Sigma] diluted in PBS. Cells were filtered through a 0.7 mm filter [BD Falcon] before flow cytometric analysis.

2.7.3 Flow cytometry

Flow cytometry analysis of GFP fluorescent or intracellular immunostained cells was performed using CYAN apparatus [Dako] or MACS Quant and Summit software [Beckman Coulter]. Cells lacking the GFP were used as a negative control. In the case of immunostaining, cells without the epitope recognised by the antibody were used. Readout of at least 20000 cells enabled an accurate determination of as little as 0.5% percentage of positive cells with a confidence interval of 0.01. However, in most cases the infectivity was higher, and usually from a single assayed well, at least 50000 cells were counted.

The adjustment of minimal sample size according to the probability of the event is shown in the formula below.

Sample size = $Z^2 \times (P) \times (1\text{-}P) / c^2$

Z = Z value (e.g. 1.96 for 95% confidence level)

P = percentage picking a choice, expressed as decimal

c = confidence interval, expressed as decimal

The percentage of positive cells infected by A3 containing stocks or their median fluorescence values, were compared to cells infected by a reference "no A3" virus stocks. The relative infectivity values were obtained from the average percentage of positive cells in wells infected by the test virus, divided by the average percentage value of positive cells infected by the control virus (ie., virus prepared in the absence of A3. Error bars on plots reflect the experimental variability and show the standard deviation values between wells infected in triplicate by the same virus stocks. The relative fluorescence intensity values were calculated similarly to the relative infectivity, but taking into account the median fluorescence of positive cells. The student two-tailed t-test method with unequal variance was used to verify the significance of results. Due to a multiple comparison, obtained p-values were corrected using the Bonferroni method.

2.8 Sucrose gradient purification of retroviral particles

In order to enhance the purification of retroviral particles, sucrose gradient ultracentrifugation was performed. Retroviral particles are purified on the principle that their virion buoyant density is approximately 1.16 g/ml which corresponds to a particular sucrose concentration (York et al., 1991, Palmarini et al., 1995, Palmarini et al., 1999b). Initially, sucrose solutions of 65%, 42%, 33% and 20% (weight to volume) in TNE buffer were prepared**,** which were subsequently sterilised by 0.2 μm filtering and stored at 4°C. Equal volumes of sucrose solutions were added slowly to a centrifuge tube, starting with a highest concentration of sucrose, then tubes were stored vertically on ice for approximately 1 h. Samples were applied on the surface: for 36 ml tubes the maximum of 2 ml was applied and for 13 ml tubes up to 0.5 ml of a sample was added. Tubes were balanced for centrifugation by adding a small amount of TNE buffer.

Tubes containing the sucrose step gradients were centrifuged at 100,000 × *g* at 4°C for 16 h using the "slow acceleration" and "brake off" deceleration functions in order to avoid disturbing the density gradient. After centrifugation, the tube was placed vertically and the bottom of the tube was punctured by a 19G needle and fractions (0.5 ml) were collected.

The density of fractions was measured by refractometer [Bellingham-Stanley] using the formula:

Density [g/ml] = [2.6465 × (refractive index)] – 2.5286 (Griffiths, 1996)

Samples were stored at -80°C prior to further experiments.

2.9 Concentration of lung fluid

Lung fluid was obtained from OPA sheep, filtered through gauze and clarified first by centrifugation for 10 min at 430 × *g* and 4°C, followed by 1800 × *g* at 4°C for 10 min. The supernatant was then applied to a glycerol cushion in a SW 32Ti ultracentrifuge tube. The glycerol cushion consisted of a bottom layer of 1.5 ml of 50% glycerol / TNE (ingredients TNE) and 1.5 ml top 25% glycerol / TNE. Lung fluid was concentrated at least 200 × by ultracentrifugation at 100,000 × *g* at 4°C for 2 h and suspended in TNE buffer.

2.10 Materials and methods regarding APOBEC experiments

2.10.1 Cloning of sheep, goat, cow APOBEC3 proteins

RNA purified (see Section 2.3.10) from the cell lines CPT-Tert (sheep), TIGEF (goat) and BOMAC (cow) was used as a template for RT-PCR amplification of ruminant *A3-Z2, A3-Z3, and A3-Z2Z3* genes. In order to amplify sheep and cow A3Z1, mRNA isolated from small intestine was used as a template. Consensus primers were designed to sequences located external to reading frames and used to amplify the *A3* genes.

The mix used was as described in Section 3.11 and the RT-PCR program used was 50°C 30 min, 94°C 30s, 40 cycles (94°C 15s, 50°, 55° or 60°C 30s, 72°C 1 min), 72°C 10 min.

RT-PCR products were gel purified (see Section 2.3.7) and ligated into pGEM-T Easy (see Sections 2.3.9 and 2.3.14), which enabled sequencing using SP6 and T7 primers to identify clones with the desired sequences. The selected pGEM-T Easy clones were used as templates for high fidelity PCR using KOD polymerase [Novagen] (see Section 2.3.13). Subsequently, additional primers were used to add a C-terminal HA tag coding sequence and appropriate restriction sites to *A3* sequences to facilitate their cloning into the mammalian expression vector pCI-Neo. The primer sequences are shown in Table 2.2. The details for construction of each vector are described below. The PCR program was 94°C 2 min, 25 cycles (94°C 15s, 50 or 55 or 60°C 30s, 72°C 1 min), 72°C 10 min. Products were gel purified before digestion and ligation (see Section 2.3.7, 2.3.9). pCI-Neo was digested using SalI and NotI and was gel purified (see Sections 2.3.8 and 2.3.7) in order to prepare it for subsequent ligations.

The cow and sheep A3-Z1 coding sequences were amplified by RT-PCR utilising consensus external primers designed to ruminant *A3-Z1* open reading frame, A3Z1-F and A3Z1-R. The sheep *A3-Z1HA* sequence was reamplified from gel-purified RT-PCR product (see Section 2.3.13) using KOD polymerase [Novagen]. Forward primer A3Z1-OA_Ex_F added an XhoI site and a Kozak consensus site upstream of the start codon. A haemagglutinin tag and NotI restriction site was added to the 3' of the ORF using A3Z1-OA_ExHA_R primer. The PCR product was digested using XhoI and NotI restriction enzymes and inserted into SalI and NotI gel-purified digested pEGFP-FLAG (see Section 2.1.6), which enabled sequencing. In order to clone sheep *A3-Z1HA* into pCI-Neo, pEGFP-Ci S *A3-Z1* was cut using XhoI and NotI and ligated into pCI-Neo using T4 Ligase [Promega]. The cow *A3-Z1HA* was reamplified from RT-PCR product using KOD polymerase [Novagen]. The forward primer A3Z1-BT_Ex_F added the SalI site and Kozak consensus site upstream of start codon. The reverse primer A3Z1-BT_ExHA_R added the NotI restriction site and a HA tag to the 3' of the ORF which enabled cloning into pCI-Neo.

For RT-PCR amplification of ruminant *A3-Z2*, primers A3Z2-F and A3Z2-R were used. Reamplification and cloning of sheep and goat *A3-Z2* into pCI-Neo, was enabled by forward A3Z2Z3-Ov-Exp-F and reverse primer A3Z2-OaBT_ExHA_R. The cow *A3-Z2* was reamplified utilising the selected pGEM-T Easy clone as a template and using A3Z2-BT_Ex_F and A3Z2-OaBT_ExHA_R primers. *A3-Z2* PCR products were digested by SalI and NotI, gel-purified and cloned into SalI and NotI digested pCI-Neo.

In order to amplify *A3-Z3* RT-PCR used the same reverse primer, A3Z2Z3-R, for all ruminants together with reverse primer A3Z3-Oa_ExF for sheep and goat *A3-Z3* or A3Z3-BT_Ex_F for cow *A3-Z3*. *A3-Z3HA* reamplified using reverse primer A3Z3-BT_ExHA_R together with forward primer A3Z3-Oa_ExF for sheep, A3Z3-CAPHA_Ex_R for goat, or A3Z3-BT_Ex_R for cow. PCR products were digested by SalI and NotI, gel purified and cloned into pCI-Neo cut with the same enzymes.

RT-PCR amplification of ruminant *A3-Z2Z3* employed forward primer A3Z2Z3-F and reverse A3Z2Z3-R. Sheep and goat *A3-Z2Z3HA* was reamplified by forward primer A3Z2Z3-Ov-Exp-F and reverse A3Z2Z3HA-ExpR. The cow *A3-Z2Z3* was reamplified using A3Z2-BT_Ex_F and A3Z2Z3HA-ExpR. PCR products were digested by SalI and NotI, gel-purified and cloned into pCI-Neo cut with same enzymes.

2.10.2 JSRV vector production for APOBEC3 experiments

JSRV vectors were produced by transient transfection of 293T cells (see Section 2.4.1 and 2.4.2). Retroviral vectors derived from the infectious molecular clone pCMV2JS$_{21}$, were employed in this study. Production of virus stocks was performed either in T-75 flasks or 6-well plates.

JSRV-based vectors were produced by transient transfection of confluent T75 flask of 293T cells with 14 µg of DNA (see Table 2.3) using 42 µl of transfection reagent Fugene-HD (Roche) according to the manufacturer's instructions (see Section 2.4.2).

Sixteen hours post-transfection, transfection complexes were replaced with 10ml fresh medium supplemented with additionally 5 mM sodium butyrate. Virus-containing supernatant (SN) was harvested after 42 h and 66 h post transfection, centrifuged at 1800 × *g* for 10 min at 4°C, filtered through a 0.45 µm filter [Sartorius] and frozen at -80°C. Then 42 h and 66 h supernatants were pooled and then concentrated × 25 by ultracentrifugation at 100,000 × *g* for 2 h at 4°C and resuspended in serum free IMDM [Sigma]. Aliquots were stored at -80°C.

Table 2.3 Plasmids used in transfection to create JSRV stocks carrying APOBEC3

Virus Stock	JSRV vector encoding plasmids	A3 Expression vector	pCI-Neo
No A3	pCMV2JS$_{21}$ 10 µg OR pCMVJS-ΔE-CG 7 µg pCMV JSE SP-FLAG 2 µg Envelope encoding vector 1 µg (pCAG-JSEnv or pVSV-G)		4 µg
0.25 S A3		pCI-Neo S A3 0.25 µg	3.75 µg
1 S A3		pCI-Neo S A3 1 µg	3 µg
4 S A3		pCI-Neo S A3 4 µg	
0.25 G A3		pCI-Neo G A3 0.25 µg	3.75 µg
1 G A3		pCI-Neo G A3 1 µg	3 µg
4 G A3		pCI-Neo G A3 4 µg	
0.25 C A3		pCI-Neo C A3 0.25 µg	3.75 µg
1 C A3		pCI-Neo C A3 1 µg	3 µg
4 C A3		pCI-Neo C A3 4 µg	

Table 2.3 DNA used in transfection in order to produce JSRV vectors on a T-75 flask scale.
Ten different stocks were made in each experiment (No A3-no APOBEC3, S- sheep, G- goat, C- cow; numbers represent µg of A3 encoding plasmid used during transfection of a confluent T-75 flask). For each stock 10 µg of DNA encoding viral proteins was included in the premix. In order to produce wild type JSRV, pCMV2JS$_{21}$ was used. To make JSRV-GFP three plasmids were used (pCMVJS-ΔE-CG, pCMV JSE SP-FLAG and an envelope encoding vector (pCAG-JSEnv or pVSV-G). Various A3 genes were provided as a pCI-Neo vector in three different quantities for each species homologue (0.25 µg, 1 µg or 4 µg). The total amount of DNA was adjusted by the addition of empty pCI-Neo vector. The same type of A3-containing stocks; either one of four paralogues Z1, Z2, Z3 or Z2Z3) were made in a single experiment.

2.10.3 *In vitro* infections

The CRFKovH2 cells were maintained in 10% FCS IMDM and infected in medium containing 8 μg/ml polybrene. 1×10^5 CRFKovH2 cells were plated in each well of twelve well plates on the day prior to infection. Virus was then added to the cells and incubated for 16 h. Volume of virus stock used was adjusted in order to balance the input amount of Gag on the basis of WB. Three days post-infection cells were harvested and either analysed by flow cytometry or subjected to DNA extraction. As a negative control non-infected cells and cells infected by heat inactivated virus (virus was incubated at 70°C for 20 min) were used.

2.10.4 Quantitative PCR

In order to determine the number of viral integration events, qPCR (quantitative PCR) was performed using DNA extracted from infected CRFKovH2 cells as a template.

Virus stocks used for these series of infections and heat inactivated controls were treated for 1 h at 37°C with DNAse [Ambion] (4U of enzyme per 100 μl of virus stock) and the addition of supplied 10× buffer [Ambion] in order to remove residual DNA carried over from the transfection process.

The 25 μl qPCR reaction mixture contained 2×PCR reaction mix [Applied Biosystems] and 14.8 mM $MgSO_4$. Amplification and detection of exogenous JSRV was enabled by P1 and P6 primers (50 μM) (Holland et al., 1999, Palmarini et al., 1996) and the JSRV-T-FAM probe (10 μM) (Cousens et al., 2009) (see Section 2.2.).

Initially, the DNA concentration in the samples analysed was standardised to 50 ng/μl and 200 ng (4 μl) was added to each qPCR reaction. As a negative control, water was used or DNA was extracted (see Section 2.3.11) from non-infected cells and from cells subjected to heat inactivated virus stocks. As a positive control and standard for the number of JSRV copy number used, dilutions of DNA extracted from JS7 cells, which contain a single integrated JSRV provirus per cell (DeMartini et al., 2001), were used. These were diluted in the DNA extracted from non-infected CRFKovH2 cells in order

to have the same total amount of genomic DNA in each tube (see Sections 2.3.11 and 2.4.1).
Amplification, data acquisition and data analysis were performed on a Prism SDS7000 (Applied Biosystems). Reaction conditions were 94°C for 10 min followed by 40 cycles of (95°C for 15 s, 59°C for 30 s and 60°C for 30 s).

2.10.5 Analysis of APOBEC3 induced hypermutations

CRFK cells were infected with "APOBEC3 containing" or "No APOBEC3" virus stocks. As a negative control heat-inactivated virus was used. Cells were harvested three days post-infection and DNA was purified using Qiagen Blood and Tissue DNA extraction kit (see Section 2.3.11). A 928 bp fragment of GFP was amplified using primers GFP 1164 F and GFP 1164 R (see Table 2.1). PCR products were purified using Qiagen PCR purification kit and ligated into pGEM-T Easy which enabled sequencing. The Hypermut 2.0 program [www.hiv.lanl.gov] was used to identify the mutations present in each clone.

2.10.6 Production of virus stocks containing human and mouse APOBEC

Virus stocks made in the presence of human APOBEC were prepared by transfection of 293T cells plated in a six well plate using 2.8 μg of DNA for each well, according to Section 2.4.2. The DNA used in the transfection contained 2 μg of viral vector encoding genes (see Section 1.4 μg pCMVJS-DE-CG-1164, 0.4 μg pCMV JSE SP-FLAG, 0.2 μg pCAG Env) and 0.8 μg of vector encoding APOBEC (pcDNA – human and mouse APOBEC; pCI-Neo – sheep A3-Z2Z3) or empty pCI-Neo plasmid as a negative control. The mass ratio of vector plasmid to APOBEC plasmid was similar to "4 μg stocks" (see Table 2.3).

The pcDNA3 expression vectors for human APOBEC1, human APOBEC2, huA3DE, huA3F, huA3G and murine A3 were provided by Dr. B. Matija Peterlin and Dr Yong-Hui Zheng (University of California, San Francisco USA).

Each stock was prepared using two wells of a six well dish and supernatants from duplicate wells were pooled. Virus stocks were harvested, concentrated 50 × and

stored according to Section 2.5.1 Cellular extracts from producer cells were prepared according to Section 2.5.2.

2.10.7 Western blot detection of V5-tagged human and mouse APOBEC

Western blotting for detection of human and mouse V5-tagged APOBEC proteins was performed according to Section 2.6. The total volume of 15 µl of concentrated stock or cellular extract per well was utilised. Anti-V5 HRP antibodies [Invitrogen] diluted 1:2000 were used for detection of human and mouse V5-tagged APOBEC proteins.

2.10.8 Detection of APOBEC3 expression in sheep

Detection of A3 expression in vivo has been performed by RT-PCR, lung immunohistochemistry and western blotting of concentrated lung fluid.

Origin of anti sheep A3-Z2 and A3-Z3 antibodies

Rabbit polyclonal antibodies to ovine A3-Z2 and A3-Z3 were provided by David Griffiths. These antibodies were generated by subcloning the coding sequence of each gene separately into pET-DUET (a bacterial expression plasmid; Merck) in-frame with an N-terminal polyhistidine tag. Expression of each protein in *E.Coli* was confirmed by IPTG induction prior to submitting purified plasmid DNA to a commercial provider (Proteintech) for large scale protein expression and immunisation of rabbits. Post-immune sera were affinity purified for use in western blots (Proteintech).

2.10.8.1 Collection of tissue samples

Tissue samples were collected from sheep post mortem. Freshly dissected tissue pieces were put into tubes and snap frozen in liquid nitrogen before storage at -80°C. Samples from grossly unaffected normal lung, OPA affected lung, spleen, liver, kidney, muscle and lymph node were collected.

2.10.8.2 RT-PCR amplification of APOBEC3 and TRIM5 using RNA from various tissues

RT-PCR was performed in order to determine if A3 and T5 were expressed in a panel of different sheep tissues. Template RNA extracted from sheep lung, liver, intestine, kidney, lymph node, muscle, spleen and OPA tumour was used (see Section 2.3.11). As a positive control RNA from the CPT-Tert cell line was used. The primers and RT-PCR programs utilised were identical to the ones used in RT-PCR for the first step cloning (see Section 2.10.1.1).

2.10.8.3 Immunohistochemistry

Processing cell pellets and embedding in wax

In order to incorporate cells into wax blocks, they were initially dispersed by trypsin and pelleted by centrifugation at 430 × *g* for 5 min, then fixed by incubation in 1 ml of 10% buffered formalin. Afterwards, cells were pelleted by centrifugation and resuspended in PBS, then the washing step was repeated. Finally the cells were suspended in a small volume of 5% gelatin PBS solution. After solidification of gelatin the pellet was left in 80% ethanol overnight in order to dehydrate it. On the next day the gelatin pellet was placed in the processor on the overnight cycle and afterwards the pellet was embedded in wax.

Immunohistochemistry method

Initially sections were cut at 4 μm and mounted onto SUPERFROST®PLUS slides [Thermo Scientific] then dried overnight at 37°C. The wax was removed from sections using in xylene by two subsequent 5 min washes. Slides were rinsed in 100% ethanol for 2 min then 95% ethanol for 2 min, then placed in 3% hydrogen peroxide methanol for 20 min at room temperature and stirred in order to remove endogenous peroxidase. Slides were washed using running tap water for 5 min. Slides were placed in a metal rack in a 2 litre beaker containing antigen retrieval buffer (citric acid in one litre water add approx 25 ml of 1 M NaOH to pH 6**)** autoclave at 121°C for 10 min. After cooling to 50°C, slides were washed in water for 5 min. Slides were loaded into Sequenza chambers and washed in 0.05% Tween20 diluted in PBS.

In order to block any non-specific binding sites, 100 µl of 25% normal goat serum (Vector Laboratories S-1000) was applied for 30 min at room temperature. Afterwards applied primary antibody (1:10000 anti-A3-Z2; 1:20000 anti-A3-Z3 or pre-immune sera as a negative control) and incubated overnight at 4°C (origin of antibodies is shown in Section 2.10.8). On the next day slides were washed three times using 0.05% Tween20 diluted in PBS. Then 100 µl of secondary goat anti-rabbit HRP (Envision - Dako), was applied for 30 min at room temperature. Then the slides were washed three times using 0.05% Tween20 diluted in PBS, and applied 100 µl of DAB (3,3′-Diaminobenzidine) solution, prepared according to the manufacturer's instructions. The slides were rinsed with water, removed from the Sequenza machine then washed in running water. Nuclei were stained with haematoxylin [Cellpath] for 2 min, washed in water for 2 min, and then blued using STWS (Scots tap water substitute – 3.5 g sodium bicarbonate, 20 g magnesium sulphate, 1 litre water). Afterwards the slides were washed in running tap water for 2 min and dehydrated through graded ethanol (70%, 95%, 100%) and rinsed in xylene twice. Finally coverslips were mounted on the sections using Thermo Shandon mountant [Thermo Scientific].

2.10.9 Reverse transcriptase assay

The Colorimetric Reverse Transcriptase Assay [Roche] was utilised to analyse the activity of RT present in virus stocks. The protocol was adjusted to test concentrated JSRV supernatant in each well. Initially, instead of suspending the viral pellet directly in lysis buffer, 5 µl of each of concentrated virus stock was mixed with 35 µl of the provided lysis buffer. Optionally the volume of virus stock used was adjusted in order to balance the input amount of Gag on the basis of WB. The following steps were performed according to the manufacturer's instructions, utilising the provided poly-A as RNA template and allowing 3 h incubation for the reverse transcription step.

Two-fold dilutions of the provided HIV-1 RT were employed in order to plot a standard curve, ranging from 1 ng to 15.6 pg per well. As a negative control 5 µl of serum free IMDM medium was used. Each virus stock was tested in triplicate. The interpretation of RT content in the virus stocks was based on the standard curve, where the absorbance of tested samples was within the range of standards. The RT activity values of A3 containing stocks, were compared to reference "no A3" virus stocks. The

student two-tailed t-test method with unequal variance, was used to verify the significance of the results. Due to a multiple comparison, obtained p-values were corrected using the Bonferroni method.

2.11 Materials and methods regarding TRIM5 experiments

Initially, T5 encoding ORFs were cloned into retroviral vector plasmids (see Section 2.11.1). Afterwards, retroviral mediated transduction of CRFKovH2 cells, followed by their antibiotic selection enabled the creation of cell lines which stably express various T5 homologues. Expression of T5 was confirmed by flow cytometric analysis of anti-HA labelled cells. The impact of T5 on HIV-1 and JSRV replication was performed according to Section 2.11.3.

2.11.1 Cloning of TRIM5 encoding sequences.

Sheep and goat T5 sequences were isolated by RT-PCR, cloned into pGEM-T Easy vectors and after selection of representative clones by sequencing, they were subsequently reamplified by a high fidelity PCR and cloned into pLNCX-2 vectors. Two bovine T5 coding sequences in pLPCX were kindly provided by Dr Joseph Sodroski (Dana-Farber Cancer Institute, USA).

The pLPCX vectors encoding human and rhesus macaque T5α were obtained through the AIDS Reagent Program, Division of AIDS, NIAID, NIH - originally from Dr Joseph Sodroski, Dana-Farber Cancer Institute, USA). Both pLNCX-2 and pLPCX vectors with cloned T5 were further modified by insertion of an IRES-Hyg cassette in order to enhance their transduction ability (see Section 2.11.1.4).

2.11.1.1 Isolation of sheep and goat TRIM5 sequences by RT-PCR

Primers utilised in RT-PCR were designed to consensus fragments of sheep and cow sequences located external to the T5 reading frame (forward primer TRIM-F1 and reverse primer TRIM-R1 sequences are shown in Table 2.1).

RNA purified (Section 2.3.10) from goat PBMCs or sheep cell line CPT-Tert (Section 2.7.1) was used as a template for amplification of sheep and goat *T5* genes. Superscript 2 one-step platinium Taq [Invitrogen] was used for this reaction (see Section 2.3.12). The RT-PCR program used was 50°C 30 min, 94°C 30 s, 40 cycles (94°C 15 s, 55°C or 60°C 30 s, 72°C 1 min), 72°C 10 min.

2.11.1.2 Cloning of sheep and goat TRIM5 ORFs into pGEM-T Easy

RT-PCR products were gel purified (see Section 2.3.7) and cloned into pGEM-T Easy (see Section 2.1.1), which enabled sequencing using SP6 and T-7 primers in order to identify desired clones.

2.11.1.3 Cloning of sheep and goat TRIM5 ORFs into retroviral vectors

T5 ORFs were reamplified from selected plasmid clones by high fidelity PCR (see Section 2.3.13). Sequence similarity at the 5' and 3' ends of the goat and sheep T5 ORF allowed further cloning using the same set of primers (forward primer Oa-TRIM-F-BCL and reverse primer BtOa-TRIM-HA-R sequences are shown in Table 2.1). The forward primer inserted a Kozak consensus sequence and BclI restriction site upstream the T5 start codon. The reverse primer inserted the HA tag and SalI site encoding sequence to the 3' end of T5.

High fidelity KOD polymerase was used in this reaction (see Section 2.3.13). The PCR program was 94°C 2 min, 25 cycles (94°C 15 s, 55 and 60°C 30 s, 72°C 1 min), 72°C 10 min.

The addition of BclI and SalI restriction sites enabled the insertion of reamplified, digested and gel purified T5 ORF into BglII and SalI digested pLNCX-2 expression vector (See Table 2.1). The *T5* and HA-tag sequences present in the selected recombinant pLNCX-2 plasmids were verified by sequencing.

2.11.1.4 Addition of IRES-Hyg cassette to TRIM5 carrying pLNCX-2 or pLPCX vector.

Insertion of the hygromycin B phosphotransferase (hygromycin resistance gene) and a IRES Internal Ribosome Entry Site (derived from encephalomyocarditis virus) located downstream of T5-HA ORF enabled the expression of both genes from the same transcript.

High fidelity PCR using KOD polymerase (see Section 2.3.13) amplified an IRES and hygromycin cassette from plasmid pIREShyg3 (see Table 2.1). SalI and XhoI restriction sites were added during this reaction. The PCR program was 94°C 2 min, 25 cycles (94°C 15 s, 55°C and 60°C 30 s, 72°C 1 min) 72°C 10 min.

IRES-Hyg PCR products were gel purified and digested with SalI and XhoI which enabled cloning into pLNCX-2 carrying T5 ORF (linearised with SalI, treated with alkaline phosphatase and gel purified). Similarly the IRES-Hyg cassette was cloned into pLNCX-2 with the *LacZ* gene (provided by David Griffiths).

All ruminant T5 ORFs and IRES-Hyg cassette junctions were sequenced in both directions to confirm their correctness using primers TRIM5-F2, TRIM5-F3, TRIM5-R2, TRIM5-R6, LN-F, CX-R (see Table 2.1). Human and rhesus monkey T5 carrying plasmids were verified by LN-F and CX-R primers (see Table 2.1).

2.11.2 Creation of cell lines stably expressing TRIM5α

Cell lines that stably express various T5 proteins were generated in order to analyse the impact of those proteins on retroviral replication. Initially, MLV vectors were prepared (see Section 2.11.2.1) in order to transduce CRFKovH2 cells (see Section 2.11.2.2). Antibiotic selection enabled the creation of cell lines expressing various T5 (see Section 2.11.2.2), which was confirmed by RT-PCR (see Section 2.11.2.4) and flow cytometric analysis of anti-HA labelled cells (see Section 2.11.2.5). β-galactosidase activity assay was performed to verify the transduction process (see Section 2.11.2.3).

2.11.2.1 Production of MLV retroviral vectors for TRIM5α experiments

Murine leukaemia virus based vectors were made for efficient transduction of mammalian cells. Confluent 293T cells plated in six well plates were transfected (see Section 2.4.2) using 1 µg of DNA and 3 µl of Fugene HD per well. The DNA used for each transfection contained 0.3 µg pHIT60 (encoding MLV structural proteins) (Soneoka et al., 1995), 0.2 µg pVSV-G (envelope), 0.5 µg pLNCX-IH or pLPCX-IH (vectors containing MLV packaging signal, *T5* or β-galactosidase encoding sequences, IRES-Hyg cassette see Table 2.1). MLV vectors carrying the *T5* or *LacZ* gene were harvested on the second and third day post transfection, then filtered (0.45 µm), aliquoted and frozen at -80ºC.

2.11.2.2 Transduction of CRFKovH2 cells in order to stably express TRIM5

CRFKovH2 cells (see Section 2.4.1) were plated on the day before infection in a six well plate at a density of 10^6 cells per well. Cells were infected by 3 h exposure to 0.5 ml of MLV vector carrying various T5 or *LacZ* coding sequences.

Selection of cells was based on a hygromycin resistance gene present in transduced cells. Antibiotic selection of T5α transduced cells was applied three days post-infection. Non-transduced CRFKovH2 (see Section 2.4.1) were put under antibiotic selection in parallel. Hygromycin [Invitrogen] 500 µg/ml enabled the elimination of all non-transduced cells within two weeks. Successful selection was initially confirmed by the death of non-transduced cells after two weeks and expression of β-galactosidase in *LacZ* transduced cells.

2.11.2.3 Beta-galactosidase staining of transduced cells

β-galactosidase staining was used in order to detect transduction of cells and verify successful stable expression of the *LacZ* transgene after antibiotic selection. The medium was removed and cells were washed once with PBS. The cells were fixed for 15 min using 0.5% glutaraldehyde [BDH] dissolved in PBS, then washed once with PBS before adding X-Gal substrate (5 mM potassium ferricyanide, 5 mM potassium

ferrocyanide, 2 mM magnesium chloride, 0.01% sodium deoxycholate, 0.02% NP40, 2% DMF and 1 mg/ml X-gal [Promega]), and incubating at 37 ˚C for 1-4 h. After the colour had developed, the substrate was removed and PBS was added to wells.

2.11.2.4 Immunolabelling of TRIM5α HA expressing cells

The percentage of T5-expressing cells was determined by flow cytometry of intracellularly anti-HA labelled cells. Cells were dispersed by trypsin and diluted to 5×10^5 cells in PBS containing 5% of heat inactivated fetal calf serum. Then cells were centrifuged at 430 × *g* for 1 min and washed in PBS, before fixing in 1% PFA/PBS for 10 min at room temperature. Cells were again washed with PBS and suspended overnight at 4^{o}C in 1 ml of permeabilisation and block buffer, which was a 0.2% saponin [Sigma] solution in PBS and 20% heat inactivated goat serum [Moredun Research Institute].

On the next day cells were pelleted at 430 × *g* for 1 min and then resuspended in 200 µl of permeabilisation buffer, which is 0.2% saponin [Sigma] solution in PBS, containing primary antibody 1:1000 (Covance anti-HA) and incubated for 1 h at room temperature. The cells were then washed twice using permeabilisation buffer and incubated in FTIC-labelled secondary goat anti mouse antibody 1:1000 [Alexa Fluor] for 1 h at room temperature. Afterwards, cells were washed twice using permeabilisation buffer, and once using PBS. The cells were fixed in 1% PFA for 10 min at room temperature, then washed in PBS and kept at 4^{o}C until flow cytometric analysis. As a negative control, cells were incubated only with secondary antibody and also *LacZ* transduced CRFKovH2 was tested using the full-length protocol.

2.11.3 HIV-1-GFP production

HIV-1 GFP VSV-G pseudotyped vector was made in order to verify its restriction in cells stably expressing cow and rhesus macaque T5α. Confluent T75 flasks of 293T cells (see Section 2.4.1) were transiently transfected using 30 µl Fugene and 10 µg of DNA (see Section 2.4.2), which contained 3 µg pMDLg/pRRE (Dull et al., 1998), 4.5 µg pCS-CG; 1 µg pCNCrev and 1.5 µg pVSV-G. After 16 h, transfection

complexes were removed and the media was replaced. Virus containing supernatant was harvested 48 h and 72 h after transfection, cellular debris was removed by centrifugation for 10 min at 1800 × *g* at 4°C and filtered through a 0.45 µm filter [Sartorius]. Then virus was aliquoted and frozen at -80°C.

Chapter 3 - Impact of ruminant APOBEC3 on JSRV replication

3.1 Introduction

The A3 family of proteins has been identified (Harris and Liddament, 2004) as a species specificity determinant for a number of viral infections (Holmes et al., 2007b, Mariani et al., 2003) (see Section 1.8.1). Due to its viral genome editing potential, this restriction factor has a significant impact on the evolution rate of many viruses (Jern et al., 2009) and retroelements (Anwar et al., 2013).

The activity of ruminant A3 proteins against various retroviruses has been previously studied by a few groups (Dorrschuck et al., 2011, Jonsson et al., 2006, LaRue et al., 2008). However, this project is the first study of the effect caused by ruminant A3 on JSRV replication and its relevance to OPA epidemiology. JSRV restriction mediated by ruminant A3 was analysed and the mechanism of this process was investigated according to the plan of experiments shown in Fig. 3.1.

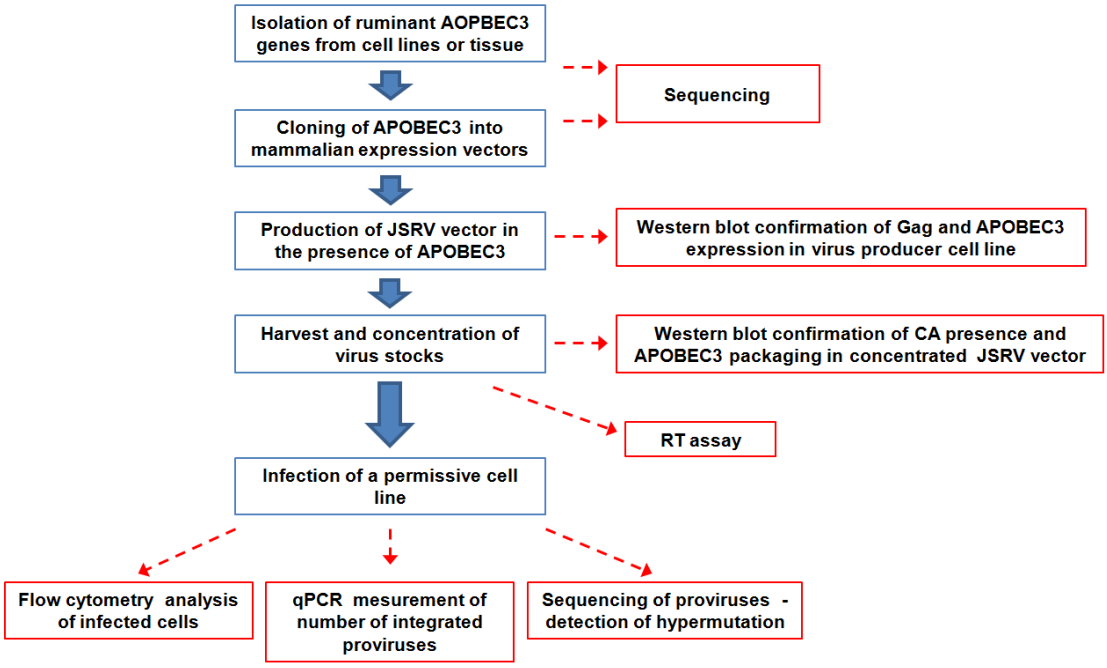

Fig. 3.1 The plan of investigation of the effect of ruminant APOBEC3 on JSRV replication *in vitro*.
Blue boxes: assays; Red boxes: results

3.2 Results

Initially, ruminant A3 genes were cloned (see Section 3.2.1) and their activity was investigated *in vitro* (see Sections 3.2.2 to 3.2.7). The experiments on the *in vivo* significance of A3 during JSRV infection are described in Sections 3.2.8; 3.2.8 and 3.3.4.

3.2.1 Cloning of ruminant APOBEC3 genes

As a first step towards studying the activity of ruminant A3 against JSRV, each A3 coding region was isolated by RT-PCR and subsequently cloned into a mammalian expression vector. This process is shown in Fig. 3.2.

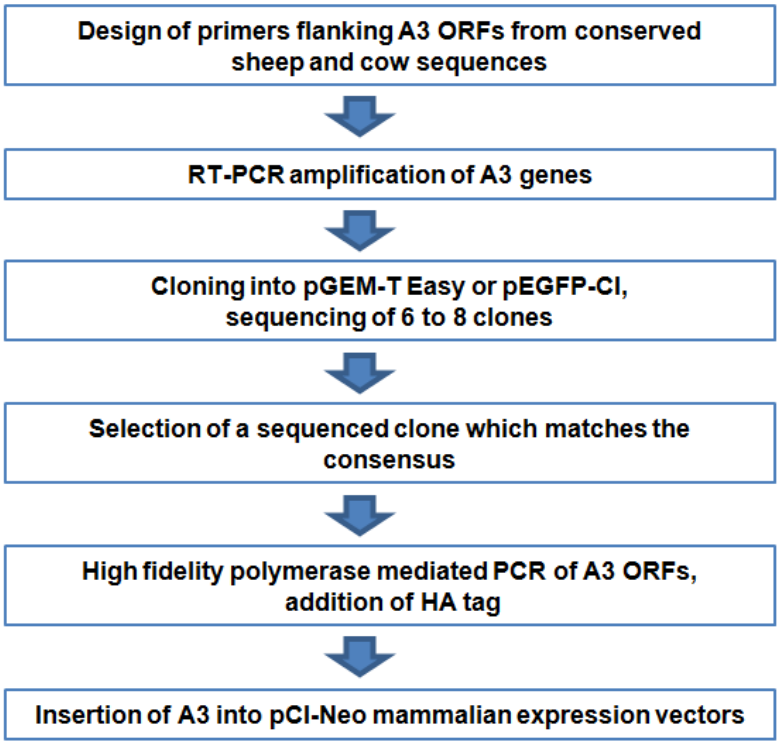

Fig. 3.2 Cloning strategy of APOBEC3 Z2 and Z2Z3 coding regions
Ruminant A3-Z3 and cow A3-Z2 were isolated using a forward primer overlapping the start codon, while external primers were utilised for other isolated A3 proteins, A3-Z1 coding sequences were cloned into pEGFP-CI instead of pGEM-T Easy prior to cloning into pCI-Neo. A3-Z3 open reading frames were reamplified from pGEM-T Easy and then cloned to pEGFP-C1 prior to cloning into pCI-Neo mammalian expression vectors.

3.2.1.1 APOBEC3 primer design

Isolation and cloning of ruminant A3 genes was based on available sequences of cow and sheep A3 that had been published previously (LaRue et al., 2008). Primers were designed based on the nucleotide sequence alignment of sheep and cow A3 sequences shown in Table 3.1.

Table 3.1 Published ruminant A3 gene sequences

APOBEC3	gene ID number
Sheep A3-Z1	GI 238637212
Sheep A3-Z2	GI 238637214
Sheep A3-Z3	GI 238637216
Sheep A3-Z2Z3	GI 199945618
Cow A3-Z1	GI 255652988
Cow A3-Z2	GI 197359096
Cow A3-Z3	GI 197359098
Cow A3-Z2Z3	GI 118150803

Where possible, consensus primers (see Section 2.2) were designed to sequences located external to coding regions. The consensus primers were used to amplify sheep and cow A3 coding sequences A3-Z2 (see Fig. 3.3) and A3-Z2Z3 (see Fig. 3.4). RNA purified from the cell lines CPT-Tert (sheep) and BOMAC (cow) was used as a template for RT-PCR amplification of ruminant A3-Z2, A3-Z3 and A3-Z2Z3 coding regions (see Section 2.3.12) (see Section 2.10.1).

Sheep and cow A3-Z3 were amplified using forward primer A3Z3 OA-BT ExpF and the external reverse primer A3Z2Z3-R. Because of a lack of conserved sequences in the A3-Z3 transcript upstream of the start codon, a primer overlapping the start codon was used (see Fig. 3.5). Despite the nucleotide sequence polymorphism between those two homologues downstream of the start codon, the N-terminal protein sequence is conserved among cow and sheep.

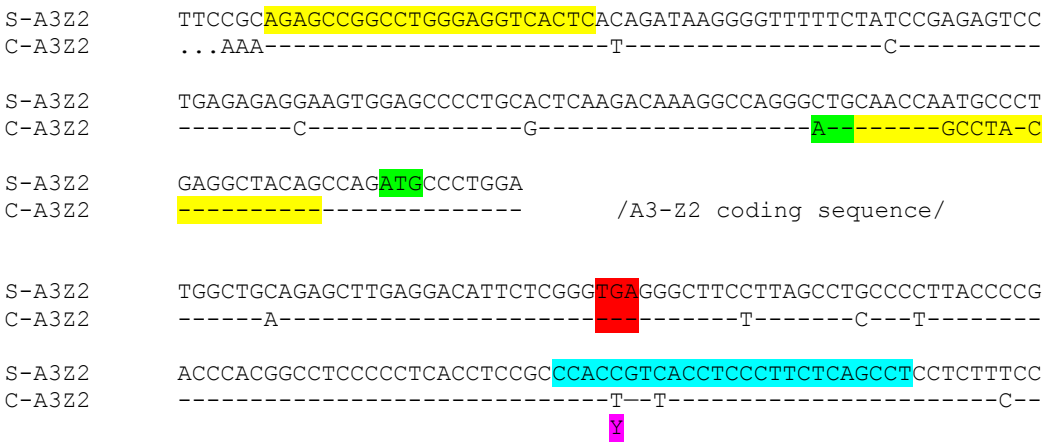

Fig. 3.3 Alignment of sheep and cow sequences located external to the A3-Z2 reading frame

Forward primers A3Z2F-Ov and A3Z2F-Bt were designed to match sheep (S- GI 238637214) or cow (C- GI 197359096) mRNA sequence respectively (yellow). Two primers were necessary due to different locations of the start codons (green). The reverse primer is complementary to a consensus ruminant sequence (blue) located downstream of the stop codons (red). The highlighted residue (Y) indicates a degenerate base in the primer in order to permit the amplification of both genes. The majority of the ruminant A3-Z2 coding region is not shown. Dashes indicate sites where cow sequence is identical to sheep; polymorphic residues are highlighted by letters in the cow sequence; dots indicate gaps in the alignment.

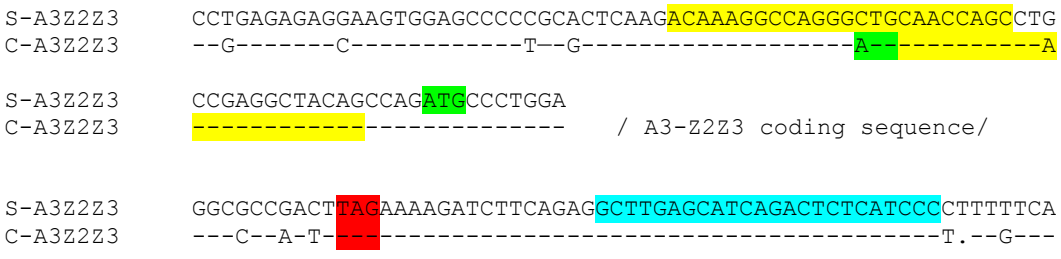

Fig. 3.4 Alignment of sheep and cow sequences located external to the A3-Z2Z3 reading frame

Forward primers A3Z2F-Ov or A3Z2-Bt were designed to match sheep (S- GI 199945618) or cow (C- GI 118150803) mRNA sequence respectively (yellow). Two primers were necessary due to the different location of the start codons (green). The reverse primer is complementary to consensus region (blue) located downstream of the stop codon (red). The majority of the A3-Z2Z3 coding region is not shown. Dashes indicate sites where cow sequence is identical to sheep; polymorphic residues are highlighted by letters in cow sequence; dots indicate gaps in alignment.

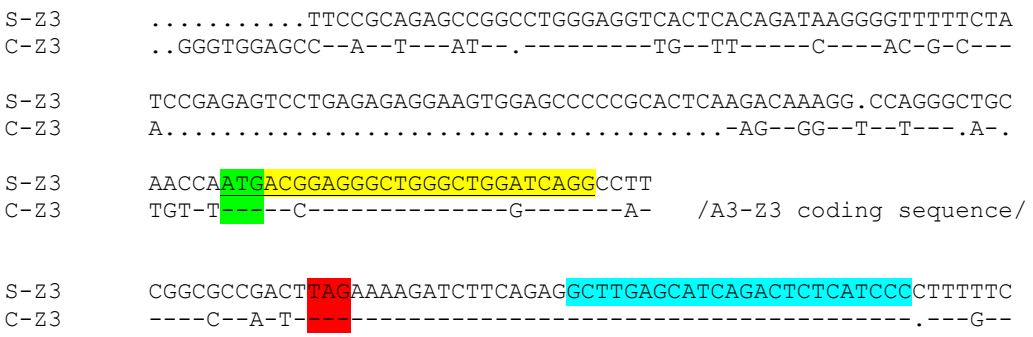

Fig. 3.5 Alignment of sheep and cow sequences located external to A3-Z3 reading frame

The forward primer A3Z3-F was designed to bind a conserved sequence in the sheep (S- GI 238637216) and cow (C- GI 197359098) mRNAs (yellow and green underlined) overlapping the start codon (green). The reverse primer A3-Z3-R is complementary to a conserved ruminant sequence (blue) located downstream of the stop codons (red). The majority of ruminant A3-Z3 coding region is not shown. Dashes indicate sites where cow sequence is identical to sheep; polymorphic residues are highlighted by letters in cow sequence; dots indicate gaps in alignment.

Cloning of sheep and cow A3-Z1 was more difficult than Z2, Z3 and Z2Z3. There were a number of unsuccessful RT-PCR amplifications using RNA extracted from sheep cell line CPT-Tert sheep as well as the cow cell lines: MDBK, BOMAC (see Section 2.4.1). Similarly there was a lack of A3-Z1 amplification when RNA extracted from a panel of sheep tissues including lung, muscle, spleen, liver, testicle, kidney, OPA tumour and mediastinal lymph node was used (data not shown). Additionally, RNA extracted from cow lung was tested, but still failed to yield a positive amplification product for A3-Z1. Neither utilisation of external primers nor primers designed for cloning into pCI-Neo failed to amplify A3-Z1. However, other A3 paralogues were successfully amplification of from RNA, extracted from these tissues.

Referring to submitted sequence of sheep Z1 in GenBank, it was identified in EST library that had been prepared from small intestine. Subsequently, cow and sheep intestine RNA was obtained (Craig Watkins, Moredun Research Institute) and A3-Z1 was successfully amplified from both by David Griffiths (Moredun Research Institute).

Cow and sheep A3-Z1 were amplified by RT-PCR utilising consensus external primers (A3Z1-F, A3Z1-R) to ruminant A3-Z1 ORF (see Fig. 3.6).

```
S-Z1      -CTCCTGCCGCTTGAACAACTTCAAGGAGGAGGCCACAGGCTGTGACTGAGCATAGCATC
C-Z1      AGG-----------------------------------..C-----------C----

S-Z1      AGAGGACTCGGAGCCAGGGACGACGCCTGATGGATGAA
C-Z1      ----------------------A----------C--- /A3-Z1 coding sequence/

S-Z1      AACTGAAGGACGGACGCCAGCCTCTCTA.AGATGGCAGGAGGCCTCTATTCAACAGCAGC
C-Z1      ---------T----------------A---A--------A----------------A

S-Z1      ACAAAACACCTTCTTTCAAGAAATGTAAACATGCCATATGCTACTGTCTCCAGACTGATC
C-Z1      ---------T-----------G----------A---T--------------------T
                                                                    Y

S-Z1      CAAACAGAC
C-Z1      ---------
```

Fig. 3.6 Alignment of sheep and cow sequences located external to A3-Z1 reading frame

The forward primer A3Z1-F was designed to consensus sheep (S- GI:238637212) and cow (C- GI:255652988) sequence (yellow) upstream the start codons (green). The reverse primer is complementary to consensus ruminant sequence (blue) located downstream of the stop codons (red). The highlighted residue (Y) indicates a degenerate base in the primer in order to enhance the amplification of both genes. The majority of the ruminant A3-Z1 gene is not shown. Dashes indicate sites where cow sequence is identical to sheep; polymorphic residues are highlighted by letters in cow sequence; dots indicate gaps in alignment.

The sheep and cow A3-Z1HA sequence was reamplified from purified RT-PCR product using high fidelity KOD polymerase. The PCR product was digested and inserted into SalI and NotI digested pEGFP-FLAG (see Section 2.1.16 and 2.10.1) for expression in mammalian cells.

3.2.1.2 Cloning of goat APOBEC3 genes

Goat A3 gene sequences have not been published previously but the cloning strategy for goat A3 genes was similar to the sheep and cow homologues. Therefore, external primers derived from the sheep and cow sequences flanking ORFs were utilised for isolation of goat A3.

This approach was successfully used to clone goat A3-Z2, A3-Z3 and A3-Z2Z3 from RNA from a goat cell line (TIGEF). However, it was not possible to clone goat A3-Z1 from TIGEFs and goat intestine tissue was not available for study. Therefore, goat A3-Z1 was not analysed in this project.

In order to eliminate the uncertainty connected with cloning A3-Z3 caused by the utilisation of a forward primer that overlaps the start codon (see Fig. 3.5), the goat A3-Z3 locus was investigated at the genome level. DNA extracted from the goat cell line TIGEF was used as a template for PCR. Consensus primers were designed based on sheep and cow sequences, located upstream of the A3-Z3 start codon (Z3xtF2) and downstream (Z3xtR1, Z3xtR2) (see Fig. 3.7). PCR products were cloned into pGEM-T Easy and sequenced. Moreover, recently some caprine genome sequence has become publically available (GenBank Accession: LOC102184324). This confirms that an authentic goat A3-Z3 was used in this study.

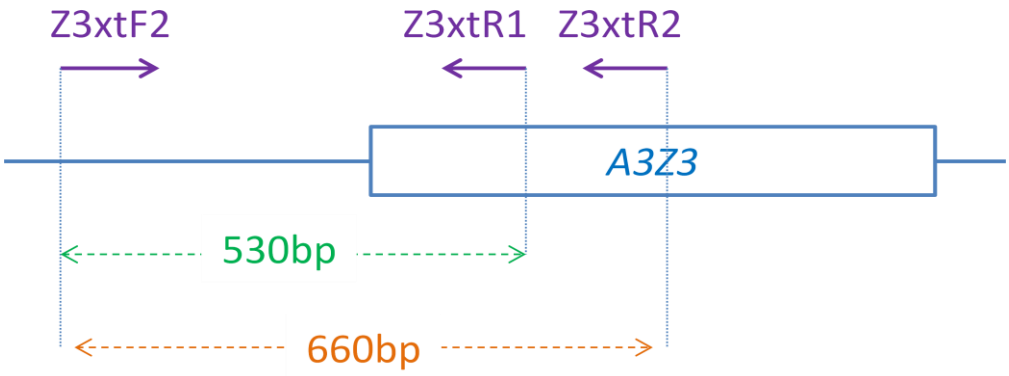

Fig. 3.7 Investigation of goat 5' A3-Z3 locus
Locations of primers used are indicated in violet. They were used to amplify two sequences overlapping the 5' region of the goat A3-Z3 coding sequence (green and orange).

Amplified genes were cloned into pGEM-T Easy (see Section 2.1.1) and several clones of each PCR product were sequenced in order to avoid the selection of a clone with RT-PCR errors. More goat A3 clones were sequenced than sheep and cow, because the goat sequences had not been published at the time. For each A3 protein, a clone was selected that matched the consensus of all sequenced clones.

The A3 clones selected for expression analysis all had amino acid sequences identical to the previously published sequences (LaRue et al., 2008) with the exception of four mismatches present in cow A3-Z1 and one sheep A3-Z1 residue (14^{th}) was R in this study but G in the published sequence (see Fig. 3.8).

All the analysed ruminant A3 homologues share high sequence similarity, however the newly identified goat sequences were more similar to their sheep than cow homologues, which reflects the closer relatedness of sheep and goats (see Fig. 3.8 to 3.11).

A3-Z1

Fig. 3.8 Alignment of sheep and cow A3-Z1 protein sequences
The sheep (S- GI 238637212) and cow (C- GI 255652988) A3-Z1 have typical features which include the presence of conserved motifs (underlined; bold-conserved residues are discussed in section 1.5.1.2) (LaRue et al., 2009). A mismatch to the published sheep sequence is highlighted in pink, differences to published cow sequence are highlighted in red (published sequence amino acids are displayed above-sheep, or below – cow GI 255652988). The motif which includes isoleusine after arginine is unique to all Z1 domains (highlighted in green) (LaRue et al., 2009). Dashes indicate sites where cow sequence is identical to sheep; polymorphic residues are highlighted by letters in cow sequence; dots indicate gaps in alignment.

A3-Z2

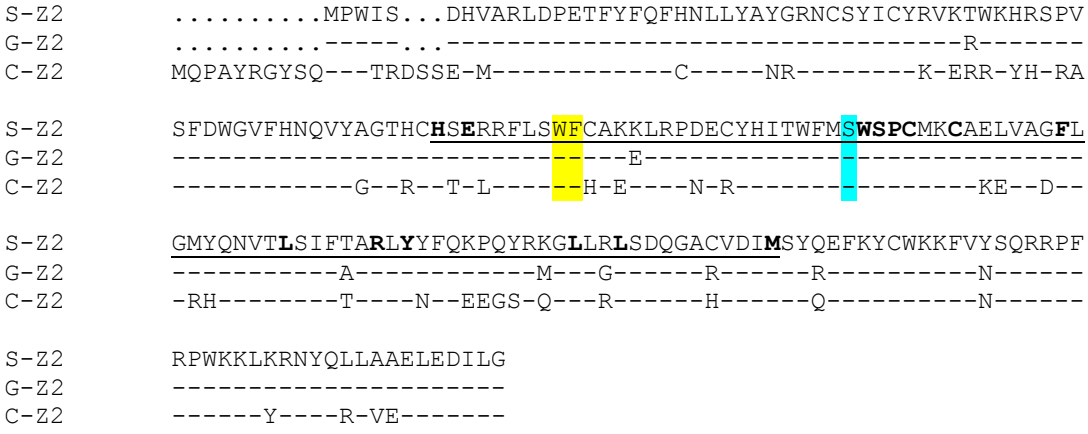

Fig. 3.9 Alignment of sheep, goat and cow A3-Z2 protein sequences
The sheep (S-), cow (C-) and goat (G-) A3s have typical features which include the presence of conserved motifs (underlined; bold-conserved residues are discussed in section 1.5.1.2) (LaRue et al., 2009). There is a WF tryptophan-phenylalanine motif five residues after glutamate in the Z2 domain and a zinc-binding motif SWSPC$x_{2\text{-}4}$C, where "x" could be any amino acid. Dashes indicate sites where goat or cow sequence is identical to sheep; polymorphic residues are highlighted by letters in the cow sequence; dots indicate gaps in alignment.

A3-Z3

```
S-Z3        MTEGWAGSGLPGRGDCVWTPQTRNTMNLLRETLFKQQFGNQPRVPPPYYRRKTYLCYQLK
G-Z3        ------------Q-----------------------------------------------
C-Z3        ---------H--Q-A-----G----------V-------------A--------------

S-Z3        ELDDLMLDKGCFRNKKQRHAEIRFIDKINSLNLNPSQSYKIICYITWSPCPNCASELVDF
G-Z3        Q----T---------R-------------------------------------------
C-Z3        QRN--T--R------R---------------D-------------------N---N-

S-Z3        ITRNDHLNLQIFASRLYFHWIKPFCRGLQQLQKAGISVAVMTHTEFEDCWEQFVDNQLRP
G-Z3        ------------------------WK---K----------T-------------------
C-Z3        ----N--K-E------------S-KM---D--N-------------------------S--

S-Z3        FQPWDKLEQYSASIRRRLQRILTAPT
G-Z3        --------------------------
C-Z3        --------------------------
```

Fig. 3.10 Alignment of sheep, goat and cow A3-Z3 protein sequences
The sheep (S-), cow (C-) and goat (G-) A3s have typical features which include the presence of conserved motifs (underlined; bold-conserved residues are discussed in section 1.5.1.2) (LaRue et al., 2009). There is a zinc-binding motif TWSPC$x_{2\text{-}4}$C characteristic of the Z3 domain (bold and underlined), where "x" could be any amino acid. Dashes indicate sites where goat or cow sequence is identical to sheep; polymorphic residues are highlighted by letters in cow sequence; dots indicate gaps in alignment.

The sequences of cloned ruminant A3 proteins were identical to published ones with the exception of one residue of sheep A3-Z1 and four residues in cow A3-Z1. Therefore, it makes them reliable for comparison to previously published studies.

A3-Z2Z3

```
S-Z2Z3    ..........MPWIS...DHVARLDPETFYFQFHNLLYAYGRNCSYICYRVKTWKHRSPV
G-Z2Z3    ..........-----...---------------------------------R-------
C-Z2Z3    MQPAYRGYSQ---TRDSSE-M------------C-----NR--------K-ERR-YH-RA

S-Z2Z3    SFDWGVFHNQVYAGTHCHSERRFLSWFCAKKLRPDECYHITWFMSWSPCMKCAELVAGFL
G-Z2Z3    ------------------------------E----------------------------
C-Z2Z3    ------------G--R--T-L------H-E----N-R---------------KE--D--

S-Z2Z3    GMYQNVTLSIFTARLYYFQKPQYRKGLLRLSDQGACVDIMSYQEFKYCWKKFVYSQRRPF
G-Z2Z3    -----------A------------M---G------R------R-----------------
C-Z2Z3    -RH---------S---K--EEGS-Q----------H-----------------------

S-Z2Z3    RPWKKLKRNYQLLAAELEDILGNTMNLLRETLFKQQFGNQPRVPPPYYRRKTYLCYQLKE
G-Z2Z3    ------------------------------------------------------------Q
C-Z2Z3    ------D----R-VE---------------V-------------A--------------Q

S-Z2Z3    LDDLMLDKGCFRNKKQRHAEIRFIDKINSLNLNPSQSYKIICYITWSPCPNCASELVDFI
G-Z2Z3    ----T---------R-----------------------------------------------
C-Z2Z3    RN--T--R----------------------D----------------------N---N--

S-Z2Z3    TRNDHLNLQIFASRLYFHWIKPFCRGLQQLQKAGISVAVMTHTEFEDCWEQFVDNQLRPF
G-Z2Z3    ----------------------WK---K-----------------------------
C-Z2Z3    ---N--K-E------------S-KM---D--N-----------------------S---

S-Z2Z3    QPWDKLEQYSASIRRRLQRILTAPT
G-Z2Z3    -------------------------
C-Z2Z3    ------------------------I
```

Fig. 3.11 Alignment of sheep, goat and cow A3-Z2Z3 protein sequences
Residues different to sheep sequence (top) are displayed with letters; dashes indicate consensus residues; dots were used to highlight gaps in alignment. The sheep (S-), cow (C-) and goat (G-) A3s have typical features which include the presence of conserved motifs (underlined; bold-conserved residues are discussed in section 1.5.1.2) (LaRue et al., 2009). There is a WF tryptophan-phenylalanine motif five residues after glutamate in the Z2 domain and a zinc-binding motif SWSPC$x_{2\text{-}4}$C and a zinc-binding motif TWSPC$x_{2\text{-}4}$C characteristic for the Z3 domain, where "x" could be any amino acid. Dashes indicate sites where goat or cow sequence is identical to sheep; polymorphic residues are highlighted by letters in cow sequence; dots indicate gaps in alignment.

3.2.1.3 Cloning of APOBEC3 genes into mammalian expression vectors

In order to perform *in vitro* experiments, ruminant A3 genes were cloned into the mammalian expression vector pCI-Neo. The desired A3 pGEM-T Easy or pEGFP-CI (A3-Z1) clones were reamplified by a high fidelity PCR (see Section 2.3.13). When the similarity of ruminant A3 proteins allowed, then the same pair of primers was used for amplification of each A3 homologue. However, in some cases the protein sequence at the 5' or 3' end varied among different species and then species specific primers

were utilised. For example, the cow A3-Z2 domain has 10 more amino acids at the N-terminus and there is a polymorphism present in either C- or N- end of the A3-Z1 and A3-Z2 protein.

Each forward primer for expression inserted a Kozak consensus sequence (ACCGCC) (Kozak, 1987) upstream of the start codon and a haemagluttinin tag was added to the N-terminus of the sequence by the reverse primers. The primers used in those reactions contained restriction sites, which enabled cloning into pCI-Neo (see Section 2.1; 2.2.2.; 2.10). Sheep and cow A3-Z1 were cloned into pEGFP-CI by replacing the GFP ORF (see Section 2.10.1) prior to subsequent cloning into pCI-Neo.

3.2.2 JSRV packages ruminant APOBEC3s *in vitro*

The antiviral activity of A3 proteins requires their expression in virus producing cells, where encapsidation occurs during virus assembly (Harris and Liddament, 2004). To determine whether JSRV encapsidates ruminant A3 proteins, they were coexpressed with plasmids encoding JSRV in 293T cells (see Section 2.10.2.2). Three different amounts of each A3 expressing plasmid were tested in these experiments (see Table 2.3). Currently, there is no permissive cell line that enables JSRV replication *in vitro*, therefore retroviral vector pCMV2JS$_{21}$ (see Section 2.1.3) (Palmarini et al., 1999), which is an infectious molecular clone of JSRV and its derivative reporter virus pCMVJS-ΔE-CG that encodes a CMV-EGFP reporter cassette were employed in this study (see Section 2.1.9).

The expression of JSRV in 293T cells was detected using rabbit anti-Gag antibody by western blotting of cellular lysates and concentrated virus from culture supernatants (see Fig. 3.12 – 3.15) (see Sections 2.6. and 2.10.7). This antibody detected mainly unprocessed Gag in cellular extracts of transfected cells and processed CA protein of viral particles present in concentrated supernatant. The intensity of CA bands in concentrated supernatant was used to standardize inocula of the different virus stocks that were used to infect cells. A variation in the amount of CA detected in concentrated JSRV-GFP containing supernatant was observed. JSRV-GFP stock made by cotransfection with 4 µg of sheep or goat A3-Z2 HA or APOBEC Z2Z3 HA contained a decreased amount of CA in comparison to other stocks prepared at the

same time. Therefore the volume of those “4 µg stocks” was increased for infections. As an example a western blot picture of A3-Z2 stocks is shown in Fig.3.12.

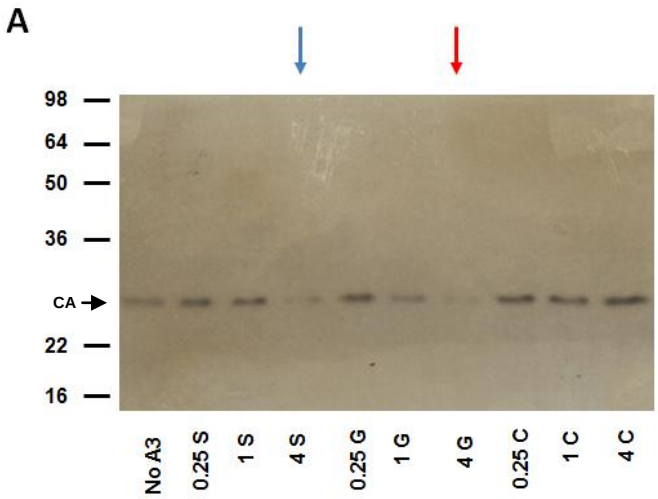

B

stock	amount of CA vs No A3
No A3	100
0.25 S	165.37
1 S	148.31
4 S	**55.75**
0.25 G	197.15
1 G	95.44
4 G	**39.11**
0.25 C	189.61
1 C	144.88
4 C	141.67

Fig. 3.12 Imbalance of CA content in stocks made in the presence of A3-Z2

Panel (A) western blot detection of CA in concentrated JSRV-GFP made in the presence of ruminant A3-Z2. Transfection was performed in the presence of the indicated A3s (C- cow, G- goat, S- sheep) and a vector control (no A3). Numbers represent µg of A3 encoding vector during transfection. Arrows indicate bands where a lower amount of CA was detected (blue – 4 µg of sheep A3-Z2; red - 4 µg of goat A3-Z2). Molecular weight marker See Blue2 bands representing protein size (kDa) are displayed on the left side of figure. Panel (B) amount of CA compared to “No A3 stock”, band density values were approximated using the ImageQuant TL Array software by the image rectangle background subtraction method.

Figure 3.12 clearly shows the decreased CA content of JSRV-GFP stocks made by cotransfection with 4 µg of sheep and goat A3-Z2. The image shown was intentionally captured by relatively short exposure time in order to emphasise the disproportions.

Notably, this effect was not seen with “4 µg cow A3-Z2 or Z2Z3 stocks” or $JSRV_{21}$ stocks. The blots presented in Fig. 3.13 - 3.16 were performed using standardized volumes of concentrated supernatant in order to ensure to infect cells with a similar amount of virus. In practice this means that identical volumes of each stock were used for infections and RT-assays, with the exception of sheep and goat A3-Z2 and A3-Z2Z3 stocks which were adjusted on the total content of Gag by immunoblot comparison with dilutions of “No A3” stock or by analysis utilising ImageQuant TL Array software. Notably, RT-assay should not be used to normalise input amount of virus in those experiments because of the potential interference of A3 on reverse transcription.

The expression of HA-tagged ruminant A3 proteins in 293T cellular extracts and their encapsidation by JSRV-GFP was confirmed by anti-HA Western Blot (see Fig. 3.13 to 3.16), (see Section 2.6). The filtration of virus containing supernatant and further ultracentrifugation ensured that the signal from HA-tagged A3 is from virus-associated protein, which is likely packaged into virions and is not an artefact of cellular debris or secreted protein present in the culture supernatant. To confirm this, the supernatant was analysed from cells transfected only with A3 expression vector without any virus encoding DNA.

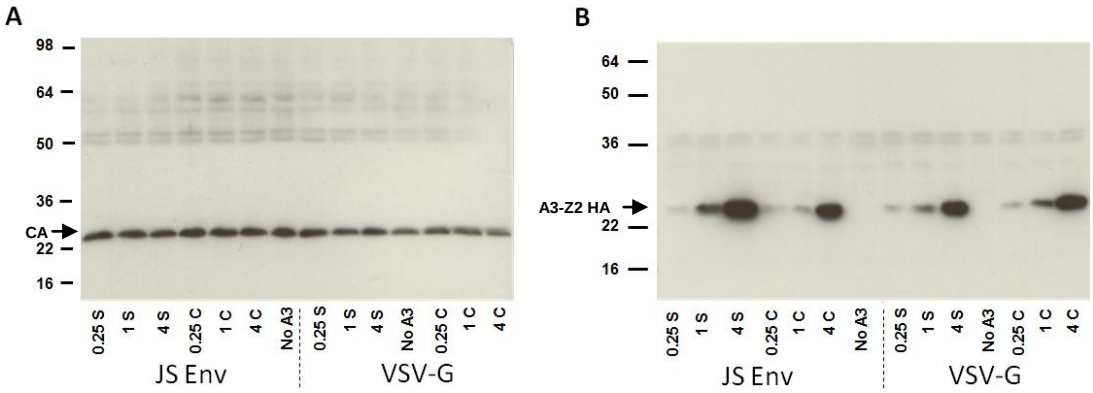

Fig. 3.13 JSRV encapsidates ruminant A3-Z1
Panel (A) shows Western blot detection of Gag proteins in concentrated JSRV. Panel (B) demonstrates encapsidation of ruminant A3-Z1 by JSRV in analysed concentrated supernatants. JSRV Virus stocks were made by transfection together with the indicated A3s (C- cow, G- goat, S- sheep) or a vector control (no A3). Numbers represent µg of A3 encoding vector during transfection. Blots presented represent concentrated JSRV-GFP pseudotyped with JSRV Env or VSV-G Env (described below each image). Molecular weight marker See Blue2 bands representing protein size (kDa) are displayed on the left side of figure.

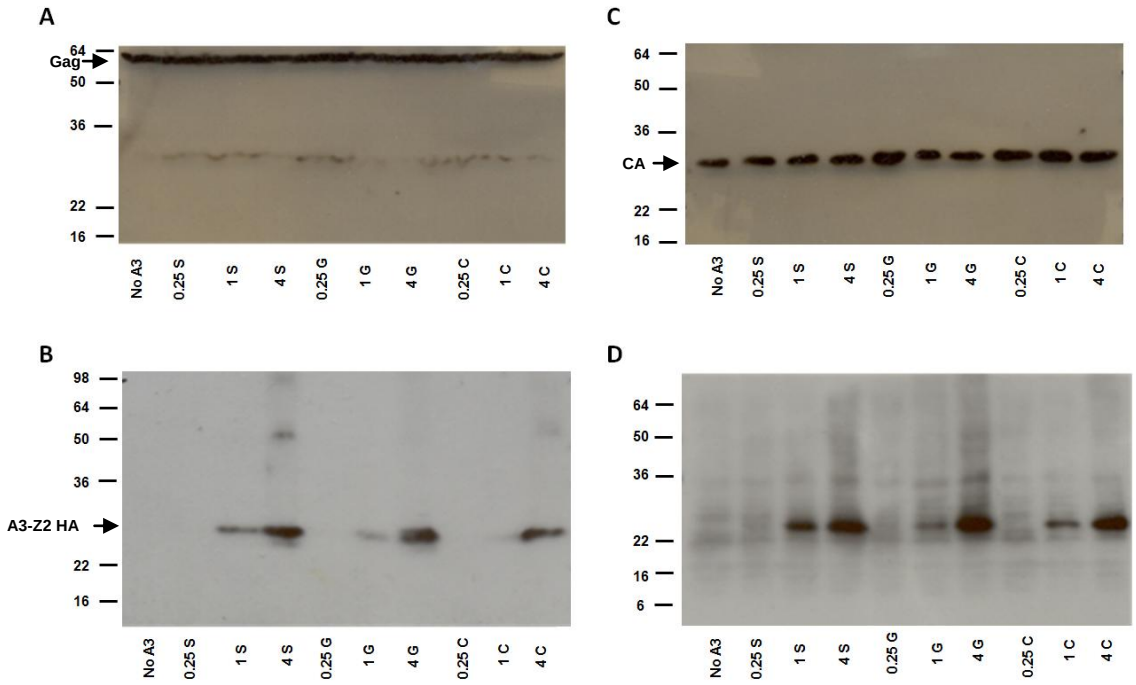

Fig. 3.14 JSRV encapsidates ruminant A3-Z2

Panel (A) shows Gag detection in cellular extract of 293T coexpressing ruminant A3-Z2. Panel (C) shows Western blot detection of Gag proteins in concentrated JSRV-GFP. Panel (B) shows detection of haemagglutinin tagged ruminant A3-Z2 in cellular extract of 293T. Panel (D) demonstrates encapsidation of ruminant A3-Z2 by JSRV in concentrated supernatants. JSRV Virus stocks were made by transfection together with the indicated A3s (C- cow, G- goat, S- sheep) or a vector control (no A3). Numbers represent µg of A3 encoding vector during transfection. Molecular weight marker See Blue2 bands representing protein size (kDa) are displayed on the left side of figure.

The amount of encapsidated A3 present in the JSRV-GFP and expressed in producer cell line lysates increased with increasing amount of A3 expression plasmid used in transfection (see Fig. 3.13 to Fig. 3.16). A stronger band was observed where 4 µg of A3 expression vector was used than 1 µg, while 0.25 µg rarely gave a visible band. No HA signal was detectable by western blot of filtered and ultracentrifuged supernatant from cells transfected only with 4µg sheep A3-Z2Z3HA pCI-Neo (data not shown).

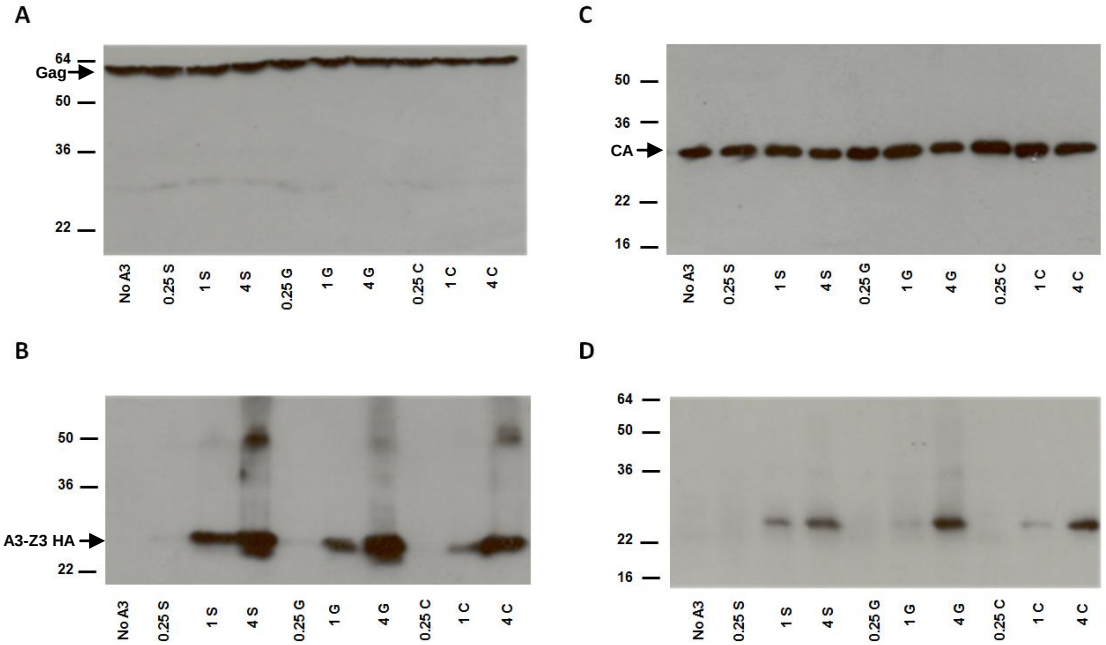

Fig. 3.15 JSRV encapsidates ruminant A3-Z3

Panel (A) shows Gag detection in cellular extract of 293T coexpressing ruminant A3-Z3. Panel (C) shows western blot detection of Gag proteins in concentrated JSRV-GFP. Panel (B) shows detection of haemagglutinin tagged ruminant A3-Z3 in cellular extract of 293T. Panel (D) demonstrates encapsidation of ruminant A3-Z3 by JSRV in concentrated supernatants. JSRV Virus stocks were made by transfection together with the indicated A3s (C- cow, G- goat, S- sheep) or a vector control (no A3). Numbers represent µg of A3 encoding vector during transfection. Molecular weight marker See Blue2 bands representing protein size (kDa) are displayed on the left side of figure.

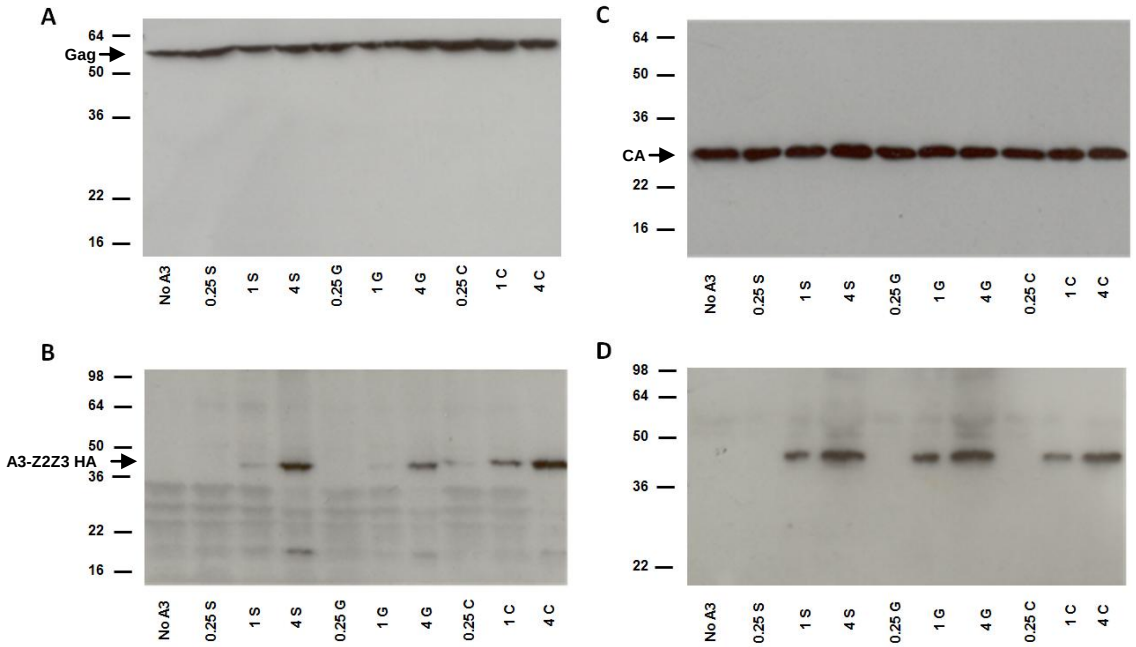

Fig. 3.16 JSRV encapsidates ruminant A3-Z2Z3

Panel (A) shows anti-Gag analysis of cellular extract of 293T coexpressing ruminant A3-Z2Z3. Panel (C) shows western blot detection of Gag proteins in concentrated JSRV-GFP. Panel (B) shows detection of haemagglutinin tagged ruminant A3-Z2Z3 in cellular extract of 293T. Panel (D) demonstrates encapsidation of ruminant A3-Z2Z3 by JSRV in analysed concentrated supernatants. JSRV Virus stocks were made by transfection together with indicated A3s (C- cow, G- goat, S- sheep) or a vector control (no A3). Numbers represent µg of A3 encoding vector during transfection. Molecular weight marker See Blue2 bands representing protein size (kDa) are displayed on the left side of figure.

3.2.3 Ruminant APOBEC3 restricts JSRV *in vitro*

Having demonstrated that all the analysed ruminant A3 proteins were encapsidated by JSRV, it was next determined whether these proteins can restrict JSRV infectivity. As there is no permissive cell culture system supporting JSRV replication, retroviral vectors $pCMV2JS_{21}$ (see Section 2.1.3) and its GFP-carrying derivative $pCMV_2JS$-ΔE-CG were employed in this study (see Section 2.1.9). The use of GFP as a reporter enabled the study of their infectivity by flow cytometry (see Section 2.8.3). Parallel experiments were performed with viruses pseudotyped with JSRV Env or VSV-G.

The number of infected cells (GFP expressing) was reduced when cells were infected with JSRV encapsidating any of ruminant A3s, however A3-Z1 and A3-Z3 did not cause as strong restriction as that mediated by A3-Z2 and A3-Z2Z3. The infectivity of JSRV-GFP decreased with increasing amounts of A3 expression plasmid used in transfection of 293T cells. Flow cytometric analysis of CRFK-ovH2 cells infected with JSRV-GFP demonstrated the ability of ruminant A3-Z1, Z2 and Z2Z3 to restrict JSRV *in vitro* (see Fig. 3.17). Notably, sheep A3-Z1, Z2 and Z2Z3 were able to inhibit infection almost with similar efficiency as their goat and cow homologues (as illustrated in Fig. 3.17).

In addition to a decreased number of positive cells (see Fig. 3.17 and Fig. 3.19), there was a decrease in the fluorescence intensity of cells infected with JSRV-GFP made in the presence of increased amounts of A3 (see Fig. 3.18). The median fluorescence intensity of GFP-positive cells was reduced when cells were infected by JSRV-GFP carrying all ruminant A3s, however this effect was mild in cells infected by A3-Z3 stocks (see Fig. 3.17). The GFP-positive cells infected by stocks made by co-transfection with 4 μg of A3 are characterized by a FITC median value close to the baseline separating the GFP-positive from the GFP negative population.

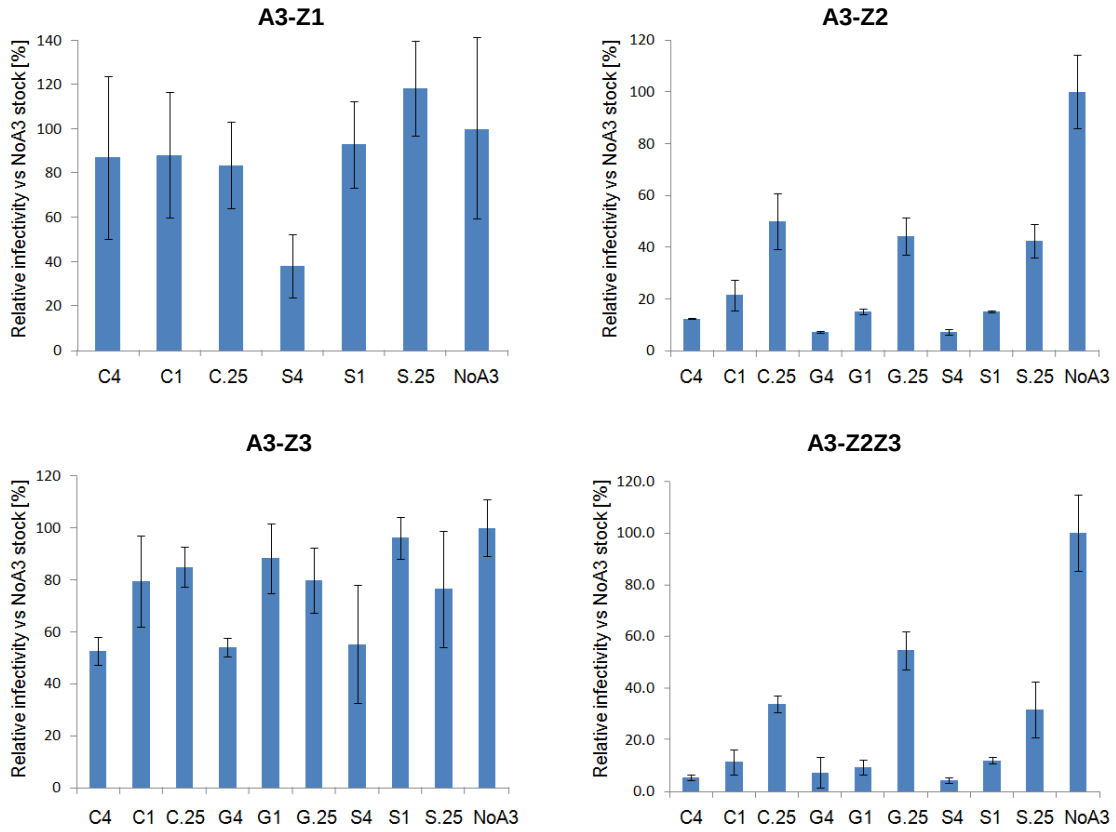

Fig. 3.17 Restriction of JSRV by ruminant A3 proteins
Bars represent relative infectivity of JSRV-GFP stocks made in the presence of various A3s (Z1, Z2, Z3 and Z2Z3). Flow cytometric results of CRFKovH2 cells infected by JSRV-GFP. The relative percentage of cells infected by virus produced in the presence of the indicated A3s (C- cow, G- goat, S- sheep) and a vector control (no A3), numbers on X-axis represent µg of A3 encoding vector during transfection. Values are based on the ratio of percentage GFP-positive cells infected by "A3 stocks" compared to cells infected by "No A3 stock". The student two-tailed t-test method with unequal variance was used to verify the significance of results. The error bars report the standard deviation value between wells infected in triplicate. Plots present relative infectivity values of one of at least 2 experiments.

There was a possibility of false positive readings of fluorescent cells due to their uptake of DNA which was carryover from the virus production process. That is why all analysed virus stocks were concentrated and heat inactivated virus was used as a negative control in every infection assay along with non-infected cells. Cells subjected to heat inactivated virus rarely contained any GFP-positive cells. Therefore, the passive transduction caused by DNA carryover was minimal since heat inactivated controls never contained more than 0.03% of GFP-positive cells.

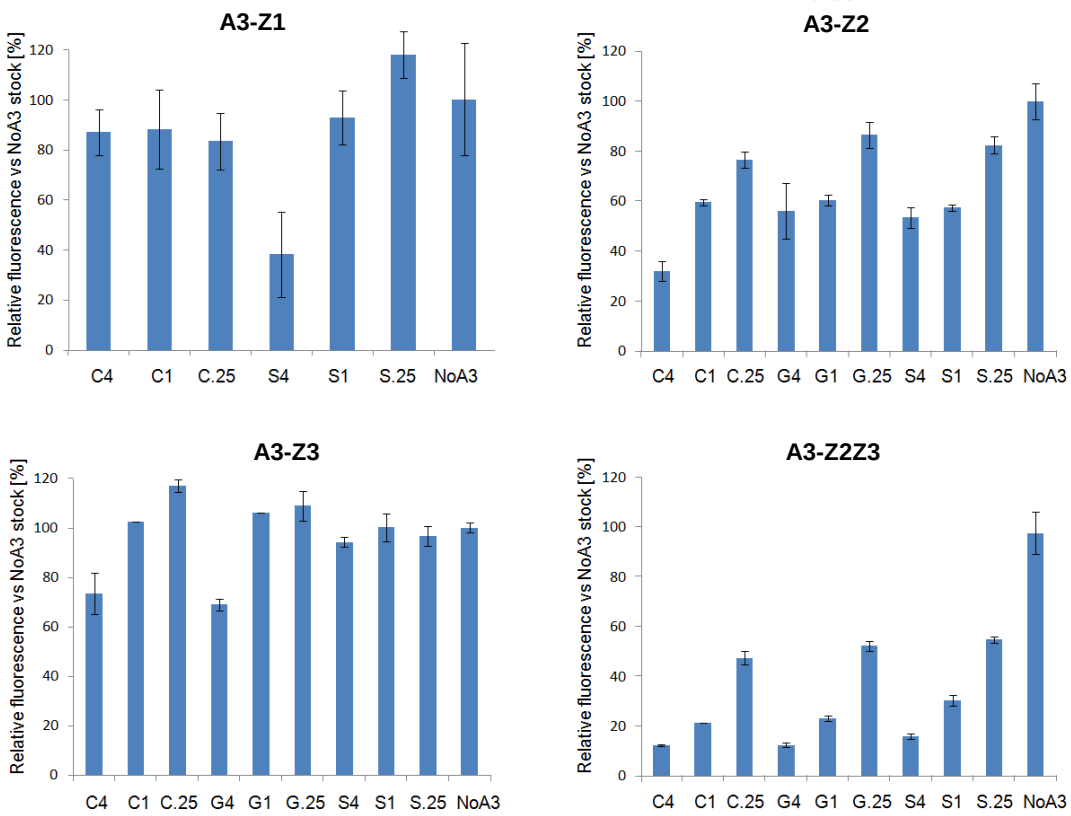

Fig. 3.18 The impact of ruminant A3 on fluorescence of JSRV-GFP infected cells
Bars represent fluorescence intensity median of cells infected by stocks made in presence of various A3s (Z1, Z2, Z3, Z2Z3). Flow cytometric results of CRFKovH2 cells infected by JSRV-GFP – the relative median fluorescence of cells infected by virus produced in the presence of the indicated A3s (C- cow, G- goat, S- sheep) and a vector control (no A3), numbers represent µg of A3 encoding vector during transfection. Values are based on the fluorescence intensity median of GFP-positive cells infected by "A3 stocks" compared to cells infected by "No A3 stock". The student two-tailed t-test method with unequal variance was used to verify the significance of results. The error bars report the standard deviation value between wells infected in triplicate. Plots present relative fluorescence intensity values of one of at least 2 experiments.

3.2.4 VSV-G and JSRV Env pseudotyped viruses are restricted by APOBEC3 to the same degree

The experiments shown in Section 3.2.3 utilised wild type JSRV Env. In order to determine whether the envelope protein used influences the results, experiments utilising VSV-G pseudotyped JSRV-GFP were also performed (see Fig. 3.19). The detected lack of strong A3-Z1 and A3-Z3 inhibition of JSRV Env pseudotyped virus (see Fig. 3.17 and 3.18) required an investigation if JSRV Env does not mediate an evasion potential against those A3.

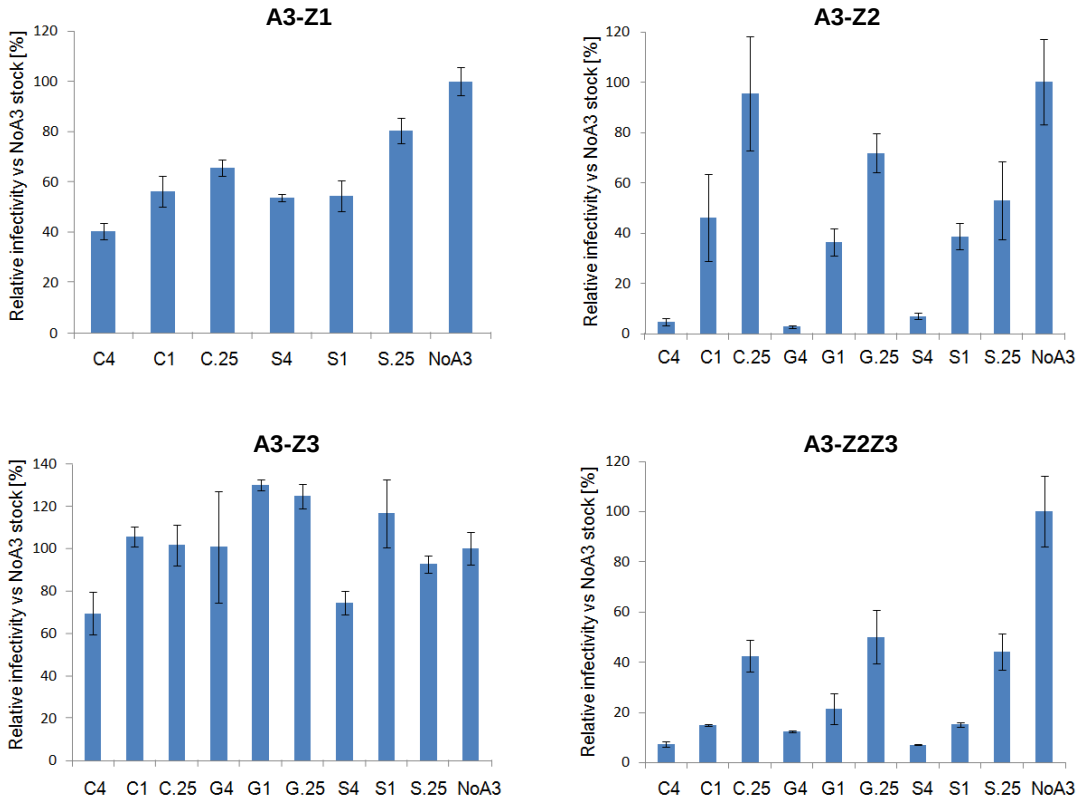

Fig. 3.19 Restriction of JSRV (VSV-G) by ruminant A3 proteins

Bars represent relative infectivity of JSRV-GFP stocks made in presence of various A3s (Z1, Z2, Z3 and Z2Z3). Flow cytometric results of CRFKovH2 cells infected by JSRV-GFP. The relative percentage of cells infected by virus made in the presence of the indicated A3s (C- cow, G- goat, S- sheep) and a vector control (no A3), numbers on X-axis represent µg of A3 encoding vector during transfection. Values are based on the ratio of percentage GFP-positive cells infected by "A3 stocks" compared to cells infected by "no A3 stock". The student two-tailed t-test method with unequal variance was used to verify the significance of results. The error bars report the standard deviation value between wells infected in triplicate. Plots present relative infectivity values of one of at least 2 experiments.

Although A3 is thought to act independently of the infected target cell type, in order to verify this statement the VSV-G pseudotyped JSRV-GFP were prepared in other cell lines, which are non permissive for JSRV Env mediated entry. The JSRV-GFP pseudotyped either with JSRV or VSV-G envelope protein, were restricted to a similar degree by ruminant A3s (see Fig. 3.19). Flow cytometry results showed that there is a similar decrease in the percentage of GFP-positive cells and their fluorescence intensity caused by ruminant A3 irrespective of envelope used.

Therefore no evasion of A3 mediated by JSRV envelope was detected. It should be noted that all JSRV-GFP production occurred by a co-transfection with SP-FLAG which is a fragment of JSRV *Env* gene, in order to enhance the stock titre. There is a need to be aware that SP may influence the ratio of transcripts, since it has been described to act as a postranstriptional regulator of expression (Caporale et al., 2009).

3.2.5 Effect of sheep APOBEC3 on the number of integrated proviruses

In order to further investigate the detected inhibition of JSRV by sheep A3 the integrated proviruses were quantified. The activity of sheep A3 against the wild type JSRV virus and JSRV-GFP was measured by qPCR (see Section 2.10.4). Integration events which occurred as the effect of JSRV-GFP or $JSRV_{21}$ infections were compared (see Fig. 3.20). Note that this was a preliminary experiment and requires further confirmation, preferably with utilisation of stocks made in presence of other quantities of A3 expressing vector.

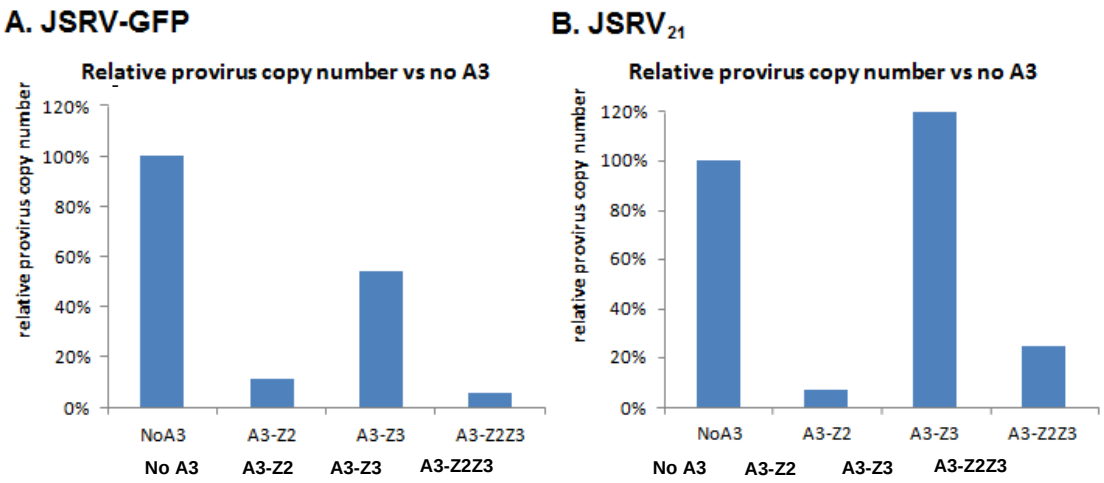

Fig. 3.20 Reduction of JSRV integration events by sheep A3 proteins
The qPCR measured the relative number of proviruses in cells infected by JSRV-GFP (A) or $JSRV_{21}$ (B). Virus was produced in the presence of the indicated sheep A3s (4µg of A3 encoding vector used during transfection) and a vector control (no A3). Results show an average of duplicate qPCR samples.

The results show there were at least four-fold fewer proviruses detected in cells infected by either JSRV-GFP or a wild type $JSRV_{21}$ containing A3-Z2 or Z2Z3 virus stocks compared to cells infected by "No A3" stock. Due to time constraints this assay was only done once, therefore it needs to be repeated in order to confirm the result obtained. As negative controls heat inactivated or heat inactivated and DNAse treated viruses were used. However, carryover DNA was detected in some negative controls and those values were subtracted during interpretation of the proviral copy number.

3.2.6 Hypermutation caused by sheep APOBEC3

The previous experiments provide clear evidence that ruminant A3 can restrict JSRV, at least *in vitro*. As hypermutation mediated by the cytidine deaminase activity of A3 is a common mechanism of viral restriction mediated by A3 in other species, I next examined whether sheep A3 proteins also exhibit this activity against JSRV. Genomic DNA was extracted from cells infected by $JSRV_{21}$ and JSRV-GFP made in the presence of sheep A3-Z2, Z3 and Z2Z3. The DNA was subjected to high fidelity amplification of 928 bp fragments of *EGFP* (JSRV-GFP) or *env* ($JSRV_{21}$) sequences present in those proviruses. Subsequently, the amplified sequences were cloned into pGEM-T Easy (see Section 2.10.7), and up to 21 clones of each were sequenced to identify possible hypermutation.

Countermeasures were introduced to minimise the risk of amplifying the possible carryover of DNA which was used during transfection during virus production. All virus stocks were treated with DNAse prior to infection (see Sections 2.3.11 and 2.10.5) and cells were washed twice after the infection before adding the medium. In addition, DNA was extracted from non-infected cells and from cells exposed to a heat inactivated "no A3" stock and was utilised as a negative control for PCR. Provirus fragments from up to 21 separate integration events were sequenced for each of the A3 variants. The mutation frequency caused by the various A3s is shown in Table 3.2.

The results provided evidence of deamination of JSRV-GFP by sheep A3-Z2 and Z2Z3. Cells infected with "No A3" virus stocks provided DNA which was used to characterise the background error of sequences readout in the assay.

Table 3.2 Mutation frequencies observed in proviruses affected by sheep A3

APOBEC3	No of clones sequenced	Bases sequenced	G→A	other	G→A freqency
no A3	19	17632	2	2	0.00011
Z2	17	15776	178	3	0.01128
Z3	17	15776	3	1	0.00018
Z2Z3	21	19488	51	4	0.00275

In this experiment A3-Z2 was identified as being a stronger JSRV hypermutator than A3-Z2Z3 (see Table 3.2). Sheep A3-Z2 and A3-Z2Z3 G to A mutation frequency was 89-fold and 25.5 fold higher respectively than the negative control, which contained only one G to A mutation in the total of ninety 928 bp length fragments of proviruses from cells infected by "No A3" stock. Mutations observed in sequenced "A3-Z3" proviruses were close to the background of the assay.

The experiment demonstrated that sheep A3-Z2 and A-Z2Z3 are able to hypermutate JSRV *in vitro*. The sequencing results shown in graphs generated by Hypermut software (see Fig. 3.21) demonstrate the distribution of mutations among a group of sequenced individual provirus clones from two separate experiments.

There was an apparent difference in the editing pattern of A3-Z2 and A3-Z2Z3 on JSRV-GFP. Proviruses deaminated by A3-Z2Z3 showed a dispersed distribution of mutations among different sequences, whereas A3-Z2 induced hypermutation was focused on a smaller number of sequences which were edited more intensively than others (e.g. clones A3-Z2 marked by asterisk in Fig.3.20). This result could suggest a different enzymatic activity mechanism between A3 paralogues. The bases located next to a guanidine have impact on the occurrence of deamination (Ebrahimi et al., 2014). This experiment determined the site preference of mutations caused by sheep A3-Z2 and A3-Z2Z3 (see Table 3.3). The most commonly mutated sites were GA (cyan), followed by GG (red) to GC (green) (see Fig. 3.21 and Table 3.3). The deamination site preference of analysed sheep A3 is shown in Table 3.3.

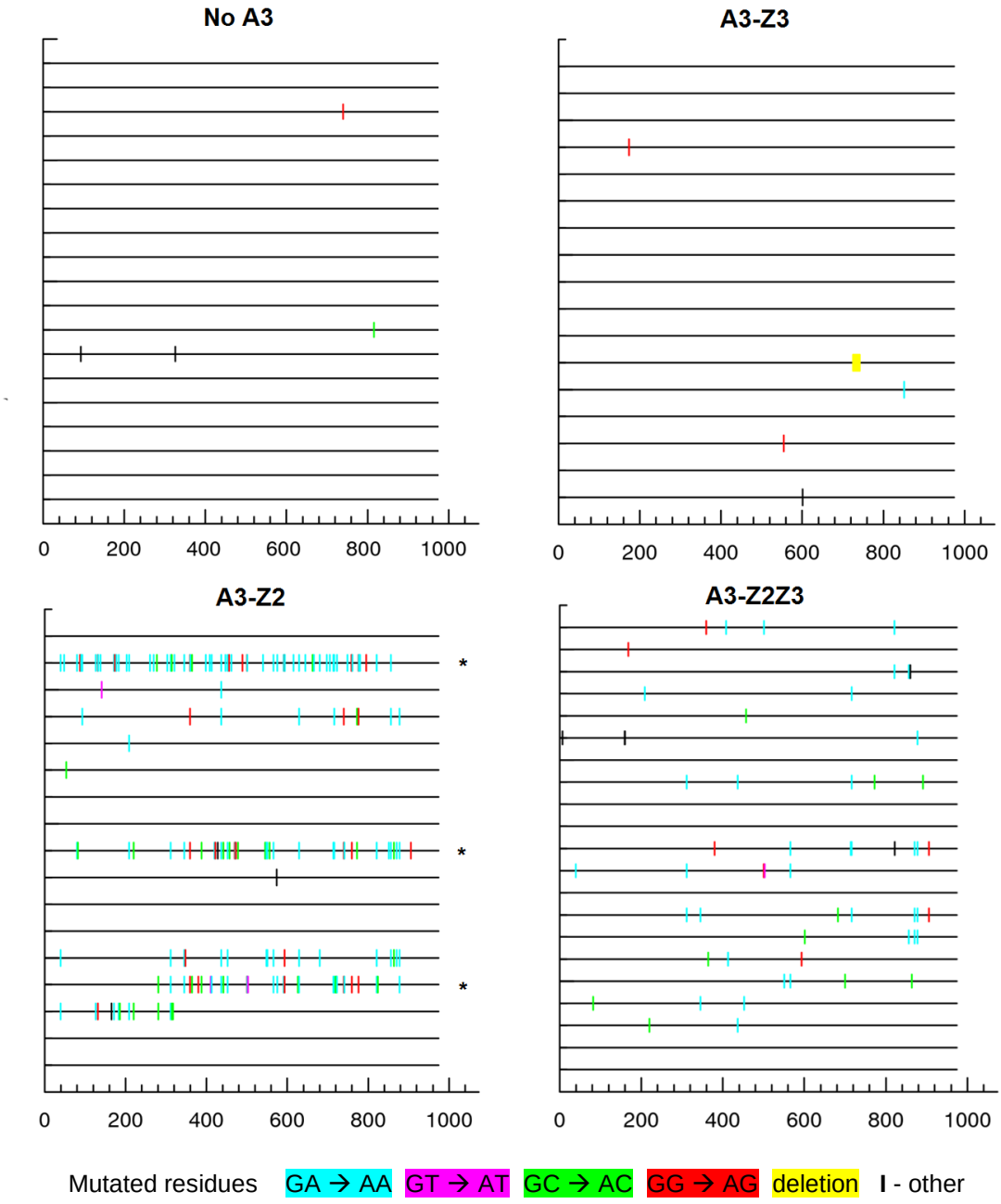

Fig. 3.21 Hypermutation of proviral genome caused by sheep A3
Graphs were generated using Hupermut software. Horizontal lines represent 928 bp fragments of individually sequenced proviruses (letters). Coloured short vertical lines indicate mutation, indicating the base downstream of the mutated guanidine. Short black vertical lines represent non G → A mutations.

Table 3.3 G to A mutation context observed in proviruses affected by sheep A3

APOBEC3	GG	GA	GC	GT
no A3	1	0	1	0
Z2	32	113	30	3
Z3	2	1	0	0
Z2Z3	7	33	10	1

3.2.7 Ruminant APOBEC3 inhibits the enzymatic activity of JSRV's RT

Work on other retroviruses has shown that A3 proteins can restrict infection by mechanisms that do not involve hypermutation (Stenglein and Harris, 2006). In particular, several steps in reverse transcription may be inhibited by A3. In order to examine the mechanism of restriction, the effect of each of the A3 proteins on JSRV-mediated reverse transcription was measured using a commercial colorimetric RT assay (see Section 2.10.9). The same virus stocks that were used in infectivity assays were subjected to analysis of their RT activity. Therefore, the detection of possible reverse transcription interference by A3 was performed by comparison to RT activity of "no A3" stocks. Similarly to infectivity experiments, standardized amounts of virus were tested. As a negative control for background control of the assay, the IMDM medium which had been used for resuspension of ultracentrifuged virus was utilised (see section 2.5.1).

All of the ruminant A3s analysed inhibited JSRV reverse transcription in Roche Reverse Transcriptase Colorimetric assay's settings (see Section 2.10.9) (see Fig. 3.22). The results indicated that ruminant A3 proteins may influence the JSRV reverse transcription by a cytidine deamination independent mechanism.

For all the A3 analysed, the highest amount decreased the RT efficiency. Notably, the intermediate amounts A3-Z2 and A3-Z2Z3 also reduced the JSRV RT activity, in contrast to A3-Z1 and A3-Z3 where only the highest amounts of A3 inhibited RT.

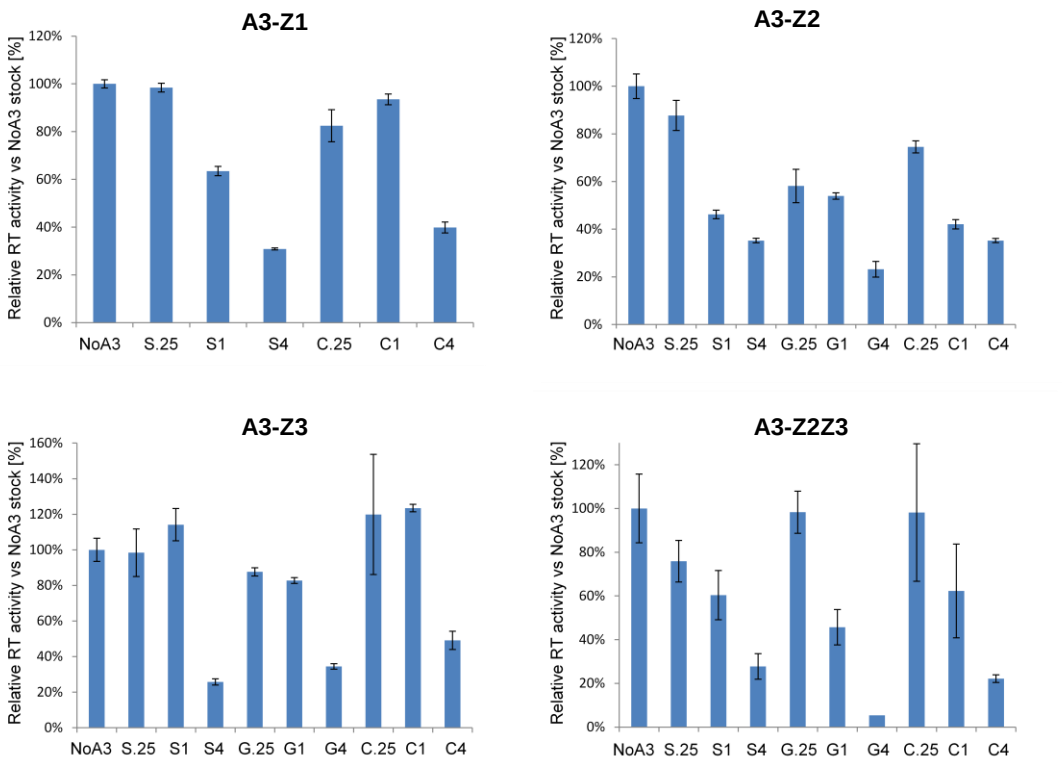

Fig. 3.22 Inhibition of JSRV reverse transcriptase by ruminant A3 proteins
Reverse transcriptase assay performed on concentrated JSRV-GFP produced in the presence of the indicated A3 (S- sheep, G- goat, C- cow) and a vector control (NoA3). Numbers represent µg of A3 encoding vector during transfection. Plots present relative reverse transcriptase activity compared to "NoA3" stock. Presented values show one of at least 2 experiments. The student two-tailed t-test method with unequal variance was used to verify the significance of results. The error bars report the standard deviation value between wells infected in triplicate.

3.2.8 APOBEC3 Z2, Z3 and Z2Z3 are not detected in lung fluid from OPA affected animals.

The experiments described so far show that sheep, goat and cow A3 proteins can restrict JSRV by both deaminase dependent and deaminase independent mechanisms in an *in vitro* assay system. In order to investigate whether such restriction is also active *in vivo*, I examined virus from lung fluid from natural cases of OPA for evidence of A3 encapsidation.

In order to determine whether lung fluid containing JSRV includes packaged A3, JSRV was purified and concentrated, and subsequently analysed by western blot. Antibodies against JSRV Gag (see Section 2.6) were used to confirm the presence of

JSRV in lung fluid and polyclonal antibodies against sheep A3-Z2 or A3-Z3 (see Sections 2.9 and 2.10.8) were utilised to investigate if sheep A3 was associated with the purified virus.

JSRV was purified from LF of 6 OPA cases by ultracentrifugation followed by a sucrose gradient purification and a second ultracentrifugation of fractions. The cases were natural OPA in sheep donated by farmers to Moredun Research Institute. Lung fluid samples had been stored at -80ºC for a few days up to six years prior to analysis. Concentration and purification of JSRV from lung fluid was necessary to perform accurate detection of proteins included in virions, and to avoid the detection of proteins in cellular debris or in the fluid itself. The procedure followed is shown in Fig. 3.23.

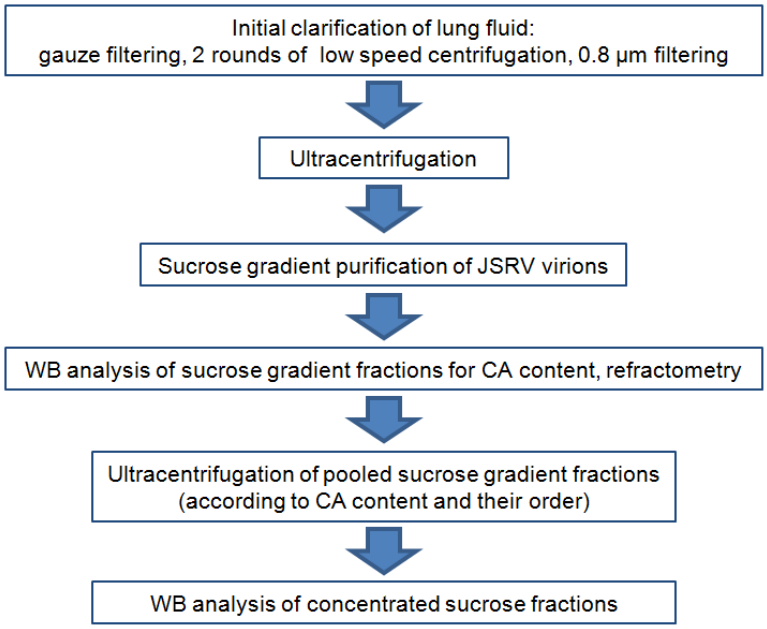

Fig. 3.23 Process of concentration and purification of JSRV from lung fluid
Where necessary, samples were stored at -80ºC between steps.

Prior to the analysis, lung fluid obtained from OPA affected animals was clarified, concentrated and purified according to Section 2.9. In order to enhance JSRV purity, sucrose gradient purification was performed (see Section 2.8). Fractions were collected and those containing virus were identified by WB for detection of Gag protein. The sucrose fractions were pooled into four samples (W-Z). Fractions were pooled depending on the initial detection of Gag on western blot (see Fig. 3.24, panel A).

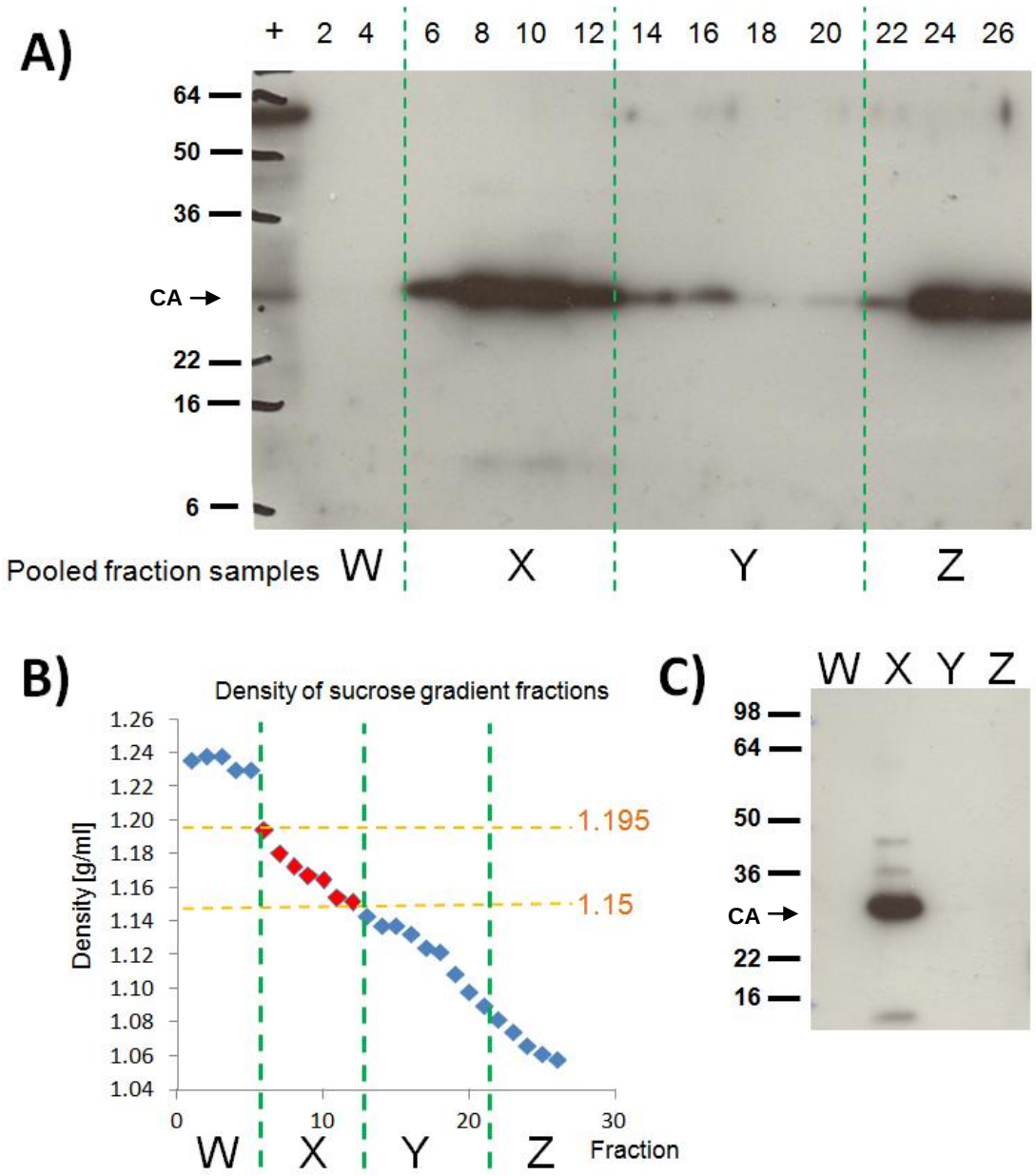

Fig. 3.24 Detection of JSRV Gag in sucrose gradient fraction samples
A) Every second gradient sample was tested (numbers top) by WB using anti-Gag antibody. Fractions were pooled (letters W-Z) according to the presence of Gag. B) Density gradient of each gradient fraction (points); density of fractions where JSRV was purified (red) are highlighted in orange C) Detection of JSRV Gag (CA) in pooled fraction samples after being further concentrated. Molecular weight marker See Blue2 bands representing protein size (kDa) are displayed on the left side of blots.

The first sample (sample W) contained fractions from the bottom of the gradient with the highest concentration of sucrose, where no JSRV Gag was detected. The second sample (X) contained the Gag-rich fractions with densities in the range of 1.15 to 1.19 g/ml. The peak of Gag reactivity was in fractions in the range from 1.15-1.16 g/ml which is the expected density of retroviral particles (York et al., 1991, Palmarini et al., 1995, Palmarini et al., 1999b). The third sample (Y) was a pool of Gag-negative fractions of lower sucrose concentration (density 1.09-1.14 g/ml). The last sample (Z) included the lowest concentration sucrose fractions from the top of the gradient (see Section 1.05-1.09 g/ml) where Gag was detected, which likely represents solubilised Gag proteins and the presence of virion debris (see Fig. 3.24).

Each pool was concentrated by centrifugation at 100,000 × *g* at 4°C for 2 h and resuspending the pellet in a minimum volume (at least 100 μl) of TNE. The resuspension volume was adjusted depending on the total volume of pooled fractions in order to keep the same × 50 concentration factor. After the ultracentrifugation only sample X contained JSRV Gag (see Fig.3.24, panel C). The lack of Gag concentration in pooled fraction Z can be attributed to the presence of Gag in solution, but not in virions, as it was confirmed by Gag detection only in sucrose gradient fractions (see Fig.3.13.A. 22,24,26) and not after their subsequent concentration (see Fig.3.24, panel C. sample Z). Assuming that only sample X contained virus, it was concentrated approximately 200 times. Western blot detection of Gag, A3-Z2 or A3-Z3 in concentrated JSRV-GFP stocks or concentrated and purified lung fluids from 8 animals (virus rich "X" fraction of each stock) is shown in (see Fig. 3.25).

Western blot demonstrated that there is usually more Gag antigen in purified lung fluids than in concentrated JSRV-GFP stocks (see Fig. 3.25.A). There was no signal characteristic for A3-Z2 or A3-Z3 protein size corresponding to JSRV-GFP positive controls. However, there were other bands which may be a result of polyclonal antibody cross-reactivity with other antigens, present both in virus supernatants and analysed lung fluids. Notably, anti-Z2 antibody only weakly detected A3-Z2Z3 in JSRV-GFP samples (see Fig. 3.25B) but anti-Z3 efficiently detected this antigen. This result could be attributed to lower CA content of A3-Z2Z3 stock than present in other stocks (see Fig. 3.25A).

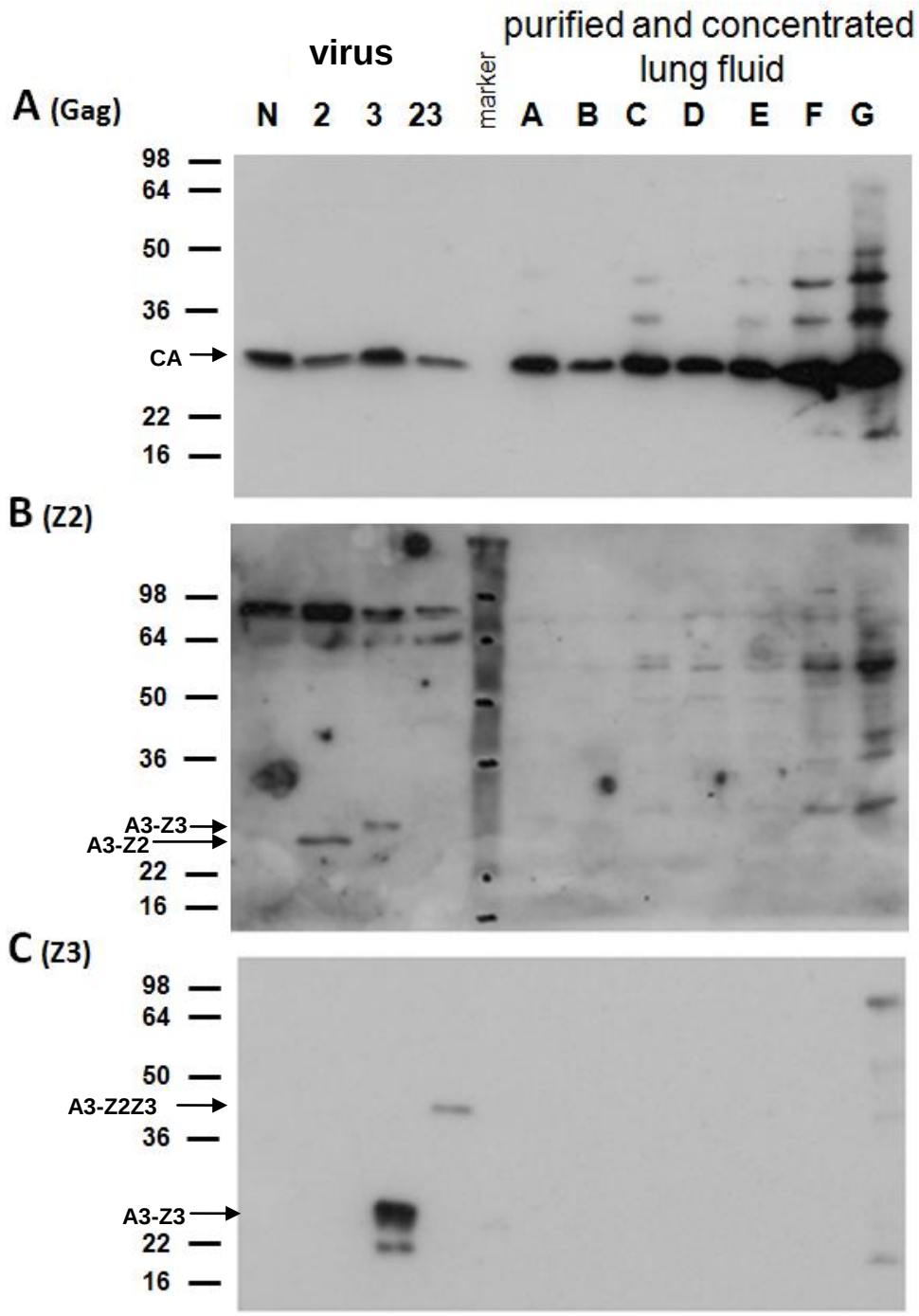

Fig. 3.25 Western blot analysis of JSRV concentrated and purified lung fluid from OPA affected sheep.

Antibodies against Gag (A), anti-Z2 (B) or anti-Z3 (C) were utilised. Samples tested included concentrated JSRV-GFP vector (N – No A3; 2 – sheep A3-Z2; 3 – sheep A3-Z3; 23 – sheep A3-Z2Z3) and concentrated and purified lung fluids (right, A to G). Molecular weight marker See Blue2 bands representing protein size (kDa) are displayed on the left side of figure.

3.2.9 Determination of sensitivity of anti A3-Z2 and A3-Z3 immunoblot

In order to estimate the sensitivity of the method used, serial dilutions of sheep A3-Z2 and A3-Z3 recombinant proteins (provided by the antibody provider, Proteintech) were analysed by western Blot in parallel with virus made *in vitro* (see Fig. 3.24). The result obtained highlighted the cross-reactivity of the anti-sheep Z2 antibody with sheep Z2 and Z3 proteins.

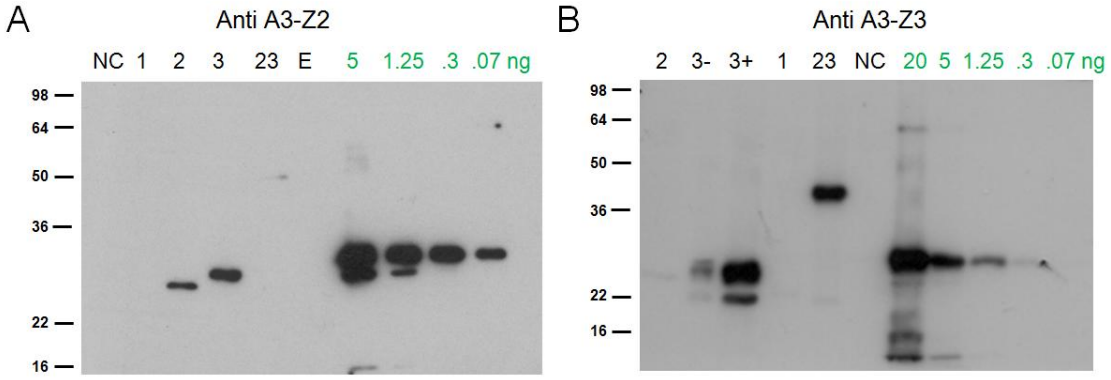

Fig. 3.26 Estimation of the threshold amount of A3 detectable by western blot.
The performance of antibodies, anti-sheep A3-Z2 (panel A) and anti-sheep A3-Z3 (panel B), was analysed by detection of A3 present in virus stocks prepared *in vitro* and serial dilutions of recombinant A3 peptide. Samples included concentrated virus stocks made *in vitro*: NC (15 µl "no A3" stock); 1 (15 µl A3-Z1); 2 (15 µl A3-Z2); 3- (5 µl A3-Z3); 3+ (15 µl A3-Z3); 23 (15 µl A3-Z2Z3); E empty well. Numbers highlighted in green 20, 5, 1.25, 0.3, 0.07 are ng of serially diluted recombinant A3 proteins used to immunise rabbits in order to produce the antiserum. Molecular weight marker See Blue2 bands representing protein size (kDa) are displayed on the left side of figure.

According to the recombinant A3 protein concentration provided, the WB assay can detect as little as 0.07 ng of A3. The anti-Z2 antibody cross-reacted with A3-Z3 and weakly detected A3-Z2Z3 in concentrated virus stocks made *in vitro* (panel A). The anti-Z3 antibody is specific to A3-Z3 and effectively detects A3-Z2Z3 (panel B), but using this exposure its estimated threshold of detection is limited to 0.3 ng. Therefore the antibodies provided could be utilised for *in-vivo* detection of A3, however their non-specific cross-reactivity, should be taken into account.

3.3. Chapter Discussion

This project is the first study of the impact of A3 on JSRV replication. During this study the goat A3-Z2, A3-Z3 and A3-Z2Z3 were identified, cloned and their role in JSRV restriction was characterized.

Initially ruminant A3 genes were isolated and cloned into mammalian expression vectors and their sequences were confirmed (Sections 3.2.1). After confirmation that JSRV is able to encapsidate ruminant A3 (Section 3.2.2), the restriction potential of ruminant A3 against JSRV was demonstrated by infection of a permissive cell line. Flow cytometry results (see Sections 3.2.3 and 3.2.4), qPCR quantification of integrated proviruses (see Section 3.2.5), sequencing of proviral sequences (see Section 3.2.6) and reverse transcriptase assays (See Section 3.2.7) provided insights into the restriction mechanism. However, no A3 proteins were detected in lung fluid (see Section 3.2.8). Collectively, these data indicate that JSRV is sensitive to restriction mediated by ruminant A3, but suggest that *in vivo* A3 does not act as a restriction factor because it is not packaged into virions present in lung fluid.

3.3.1 Sheep APOBEC3 is not responsible for species specificity of JSRV infection

Experiments conducted *in vitro* demonstrated the inhibitory potential of ruminant A3 and investigated the restriction mechanism. Assuming that even minor sequence polymorphism among restriction factor homologues may be responsible for species-specificity of infection it was possible that ruminant A3 plays such a role in species infectivity of JSRV. Unexpectedly the results showed that sheep A3 had similar properties *in vitro* to its ruminant homologues from goat and cow. Therefore, these *in vitro* experiments did not identify A3 as the species specificity factor.

The comparable ability of ruminant A3-Z2 and A3-Z2Z3 homologues to interfere with JSRV *in vitro,* could be explained by an extremely high sequence similarity among the ruminant A3 homologues. However, this striking identity was quite unexpected and in future, attempts to clone various haplotypes from a larger group of animals and

different breeds might reveal A3 genes with other antiviral potential. Moreover, identification of other A3 homologues from both farm and wildlife ruminants might explain some aspects of JSRV epidemiology and species specificity.

Despite the data showing that ovine A3 restricts JSRV replication, JSRV clearly successfully infects sheep. This suggests that JSRV might have an evasion strategy specific to endogenous A3 or alternatively that the restriction factor is not expressed to a sufficient level in cells where JSRV replicates (see Section 3.3.4). Therefore, A3 is not detected in field samples. There is also the possibility that various alleles of A3 might have different antiviral potential among its various haplotypes (Krupp et al., 2013). Results presented in this chapter identified a similar potential of sheep, goat and cow A3 to restrict JSRV *in vitro*. The similarity of results of experiments performed using JSRV pseudotyped with VSV-G or wtJSRV Env, strengthen the statement that wild type JSRV envelope does not protect against A3.

The *in vitro* experiments described in this study have some nuances which could potentially lead to misinterpretation of conclusions. The lack of a robust *in vitro* model which supports complete JSRV replication made experiments only possible by transient transfection of a producer cell line. It needs to be taken into account that transient transfection creates an artificial stoichiometry of viral and A3 proteins. In nature, viral proteins and A3 may not be expressed to such a high level. However, even the smallest measured amount of A3-Z2 or A3-Z2Z3 expression vector decreased JSRV infectivity (see Fig. 3.17 and Fig. 3.19).

3.3.1.1 Comment on flow cytometric analysis of A3 activity

Several factors influenced the flow cytometry result of JSRV-GFP infectivity. To properly interpret the readout of the A3 and JSRV-GFP experiment, there is a need to be aware of the fact that some positives (especially those characterized by low fluorescence) come from cells which contained an edited either GFP gene or CMV promoter sequence. It is likely, that mutated GFP has less intense fluorescence or its expression is downregulated by mutations of its promoter (Harris et al., 2003). It is possible, that some negative cells contained a provirus mutated to a degree which prevented the GFP expression to a detectable level. Flow cytometry analysis of

samples containing low positives was quite troublesome due to the fact that it was difficult to distinguish truly non-infected negative cells from low fluorescent cells, possibly containing A3-edited GFP within the provirus. Flow cytometry based sorting of cells, whose DNA would be subjected to PCR for the detection of integrated proviruses would provide additional conclusions and improved quality control to the assay.

There was a possibility of false positive readings of fluorescent cells due to the uptake of DNA carried over in transfection complexes from the virus production process. Moreover, previous studies have demonstrated that the use of VSV-G in retroviral pseudotyping can produce artifactual false positives. This phenomenon can arise from the transfer of GFP inside vesicles. When VSV-G viruses were prepared, tubovesicular structures carrying DNA might have been formed (Pichlmair et al., 2007). Therefore, all analysed virus stocks were concentrated and heat inactivated virus was used as a negative control in every infection assay along with non-infected cells.

Flow cytometry needs to be properly conducted and interpreted. In order to allow quantitative analysis, these experiments were performed using virus at multiplicity of infection (MOI) ideally higher than 0.01. By keeping the MOI low, the possibility of individual cells being infected by more than virus was minimized. In addition, maintaining at least 1% of infected cells ensured these results included an adequate sample size. To address this issue, in each experiment the "No A3" stock's titre was estimated on a small scale prior to infection of cells with all stocks included in the experiment. To ensure a reliable result, cells were infected by two different amounts of a single virus stock in triplicate.

3.3.1.2 Comment on RT assay based assessment of A3 activity

All the analysed ruminant A3 proteins inhibited JSRV RT. However, only the highest concentration of A3-Z1 or A3-Z3 decreased reverse transcription. The Roche Colorimetric RT assay utilised here, works using virions that are lysed prior to the reverse transcription step. The detected inhibition of reverse transcriptase activity showed the enzymatic potential of A3. However, inside a virion there is a possibility

that A3 proteins are packaged in a location physically separated from where the reverse transcription takes place, because A3 must have access to ssDNA. Moreover, polyA RNA template was added to samples before the reverse transcription step, which might have influenced the result obtained.

I utilised the Roche Colorimetric RT assay due to its robustness and the fact that there are publications where this kit was used (Kolokithas et al., 2010, Giroud et al., 2013). Other groups studying deaminase–independent A3 restriction have utilised an endogenous RT assay in which the RT step is conducted as the native retroviral RNA is reverse transcribed by viral particle components (Iwatani et al., 2007, Holmes et al., 2007b, Holmes et al., 2007a). In order to verify those issues, an assay should be performed based on *in situ* reverse transcription without the virion lysis step and addition of artificial polyA template.

The results obtained show that with the increase of A3 concentration inside a virion there is a gradual decrease of RT activity which confirms the statement of the inhibitory role of A3. However, the precise step of the JSRV RT reaction which is particularly inhibited by ruminant A3 remains unknown. Work on HIV and MLV has found that A3 can block reverse transcription at several steps including its initiation (Adolph et al., 2013), strong stop signal synthesis (Mbisa et al., 2007), first and second strand transfer (Mbisa et al., 2007) and accumulation of reverse transcriptase products (Bishop et al., 2008). In order to get an improved insight into the mechanism of JSRV RT interference caused by ruminant A3, a more detailed analysis of reverse transcription should be performed to identify the precise the step where interference occurs.

3.3.1.3 Comment on analysis of hypermutations caused by sheep A3.

Sequencing of JSRV proviruses clearly demonstrated the cytidine deaminase activity of sheep A3-Z2 and A3-Z2Z3. In contrast the small number of sequence alterations observed in proviruses of A3-Z3 stocks could be attributed to the background of the assay. Those mutations could be caused by a mutation arising during JSRV-GFP production, reverse transcription, somatic mutation during cellular division, PCR error and finally mutations occurring in bacterial cultures used to amplify pGEM clones.

Mutations other than G to A changes indicate non-A3 induced mutations and are an additional measurement of the experimental background. The calculated mutation frequency readout is affected by the sequence itself and is caused by the surrounding bases sequence context to guanidines (Harris and Liddament, 2004, Ebrahimi et al., 2014).

However, there is a need to be aware that the calculated frequencies of editing may be altered by a preference of PCR to more robustly amplify non-edited templates. This effect could be caused due to possible mis-matching of primers to edited sequences. Moreover denaturation temperature could decrease, due to the fact that the edited DNA which contains more A and T and in consequence makes it easier to dissociate than the one with higher G and C content.

Moreover, bands were relatively fainter on agarose gel in all PCR amplifications when DNA from cells infected with A3-Z2 or A3-Z2Z3 stocks was used (data not shown). Therefore, taking into account the number of cycles used, the lower amount of product may not only be connected with decreased proviral copy number but may also be a result of decreased PCR performance. Additionally a selective PCR might be partially responsible for alteration of mutation frequencies between A3-Z2 and A3-Z2Z3, because of the different distribution pattern of mutations (see Fig. 3.21). Therefore, I speculate that the actual A3-Z2 hypermutation frequency could be even higher than measured. In order to examine this further, an extensive analysis of other regions in proviruses could be performed using multiple sets of primers and lower denaturation temperatures (MacMillan et al., 2013).

In order to clarify the potential of sheep A3 to hypermutate JSRV, sequencing of proviruses resulting from $JSRV_{21}$ containing A3 was performed. Sequencing of 1kb fragments of the *env* gene in proviruses demonstrated that $JSRV_{21}$ may be hypermutated by sheep A3-Z2 and A3-Z2Z3 similarly to the JSRV-GFP. This finding suggests a possibility that JSRV might have an A3 evasion strategy *in vivo*, as there is a very low level of polymorphism among different isolates and lack of quasispecies.

3.3.2 JSRV appears not to have an interference mechanism against APOBEC3

In a number of cases A3 is a determinant of species specificity in retroviral infections. Some retroviruses have evolved sophisticated evasive mechanisms targeted against their host's A3, while remaining vulnerable to A3 proteins of other species. It could be speculated that JSRV might have a specific mechanism for inhibiting endogenous A3 that is active *in vivo* but not in *in vitro* assays.

Although A3-Z1 and A3-Z3 were packaged into JSRV virions *in vitro*, they did not have such a dramatic effect on JSRV infectivity as A3-Z2 or A3-Z2Z3. This suggests the possibility that JSRV might have a mechanism to protect against A3-Z1 or A3-Z3 but not A3-Z2. It would partially explain the two results appearing to be contradictory. Firstly, the lack of detected hupermutations and lack of dramatic infectivity reduction among A3-Z3 stocks was demonstrated. Secondly, the reverse transcriptase activity was decreased in stocks containing the highest amounts of A3-Z1 and A3-Z3. There is a possibility that there are uncharacterised traits of JSRV virion structure or the existence of an interference mechanism against A3 might make it resistant to packaged A3-Z1 and A3-Z3. The A3-induced decrease of RT activity was detected in virions that were lysed during the RT assay. It is possible that the lysis step might bypass JSRV potential evasive mechanisms against A3.

3.3.2.1 Could the use of an *in vitro* system have influenced the results?

The observed vulnerability of JSRV to ruminant A3 *in vitro* may potentially be an artefact of the reporter vector system utilised and the lack of an *in vitro* method which permits complete replication. For example, the high expression of A3 proteins might have reduced the amount of extrachromosomal transfected DNA, which in turn may have affected the dynamics of virus production (Stenglein et al., 2010).

The JSRV-GFP might have slightly different properties than $JSRV_{21}$. However, this is unlikely to be the case because sheep A3 reduced provirus copy number and hypermutated the viral genome for both the JSRV-GFP and the $JSRV_{21}$. However, the possibility that the virus producer cell line influenced the *in vitro* experiments should

not be excluded. JSRV was made in human derived 293T cells with a phenotype that is very different to the cells in which JSRV replicates *in vivo*. JSRV might have an unidentified factor which may be expressed or be active in sheep lung cells but not 293T. In addition, endogenous retroviral proteins in sheep cells *in vivo* could potentially influence the activity of A3 (Arnaud et al., 2007a). However, the expression of enJSRV RNA in lung tissue is low (Palmarini et al., 1996). There is a chance that in cells where JSRV replicates, so far unidentified interactions could occur between both viral and host proteins and nucleic acids. The possibility of a role for the bacterial flora or the cellular miRNA transcriptome within the lung in JSRV biology cannot be excluded. Moreover, the state of cells to permit replication might be dependent on the chemokine environment and other factors linked to the fact that infection occurs *in vivo*. Additionally, the virus producing cells make replication-defective virions and this effect is difficult to estimate both *in vitro* and *in vivo*, but possibly affects the dynamics of incorporation of molecules such as A3.

Both the proteome and miRNA transcriptome of lung epithelial and OPA tumour cells might enable potential virus-host interactions that have not yet been characterized (Nathans et al., 2009, Bogerd et al., 2014). To address these uncertainties, an extensive comparison between the proteome and transcriptome of *in vitro* models and both the healthy lung and OPA tumour in the various stages and different age of animals could be performed. Additionally, cases of non-virally originated sheep and human lung tumours should be compared in this way in order to identify transformation patterns and eventual expression of viral genes. Such extensive comparison could provide a list of proteins and RNAs involved in the support or inhibition of JSRV replication.

3.3.3 APOBEC3 is not detected in lung fluid samples from OPA sheep

The *in vitro* experiments performed during this study demonstrated that ruminant A3 has the potential to inhibit JSRV and suggests that hypermutation is an important mechanism of restriction. However, the high conservation of the JSRV genome among different field isolates and the lack of emergence of quasispecies during disease progression (Griffiths et al., 2010), suggests that JSRV is not affected by A3 activity

in vivo. Therefore, lung fluid from natural OPA cases was analysed in order to determine whether A3 is present inside *in vivo* produced JSRV (see Section 3.2.8).

Analysis of the presence of A3-Z2 and A3-Z3 did not detect those proteins in lung fluids from OPA affected animals. The lung fluid was not analysed for the A3-Z1 content, because RT-PCR analysis indicated that A3-Z1 is not expressed in sheep and cow lung tissue (see Section 2.2.1). Other experiments showed that A3-Z1 does not impact the disease pathology. Therefore, the lack of strong inhibition of JSRV *in vitro* by sheep and cow A3-Z1 discouraged the need to develop antibodies against this protein.

Since A3-Z2, A3-Z3 or A3-Z2Z3 were not detected in field samples (see Sections 3.2.8 and 3.3.4), it was necessary to determine the sensitivity of the assay. Therefore, I extrapolated from published studies on A3 content in ΔVif HIV virions in order to estimate the assay's sensitivity threshold.

Previous studies on A3 encapsidation by ΔVif-HIV provided an estimate of the quantities of structural proteins forming a single virus. Analysis performed on ΔVif HIV produced in the presence of 2 μg of pcDNA huA3G mammalian expression vector estimated by HPLC that the molar ratio of encapsidated huA3G to Gag is 1:439 (Xu et al., 2007). Assuming that in a single HIV virion there are approximately 1500 (Zhu et al., 2003) or 5000 (Briggs et al., 2004) Gag molecules, then according to the estimated molar ratio there should be 3-11 huA3G molecules per single virion. Therefore, there is a possibility that the method utilised in the present study was not sensitive enough to detect such a small amount of A3. Taking into account the Gag content in a single virion, I estimate that there are 4 or 20 molecules of A3 packaged as a result of 1 μg or 4 μg of A3 expression vectors utilised in transfection. Therefore, based on the molecular mass of A3-Z2Z3, there are between 200 kDa (4 × 50 kDa) and 1000 kDa (20 × 50 kDa) in a single virion, which is equal to 3.32×10^{-18} g and 1.62×10^{-17} g respectively.

The analysis performed by Cousens et al. demonstrated that there is from 10^4 to 10^8 copies of JSRV RNA in 1 μl of lung fluid of sheep affected by OPA (Cousens et al., 2009). Therefore, on average, 1 μl of lung fluid contains 5×10^5 virions. In the present

study, lung fluid was concentrated 200 times to yield approximately 10^9 virions in each 10 µl sample analysed by western blot. The western blot analysis of Gag content showed that there is more JSRV present in the concentrated lung fluid samples, than in the virus produced *in vitro*. Therefore, extrapolating from values calculated above based on the HIV studies, we might expect that there should be at least 1.62 ng of A3-Z2 or A3-Z3 per lane. This should be detectable, given the sensitivity of the western blot (see Section 3.2.9). Thus, significantly less than the estimated 1.62 ng of A3 present in each sample of virus produced *in vitro*. In conclusion, I hypothesise that there is no A3-Z2, A3-Z3 or A3-Z2Z3 in JSRV from the lung fluid samples tested, to a level which is sufficient for JSRV restriction. These calculations are summarised in Fig. 3.27.

N_{gag} - Number of Gag molecules per single HIV -1 virion ~ 1500 to 5000 (Zhu et al. 2003; Briggs et al. 2004)

$R_{A3\,/\,Gag}$ - Molal ratio of Gag to encapsidated A3 ~ 439 : 1 (Xu et al. 2007)

$N_{A3\,/\,VIR}$ - Number of A3G molecules per ΔVif HIV-1 virion (amount of Gag / 439) ~ 7±4 (Xu et al. 2007)

Estimated number of A3-Z2Z3 molecules when 1 µg or 4 µg of expression vector are used in transfection ~ 4 (1 µg) or 20 (4 µg)

$M_{A3\,/\,VIR}$ - Estimated mass A3-Z2Z3 in a single virion (A3-Z2Z3 molecular mass ~50 kDa)

There are 200 kDa (4 × 50kDa) or 1000 kDa (20 × 50kDa) in a single virion, which is equal to 3.32×10^{-19} g and 1.62×10^{-18} g

N_{JSRV_LF} - Number of JSRV RNA copies in 1 µl of lung fluid is 10^4 to 10^8 (Cousens et al. 2009) ~ 5×10^5 virions

$N_{concsample.LFJSRV}$ Number of JSRV virions in tested 10 µl of 200 × concentrated lung fluid ~ 10^9

$MA3_{SAMPLE}$ - Estimated minimum total mass of A3-Z2Z3 in tested sample (where is less Gag than in 10 µl of concentrated lung fluid)

$$MA3_{SAMPLE} = (N_{gag} / R_{A3\,/\,Gag}) \times M_{A3\,/\,VIR} \times N_{JSRV\_LF} \times 200 \text{ (concentration factor)} \times 10 \text{ (volume of sample tested)}$$

$MA3_{SAMPLE}$ Extrapolating from a calculated mass of A3 content in ΔVif HIV, the expected total mass of A3-Z2Z3 in 10 µl of concentrated "4 µg stock" is 1.62 ng

Fig. 3.27 Estimation of A3 content in the JSRV samples produced *in vitro*
Calculations are based on the reported estimated Gag content in HIV-1 and number of encapsidated A3 in ΔVif Virions and on the average amount of JSRV from lung fluid samples.

The ideal imaging technique for the detection of A3 encapsidated inside a virion might be electron microscopy utilising gold labelled antibodies. Such an experiment might potentially determine the precise location of A3 proteins inside a virion. However, a relatively small number of encapisdated A3 protein molecules inside a single virion might still be difficult to detect with such an approach.

In summary, *in vitro* produced JSRV is restricted by A3, even when made in the presence of 0.25 or 1 µg of A3-Z2 and A3-Z2Z3 expression vector. *In vivo* produced JSRV does not encapsidate a detectable amount of A3.

3.3.4 JSRV target cells in the lung do not express A3

The failure to detect A3 in OPA lung fluid suggests that A3 does not restrict JSRV *in vivo* in lung epithelial cells. Despite the calculation presented in the preceding section, there remains a theoretical possibility that lung fluid may still contain a small but undetectable amount of A3-Z2 or A3-Z2Z3. However, the fact that the JSRV genome is stable among field isolates supports the finding that A3 is not present in JSRV virions.

In order to clarify whether JSRV avoids A3 restriction *in vivo* because this restriction factor is not expressed in cells where JSRV replicates, OPA and normal healthy lung were analysed by immunohistochemistry (IHC) using antibodies to ovine A3-Z2 and A3-Z3 (see Section 2.10.8). (Note that the similarity of A3 protein sequence between ruminants should allow antibodies generated against sheep proteins to also be utilised against goat and cow). Due to time constraints the IHC was done by Jeanie Finlayson (MRI, Pathology Department). IHC of sheep and goat JSRV- transformed lung tissue labelled with anti A3-Z2 antibody or pre-immune serum is shown in Fig. 3.28.

Antisera raised against sheep Z2 (Figure 3.28) or Z3 (not shown) did not label either normal lung epithelium or JSRV-transformed lung tissue. Similar results were observed in lung tissue from experimentally infected sheep and experimentally infected goats (from a previously published study (Caporale et al., 2013a) and kindly provided by Marco Caporale). In contrast, alveolar macrophages in both species labelled positively with the antibodies against Z2 and Z3 (see panels A and B in Fig. 3.2). These results suggest that there is a lack of A3 expression in lung epithelial cells (the targets of JSRV replication) and suggests that JSRV avoids the activity of A3 proteins *in vivo* by infecting cells that do not express this restriction factor. Furthermore, the similar pattern of labelling in goats as in lambs suggests that A3 expression *in vivo* is not responsible for the species specificity of OPA for sheep. Further experiments are needed to determine whether cow lung epithelial cells express A3.

Additional controls used in the IHC included analysis of transfected 293T cells expressing the different ruminant A3 proteins. These were embedded in gelatin and

fixed in wax blocks to mimic the tissue (see Section 2.10.10.3). These controls verified the cross reactivity of anti-Z2 and anti-Z3 between different ruminant A3 family members.

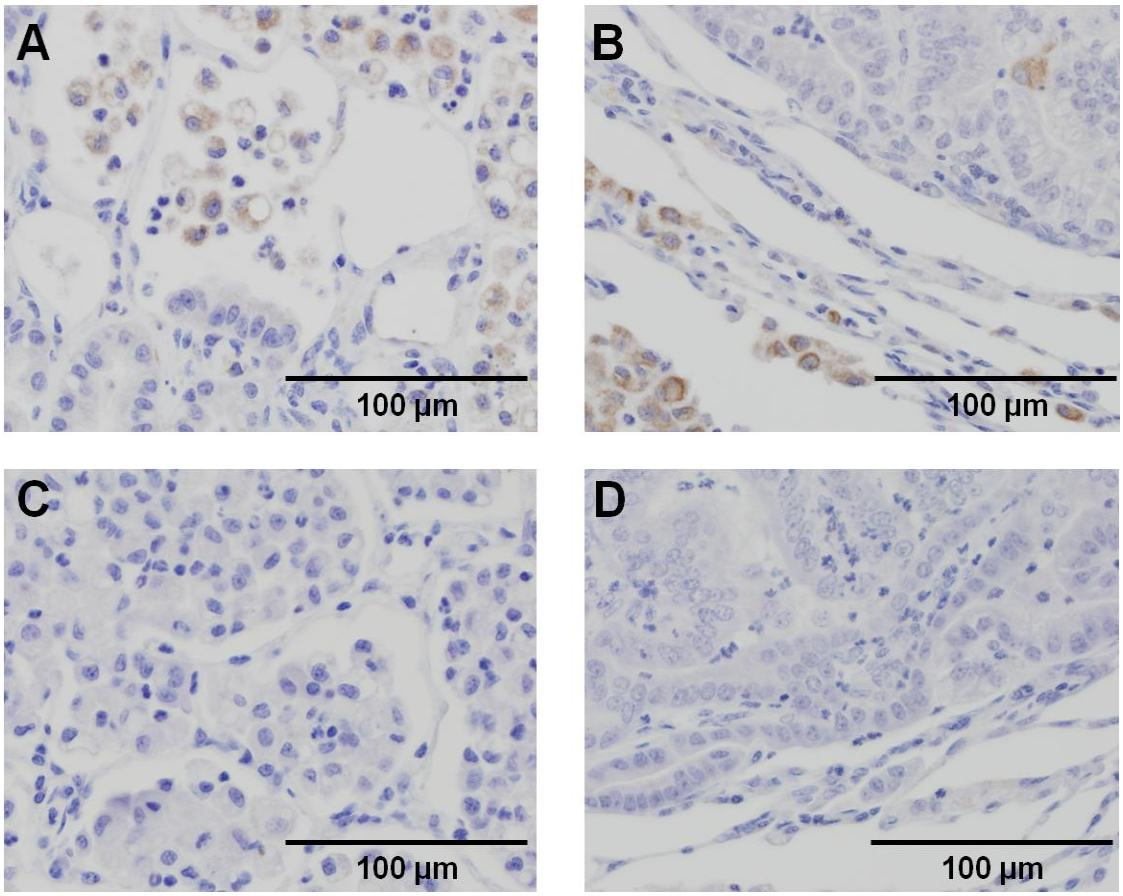

Fig. 3.28 Immunohistochemistry analysis of sheep and goat lung transformed by JSRV
Anti A3-Z2 antibody labels only infiltrating macrophages in sheep (Panel A) and goat (Panel B) JSRV-transformed lung. Pre-immune sera from the same rabbit was utilised as a negative control for non-specific labelling of sheep (Panel C) and goat (Panel D) JSRV-transformed lung. Scale is indicated at the right bottom of each panel figure.

Despite the data obtained so far, further analysis is required to rule out any role for evasion of A3 function by the product of the JSRV *orf-x* gene. However, there is an indication that Orf-X does not have any important role in tumourigenesis since experimentally animals infected by $JSRV_{21}$ carrying a truncated *orf-x* resulted in no difference compared to wild type $JSRV_{21}$ in experimental infections (Cousens et al., 2007).

3.3.5 Impact of APOBEC3 on OPA epidemiology – Conclusions

Only sheep develop OPA. Therefore, it is perhaps surprising that sheep A3-Z2 and A3-Z2Z3 are able to inhibit virus replication *in vitro* to a similar degree as their ruminant homologues in cows and goats. However, JSRV isolates are characterized by a stable genome among different isolates, and quasispecies do not emerge during infection, suggesting that there is a lack of ongoing hypermutation *in vivo*. Both the *in vitro* potential of sheep A3 to inhibit JSRV and the lack of hypermutation signatures present in infected animals, could be explained by a JSRV-specific evasion strategy against restriction factors or simply the lack of expression of A3 in the cells where JSRV replicates. The lack of detectable A3 in virus isolated from lung fluid from OPA-affected sheep and the absence of A3 protein in lung epithelial cells of both normal and transformed lung tissue strongly indicate that JSRV avoids A3 activity *in vivo* by replication in cells that do not express it. The evolution of retroviruses to use this strategy to avoid the activity of A3 has not been described previously.

Chapter 4 - The effect of mouse and human APOBEC3 on JSRV replication

4.1 Introduction

The results presented in Chapter 3 demonstrate the restrictive activity of ruminant A3 proteins against JSRV. To extend these studies, I next investigated the interplay between JSRV and mouse APOBEC3 (muA3) and several human APOBEC proteins (huA1, huA2, huA3DE, huA3F, huA3G) *in vitro*. Although JSRV does not seem to be pathogenic among mice or humans, these experiments were performed in order to improve the understanding of species specificity of A3-JSRV interactions.

4.1.1 Why study the interaction of human APOBEC3 with JSRV?

Humans are not recognised as a natural host for JSRV and there is no documented human disease resembling the clinical signs of OPA. However, some forms of non-invasive human lung cancer have features that resemble OPA at the histological level (Palmarini and Fan, 2001, Mornex et al., 2003) (See Section 1.1.4). In addition, this type of lung tumour has the weakest association with smoking, which suggests a possible role for genetic factors or other environmental factors, such as viruses (De las Heras et al., 2007, Sun et al., 2007). Notably, human Hyal-2 can be utilised as an entry receptor for JSRV and JSRV Env can transform some rodent and human cell lines *in vitro* (Maeda et al., 2001, Miller, 2008, Wootton et al., 2006a).

Several groups have attempted to define the possible connection of human non-invasive lung cancer with a viral aetiology. Most of those studies have focused on the detection of a virus related to JSRV in human tumour specimens (Hopwood et al., 2010). Approximately 30% of human lung adenocarcinomas were positive for the presence of an epitope reacting with anti-JSRV Gag antibody (De las Heras et al., 2000b). Additionally, a recent study reported the presence of an antigen related to JSRV Env and the presence of JSRV Env related sequences in a subset of lung adenocarcinomas and squamous cell carcinomas (Linnerth-Petrik et al., 2014). The positive staining of some lung tumour sections could be caused by expression of an endogenous retrovirus whose potential impact on transformation is not yet characterised. Alternatively, it might be a result of a non-specific cross-reaction of antibodies with a non-viral cellular protein, whose expression is upregulated by

transformation (De las Heras et al., 2007, Hopwood et al., 2010). Despite the lack of other viral markers in lung tumours, the possibility that the aetiology of these tumours is connected with an unknown exogenous retrovirus cannot be ruled out (Hopwood et al., 2010). In light of these studies of human infection with JSRV, it is of interest to ask whether human A3 proteins can restrict JSRV.

4.1.2 Reasons for studying the effect of mouse APOBEC3 on JSRV replication

An *in vivo* disease model of OPA in new-born lambs has been available for many years (Palmarini et al., 1999a). However, although this model has provided valuable insights into OPA pathogenesis it does have some disadvantages. For example, experiments in sheep are expensive and only available to a small number of laboratories with facilities capable of handling large animals. Therefore, the development of a small animal model of OPA would provide a more tractable *in vivo* tool for investigating JSRV biology and its role in carcinogenesis.

Mice would be an ideal candidate as a small animal model of OPA due to the availability of reagents and a significant publication background as a cancer model. Notably, mice have already been used in experiments for JSRV Env-induced tumourigenesis. However, adeno-associated virus vectors were utilised in those experiments (Wootton et al., 2006a, Wootton et al., 2006b, Vaughan et al., 2012).

An additional limitation for the utilisation of mice as a model for OPA is that mouse Hyal-2 is only a weak JSRV receptor (Miller, 2008). However, this issue could potentially be solved by the creation of a transgenic line expressing a permissive receptor or by utilising JSRV pseudotyped with an alternative envelope protein.

Investigation of mouse restriction factors against JSRV may direct the development of a small animal model of OPA and further extend understanding of the species specificity of JSRV infection. In this project I investigated the impact of mouse A3-Z2Z3 on JSRV replication.

4.2 Results

4.2.1 Impact of mouse and human APOBEC on JSRV replication

In order to investigate the role of mouse and human APOBEC proteins on JSRV replication *in vitro*, mammalian expression plasmids encoding these proteins were obtained from AddGene. Murine A3 (muA3) and several human APOBEC proteins (huA1, huA2, huA3DE, huA3F, huA3G) were used in the JSRV-GFP reporter assay in parallel with sheep A3-Z2Z3 (see Section 2.10.6).

4.2.2 Human and mouse APOBEC are packaged by JSRV

The detection of encapsidation of APOBEC by JSRV was the first step in investigating of restriction mediated by mouse and human APOBEC proteins. Concentrated virus stocks were made in the presence of V5 epitope-tagged muA3 and huAPOBECs and then tested by western blot for evidence of their encapsidation (See section 2.10.7 and Fig. 4.1). Virus stocks were produced by cells transfected in 6-well plates, utilising 0.8 µg of APOBEC expressing vector (the molar ratio of Gag-Pol and envelope encoding DNA used is equivalent to the 4 µg samples on a T-75 flask scale; the highest amount tested in Chapter 3).

This analysis indicated that mouse A3 and human A3DE, A3F, A3G and A2 are packaged by JSRV-GFP (JSRV Env pseudotyped), as shown by the detection of V5-tagged proteins by western blotting of concentrated virus (see Fig. 4.1.A). In contrast, hA1 was not packaged by JSRV in these experiments, supporting the specificity of encapsidation of the other APOBEC proteins. Note that, spill over of sample occurred in panel (A), since there is a faint band in the "No A3 stock" lane, but the "S A3-Z2Z3" which lacks a V5 epitope tag and "No A3 cellular extract" lanes are negative.

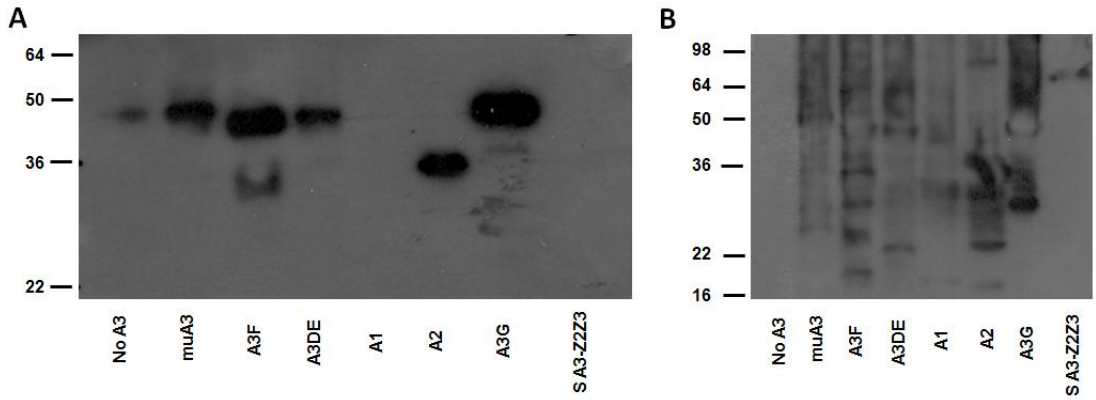

Fig. 4.1 JSRV encapsidates V5-tagged human and mouse APOBECs
Panel (A) demonstrates encapsidation of V5-tagged APOBEC proteins in concentrated JSRV virus stocks. Panel (B) shows detection of V5-tagged APOBECs in cellular extracts of transfected 293T cells. JSRV virus stocks were made by transfection together with the indicated A3s (mu-mouse, S-sheep, human APOBECs are described by their original names – letters and numbers) or a vector without A3 (No A3). The molecular weight marker bands representing protein size (kDa) are displayed on the right side of each figure.

4.2.3 Effect of mouse and human APOBECs on JSRV infectivity

The previous experiment showed that JSRV is able to package mouse and human APOBECs. Next, I tested the infectivity of these virus stocks *in vitro*, as had been done with ruminant A3s (see Chapter 3). Flow cytometric analysis demonstrated that JSRV-GFP (JSRV VSV-G pseudotyped) infectivity is reduced by mouse A3 and some of the human APOBECs tested (see Fig. 4.2).

The mouse A3 was identified as a strong inhibitor of JSRV and was active to a similar degree as sheep A3-Z2Z3. Human A3F restricted the infectivity of JSRV GFP six-fold, while A3G reduced the infectivity by 50% and A3DE had a mild restrictive activity. Although huA2 was packaged by JSRV GFP (see Fig.4.2. A), it did not show any antiviral activity. Since huA1 was not packaged, this stock became an additional internal reference control for infectivity. The difference of infectivity and fluorescence of cells infected by “A1” and “No A3” stocks, are most likely to be caused by variation in the assay system. The data presented in Fig. 4.2 shows the readout of one of two experiments, values represent an average of wells infected in duplicate. However, two virus amounts were tested and the results shown represent the average of cells infected in duplicate by the higher amount of virus.

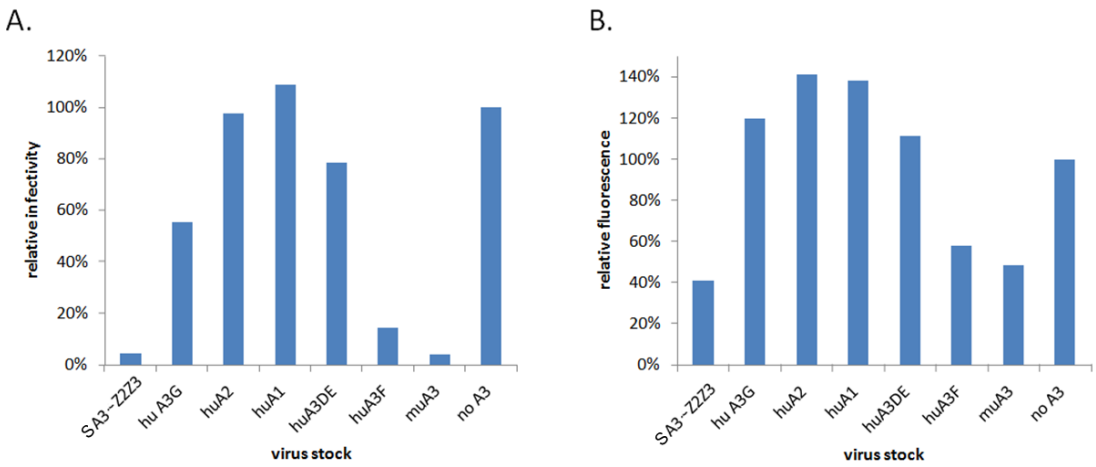

Fig. 4.2 The impact of mouse and human APOBEC proteins on JSRV infectivity
Flow cytometric result of CRFKovH2 cells infected by JSRV Env pseudotyped JSRV-GFP. Graph (A) shows the relative percentage of cells infected by virus produced in the presence of the indicated A3s (mu-mouse, hu-human, S-sheep) and a vector control without A3 (no A3). Graph (B) shows the relative fluorescence intensity (FITC median) of infected CRFKovH2 cells. The relative infectivity values are based on the proportion of GFP-positive cells infected by "APOBEC stocks" compared to cells infected by "no A3 stock".

4.3 Discussion

In this Chapter, mouse A3 was shown to be a strong inhibitor of JSRV replication. The human A3 proteins tested were packaged by JSRV but their impact on its replication was not as strong compared to the potent restriction of JSRV caused by muA3 and sheep A3-Z2Z3.

While these data appear reproducible, it should be noted that the experiment was only performed twice and further work should be conducted to perform more replicates and analyse the impact of intermediate amounts of APOBEC. In addition, further analysis of the restriction mechanism by sequencing of proviral clones and RT-assays performed on virus stocks would extend understanding of the restriction mechanism of mouse and human A3s in JSRV.

4.3.1 Restrictive character of mouse APOBEC3

Mouse A3 was identified as a potential JSRV restriction factor. However, as shown in Chapter 3 in ruminants, *in vitro* assays may not predict whether restriction factors are *in vivo*. Therefore, determining whether A3 is expressed in mouse lung epithelial cells would provide further clues towards understanding OPA species-specificity and the possibility of using mice as a small animal model. Even if mice do not express A3 in lung epithelial cells then the different anatomy of the mouse respiratory tract compared to that in sheep would need to be taken into account during interpretation of *in vivo* experiments.

Mice would be a robust tool as a small animal model of OPA, because of the easy access to different lines or breeds, various reagents and a number of publications concerning carcinogenesis, where these animals were utilised. Moreover, the genetic engineering techniques available in mice are at a far more advanced level in comparison to other mammalian species. Mice deficient in A2 or A3 have been created and their deletion did not have any major effect on their survival or fertility (Mikl et al., 2005). Although A2 is expressed in all vertebrates in muscles, the tissue histology features of A2 knockout mice was unaffected. Notably, muA3 deficiency results in an increased vulnerability to retroviral infections caused by MMTV (Okeoma et al., 2009b) and MLV (Nair et al., 2014).

Mouse APOBEC1 has been shown to restrict Friend-mouse leukaemia virus (Petit et al., 2009), and it would be interesting to determine its restriction potential against JSRV. However, creation of mice deficient in APOBEC1 could be difficult, because of its physiological function in gastrointestinal tissues, where it deaminates cytosine to uracil at position 6666 in the RNA encoding apolipoprotein B (Navaratnam et al., 1993). Since mouse APOBEC1 may act as a potential restriction factor, it would also be interesting to evaluate the role of its ruminant homologue against JSRV.

Although mice have only one A3 gene, several different alleles and splice variants have been described, and these different forms have a variety of inhibitory activities against MMTV (Okeoma et al., 2009b). A single nucleotide polymorphism present in

some A3 alleles affects its mRNA splicing pattern, and this impacts on the amount of muA3 packaged into MMTV and in consequence its infectivity (Okeoma et al., 2009b). Therefore, this observation could direct further research on the epidemiology of OPA in different breeds and species of sheep, which may be dependent on A3 allele polymorphism. It is perhaps unlikely that there exists an allelic variant which protects against OPA significantly more than others, because it would be positively selected during the course of evolution of *Ovis.* Notably, the selection of a putative protective A3 variant would be difficult due to the fact that sheep develop disease after they reproduce. Moreover, since sheep A3 is not expressed in sheep lung epithelium (see Section 3.3.4), this suggests that JSRV avoided its restriction, by selecting a tissue tropism enabling its replication in the absence of A3 (see Chapter 4) and tetherin (Arnaud et al., 2010). I speculate that promoter polymorphism could contribute to variation in the expression pattern of A3 or other restriction factor's in tissues, which might partially explain the differential susceptibility of some sheep to OPA among flocks.

The weak interaction of murine Hyal-2 receptor with JSRV Env is a major factor limiting the utilisation of those animals as model organisms for OPA. When this difficulty regarding the utilisation of mice as a model for OPA is bypassed, it will be necessary to verify A3 expression patterns. If A3 is expressed in mouse lung epithelium, then there would be a need to utilise mice which are deficient in functional A3 (already available). However, utilising A3 knockout mice may also alter the tissue tropism of the virus.

Published work on mouse APOBEC has demonstrated the significance of endogenous A3 in the context of protecting against retroviruses pathogenic in the same species (Ross, 2009). Furthermore, the observed restriction caused by endogenous A3 may in some way be beneficial for the virus, because mild restriction of infection prolongs the life of the virus-shedding animal. Moreover, A3 mediates the editing of the viral genome, which contributes to its increased evolution rate (Jern et al., 2009).

4.3.2 Restriction of JSRV by human APOBEC3

Some human APOBEC proteins were identified as potential determinants of OPA species-specificity. Even though the majority of huAPOBECs are packaged by JSRV, only huA3F has relatively strong inhibitory potential against JSRV, almost as strong as its sheep and mouse paralogues. The huA3G is known to be one of the strongest retroviral inhibitors of ΔVif HIV-1, but it has only mild activity on JSRV. There is a possibility that some human A3 alleles might be more or less protective against JSRV, similar to the reported variable antiviral activity of various primate A3G haplotypes against SIV (Krupp et al., 2013). Moreover, other human A3 proteins which were not investigated in this project (huA3A, huA3B, huA3C, huA3H) may have different inhibitory potential against JSRV. Notably, human and mouse APOBECs were expressed by transfection utilising pcDNA1 not pCI-Neo vectors as was done with sheep A3-Z2Z3 (see Sections 2.1 and 2.10.6), which might have resulted in difference of their expression levels and there is a need to be aware of its possible influence on results.

The function of human A2 is still largely unknown and there are no reports of its antiviral potential. Therefore, this study is exceptional due to the demonstration of A2 being encapsidated by JSRV as previous studies have not reported A2 encapsidation by retroviruses, even in overexpression conditions. Even though encapsidated it was not antiviral.

Although, there are no reports of JSRV being responsible for human disease, the results obtained indicate that the human APOBECs analysed protect against JSRV. However, other restriction factors may contribute to species specificity and JSRV may simply require other crucial host factors which enable it to cause tumours in sheep.

There is only weak evidence of a possible association of JSRV-like virus causing human lung cancer. Firstly, the immunoreactivity of some lung tumour with polyclonal antibodies to betaretroviral Gag (see Section 4.1) and anti-JSRV Env (Linnerth-Petrik et al., 2014). Secondly, there is a study presenting correlation of the occurrence of lung tumours among farmers working with goats (Lutringer-Magnin et al., 2012). However, goats do not develop OPA and the highest occupational exposure

to JSRV is expected to be among sheep farmers and this group was not identified as under a high risk in that study (Lutringer-Magnin et al., 2012). In my opinion, examination of prevalence of the lung tumours in a group of farmers with ocupational exposure to JSRV could provide direct epidemiological evidence for JSRV-induced pathogenesis in humans.

The detection of betaretroviral sequences from blood has been reported in only a few samples from African patients (Morozov et al., 2004). However, extensive attempts to detect the virus by PCR failed suggesting that if there is a virus responsible for some forms of lung cancers then it remains to be characterised (De las Heras et al., 2000b, Yousem et al., 2001, Hopwood et al., 2010). Therefore there is an interest in examining the interaction of JSRV with human A3 as this might provide information on whether JSRV or a related virus is likely to infect humans. An extensive investigation of lung cancer adenocarcinoma transcriptome in order to identify virus-related transcripts could provide better understanding of this issue.

Upregulated expression of human endogenous retroviruses has been detected in several types of cancer and their potential role in the transformation process remains to be determined (Voisset et al., 2008, Kassiotis, 2014). Given that around 8% of human DNA is derived from ERVs (Li et al., 2001), representing around 4000 proviruses (Bannert and Kurth, 2006), there are many possible targets to look for the evidence of retroviral association with cancer. Even though people have been exposed to JSRV by contact with OPA affected sheep, there is a lack of clinical reports of human infections and the human genome does not contain enJSRV.

The results presented in this chapter imply that if there is any virus similar to JSRV, which is responsible for causing lung cancer among people, it would be restricted by huA3F. The fact that only huA3F was shown to have a strong inhibitory activity towards JSRV could be explained by the fact that primate A3 proteins evolved specifically to target their own viruses, not towards others which do not pose a threat like JSRV requiring additional host permissiveness factors for replication. Finally, the A3 expression patterns across different cell types would impact on the significance of restriction actively.

This study found that huA3G did restrict JSRV, but not as strongly as it is able to restrict ΔVif HIV (Harris and Liddament, 2004, Holmes et al., 2007a, Sheehy et al., 2002). This difference in restriction potential may be due to the fact that A3G contains the Z1 domain, which among ruminants was found to mildly restrict JSRV (see Section 3.2.3). The observed similar median fluorescence level of cells infected with JSRV stocks carrying various human APOBECs (with the exception of A3F) suggests that infected cells do not contain hypermutated JSRV proviruses, although that was not investigated directly in the present study. Additional sequencing of proviruses would provide more solid evidence regarding the deamination potential of human APOBECs against JSRV. Since huA3s have been demonstrated to cause genome editing in other viruses, this study highlights the differential sensitivity of the RT proteins of different retroviruses to diverse APOBEC family proteins.

In summary, this chapter demonstrated that JSRV can encapsidate muA3, huA3DE, huA3F, huA3G and huA2, although only muA3 and A3F strongly restricted JSRV replication. In contrast, to the A3G and A3DE caused mild restriction, while no antiviral activity of huA1 and huA2 was detected. Further understanding of the comparison between retroviral RT enzymes and their vulnerability to various APOBECs could result in the development of new disease control strategies.

Chapter 5 – Impact of TRIM5 on JSRV replication

5.1 Introduction

The TRIM family of proteins consists of approximately a hundred members in humans with a variety of different functions. Several TRIM proteins have been shown to interfere with viral replication at various stages (see Section 1.8.3.3) (Pertel et al., 2011, Huthoff and Towers, 2008, Uchil et al., 2008). Interest in TRIM5α (T5α) was stimulated by the fact that T5α mediated restriction was demonstrated to be responsible for the resistance of Old World monkeys to HIV-1 (Stremlau et al., 2004). Since then T5α has emerged as an important mediator of species-specific restriction of a number of retroviral infections (Perron et al., 2004, Si et al., 2006, Li et al., 2013b, Rahm et al., 2011).

TRIM5 (T5) proteins have been characterised mostly in primates and in several non-primate species (Li et al., 2013b, McEwan et al., 2009, Si et al., 2006, Tareen et al., 2009). This chapter investigates the sensitivity of JSRV to various T5 proteins. The restriction mediated by T5 is based on a post-entry block to incoming virions; by binding to their capsids, T5 targets them for degradation (Diehl et al., 2008). In addition to the direct inhibition of retrovirus, the ability of T5 to recognise capsids has been shown to mediate a virus sensing mechanism, which in consequence activates the signalling pathways which lead to expression of genes involved in antiviral responses (see Section 1.8.3.2) (Pertel et al., 2011, de Silva and Wu, 2011).

However, due to the rapid evolution of TRIM family genes, the analysed ruminant proteins should not be properly referred to as "alleles or homologues of T5α" (Malfavon-Borja et al., 2013). The lability of those genes makes it is difficult to precisely define their origin and relativeness (Si et al., 2006, Han et al., 2011, Malfavon-Borja et al., 2013). However, for simplicity here they are referred to as "TRIM5 alleles or homologues".

The selective pressure caused by T5 recognition of capsids can drive evolution of structural retroviral genes in order to escape restriction. For some restriction factors, notably A3 and tetherin, retroviruses have acquired proteins to counteract their activity (Mariani et al., 2003, Neil et al., 2008, Morrison et al., 2014). Currently no viral protein that inhibits T5 has been described. Therefore, T5 may be a promising target in

disease control strategies. In addition, there is a need to be aware of possible T5 mediated restriction during the development of viral vectors for use in gene therapy.

Little has been reported previously on the activity of ruminant TRIM proteins (Si et al., 2006, Fletcher and Towers, 2013). Therefore, in the present study, I investigated the possibility of T5 being involved in the species-specificity of JSRV infection among ruminants. Additionally, rhesus macaque and human homologues were also tested for their ability to restrict JSRV.

5.2 Results

At the time this study was initiated (Oct 2009), the sheep and goat T5 genes had not been identified or cloned. Therefore, initially sheep and goat T5 genes had to be isolated by RT-PCR and cloned into a MLV retroviral vector backbone (see Section 5.2.3). Subsequently, these MLV viral vectors were used to transduce the permissive cell line CRFKovH2, enabling antibiotic selection of cells stably expressing both the T5 and antibiotic resistance gene (see Section 5.2.4). Once the stable expression of T5 had been demonstrated by flow cytometric analysis performed on intacellularly labelled cells (see Section 5.2.4.2), they were subjected to infections utilising JSRV-GFP (see Section 5.2.5.2).

5.2.1 Pilot study on permissivity of cell lines to JSRV

Four cell lines were infected with JSRV-GFP (VSV-G) in order to examine their permissiveness. Three days post-infection feline CRFK, rabbit RK 13-C, bovine MDBK and murine NIH 3T3 cells were subjected to flow cytometric analysis, shown in Fig. 5.1 (see Section 2.7.3).

This preliminary experiment implied that murine NIH 3T3 and bovine MDBK cells might be protected against JSRV by a post-entry restriction factor such as T5 in contrast to the permissive CRFK. The VSV-G pseudotyped JSRV-GFP was used to avoid the effect of species differences in the JSRV receptor. Similarly, the use of a GFP reporter driven by CMV promoter avoided the requirement for JSRV-specific

transcription factors. However, it is possible that other dependency factors such as cellular division rate and molecules involved in intracellular trafficking, might have influenced the results.

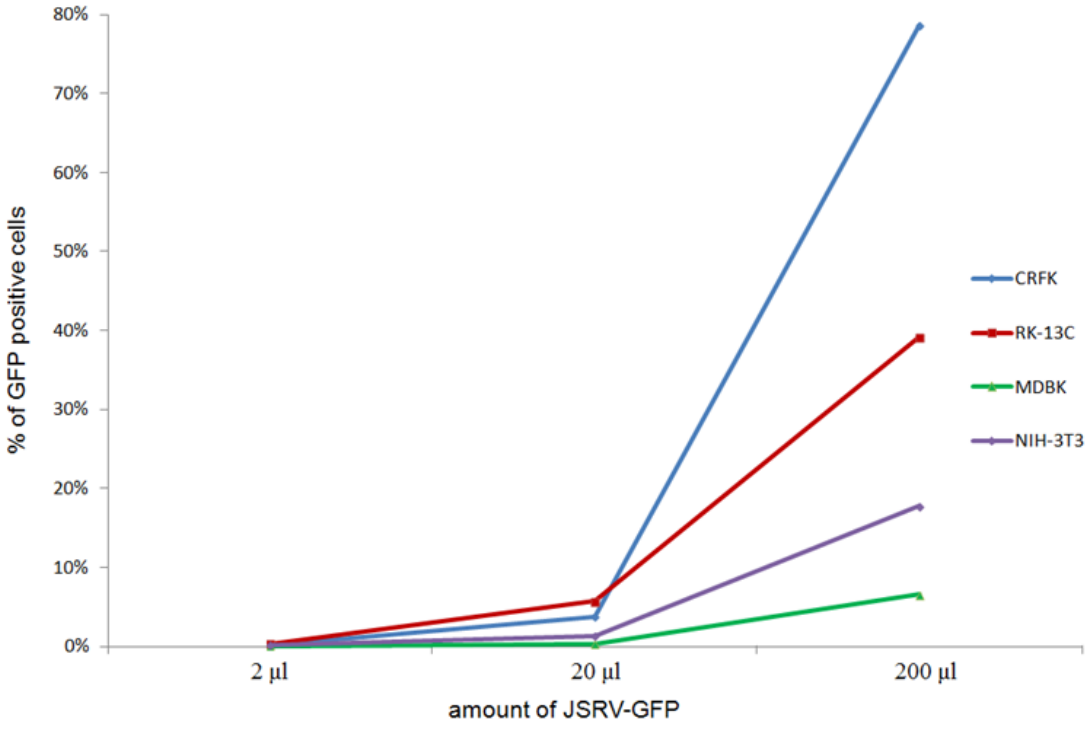

Fig. 5.1 Flow cytometric analysis of cellular permissiveness to JSRV-GFP
Analysis of JSRV-GFP VSV-G infected CRFK, RK 13-C, MDBK and NIH 3T3 cells. Cells were infected by serial dilutions of concentrated JSRV-GFP VSV-G (2 µl, 20 µl, 200 µl). The results shown indicate the percentage of GFP-positive cells obtained by infection of a single well.

5.2.2 Strategy for studying the impact of TRIM5 on JSRV replication

The experimental design is based on the utilisation of JSRV-GFP to infect cell lines that stably express T5 from various species (see Fig. 5.2). Any differences found in the permissiveness of a tested cell line would identify an antiviral T5 homologue.

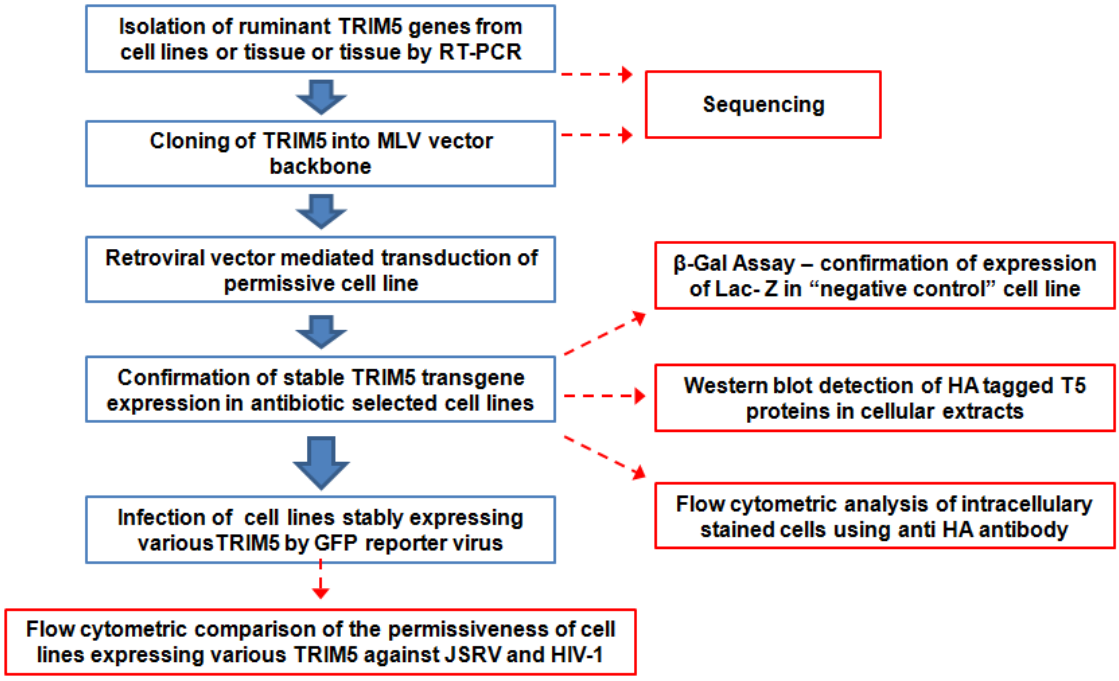

Fig. 5.2 The plan of investigation of the effect of TRIM5 on retroviral replication *in vitro*
Blue boxes: assays; Red boxes: results

5.2.3 Cloning of TRIM5 genes

Cloning of sheep T5 and identification of a goat homologue were the initial steps towards research on their relevance to OPA. At the time this study was initiated no sequences were identified as sheep T5 transcripts. A BLAST search of the EST database was performed using the cow protein (Si et al., 2006) as a query to identify EST entries from sheep and goat. The results identified several sequences overlapping part of the sequence. This approach allowed the identification of 5' and 3' termini of the T5 ORF, which allowed the design of primers for cloning (Table 5.1).

The products were amplified by RT-PCR and cloned into pGEM-T Easy, which enabled their sequencing (see Section 5.2.1.1). Representative clones were then chosen by alignment, re-amplified by high fidelity PCR and cloned into a MLV vector backbone (see Section 5.2.1.2), which was later modified by the addition of an IRES-Hyg cassette (see Section 5.2.1.3). The TRIM5 cloning steps are shown in Fig. 5.3.

Table 5.1 Sequences of ruminant TRIM5 containing mRNA

sequence origin, reference	gene reference
Cow [Moore, S.] – hypothalamus	Gb EH141776.1
Sheep [Wilson, T.] – dendritic cells	Gb EE819900.1
Sheep (Hecht et al. 2006) – bone	Gb DY491467.1
Sheep (Hecht et al. 2006) - bone	Gb DY501375.1
Sheep [Wilson, T.] – mucosal lymphoid tissue	Gb EE794007.1
Sheep [Green, J.]	Gb GT880467.1
Cow [Anderson, S.] – spleen	Gb AM031187.1
Sheep [Wilson, T.] – gall bladder	Gb EE780393.1
Sheep [Wilson, T.] – wool follicle	Gb EE855939.1
Sheep [Wilson, T.] – wool follicle	Gb EE864175.1
Sheep [Fell, M.] –Peyer's Patch, terminal illeum	Gb FE034648.1

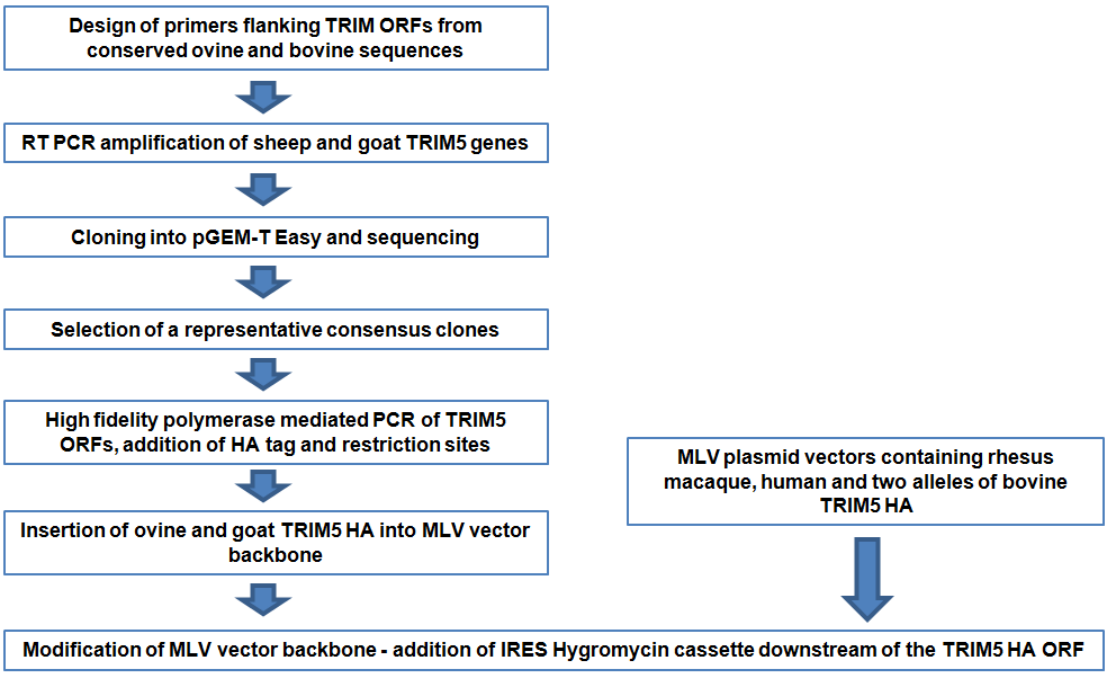

Fig. 5.3 Cloning steps of TRIM5 transgene carrying MLV plasmid vectors.

5.2.3.1 Isolation of sheep and goat TRIM5 (RT-PCR)

As a template for RT-PCR, I utilised RNA extracted from the sheep cell line CPT-Tert (Arnaud et al., 2010) and RNA from goat PBMC. Primers were designed to consensus regions located upstream of sheep and cow T5 ORF (TRIM-F1, TRIM-R1). The nucleotide alignment (see Fig. 5.4) was based on sequences shown in Table 5.1.

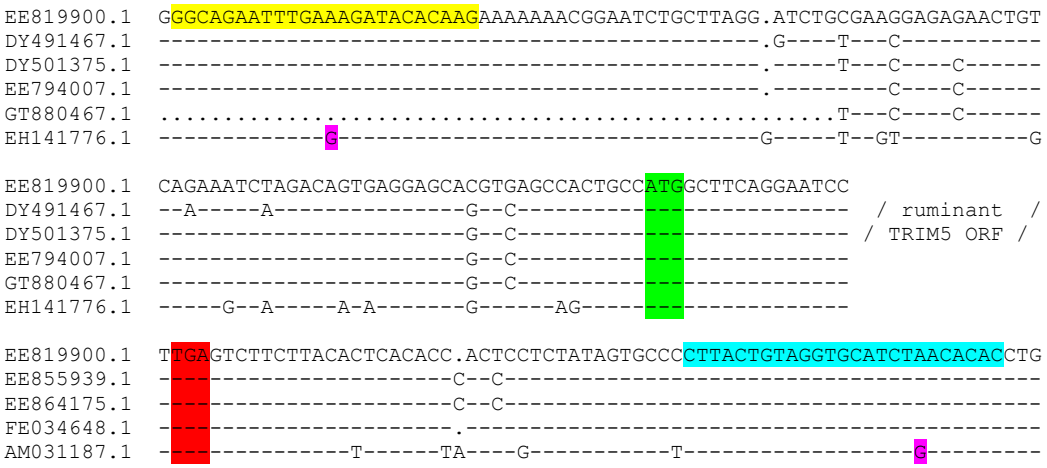

Fig. 5.4 Alignment of sequences located external to the sheep and cow TRIM5 reading frame
The forward primer (yellow) was designed to match published sheep mRNA sequence upstream of the start codon (green). The reverse primer (blue) is complementary to sheep sequences located downstream of the stop codons (red). The highlighted residue G indicates a base in the primer that was mismatched between cow (bottom sequence) and other sheep sequences. The majority of the ruminant TRIM5 coding region is not shown, dashes indicate sites where sequences are identical, dots indicate gaps or missing data.

5.2.3.2 Sequencing results and protein alignment

Amplified sequences were cloned into pGEM-T Easy and submitted for sequencing. At least ten of each sheep and goat clones were sequenced in order to choose a representative clone from each species.

Subsequently, selected sheep and goat clones were reamplified by high fidelity PCR (see Section 2.11.1.3). The forward primer incorporated a Kozak consensus sequence upstream of the start codon. The reverse primer added a haemagglutinin (HA) tag encoding sequence at the 3' of the ORF. The primers utilised also included restriction sites to facilitate the insertion of the T5 ORFs into a pLNCX-2 MLV vector backbone

(see Section 2.11.1.3). Once the T5 ORFs were cloned into pLNCX-2 vector, their sequences were again verified by sequencing (see Section 2.11.1.4).

The isolated sheep T5 sequence was more similar to the goat homologue than to the cow protein, which is shown in the protein alignment (Fig. 5.5).

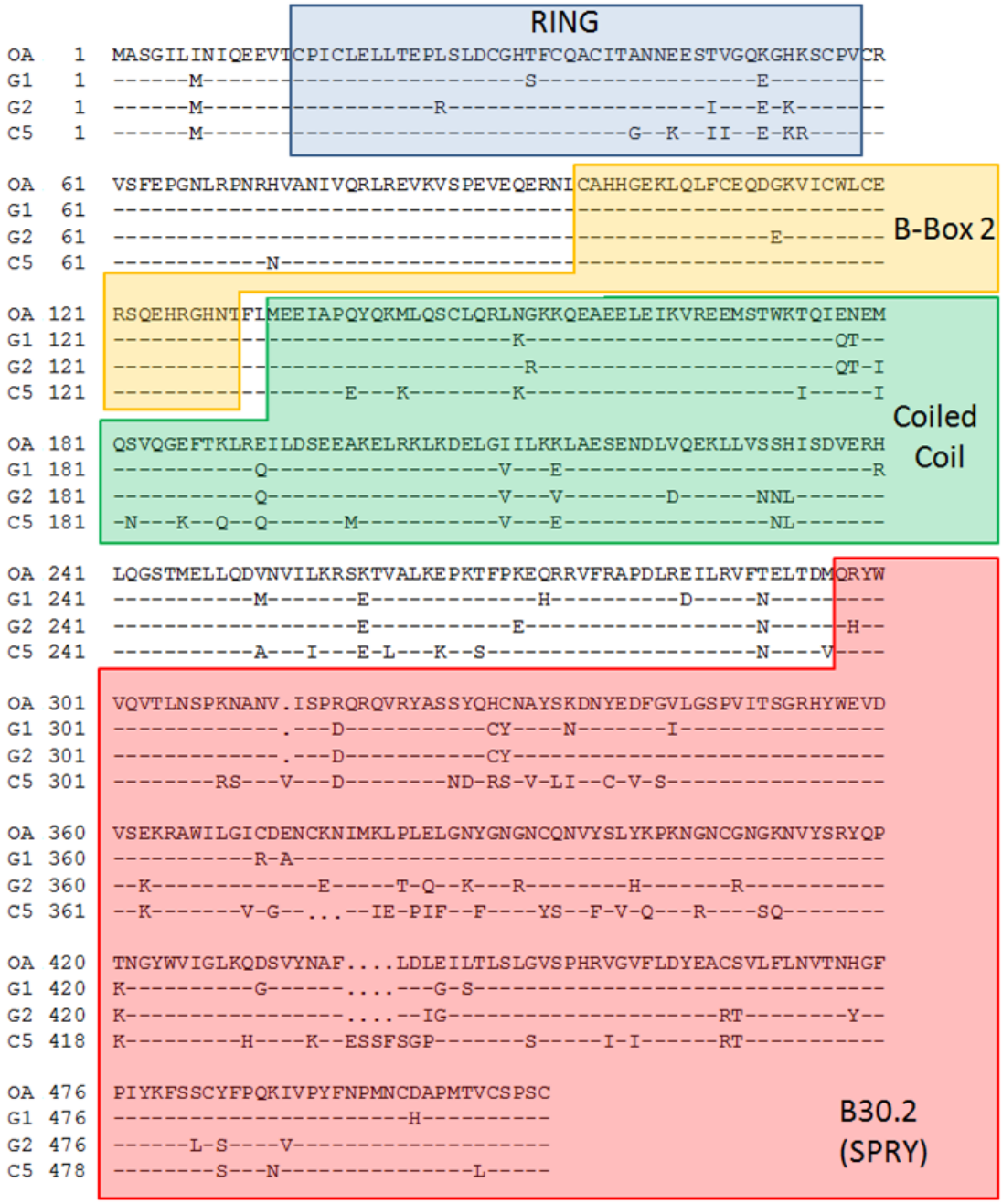

Fig. 5.5 Alignment of ruminant TRIM5 protein sequences
The sequences of the isolated sheep (OA), two goat alleles (G1 and G2) and cow LOC505265 (C5) are shown. Dashes indicate amino acid similarity. Dots indicate gaps. Polymorphic residues relative to the sheep sequence are highlighted by letters. TRIM5 domains are highlighted by shaded boxes. Numbers on the left indicate residue number.

The highest polymorphism was detected in the C-terminal B30.2 domain, while the first 120 residues of T5 were more conserved.

During the preparation of this thesis, the sequences of a number of sheep and goat T5 homologues were published (Jauregui et al., 2012). The T5 clone studied in this project is not identical to any of those homologues but most closely resembles sheep T5 "Clone OV3" (Jauregui et al., 2012). The relationship of 'the' clones with those reported by Jauregui is shown in Fig. 5.6.

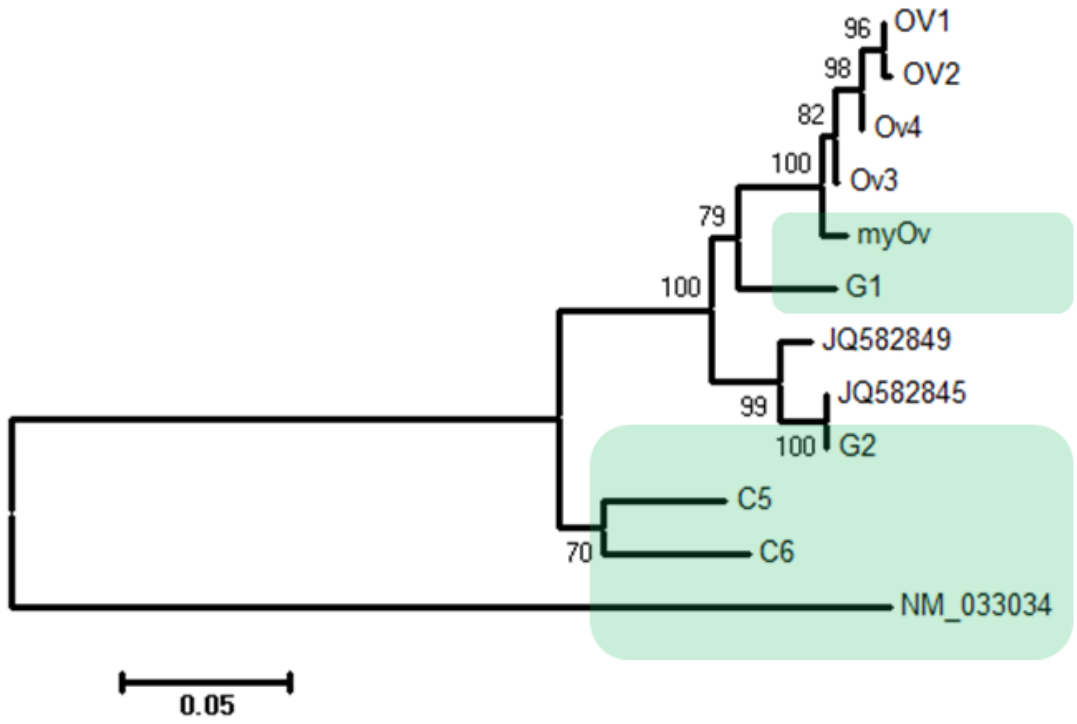

Fig. 5.6 Phylogenetic relationship of TRIM5 protein homologues
Five sheep TRIM5 alleles; 4 alleles OV1 to OV4 reported by (Jauregui et al., 2012) and the allele isolated in this study 'myOV'; four goat alleles G1 and G2 involved in this study, JQ582849 and JQ582845 reported by (Jauregui et al., 2012); two cow sequences (C5 and C6 - LOC505265, and LOC616948) (Si et al., 2006); human TRIM5α (NM_033034). T5 homologues analysed in this study are highlighted by a green background. This phylogenetic tree was generated using MEGA 6.02 Software. The evolutionary history was inferred using the Neighbor-Joining method (Saitou and Nei, 1987). The tree is drawn to scale, with branch lengths in the same units as those of the evolutionary distances used to infer the phylogenetic tree. Numbers represent bootstrap values, utilising 1000 iterations.

5.2.3.3 Cloning of T5 and *LacZ* into retroviral vectors

As a negative control, a *LacZ* transgene was cloned into pLNCX-2 instead of T5 (see Section 2.11.1.3). *LacZ* should not impact on JSRV replication and was useful for monitoring the progress of selection of cells stably expressing the transgene by staining for β-galactosidase activity (see Section 2.11.2.3).

The CRFKovH2 cell line was created in order to permit viral entry by JSRV Env-pseudotyped vectors. Effective stable expression of T5 in this cell line could not be assessed by selection based on the geneticin resistance gene (neomycin transferase) present in pLNCX-2, because this cell line already had been created by geneticin selection (see Section 2.4.3). Therefore, in order to select for stably transduced cells expressing T5 transgene, the vector backbone was modified by the addition of an Internal Ribosomal Entry Site (see Section 2.11.1.4) and hygromycin (Hyg) resistance gene cassette downstream of the T5-HA ORF. This should ensure that only cells expressing the mRNA containing T5 will survive the antibiotic selection due to the translation of Hyg^R via IRES present on the same transcript. The features of the integrated vector are shown in Fig. 5.7.

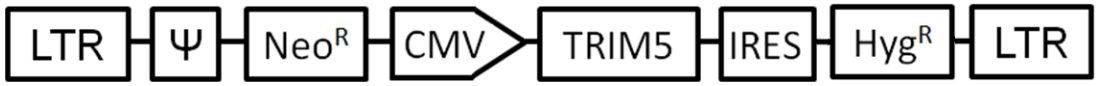

Fig. 5.7 pLNCX-2 TRIM5 IRES-Hyg vector
Features present in integrated pLNCX-2 vector: LTR – MLV 5' and 3' LTR; Ψ – packaging signal; Neo^R – neomyscin transferase (puromycin resistance gene in pLPCX vectors); CMV – CMV promoter; TRIM5 – HA tagged TRIM5; IRES – Internal Ribosomal Entry Site; Hyg^R - hygromycin resistance gene. Highlighted elements are not proportional to their actual size.

Two alleles of cow T5 (in this thesis referred as C5 and C6 - LOC505265 and LOC616948), rhesus macaque (GI 48994823) and human (NM_033034) homologues cloned into pLPCX were kindly provided by Dr Joseph Sodroski (Dana-Farber Cancer Institute, USA). These expression plasmids were modified similarly to pLNCX-2 by utilisation of a ClaI site to insert the IRES-Hyg cassette downstream of the T5-HA ORF. Features included in the integrated pLPCX vector are similar to pLNCX-2 (see Fig. 5.7), with the exception of a puromycin resistance gene, in a place of the neomycin transferase gene present in pLNCX-2.

All the clones were verified by sequencing of the TRIM5 transgene and junctions flanking the IRES-Hyg cassette (see Section 2.11.1.4).

5.2.4 Creation of cell lines stably expressing TRIM5

The creation of cell lines stably expressing different T5 homologues was the next step towards investigating the impact of T5 on JSRV replication *in vitro*. The retroviral vector method of transduction was chosen, because the expression of T5 was desired to be as high as possible and directed by the cellular genome.

MLV viral vectors were prepared by three plasmid transfection of 293T cells with pLNCX-2 (sheep, goat T5 or *LacZ*) or pLPCX (cow, rhesus macaque, human T5); pHIT60, which encodes MLV structural proteins and pVSV-G (see Section 2.11.2.1).

In order to reliably determine the ability of each T5 protein to block JSRV, a high proportion of cells expressing the analysed transgene was required. Therefore, cells were selected in the presence of antibiotic, and transgene expression was confirmed by various assays (see Sections 5.2.4.1 to 5.2.4.2).

Infection of CRFKovH2 by MLV T5 or *LacZ* carrying viral vectors was performed according to Section 2.11.2.2. Three days post-infection hygromycin was added to cell culture medium in order to select the cells which express the transgene (see Section 2.11.2.2). Two weeks of antibiotic selection eliminated all non-transduced cells in culture dish wells where no vector had been applied.

Confirmation of stable expression of transgene was monitored by β-Gal assay, performed on *LacZ* transduced cells (see Section 5.2.4.1). Immunoblotting was performed in order to detect HA-tagged T5 homologues in cellular extracts (see Section 5.2.4.3). Stable expression of T5 transgenes was assessed by flow cytometric analysis of anti-HA labelled cells (see Section 5.2.4.2).

5.2.4.1 Assessment of stable transgene expression by ß-galactosidase assay

The creation of a cell line stably expressing the *LacZ* transgene was verified by staining transduced cells for β-galactosidase activity. Note that these cells were simultaneously transduced at the same time as cells that were treated with MLV vectors carrying T5 transgenes. Cells transduced with *LacZ* express β-galactosidase and gain the ability to digest the X-Gal substrate, yielding galactose and 5-bromo-4-chloro-3-hydroxyindole, which later dimerizes and after oxidation forms the intensely blue stain 5,5'-dibromo-4,4'-dichloro-indigo (Kiernan, 2007). Therefore, β-galactosidase staining enabled the estimation of transduction efficiency by comparison of the number of *LacZ* blue coloured cells to colourless non-transduced ones (see Fig. 5.8).

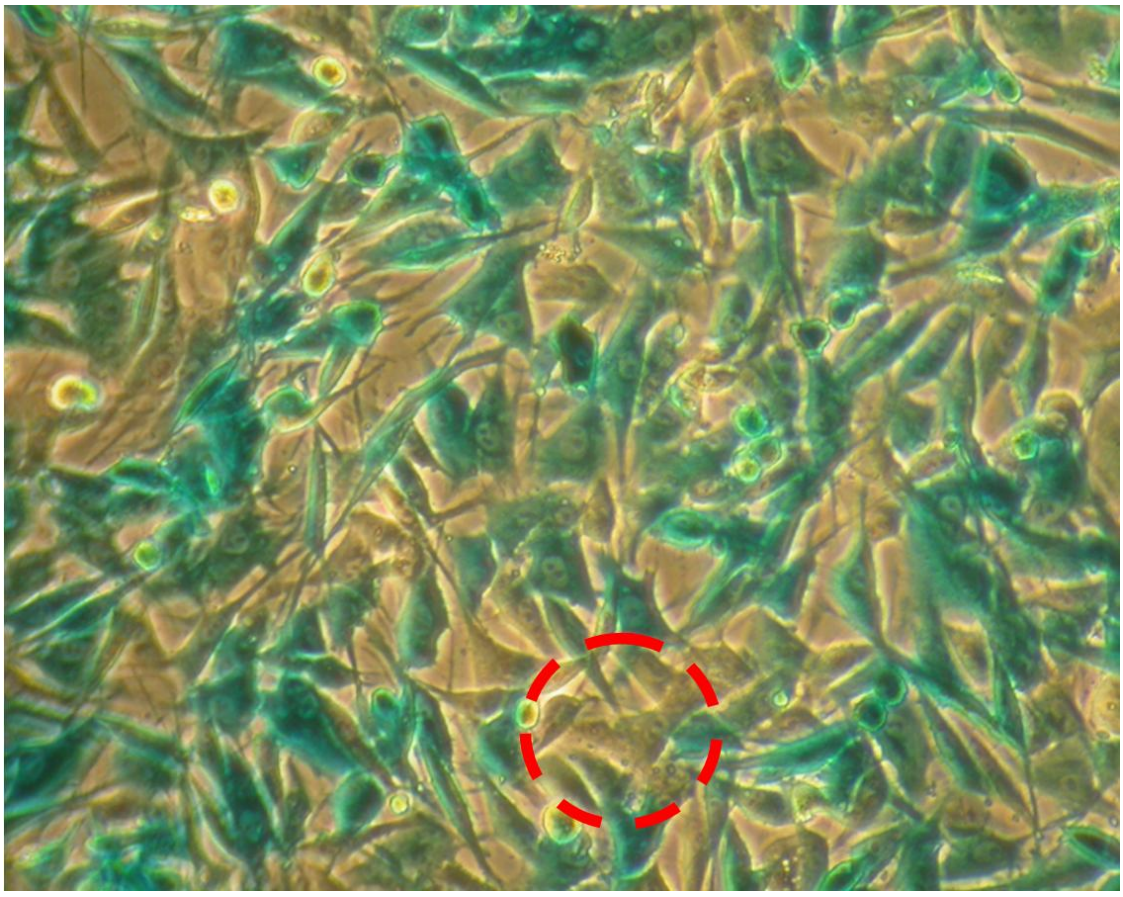

Fig. 5.8 β-Gal assay confirmation of stable *LacZ* expression in transduced CRFK cells
The majority of cells stably express the *LacZ* transgene (blue cells). However, some cells remained that did not to express β-galactosidase (an example is highlighted by a red circle).

5.2.4.2 Flow cytometry of immunocytostained cells expressing TRIM5

Confirmation of T5 expression by the vast majority of cells was necessary to qualify the cell line for analysis of T5 restriction. Initially, cells were subjected to intracellular detection of HA-tagged T5 proteins (see Section 2.11.2.5). Primary anti-HA antibody bound to C-terminally HA tagged T5, then the secondary Alexa Fluor 488 fluorescent antibody enabled the readout by flow cytometry (see Section 2.7.3).

Flow cytometric analysis of intacellularly labelled cell lines demonstrated that HA-tagged T5 is expressed by the majority of cells in each of the transduced cell lines (see Fig. 5.9). As negative controls, non-transduced cells and the cell line transduced with *LacZ* were used. An additional control, consisting of each cell line exposed only to the secondary antibody, was employed as a negative control for non-specific binding (see Section 2.11.2.5).

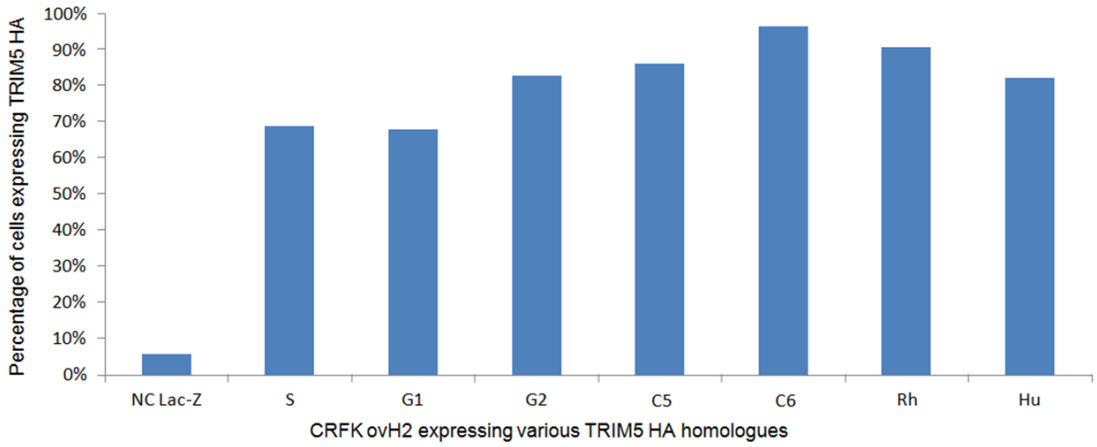

Fig. 5.9 Confirmation of stable expression of HA tagged TRIM5 homologues in transduced CRFK cell lines
Flow cytometric determination of the percentage of cells expressing various T5 in intracellularly stained cells. Cells were selected to express the following T5 homologues S- sheep; G1- goat allele "1"; G2- goat allele "2"; C5- cow allele (LOC505265); C6- cow allele (LOC616948); Rh- rhesus macaque (GI 48994823); Hu- human (NM_033034).

Cells stably transduced by cow (C5 and C6), rhesus macaque and human T5 were found to express the transgene in greater than 80% of the cell population. Sheep and "goat allele 1" of T5 was detected in approximately 70% of the cell population. It was notable that cells transduced utilising the pLPCX vector (C5, C6, Rh, Hu, T5) were characterised by a higher proportion of stable T5 expression than cells transduced

utilising the pLNCX-2 vector (S1, G1). The only exception is the G2 cell line, which was transduced with pLNCX-2 and where T5 was detected in over 80% of analysed cells. It should be noted that the assay was characterised by a relatively high background, since 6% of the *LacZ* also stained positive. However, no positive cells were detected in any of samples where only secondary Alexa Fluor 488 rabbit anti mouse antibody was utilised (not shown).

5.2.4.3 Immunoblot analysis of T5 HA cell line extracts

The expression of TRIM5 in stable expressing cell lines was tested by immunoblot detection of HA-tag present at the C-termini of those proteins. This analysis was performed in order to complement the previous flow cytometry experiments demonstrating the expression of the transgenes. Unexpectedly, the immunoblot analysis of cellular extracts did not detect any signal that corresponded to the expected size of the HA-tagged T5 (57.8 kDA).

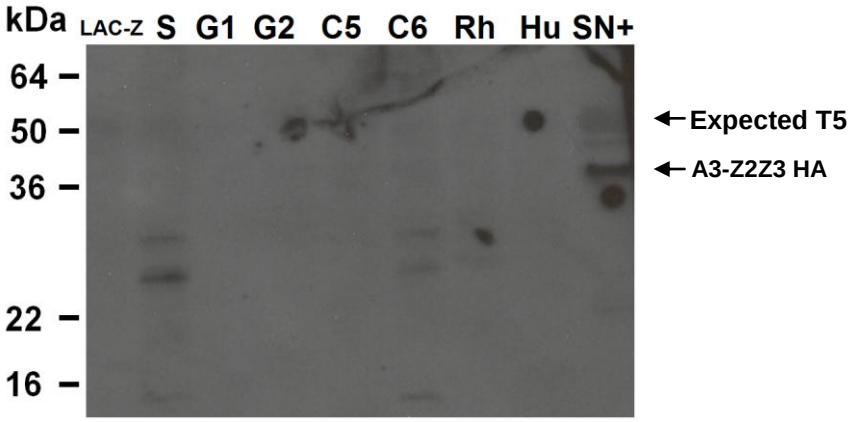

Fig. 5.10 Immunoblot analysis of cell line extracts using anti-HA antibody
Cellular extracts of cell lines transduced with the following T5: sheep (S), two goat alleles (G1 and G2); two cow variants (C5 and C6), rheseus macaque (Rh), human (Hu). Cellular extract from the Laz-Z cell line was utilised as a negative control for anti-HA activity. Detection of encapsidated sheep A3-Z2Z3 HA in 10 µl of concentrated virus stock (SN+) was utilised as a positive control for primary anti-HA antibody reactivity. Molecular weight marker (see Blue2) is shown on the left side of the figure. Note that image has a strong background signal because it was captured in overexposured conditions in an attempt to increase the assay's sensitivity.

Despite many attempts, none of the HA-tagged T5 expressing cell lines yielded any signal corresponding to the size of T5-HA by immunoblotting. Cellular extracts from cells transduced with sheep T5 (S) and cow T5 (C6) contained an immunoreactive

antigen between 22 and 36 kDa, but this is smaller than the predicted size of T5 (57.8 kDa).

Therefore, additional assays were performed to confirm T5 expression including RT-PCR detection of T5 mRNA transcripts and confirmation of previously published studies describing the ability of bovine allele (C5) and rhTRIM5 to restrict HIV-1.

5.2.5 Impact of TRIM5 on retroviral replication

Once the cell lines expressing T5 had been created and the stability of T5 expression had been confirmed, activity of each T5 was tested against JSRV (see Section 5.2.3.2). Some of the T5 proteins analysed in this study, were previously reported to restrict HIV (Stremlau et al., 2004, Si et al., 2006). Therefore, HIV-GFP infections were performed as an additional control of experimental system.

5.2.5.1 Effect of T5 on HIV-1 replication

The cell lines created in Section 5.2.4, that stably express various T5 were infected by a HIV-1-GFP in order to confirm their suitability for further experiments on the basis of comparison with previously published data. The rhT5 (GI 48994823) has been identified as a species specific determinant of HIV-1 infection (Stremlau et al., 2004). Two cow T5 alleles analysed in my project were characterised by different abilities to restrict HIV-1 restricting potential. The cow T5 LOC505265 (C5 T5) had been described as a potent HIV-1 inhibitor in contrast to the other bovine T5 allele LOC616948 (C6 T5), which is not active against HIV-1 (Si et al., 2006).

In order to evaluate the ability of ruminant, rhesus macaque and human T5 to restrict HIV-1, cells which stably expressed T5 homologues were infected by HIV-1-GFP and later analysed by flow cytometry. Six different amounts of HIV-1-GFP VSV-G pseudotyped virus were used for infections and the percentage of infected GFP-positive cells is shown in Fig. 5.11.

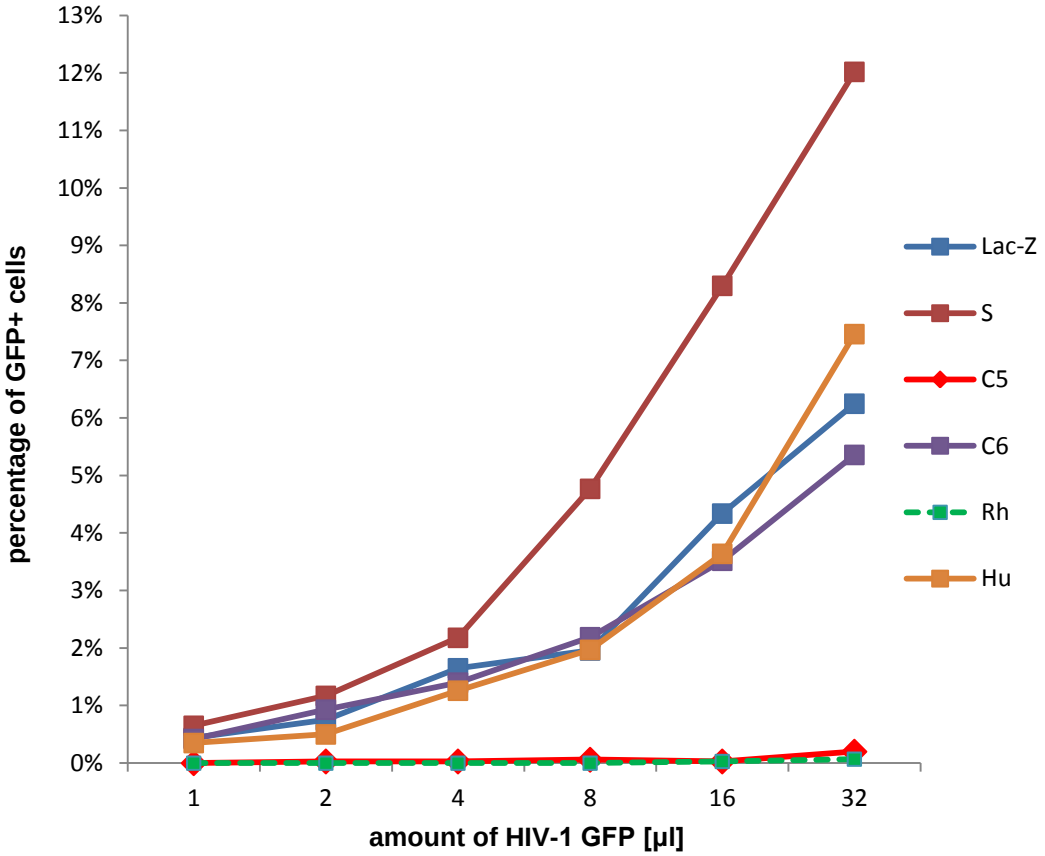

Fig. 5.11 Flow cytometric analysis of T5 impact on permissiveness to HIV-1 GFP
Analysis of HIV-1-GFP (VSV-G) infected CRFKovH2 expressing various T5 homologues S – sheep; C5 – LOC505265; C6 – LOC616948; Rh – Rhesus monkey (GI 48994823); Hu – human (NM_033034). Each cell line was infected using 6 different amounts of virus utilised for infection 1; 2; 4; 8; 16 and 32 µl. *LacZ* transduced cells were used as a negative control for T5 function.

This experiment showed that Rh and C5 T5 could restrict HIV-1. These results are in agreement with previous reports (Stremlau et al., 2004, Si et al., 2006). Therefore, although western blotting did not detect T5 expression (see Section 5.2.4.3), the confirmation of a biological effect exhibited by rhesus (Rh) T5 and cow (C5) T5 supports the flow cytometric analysis that these cell lines do express T5.

Comparing to *LacZ* cell line permissiveness, the expression of sheep and human T5 did not protect against HIV-1 infection. The result obtained did not show the ability of huT5 to protect at all against HIV-1 in contrast to published work where huT5 restricted HIV-1 but not as strongly as its macaque homologue (Stremlau et al., 2004).

5.2.5.2 Effect of T5 on JSRV replication

In order to determine the ability of ruminant and human T5 to restrict JSRV, cells which stably expressed T5 homologues were infected by JSRV GFP and analysed by flow cytometry. The T5-expressing cell lines were plated in 12-well cell culture dishes in equal amounts and were then infected in triplicate by four different amounts of JSRV-GFP VSV-G vector. The percentage of GFP-positive cells is shown in Fig. 5.12.

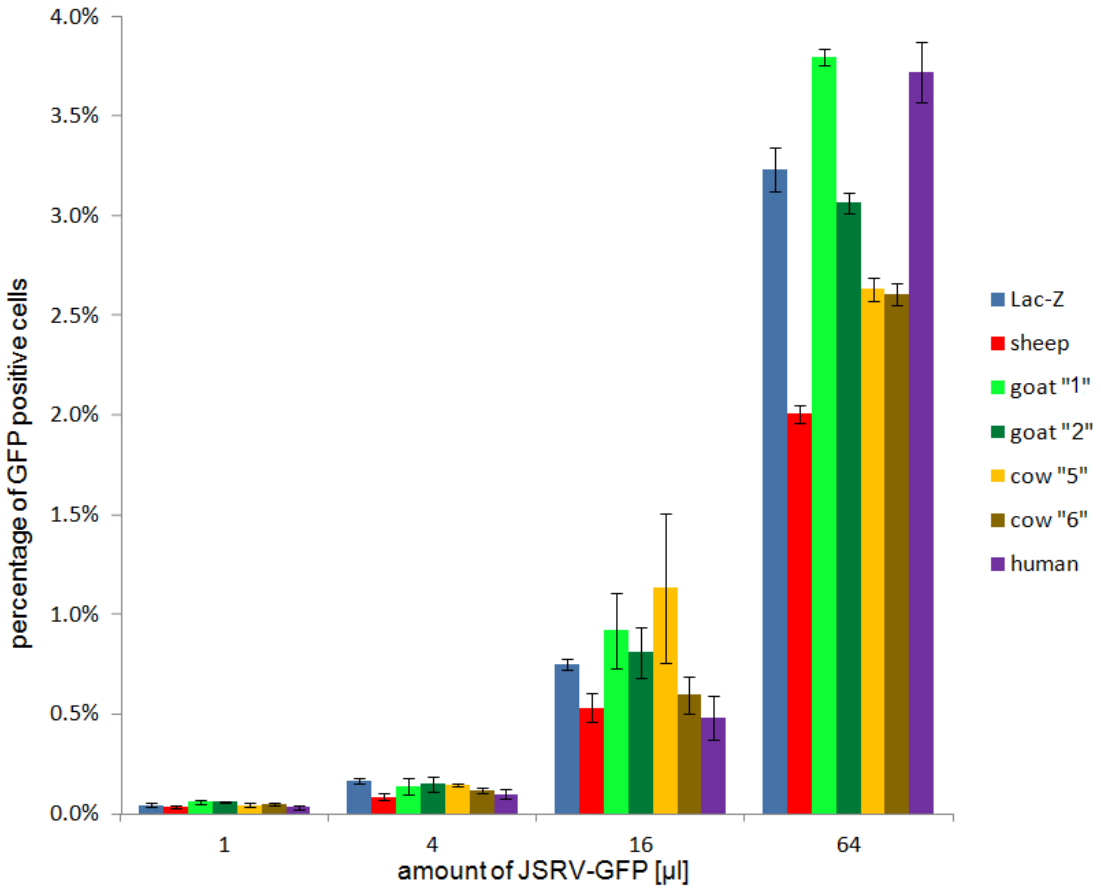

Fig. 5.12 Flow cytometric analysis of T5 impact on permissiveness to JSRV-GFP
Analysis of JSRV-GFP VSV-G infected CRFKovH2 expressing various T5 homologues (right legend) sheep; goat T5 allele "1" and "2"; cow "5" – LOC505265; cow "6" – LOC616948; human. Each cell line was infected using 4 different amounts of virus 1; 4; 16 and 64 µl. *LacZ* transduced cells were used as a negative control for T5 function. The student two-tailed t-test method with unequal variance was used to verify the significance of results. The error bars report the standard deviation value between wells infected in triplicate.

Flow cytometric analysis of cell lines expressing T5 homologues did not demonstrate any dramatic restriction caused by any of the analysed T5. The permissiveness of the tested cell lines which stably express various T5 was similar to *LacZ* NC. Notably, cells expressing the sheep T5 were about 30% less permissive to JSRV than the *LacZ*

cell line. However, this is a relatively modest restriction and further analysis is required to confirm whether this is reproducible.

5.3 Discussion

The experiments described in this chapter represent the first analysis of the potential role of T5 in JSRV replication. During this study one sheep allele, two goat alleles, two cow alleles and are human T5 homologue were examined for their ability to restrict JSRV.

As a preliminary experiment the CRFK cell line, which is highly permissive to retroviruses and does not express T5, was tested by JSRV infection in parallel with murine and ovine cell lines. The observed differences in susceptibility suggested that resistance of less permissive cell lines to JSRV might be caused by a post-entry restriction factor such as T5 (see Section 5.2.1).

Subsequently, one sheep and two goat T5 homologues were identified and cloned (see Section 5.2.3.1), then cell lines that stably express each of them were created by retroviral vector mediated transduction (see Section 5.2.5). Additionally, other cell lines were transduced with cow, rhesus macaque and human T5 homologues. Stable T5 expression in cell lines was assessed by antibiotic treatment and the detection of expressed transgene was verified by several assays (see Sections 5.2.4.1 to 5.2.4.3).

The biological function of the selected T5s was determined by infection with HIV-1, and JSRV-GFP VSV-G pseudotyped viruses (see Sections 5.2.5.1 and 5.2.5.2). Prior to the investigation of T5 activity against JSRV, the suitability of the system used was verified by demonstrating the ability of previously reported T5 homologues to inhibit HIV-1. This work has generated some data supporting the scenario that analysedT5 homologues do not exhibit inhibitory potential against JSRV. However, it should be noted that the presented experiments are preliminary and any discussion of the data is therefore speculative. Nevertheless, the data obtained so far provide a strong foundation for future work.

5.3.1 Ruminant TRIM5 does not restrict JSRV replication

Flow cytometry performed on cell lines expressing various T5 proteins did not identify any significant restriction of JSRV caused by any of the T5s analysed (see Section 5.2.5.2). For other retroviruses, the reported T5 antiviral activity in *in vitro* conditions reduce the virus titre in a range from 100 to 100,000 fold, and the restriction was more evident when smaller amounts of virus were tested (Stremlau et al., 2004).

In this study, the observed variation in the percentage of GFP-positive cells was up to two fold. Such variation is more likely an effect of such experiment factors such as minor differences in number of cells and their condition. Cells expressing the sheep T5 homologue were 33% less permissive to JSRV than *LacZ* transduced cells. However, referring to the intracellular labelling results (see Section 5.2.4.2), where the expression of sheep T5 was detected in 70% of the total cell line population, the presence of cells not expressing T5 could mask its inhibitory potential and could account in a part for fluorescence readings classified as positive. In order to resolve this uncertainty, either the infected-GFP-positive cell population should be verified for T5 expression or the proportion of cells expressing T5 should be increased.

Two cell lines expressing the human or the 'goat 1 allele' of T5 were detected as more permissive to JSRV than the *LacZ* cell line, which was used as a negative control (see Fig. 5.13). Extended analysis of observed slight increase in permissiveness to JSRV among some created cell lines, could potentially identify mechanisms responsible for this phenomena such as involvement of T5 in uncoating. However, I attribute this result as variation related to the assay depending on such factors like cell condition and their number. A similar observation was reported in a study performed by Si et al. (2006), where cells transduced with the modified cow T5 LOC616948 allele were slightly more permissive to N-MLV than cells that had been transduced with an empty vector.

5.3.1.1 Could the presence of HA tag have affected T5 activity?

It is possible that the presence of the C-terminal HA Tag might affect the activity of the analysed T5 proteins. For example, a previous study found that rhT5 inhibited SIV,

whereas HA-tagged rhT5 did not (Stremlau et al., 2004). However, in that study both tagged and untagged rhT5 and huT5 blocked HIV-1 to the same degree (Stremlau et al., 2004). Those differences may be explained by the fact that the C-terminal B 30.2 domain is responsible for binding to retroviral capsids and connecting to it an epitope tag might alter this interaction (Huthoff and Towers, 2008). Therefore, experiments on untagged and C-terminal tagged T5s may be performed in order to address this issue in the context of JSRV infection.

5.3.1.2 Comment on the suitability of the cell lines used

Since the immunoblot analysis did not detect T5 in cellular extracts of the analysed cell lines (see Section 5.2.2.3), it could be argued that either the various T5 alleles were not expressed or that their expression levels are low. It may be linked to an observation that a number of TRIM family members were described to be turned over by the proteasome, which depleted their levels (Versteeg et al., 2013). However, the intracellular flow cytometry results identified the immunoreactive HA-epitope in the majority of the population of each cell line. In addition, for rhT5 and C5 T5, actual biological activity was demonstrated in the context of HIV-1-GFP infection (see Section 5.2.5.1). However, huT5 is also reported to restrict HIV-1 although less strongly than rhT5 (Stremlau et al., 2004), but in the present study was not found to restrict HIV. Further work is needed to resolve this inconsistency. Moreover, the eventual restrictive potential of analysed T5s could be affected by a dominant negative effect due to a possible heterodimerisation with endogenous truncanted variant T5 present in CRFK cell line (Perez-Caballero et al., 2005, McEwan et al., 2009).

The stable expression of the T5 transgene in the vast majority of the cell population was desired in order to avoid the result being affected by the presence of highly permissive non-transduced cells. Therefore, flow cytometric analysis of HA-labelled cells was used to demonstrate that the majority of cells express the T5 transgene. For example, the intracellular detection of HA-tagged C5 T5 suggested that there were around 15% of cells which did not express the transgene (see Fig. 5.9). Those cells may be more permissive to infection than successfully transduced cells and subsequently the infection of this cell line should yield a higher proportion of GFP-positive cells in the readout of HIV-1 infection (see Section 5.2.5.1). My interpretation

of this observation is that the proportion of cells stably expressing T5 is actually higher than detected by flow cytometric analysis of HA-labelled cells. There is a chance that some cells might be restrictive even if they have a relatively low expression level of T5 that is not detectable by intracellular anti-HA labelling.

In addition, I speculate that some false negative readings are actually signals from improperly intracellularly stained cells. Several steps of this method might have affected the assay's performance, for example permeabilisation of cellular membranes or fixation. Such factors might possibly influence the ability of antibody to penetrate cells equally in each sample.

The flow cytometric analysis of intracellularly stained cells showed that 6% of cells in the negative control *LacZ* line were positive (see Fig. 5.9). My interpretation is that it represents a false positive and contributes to the assay's background. Alternatively, those cells scored as positive might contain a cross-reactive antigen which is responsible for background labelling. In principle, expression of such a cross-reactive antigen could be caused by an alteration of an expressed protein by provirus insertion or a response of a fraction of the cells to the antibiotic selection. However, such a scenario is unlikely, due to the fact that monoclonal anti-HA antibodies were utilised for the detection of HA-tagged T5.

In my opinion the relatively high ratio of positives (6%) in the *LacZ* cell line is unlikely to be attributed to biological factors, which should not account for such a high proportion of cells. On the other hand, antibiotic selection reduced the polyclonality of cellular population, which might in some way increase the proportion of cells expressing this putative cross-reactive epitope.

However, given the disparity of flow cytometric analysis of labelled cells (see Section 5.3.3.2) and western blot results (see Section 5.2.3.3), additional RT-PCR analysis should be performed in order to provide additional evidence of T5-HA expression.

Various variants of MLV vector backbones were utilised in order to improve the proportion of transgene expression in the cell lines generated in this study. Initial experiments showed only about 50% of cells to be detected by intracellular labelling.

The highest transgene expression proportion was found when MLV vectors containing a IRES-Hyg cassette downstream of the T5 ORF were utilised (see section 5.2.3.3).

5.3.2 Can TRIM5 be excluded as a species-specificity restriction factor for JSRV?

Initially, the feline CRFK cell line was compared to the bovine MDBK cell line by infection with VSV-G pseudotyped JSRV-GFP. The result of this preliminary experiment indicated at least 10-fold lower permissiveness of MDBK compared to CRFK cells (see Section 5.2.1). Therefore, the detected resistance of the bovine cell line against JSRV might be attributed to post-entry restriction mediated by T5, since CRFK does not express it. However, none of the created cell lines expressing any of the investigated T5 homologues was characterised by an increased resistance to JSRV. This contrasts with a dramatic effect of various T5 mediated restriction against other retroviruses reported previously (Si et al., 2006). Therefore, the observation of MDBK resistance to JSRV cannot be attributed to restriction mediated by bovine T5 molecules.

Since it has been shown in many reports that various T5 alleles may be characterised by a varying restrictive potential on viral replication (Goldschmidt et al., 2006, Rahm et al., 2013), the possibility that T5 may be responsible for the species-specificity of OPA should not be completely excluded. For example, previous work (Si et al., 2006) was confirmed here by demonstration of the ability of the cow C5 T5 allele to inhibit HIV-1 in contrast to the other bovine allele C6 T5.

Besides the direct post-entry inhibition of viral replication, T5 may be responsible for other activities which contribute to antiviral immunity (see Section 1.8.3.3). It is possible that there is a potential T5 ability to bind viral capsids, which results not in inhibition of replication, but acts as a kind of pattern recognition receptor and mediates the virus sensing mechanism (de Silva and Wu, 2011). Therefore, this project provided only data about the lack of direct T5-mediated restriction of JSRV and did not verify its other possible functions. In order to address this issue, the eventual intracellular response should be studied using a number of approaches, including transcriptomic and proteomic analysis and the identification of secreted chemokines. Moreover the

verification of the ability of T5 to bind JSRV capsids could be accessed by immunostaining followed with co-localisation using confocal microscopy. Alternatively, direct binding of T5 to capsids could be detected by protein-crosslinking or a yeast-two hybrid system. In addition, targeted mutagenesis could identify protein motifs involved in potential T5-mediated capsid recognition.

5.3.2.1 Comment on sheep TRIM5 alleles as potential JSRV limiting factors.

During the time of this project, several alleles of ovine and caprine T5 were published (Jauregui et al., 2012). In that study, the Ov1 and Ov2 alleles of sheep T5α demonstrated inhibition of MVV in contrast to the Ov4 allele which did not restrict MVV. Because the sheep T5 allele analysed in this project is similar to the OV3 (see Fig. 5.6) there is a chance that other sheep alleles might be characterised by different inhibitory potential against JSRV.

There is a need to be aware that there is ongoing co-evolution between viruses and their restriction factors. Such natural selection on the basis of resilience to pathogens also applies in the case of domestic animals, although the process may be significantly affected by breeding strategies. Moreover, sheep usually develop OPA at the time they already have some offspring.

5.3.3 Development of a strategy for effective TRIM5 expression

As described above, the vast majority of cells would ideally express T5 in order to properly determine its eventual restrictive potential. Various MLV vectors were used in order to improve the proportion of cells expressing the T5 transgene.

Initially the pBABE vector (Morgenstern and Land, 1990) was utilised for transduction of CRFK and RK-13C cells. Due to difficulties in obtaining the required percentage of transgene expressing cells, it was decided to clone the T5 ORFs into the pLNCX-2 vector [Clontech]. However, subsequent transduction of CRFK and RK-13C cells found that the percentage of T5 positive cells was still too low (not shown).

To address this issue, the IRES-Hyg cassette was cloned into the backbones of pLNCX-2 (S, G1 and G2 T5) or pLPCX vector (C5, C6, Rh, Hu T5). A similar strategy was utilised by Diehl and collegues (Diehl et al., 2008). In this study linkage of T5 to an antibiotic resistance gene within the same translational unit, improved the expression ratios in cell lines created.

The survival of some cells in hygromycin selection where T5 was not detected might be attributed to several issues. It could be speculated that the survival of cells not expressing T5 might be due to mutations generated in the T5 ORF due to RT or RNA polymerase II errors occurring during viral vector production and transduction. On the other hand it could be argued that the flow cytometry result was accurate, because cell lines stably expressing T5 have been created in parallel with *LacZ*, which contains a proportion of cells which were not stained by β-Gal assay (see section 5.2.2.1). This fraction of the cell line represents either unsuccessfully transduced cells or their *LacZ* expression was below the detection threshold.

An alternative experimental strategy would involve examination of T5 function by transient transfection of cells, as was used for example by Hwang et al., (2010). However, I decided to create cell lines stably expressing T5 from vectors integrated in the genome in order to mimic their natural expression. Additionally, taking the transient approach, transfection would be necessary to repeat transfections prior to each infectivity assay, which would add further variability to the results obtained. Moreover, transfection efficiency dependent on the cell line would impact on the results.

Some studies of T5 function have utilised T5 encoding vectors that also contain a fluorescent marker, for example, yellow fluorescent protein (YFP) (Diehl et al., 2008, Lukic et al., 2011). Taking this approach, the result is interpreted by the ratio of infected cells (GFP-positive) taking into account only transduced cells which express YFP. In my study I decided to create cell lines stably expressing T5 by an antibiotic selection in order to eliminate non-transduced cells to minimise their role in depletion of the virus pool used in infections.

In future experiments on T5 and JSRV, if biological activity of T5 is detected it would need to be confirmed by siRNA mediated knockdown to rescue infectivity (Sodroski, 2004). In order to investigate the restriction mechanism, proteasomal inhibitors could be utilised, which in some cases may rescue the original permissiveness. Moreover, mutational analysis of T5 variants generated can define motifs required for a restriction of analysed virus or for generation a gain of inhibitory function (McCarthy et al., 2013, Neagu et al., 2009).

5.3.4 Summary of TRIM5 impact on JSRV

Although none of the analysed T5 mediated the restriction of JSRV, the work in this Chapter is a first step towards examining the interaction of T5 and JSRV. The possibility remains that other T5 alleles or other TRIM family members contribute to the species specificity of JSRV infection. At the time of this project the complete family of ruminant TRIM family protein sequences was not fully characterised. Once these data are available, a high throughput analysis should be performed similar to one reported by Uchil et al. (2008), where a significant proportion of the human TRIM family members were tested for their ability to inhibit various viruses.

Notably, as the experiments on A3 demonstrated (see Chapters 3 and 4), the possible identification of TRIM mediated restriction of JSRV would require an additional confirmation that the restriction factor is expressed in cells targeted by JSRV *in vivo*. In the situation where JSRV was demonstrated to be resistant to TRIM-mediated restriction totally, then it might be utilised as a vector in a number of genetic engineering applications, which could potentially yield effective gene transduction in gene therapy or in the creation of transgenic animals.

Chapter 6 – General discussion

Recent work from many laboratories has focussed on host-pathogen interactions in retrovirus infection. In particular, a number of restriction factors have been identified that block replication at specific points in the replication cycle. For JSRV, previous work has identified tetherin (BST-2) (Arnaud et al., 2010), IFITM proteins (Li et al., 2013a) and specific enJSRV Gag and Env proteins as potential inhibitory factors (Arnaud et al., 2007b). In this thesis I examined the potential activity of A3 and T5 against JSRV within the context of species-specificity of infection. The results presented in Chapters 3 and 4 demonstrate the ability of various A3 proteins to restrict JSRV *in vitro*, but, none of the T5 homologues analysed was demonstrated to be active against JSRV (Chapter 5). These findings contribute to our understanding of host-pathogen interactions in OPA and may help to direct the future development of effective disease control strategies. In addition, this work provides improved insight into the prospect of JSRV as a potential vector in gene delivery. In addition to restriction factors, the species specificity and epidemiology of OPA could also be dependent on sequence variation of other innate immunity genes and polymorphism of dependency factors, such as alleles of the HYAL 2 receptor. Figure 6.1 summarises some known dependency and restriction factors that are relevant to OPA.

Restriction factors are now well recognised as important components of innate immunity. They are often consistently expressed but also activated by interferons and other cytokines (Koning et al., 2009, Gougeon and Herbeuval, 2012). They may act as a form of antiviral effector molecule, such as A3 and T5, and in some cases as a form of pathogen recognition sensor that triggers further cytokine expression (for example T5α). Whether the sheep homologues function in the same way remains to be determined.

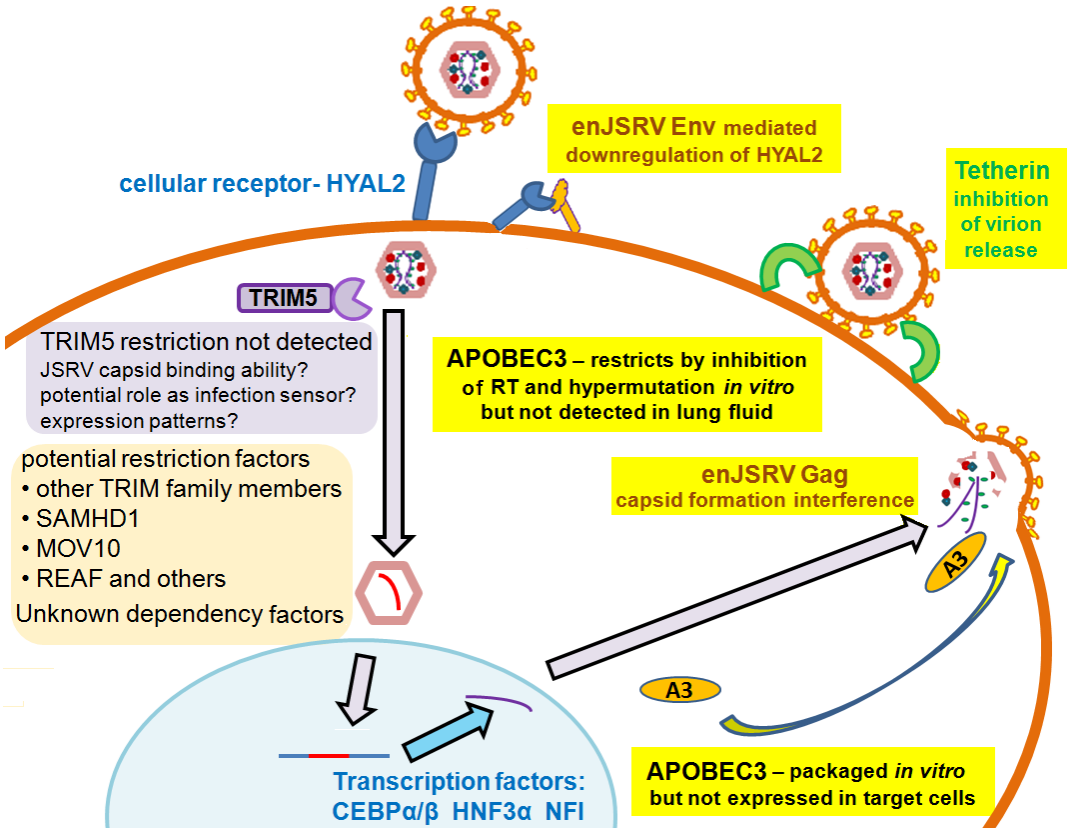

Fig. 6.1. Dependency and restriction factors relevant to JSRV replication.
Dependency factors such as the cellular receptor Hyal-2 and transcription factors are displayed in blue. Restriction factors whose activity against JSRV was confirmed *in vitro*, but are not expressed in cells where JSRV replicates, are highlighted by yellow boxes (APOBEC3, tetherin, enJSRV Gag and Env). The ability of TRIM5 to directly restrict JSRV was not detected in this study, but there are other possible functions for TRIM5 (violet box). The significance of other potential restriction factors and dependency factors remains to be investigated (orange box).

6.1 Identification of the APOBEC3 proteins as potential JSRV inhibitors

In this study, some ruminant, murine and human A3 proteins were demonstrated to be able to inhibit JSRV replication *in vitro* (see Chapter 3 and 4). Moreover, ovine A3-Z2 and A3-Z2Z3 were demonstrated to be able to inhibit JSRV replication *in vitro* by hypermutation and by direct inhibition of the reverse transcriptase reaction. However, the impact of A3 on the pathogenesis of OPA appears to be rather limited since the stability of the JSRV genome among isolates suggests no occurrence of cytidine deamination-mediated restriction *in vivo*. This correlated with a lack of detectable A3 in virus isolated from OPA lung fluid and little or no expression of A3 proteins in pulmonary epithelial cells. Collectively, the data presented in this thesis strongly indicate that JSRV avoids A3 *in vivo* by infecting and replicating in target cells that do

not express these restriction factors. This is a novel strategy and can be contrasted with the anti-A3 strategies adopted by HIV and other retroviruses.

This project was supported by a grant aiming to develop transgenic sheep that would be resistant to OPA. In studies performed in parallel to those described here, transgenic sheep were produced that expressed the enJSRV Gag and Env proteins in the lung (D. Griffiths, C. Cousens, B. Whitelaw, M. Palmarini; Unpublished Data). Identification of ovine A3s as potential JSRV inhibitors makes them disease control candidates, if their expression can be targeted to lung epithelium. However, there is a need to be aware that even endogenous A3, may contribute to uncontrolled editing of the host genome, which might lead to transformation (Nowarski and Kotler 2013; Taylor et al. 2013). In addition, there is a chance that once A3 is expressed in lung epithelium, then although it would limit JSRV infectivity, it is possible that it could also increase the rate of JSRV viral evolution. I speculate that in order to create a transgenic sheep resistant to OPA, the best results would be obtained by coexpression of some JSRV inhibitors, such as A3, tetherin and specifically designed siRNAs targeting JSRV transcripts. Although due to strict regulations such an animal would unlikely to be used in food production, it could provide a better understanding of such disease control perspectives.

6.2 Ruminant and human TRIM5 proteins do not restrict JSRV

This study demonstrated a lack of JSRV inhibition by ruminant TRIM5 proteins including one ovine, two caprine and two bovine alleles (see Chapter 5). In addition, human T5α was also not effective against JSRV. Although some of these experiments were only performed once and need to be confirmed, they suggest that T5 is not an important factor determining the species-specificity of JSRV. Nevertheless, it remains possible that other T5 alleles and other members of the TRIM family may protect against JSRV (Uchil et al., 2008). In addition, although T5 is not responsible for the direct post-entry inhibition of JSRV replication, it could still potentially function as a virus recognition factor that stimulates innate immunity signalling pathways leading to antiviral responses such as mediated by NFκB (Pertel et al., 2011, de Silva and Wu, 2011).

If JSRV is demonstrated to be completely resistant to TRIM mediated restriction, then there may be an advantage to using components of this virus as a vector in genetic engineering applications, such as gene therapy and the creation of transgenic animals.
It has been demonstrated that modification of an originally inactive T5 protein may cause a gain of virus inhibitory function. If T5 could be modified to acquire the ability to inhibit JSRV, there is the prospect of development of novel disease control strategies (McCarthy et al., 2013, Neagu et al., 2009).

6.3 Future studies on the species specificity

The work presented in this thesis has provided new information on restriction factors and JSRV. However, further restriction factors are known that could contribute to limiting the natural course of infection and may be responsible for the species-specificity of JSRV. Also, it is likely that there are additional restriction factors yet to be identified.

One strategy for identifying new restriction factors that are active against JSRV would be to perform a high throughput genetic screen similar to studies performed on HIV-1. In one study, approximately 19,000 genes were screened by selective siRNA-mediated knockdown, this study identified polymerase-associated factor 1 (PAF1) as an HIV-1 restriction factor (Liu et al., 2011). In a similar manner, RNA-associated Early-stage Anti-viral Factor (REAF) was also identified as an HIV inhibitor (Marno et al., 2014). An alternative approach for identifying novel restriction factors has been the high-throughput testing of interferon-stimulated genes for their antiviral activity (Schoggins et al., 2011), which has uncovered many new targets for future research.

It is possible that allelic variation in genes encoding restriction factors may be responsible for the apparent selection of resistant animals that is observed in flocks affected by OPA. Typically, in the first few years of an outbreak, the prevalence of OPA in affected stock ranges may be as high as 20% but in subsequent years decreases to 1% to 5% (Griffiths et al., 2010). This resistance does not appear to be related to any detectable adaptive immunity to JSRV and, instead, a host genetic factor, such as a restriction factor, may be involved. Therefore comparison of restriction factor alleles present at the beginning of an epidemic to alleles present in OPA-endemic stock might identify protective alleles. Additional information could be provided by investigation of the genomes of animals which died of OPA compared to ones which were infected with JSRV but have not developed clinical disease. Moreover, the differential distribution of restriction or permissive factor alleles among sheep breeds (Jauregui et al., 2012) might result in variable susceptibility to OPA. For example, during the OPA outbreak in Iceland in 1930-1940 nearly 90% of Gottorp breed sheep died, comparing to only around 10% of Adalbol breed sheep (Dungal, 1938).

To obtain a more global perspective on host-pathogen interactions in OPA, extensive proteomic, genomic and transcriptomic profiling comparing healthy lung and transformed lung could be performed to identify factors involved in pathogenesis. Advances in sequencing technologies over recent years have now made this a realistic possibility in OPA, even though the sheep genome sequence is not yet fully annotated. Greater understanding of the transcriptional response to JSRV infection and transformation would provide numerous avenues for dissecting host-pathogen interactions in OPA. For example, increased understanding of cellular transformation pathways would help uncover how exactly the JSRV Env protein is able to induce tumours. Similarly, identification of the local cytokine response to JSRV infection, in infected cells and in the surrounding stroma and infiltrating cells, might reveal aspects of OPA biology relating to the lack of adaptive immunity. Furthermore, this information may inform the design of new diagnostic assays and disease control strategies for OPA and would strengthen the relevance of OPA as a model for human lung cancer.

One factor that has hampered studies on JSRV has been the lack of a suitable permissive cell line capable of supporting replication of the virus *in vitro*. The data generated on A3 and T5 in this thesis has contributed to our understanding of potential blocks to JSRV replication in vitro, and will inform future studies on developing a permissive cell line. For example, there are few sheep cell lines available, and those that do exist, such as CPT-Tert used here, express A3 and so may not be ideal candidates for use in *in vitro* infectivity studies. If a permissive cell line were available, this would greatly facilitate studies on JSRV replication, including the analysis of candidate species-specific restriction factors.

6.4 Final Conclusion

In conclusion, the work in this thesis has, for the first time, investigated the role of A3 and T5 restriction factors in JSRV infection. I have shown that ovine A3 does restrict JSRV but is not expressed in the cells in which JSRV replicates, which represents a novel strategy of retroviral avoidance of this restriction factor. In addition, I have presented data supporting the notion that T5 does not restrict JSRV. The methods used, including cloning of ruminant A3 and the creation of cells that express various T5 may contribute to future studies not only on host-pathogen interactions present in OPA but also other viral diseases. Further work in this area will provide additional knowledge that can be utilised in the development of control strategies against OPA and other challenging diseases caused by retroviruses.

'Scientists have become the bearers of the torch of discovery in our quest for knowledge'.
Stephen Hawking

These words describe the mission of scientists to unravel the mysteries of nature. The aim of studying virus-host interactions is to translate the knowledge to much needed novel control strategies against many diseases including those that are currently incurable.

REFERENCES

ADOLPH, M. B., WEBB, J. & CHELICO, L. 2013. Retroviral restriction factor APOBEC3G delays the initiation of DNA synthesis by HIV-1 reverse transcriptase. *PLoS One,* 8**,** e64196.

AL SHAMSI, I. R., AL DHAHERI, N. S., PHILLIP, P. S., MUSTAFA, F. & RIZVI, T. A. 2010. Reciprocal cross-packaging of primate lentiviral (HIV-1 and SIV) RNAs by heterologous non-lentiviral MPMV proteins. *Virus Res*.

ALBERTI, A., MURGIA, C., LIU, S. L., MURA, M., COUSENS, C., SHARP, M., MILLER, A. D. & PALMARINI, M. 2002. Envelope-induced cell transformation by ovine betaretroviruses. *J Virol,* 76**,** 5387-94.

ALLOUCH, A., DI PRIMIO, C., ALPI, E., LUSIC, M., AROSIO, D., GIACCA, M. & CERESETO, A. 2011. The TRIM family protein KAP1 inhibits HIV-1 integration. *Cell Host Microbe,* 9**,** 484-95.

ANWAR, F., DAVENPORT, M. P. & EBRAHIMI, D. 2013. Footprint of APOBEC3 on the genome of human retroelements. *J Virol,* 87**,** 8195-204.

ARNAUD, F., BLACK, S. G., MURPHY, L., GRIFFITHS, D. J., NEIL, S. J., SPENCER, T. E. & PALMARINI, M. 2010. Interplay between ovine bone marrow stromal cell antigen 2/tetherin and endogenous retroviruses. *J Virol,* 84**,** 4415-25.

ARNAUD, F., CAPORALE, M., VARELA, M., BIEK, R., CHESSA, B., ALBERTI, A., GOLDER, M., MURA, M., ZHANG, Y. P., YU, L., PEREIRA, F., DEMARTINI, J. C., LEYMASTER, K., SPENCER, T. E. & PALMARINI, M. 2007a. A paradigm for virus-host coevolution: sequential counter-adaptations between endogenous and exogenous retroviruses. *PLoS Pathog,* 3**,** e170.

ARNAUD, F., MURCIA, P. R. & PALMARINI, M. 2007b. Mechanisms of late restriction induced by an endogenous retrovirus. *J Virol,* 81**,** 11441-51.

ARTEGIANI, B. & CALEGARI, F. 2013. Lentiviruses allow widespread and conditional manipulation of gene expression in the developing mouse brain. *Development,* 140**,** 2818-2822.

BAI, J., ZHU, R. Y., STEDMAN, K., COUSENS, C., CARLSON, J., SHARP, J. M. & DEMARTINI, J. C. 1996. Unique long terminal repeat U3 sequences distinguish exogenous jaagsiekte sheep retroviruses associated with ovine pulmonary carcinoma from endogenous loci in the sheep genome. *J Virol,* 70**,** 3159-68.

BANNERT, N. & KURTH, R. 2006. The evolutionary dynamics of human endogenous retroviral families. *Annu Rev Genomics Hum Genet,* 7**,** 149-73.

BARR, S. D., SMILEY, J. R. & BUSHMAN, F. D. 2008. The interferon response inhibits HIV particle production by induction of TRIM22. *PLoS Pathog,* 4**,** e1000007.

BEALE, A. J. 1963. Viral interference and interferon. *Annu Rev Med,* 14**,** 133-40.

BELLAN, C., DE FALCO, G., LAZZI, S. & LEONCINI, L. 2003. Pathologic aspects of AIDS malignancies. *Oncogene,* 22**,** 6639-45.

BENTVELZEN, P. & DAAMS, J. H. 1969. Hereditary infections with mammary tumor viruses in mice. *J Natl Cancer Inst,* 43**,** 1025-35.

BERTRAND, P., COTE, M., ZHENG, Y. M., ALBRITTON, L. M. & LIU, S. L. 2008. Jaagsiekte sheep retrovirus utilizes a pH-dependent endocytosis pathway for entry. *J Virol,* 82**,** 2555-9.

BISHOP, K. N., VERMA, M., KIM, E. Y., WOLINSKY, S. M. & MALIM, M. H. 2008. APOBEC3G inhibits elongation of HIV-1 reverse transcripts. *PLoS Pathog,* 4**,** e1000231.

BITTNER, J. J. 1942. The Milk-Influence of Breast Tumors in Mice. *Science,* 95**,** 462-3.

BLACK, S. G., ARNAUD, F., BURGHARDT, R. C., SATTERFIELD, M. C., FLEMING, J. A., LONG, C. R., HANNA, C., MURPHY, L., BIEK, R., PALMARINI, M. & SPENCER, T. E. 2010a. Viral particles of endogenous betaretroviruses are released in the sheep uterus and infect the conceptus trophectoderm in a transspecies embryo transfer model. *J Virol,* 84**,** 9078-85.

BLACK, S. G., ARNAUD, F., PALMARINI, M. & SPENCER, T. E. 2010b. Endogenous retroviruses in trophoblast differentiation and placental development. *Am J Reprod Immunol,* 64**,** 255-64.

BLOOR, S., MAELFAIT, J., KRUMBACH, R., BEYAERT, R. & RANDOW, F. 2010. Endoplasmic reticulum chaperone gp96 is essential for infection with vesicular stomatitis virus. *Proc Natl Acad Sci U S A,* 107**,** 6970-5.

BOGERD, H. P., SKALSKY, R. L., KENNEDY, E. M., FURUSE, Y., WHISNANT, A. W., FLORES, O., SCHULTZ, K. L., PUTNAM, N., BARROWS, N. J., SHERRY, B., SCHOLLE, F., GARCIA-BLANCO, M. A., GRIFFIN, D. E. & CULLEN, B. R. 2014. Replication of many human viruses is refractory to inhibition by endogenous cellular microRNAs. *J Virol,* 88**,** 8065-76.

BOHN, M. F., SHANDILYA, S. M., ALBIN, J. S., KOUNO, T., ANDERSON, B. D., MCDOUGLE, R. M., CARPENTER, M. A., RATHORE, A., EVANS, L., DAVIS, A. N., ZHANG, J., LU, Y., SOMASUNDARAN, M., MATSUO, H., HARRIS, R. S. & SCHIFFER, C. A. 2013. Crystal Structure of the DNA Cytosine Deaminase APOBEC3F: The Catalytically Active and HIV-1 Vif-Binding Domain. *Structure,* 21**,** 1042-50.

BORG, K. & NILSSON, P. O. 1985. [Ethmoid tumors in moose and roe deer]. *Nord Vet Med,* 37**,** 145-60.

BRIGGS, J. A., SIMON, M. N., GROSS, I., KRAUSSLICH, H. G., FULLER, S. D., VOGT, V. M. & JOHNSON, M. C. 2004. The stoichiometry of Gag protein in HIV-1. *Nat Struct Mol Biol,* 11**,** 672-5.

BURNS, J. C., FRIEDMANN, T., DRIEVER, W., BURRASCANO, M. & YEE, J. K. 1993. Vesicular stomatitis virus G glycoprotein pseudotyped retroviral vectors: concentration to very high titer and efficient gene transfer into mammalian and nonmammalian cells. *Proc Natl Acad Sci U S A,* 90**,** 8033-7.

BURNS, M. B., LACKEY, L., CARPENTER, M. A., RATHORE, A., LAND, A. M., LEONARD, B., REFSLAND, E. W., KOTANDENIYA, D., TRETYAKOVA, N., NIKAS, J. B., YEE, D., TEMIZ, N. A., DONOHUE, D. E., MCDOUGLE, R. M., BROWN, W. L., LAW, E. K. & HARRIS, R. S. 2013. APOBEC3B is an enzymatic source of mutation in breast cancer. *Nature,* 494**,** 366-70.

BYEON, I. J., AHN, J., MITRA, M., BYEON, C. H., HERCIK, K., HRITZ, J., CHARLTON, L. M., LEVIN, J. G. & GRONENBORN, A. M. 2013. NMR structure of human restriction factor APOBEC3A reveals substrate binding and enzyme specificity. *Nat Commun,* 4**,** 1890.

CALLAHAN, R. 1996. MMTV-induced mutations in mouse mammary tumors: their potential relevance to human breast cancer. *Breast Cancer Res Treat,* 39**,** 33-44.

CAPORALE, M., ARNAUD, F., MURA, M., GOLDER, M., MURGIA, C. & PALMARINI, M. 2009. The signal peptide of a simple retrovirus envelope

functions as a posttranscriptional regulator of viral gene expression. *J Virol,* 83**,** 4591-604.

CAPORALE, M., COUSENS, C., CENTORAME, P., PINONI, C., DE LAS HERAS, M. & PALMARINI, M. 2006. Expression of the jaagsiekte sheep retrovirus envelope glycoprotein is sufficient to induce lung tumors in sheep. *J Virol,* 80**,** 8030-7.

CAPORALE, M., MARTINEAU, H., DE LAS HERAS, M., MURGIA, C., HUANG, R., CENTORAME, P., DI FRANCESCO, G., DI GIALLEONARDO, L., SPENCER, T. E., GRIFFITHS, D. J. & PALMARINI, M. 2013a. Host species barriers to Jaagsiekte sheep retrovirus replication and carcinogenesis. *J Virol,* 87**,** 10752-62.

CAPORALE, M., MARTINEAU, H., DE LAS HERAS, M., MURGIA, C., HUANG, R., CENTORAME, P., DI FRANCESCO, G., DI GIALLEONARDO, L., SPENCER, T. E., GRIFFITHS, D. J. & PALMARINI, M. 2013b. Host Species Barriers to Jaagsiekte Sheep Retrovirus Replication and Carcinogenesis. *J Virol*.

CHARRAY, J., AMAN, N. & TANOH, K. G. 1985. [Note on an enzootic of adenocarcinoma of the pituitary nasal mucosa in Djalonke ewes]. *Rev Elev Med Vet Pays Trop,* 38**,** 406-10.

CHEN, K. M., HARJES, E., GROSS, P. J., FAHMY, A., LU, Y., SHINDO, K., HARRIS, R. S. & MATSUO, H. 2008. Structure of the DNA deaminase domain of the HIV-1 restriction factor APOBEC3G. *Nature,* 452**,** 116-9.

CHESTER, A., SCOTT, J., ANANT, S. & NAVARATNAM, N. 2000. RNA editing: cytidine to uridine conversion in apolipoprotein B mRNA. *Biochim Biophys Acta,* 1494**,** 1-13.

CHITRA, E., LIN, Y. W., DAVAMANI, F., HSIAO, K. N., SIA, C., HSIEH, S. Y., WEI, O. L., CHEN, J. H. & CHOW, Y. H. 2010. Functional interaction between Env oncogene from Jaagsiekte sheep retrovirus and tumor suppressor Sprouty2. *Retrovirology,* 7**,** 62.

CHOI, Y., KAPPLER, J. W. & MARRACK, P. 1991. A superantigen encoded in the open reading frame of the 3' long terminal repeat of mouse mammary tumour virus. *Nature,* 350**,** 203-7.

COFFIN, J. M. H., S.H.; VARMUS, H.E. 1997. *Retroviruses,* New York, Cold Spring Harbor Laboratory Press.

COTE, M., ZHENG, Y. M., ALBRITTON, L. M. & LIU, S. L. 2011. Single residues in the surface subunits of oncogenic sheep retrovirus envelopes distinguish receptor-mediated triggering for fusion at low pH and infection. *Virology,* 421**,** 173-83.

COTE, M., ZHENG, Y. M., LI, K., XIANG, S. H., ALBRITTON, L. M. & LIU, S. L. 2012. Critical role of leucine-valine change in distinct low pH requirements for membrane fusion between two related retrovirus envelopes. *J Biol Chem,* 287**,** 7640-51.

COUSENS, C., BISHOP, J. V., PHILBEY, A. W., GILL, C. A., PALMARINI, M., CARLSON, J. O., DEMARTINI, J. C. & SHARP, J. M. 2004. Analysis of integration sites of Jaagsiekte sheep retrovirus in ovine pulmonary adenocarcinoma. *J Virol,* 78**,** 8506-12.

COUSENS, C., MINGUIJON, E., DALZIEL, R. G., ORTIN, A., GARCIA, M., PARK, J., GONZALEZ, L., SHARP, J. M. & DE LAS HERAS, M. 1999. Complete sequence of enzootic nasal tumor virus, a retrovirus associated with transmissible intranasal tumors of sheep. *J Virol,* 73**,** 3986-93.

COUSENS, C., THONUR, L., IMLACH, S., CRAWFORD, J., SALES, J. & GRIFFITHS, D. J. 2009. Jaagsiekte sheep retrovirus is present at high concentration in lung fluid produced by ovine pulmonary adenocarcinoma-affected sheep and can survive for several weeks at ambient temperatures. *Res Vet Sci,* 87**,** 154-6.

CRANDELL, R. A., FABRICANT, C. G. & NELSON-REES, W. A. 1973. Development, characterization, and viral susceptibility of a feline (Felis catus) renal cell line (CRFK). *In Vitro,* 9**,** 176-85.

CURRER, R., VAN DUYNE, R., JAWORSKI, E., GUENDEL, I., SAMPEY, G., DAS, R., NARAYANAN, A. & KASHANCHI, F. 2012. HTLV tax: a fascinating multifunctional co-regulator of viral and cellular pathways. *Front Microbiol,* 3**,** 406.

DA SILVA TEIXEIRA, M. F., LAMBERT, V., MSELLI-LAKAHL, L., CHETTAB, A., CHEBLOUNE, Y. & MORNEX, J. F. 1997. Immortalization of caprine fibroblasts permissive for replication of small ruminant lentiviruses. *Am J Vet Res,* 58**,** 579-84.

DALGLEISH, A. G. & O'BYRNE, K. J. 2002. Chronic immune activation and inflammation in the pathogenesis of AIDS and cancer. *Adv Cancer Res,* 84**,** 231-76.

DANILKOVITCH-MIAGKOVA, A., DUH, F. M., KUZMIN, I., ANGELONI, D., LIU, S. L., MILLER, A. D. & LERMAN, M. I. 2003. Hyaluronidase 2 negatively regulates RON receptor tyrosine kinase and mediates transformation of epithelial cells by jaagsiekte sheep retrovirus. *Proc Natl Acad Sci U S A,* 100**,** 4580-5.

DE LAS HERAS, M., BARSKY, S. H., HASLETON, P., WAGNER, M., LARSON, E., EGAN, J., ORTIN, A., GIMENEZ-MAS, J. A., PALMARINI, M. & SHARP, J. M. 2000a. Evidence for a protein related immunologically to the jaagsiekte sheep retrovirus in some human lung tumours. *Eur Respir J,* 16**,** 330-2.

DE LAS HERAS, M., BARSKY, S. H., HASLETON, P., WAGNER, M., LARSON, E., EGAN, J., ORTIN, A., GIMENEZ-MAS, J. A., PALMARINI, M. & SHARP, J. M. 2000b. Evidence for a protein related immunologically to the jaagsiekte sheep retrovirus in some human lung tumours. *European Respiratory Journal,* 16**,** 330-332.

DE LAS HERAS, M., DE MARTINO, A., BOROBIA, M., ORTIN, A., ALVAREZ, R., BORDERIAS, L. & GIMENEZ-MAS, J. A. 2014. Solitary tumours associated with Jaagsiekte retrovirus in sheep are heterogeneous and contain cells expressing markers identifying progenitor cells in lung repair. *J Comp Pathol,* 150**,** 138-47.

DE LAS HERAS, M., GONZALEZ, L. & SHARP, J. M. 2003a. Pathology of ovine pulmonary adenocarcinoma. *Curr Top Microbiol Immunol,* 275**,** 25-54.

DE LAS HERAS, M., MURCIA, P., ORTIN, A., AZUA, J., BORDERIAS, L., ALVAREZ, R., JIMENEZ-MAS, J. A., MARCHETTI, A. & PALMARINI, M. 2007. Jaagsiekte sheep retrovirus is not detected in human lung adenocarcinomas expressing antigens related to the Gag polyprotein of betaretroviruses. *Cancer Letters,* 258**,** 22-30.

DE LAS HERAS, M., ORTIN, A., BENITO, A., SUMMERS, C., FERRER, L. M. & SHARP, J. M. 2006. In-situ demonstration of mitogen-activated protein kinase Erk 1/2 signalling pathway in contagious respiratory tumours of sheep and goats. *J Comp Pathol,* 135**,** 1-10.

DE LAS HERAS, M., ORTIN, A., COUSENS, C., MINGUIJON, E. & SHARP, J. M. 2003b. Enzootic nasal adenocarcinoma of sheep and goats. *Curr Top Microbiol Immunol,* 275**,** 201-23.

DE LAS HERAS, M., SHARP, J. M., FERRER, L. M., GARCIA DE JALON, J. A. & CEBRIAN, L. M. 1993. Evidence for a type D-like retrovirus in enzootic nasal tumour of sheep. *Vet Rec,* 132**,** 441.

DE LAS HERAS, M., SHARP, J. M., GARCIA DE JALON, J. A. & DEWAR, P. 1991. Enzootic nasal tumour of goats: demonstration of a type D-related retrovirus in nasal fluids and tumours. *J Gen Virol,* 72 (Pt 10)**,** 2533-5.

DE SILVA, S. & WU, L. 2011. TRIM5 acts as more than a retroviral restriction factor. *Viruses,* 3**,** 1204-9.

DELUCIA, M., MEHRENS, J., WU, Y. & AHN, J. 2013. HIV-2 and SIVmac accessory virulence factor Vpx down-regulates SAMHD1 enzyme catalysis prior to proteasome-dependent degradation. *J Biol Chem,* 288**,** 19116-26.

DEMARTINI, J. C., BISHOP, J. V., ALLEN, T. E., JASSIM, F. A., SHARP, J. M., DE LAS HERAS, M., VOELKER, D. R. & CARLSON, J. O. 2001. Jaagsiekte sheep retrovirus proviral clone JSRV(JS7), derived from the JS7 lung tumor cell line, induces ovine pulmonary carcinoma and is integrated into the surfactant protein A gene. *J Virol,* 75**,** 4239-46.

DEMARTINI, J. C., CARLSON, J. O., LEROUX, C., SPENCER, T. & PALMARINI, M. 2003. Endogenous retroviruses related to jaagsiekte sheep retrovirus. *Curr Top Microbiol Immunol,* 275**,** 117-37.

DEMOREST, Z. L., LI, M. & HARRIS, R. S. 2011. Phosphorylation directly regulates the intrinsic DNA cytidine deaminase activity of activation-induced deaminase and APOBEC3G protein. *J Biol Chem,* 286**,** 26568-75.

DESHAIES, R. J. & JOAZEIRO, C. A. 2009. RING domain E3 ubiquitin ligases. *Annu Rev Biochem,* 78**,** 399-434.

DIAZ-GRIFFERO, F., PERRON, M., MCGEE-ESTRADA, K., HANNA, R., MAILLARD, P. V., TRONO, D. & SODROSKI, J. 2008. A human TRIM5alpha B30.2/SPRY domain mutant gains the ability to restrict and prematurely uncoat B-tropic murine leukemia virus. *Virology,* 378**,** 233-42.

DIEHL, W. E., STANSELL, E., KAISER, S. M., EMERMAN, M. & HUNTER, E. 2008. Identification of postentry restrictions to Mason-Pfizer monkey virus infection in New World monkey cells. *J Virol,* 82**,** 11140-51.

DIRKS, C., DUH, F. M., RAI, S. K., LERMAN, M. I. & MILLER, A. D. 2002. Mechanism of cell entry and transformation by enzootic nasal tumor virus. *J Virol,* 76**,** 2141-9.

DOEHLE, B. P., BOGERD, H. P., WIEGAND, H. L., JOUVENET, N., BIENIASZ, P. D., HUNTER, E. & CULLEN, B. R. 2006. The betaretrovirus Mason-Pfizer monkey virus selectively excludes simian APOBEC3G from virion particles. *J Virol,* 80**,** 12102-8.

DONAHUE, R. E. & CLARK, S. C. 1992. Granulocyte colony-stimulating factors as therapeutic agents. *Immunol Ser,* 57**,** 637-49.

DORRSCHUCK, E., FISCHER, N., BRAVO, I. G., HANSCHMANN, K. M., KUIPER, H., SPOTTER, A., MOLLER, R., CICHUTEK, K., MUNK, C. & TONJES, R. R. 2011. Restriction of porcine endogenous retrovirus by porcine APOBEC3 cytidine deaminases. *J Virol,* 85**,** 3842-57.

DOUGLAS, J. L., GUSTIN, J. K., VISWANATHAN, K., MANSOURI, M., MOSES, A. V. & FRUH, K. 2010. The great escape: viral strategies to counter BST-2/tetherin. *PLoS Pathog,* 6**,** e1000913.

DULL, T., ZUFFEREY, R., KELLY, M., MANDEL, R. J., NGUYEN, M., TRONO, D. & NALDINI, L. 1998. A third-generation lentivirus vector with a conditional packaging system. *J Virol,* 72**,** 8463-71.

DUNGAL, N. 1938. Epizootic Adenomatosis of the Lungs of Sheep: Its Relation to Verminous Pneumonia and Jaagsiekte: (Section of Comparative Medicine). *Proc R Soc Med,* 31**,** 497-505.

DUNLAP, K. A., PALMARINI, M. & SPENCER, T. E. 2006a. Ovine endogenous betaretroviruses (enJSRVs) and placental morphogenesis. *Placenta,* 27 Suppl A**,** S135-40.

DUNLAP, K. A., PALMARINI, M., VARELA, M., BURGHARDT, R. C., HAYASHI, K., FARMER, J. L. & SPENCER, T. E. 2006b. Endogenous retroviruses regulate periimplantation placental growth and differentiation. *Proc Natl Acad Sci U S A,* 103**,** 14390-5.

DURAND, S. & CIMARELLI, A. 2011. The inside out of lentiviral vectors. *Viruses,* 3**,** 132-59.

DYKES, R. J. M., J . 1888. Lung disease in sheep caused by the Strongylus refescens. *Journal of Comparative Pathology and Therapeutics***,** 139-146.

EBRAHIMI, D., ALINEJAD-ROKNY, H. & DAVENPORT, M. P. 2014. Insights into the Motif Preference of APOBEC3 Enzymes. *PLoS One,* 9**,** e87679.

ELLERMANN, V., BANG, O. 1908. Experimentelle Leuka¨mie bei Hu¨ hnern. *Zentralbl Bakteriol Parasitenkd Infectionskr*

Hyg Abt Orig 595–609.

ENGELMAN, A. 2010. Reverse Transcription and Integration. *In:* KURTH, R. A. B., N. (ed.) *Retroviruses Molecular Biology, Genomics and Pathogenesis.* Berlin: Caister Anademic Press.

EVANS, D. T., SERRA-MORENO, R., SINGH, R. K. & GUATELLI, J. C. 2010. BST-2/tetherin: a new component of the innate immune response to enveloped viruses. *Trends Microbiol,* 18**,** 388-96.

FAN, H., PALMARINI, M. & DEMARTINI, J. C. 2003. Transformation and oncogenesis by jaagsiekte sheep retrovirus. *Curr Top Microbiol Immunol,* 275**,** 139-77.

FINKELSHTEIN, D., WERMAN, A., NOVICK, D., BARAK, S. & RUBINSTEIN, M. 2013. LDL receptor and its family members serve as the cellular receptors for vesicular stomatitis virus. *Proc Natl Acad Sci U S A,* 110**,** 7306-11.

FISCHER, A., HACEIN-BEY-ABINA, S. & CAVAZZANA-CALVO, M. 2013. Gene therapy of primary T cell immunodeficiencies. *Gene,* 525**,** 170-3.

FLETCHER, A. J. & TOWERS, G. J. 2013. Inhibition of retroviral replication by members of the TRIM protein family. *Curr Top Microbiol Immunol,* 371**,** 29-66.

FRANCIS, O., HAN, F. & ADAMS, J. C. 2013. Molecular Phylogeny of a RING E3 Ubiquitin Ligase, Conserved in Eukaryotic Cells and Dominated by Homologous Components, the Muskelin/RanBPM/CTLH Complex. *PLoS One,* 8**,** e75217.

GARCIA-GOTI, M., GONZALEZ, L., COUSENS, C., CORTABARRIA, N., EXTRAMIANA, A. B., MINGUIJON, E., ORTIN, A., DE LAS HERAS, M. & SHARP, J. M. 2000. Sheep pulmonary adenomatosis: characterization of two pathological forms associated with jaagsiekte retrovirus. *J Comp Pathol,* 122**,** 55-65.

GAUDIN, R., ALENCAR, B. C., ARHEL, N. & BENAROCH, P. 2013. HIV trafficking in host cells: motors wanted! *Trends Cell Biol*.

GIROUD, C., CHAZAL, N., GAY, B., ELDIN, P., BRUN, S. & BRIANT, L. 2013. HIV-1-associated PKA acts as a cofactor for genome reverse transcription. *Retrovirology,* 10**,** 157.

GOFF, S. P. 2007. Host factors exploited by retroviruses. *Nat Rev Microbiol,* 5**,** 253-63.

GOLDSCHMIDT, V., BLEIBER, G., MAY, M., MARTINEZ, R., ORTIZ, M. & TELENTI, A. 2006. Role of common human TRIM5alpha variants in HIV-1 disease progression. *Retrovirology,* 3**,** 54.

GOLOVKINA, T. V., CHERVONSKY, A., PRESCOTT, J. A., JANEWAY, C. A., JR. & ROSS, S. R. 1994. The mouse mammary tumor virus envelope gene product is required for superantigen presentation to T cells. *J Exp Med,* 179**,** 439-46.

GONZALEZ, L., JUSTE, R. A., CUERVO, L. A., IDIGORAS, I. & SAEZ DE OCARIZ, C. 1993. Pathological and epidemiological aspects of the coexistence of maedi-visna and sheep pulmonary adenomatosis. *Res Vet Sci,* 54**,** 140-6.

GOUGEON, M. L. & HERBEUVAL, J. P. 2012. IFN-alpha and TRAIL: a double edge sword in HIV-1 disease? *Exp Cell Res,* 318**,** 1260-8.

GRAHAM, F. L., SMILEY, J., RUSSELL, W. C. & NAIRN, R. 1977. Characteristics of a human cell line transformed by DNA from human adenovirus type 5. *J Gen Virol,* 36**,** 59-74.

GREGO, E., DE MENEGHI, D., ALVAREZ, V., BENITO, A. A., MINGUIJON, E., ORTIN, A., MATTONI, M., MORENO, B., PEREZ DE VILLARREAL, M., ALBERTI, A., CAPUCCHIO, M. T., CAPORALE, M., JUSTE, R., ROSATI, S. & DE LAS HERAS, M. 2008. Colostrum and milk can transmit jaagsiekte retrovirus to lambs. *Vet Microbiol,* 130**,** 247-57.

GRIFFITHS, D. 1996. *Investigation of a Novel Retroviral Element Isolated From Human Salivary Gland.* PhD Thesis.

GRIFFITHS, D. J., MARTINEAU, H. M. & COUSENS, C. 2010. Pathology and pathogenesis of ovine pulmonary adenocarcinoma. *J Comp Pathol,* 142**,** 260-83.

GRUTTER, M. G. & LUBAN, J. 2012. TRIM5 structure, HIV-1 capsid recognition, and innate immune signaling. *Curr Opin Virol,* 2**,** 142-50.

HACEIN-BEY-ABINA, S., VON KALLE, C., SCHMIDT, M., MCCORMACK, M. P., WULFFRAAT, N., LEBOULCH, P., LIM, A., OSBORNE, C. S., PAWLIUK, R., MORILLON, E., SORENSEN, R., FORSTER, A., FRASER, P., COHEN, J. I., DE SAINT BASILE, G., ALEXANDER, I., WINTERGERST, U., FREBOURG, T., AURIAS, A., STOPPA-LYONNET, D., ROMANA, S., RADFORD-WEISS, I., GROSS, F., VALENSI, F., DELABESSE, E., MACINTYRE, E., SIGAUX, F., SOULIER, J., LEIVA, L. E., WISSLER, M., PRINZ, C., RABBITTS, T. H., LE DEIST, F., FISCHER, A. & CAVAZZANA-CALVO, M. 2003. LMO2-associated clonal T cell proliferation in two patients after gene therapy for SCID-X1. *Science,* 302**,** 415-9.

HAMMONDS, J., DING, L., CHU, H., GELLER, K., ROBBINS, A., WANG, J. J., YI, H. & SPEARMAN, P. 2012a. The tetherin/BST-2 coiled-coil ectodomain mediates plasma membrane microdomain localization and restriction of particle release. *J Virol,* 86**,** 2259-72.

HAMMONDS, J., WANG, J. J. & SPEARMAN, P. 2012b. Restriction of Retroviral Replication by Tetherin/BST-2. *Mol Biol Int,* 2012**,** 424768.

HAN, K., LOU, D. I. & SAWYER, S. L. 2011. Identification of a genomic reservoir for new TRIM genes in primate genomes. *PLoS Genet,* 7**,** e1002388.

HARRIS, R. S., BISHOP, K. N., SHEEHY, A. M., CRAIG, H. M., PETERSEN-MAHRT, S. K., WATT, I. N., NEUBERGER, M. S. & MALIM, M. H. 2003. DNA deamination mediates innate immunity to retroviral infection. *Cell,* 113**,** 803-9.

HARRIS, R. S. & LIDDAMENT, M. T. 2004. Retroviral restriction by APOBEC proteins. *Nat Rev Immunol,* 4**,** 868-77.

HELD, W., WAANDERS, G. A., SHAKHOV, A. N., SCARPELLINO, L., ACHA-ORBEA, H. & MACDONALD, H. R. 1993. Superantigen-induced immune stimulation amplifies mouse mammary tumor virus infection and allows virus transmission. *Cell,* 74**,** 529-40.

HOFACRE, A. & FAN, H. 2010. Jaagsiekte sheep retrovirus biology and oncogenesis. *Viruses,* 2**,** 2618-48.

HOFACRE, A., NITTA, T. & FAN, H. 2009. Jaagsiekte sheep retrovirus encodes a regulatory factor, Rej, required for synthesis of Gag protein. *J Virol,* 83**,** 12483-98.

HOLLAND, M. J., PALMARINI, M., GARCIA-GOTI, M., GONZALEZ, L., MCKENDRICK, I., DE LAS HERAS, M. & SHARP, J. M. 1999. Jaagsiekte retrovirus is widely distributed both in T and B lymphocytes and in mononuclear phagocytes of sheep with naturally and experimentally acquired pulmonary adenomatosis. *J Virol,* 73**,** 4004-8.

HOLMES, R. K., KONING, F. A., BISHOP, K. N. & MALIM, M. H. 2007a. APOBEC3F can inhibit the accumulation of HIV-1 reverse transcription products in the absence of hypermutation. Comparisons with APOBEC3G. *J Biol Chem,* 282**,** 2587-95.

HOLMES, R. K., MALIM, M. H. & BISHOP, K. N. 2007b. APOBEC-mediated viral restriction: not simply editing? *Trends Biochem Sci,* 32**,** 118-28.

HOPWOOD, P., WALLACE, W. A., COUSENS, C., DEWAR, P., MULDOON, M., NORVAL, M. & GRIFFITHS, D. J. 2010. Absence of markers of betaretrovirus infection in human pulmonary adenocarcinoma. *Hum Pathol*.

HRECKA, K., HAO, C., GIERSZEWSKA, M., SWANSON, S. K., KESIK-BRODACKA, M., SRIVASTAVA, S., FLORENS, L., WASHBURN, M. P. & SKOWRONSKI, J. 2011. Vpx relieves inhibition of HIV-1 infection of macrophages mediated by the SAMHD1 protein. *Nature,* 474**,** 658-61.

HUANG, S., KAWABE, Y., ITO, A. & KAMIHIRA, M. 2010. Cre recombinase-mediated site-specific modification of a cellular genome using an integrase-defective retroviral vector. *Biotechnol Bioeng,* 107**,** 717-29.

HUDACHEK, S. F., KRAFT, S. L., THAMM, D. H., BIELEFELDT-OHMANN, H., DEMARTINI, J. C., MILLER, A. D. & DERNELL, W. S. 2010. Lung tumor development and spontaneous regression in lambs coinfected with Jaagsiekte sheep retrovirus and ovine lentivirus. *Vet Pathol,* 47**,** 148-62.

HULL, S. & FAN, H. 2006. Mutational analysis of the cytoplasmic tail of jaagsiekte sheep retrovirus envelope protein. *J Virol,* 80**,** 8069-80.

HUTHOFF, H. & TOWERS, G. J. 2008. Restriction of retroviral replication by APOBEC3G/F and TRIM5alpha. *Trends Microbiol,* 16**,** 612-9.

HWANG, C. Y., HOLL, J., RAJAN, D., LEE, Y., KIM, S., UM, M., KWON, K. S. & SONG, B. 2010. Hsp70 interacts with the retroviral restriction factor TRIM5alpha and assists the folding of TRIM5alpha. *J Biol Chem,* 285**,** 7827-37.

IKEDA, T., ABD EL GALIL, K. H., TOKUNAGA, K., MAEDA, K., SATA, T., SAKAGUCHI, N., HEIDMANN, T. & KOITO, A. 2011. Intrinsic restriction activity by apolipoprotein B mRNA editing enzyme APOBEC1 against the mobility of autonomous retrotransposons. *Nucleic Acids Res,* 39**,** 5538-54.

IKEDA, Y., TAKEUCHI, Y., MARTIN, F., COSSET, F. L., MITROPHANOUS, K. & COLLINS, M. 2003. Continuous high-titer HIV-1 vector production. *Nat Biotechnol,* 21**,** 569-72.

ISMAIL, S. I., KINGSMAN, S. M., KINGSMAN, A. J. & UDEN, M. 2000. Split-intron retroviral vectors: enhanced expression with improved safety. *J Virol,* 74**,** 2365-71.

IWATANI, Y., CHAN, D. S., WANG, F., MAYNARD, K. S., SUGIURA, W., GRONENBORN, A. M., ROUZINA, I., WILLIAMS, M. C., MUSIER-FORSYTH, K. & LEVIN, J. G. 2007. Deaminase-independent inhibition of HIV-1 reverse transcription by APOBEC3G. *Nucleic Acids Res,* 35**,** 7096-108.

JAUREGUI, P., CRESPO, H., GLARIA, I., LUJAN, L., CONTRERAS, A., ROSATI, S., DE ANDRES, D., AMORENA, B., TOWERS, G. J. & REINA, R. 2012. Ovine TRIM5alpha can restrict visna/maedi virus. *J Virol,* 86**,** 9504-9.

JERN, P., RUSSELL, R. A., PATHAK, V. K. & COFFIN, J. M. 2009. Likely role of APOBEC3G-mediated G-to-A mutations in HIV-1 evolution and drug resistance. *PLoS Pathog,* 5**,** e1000367.

JOHNSON, C., SANDERS, K. & FAN, H. 2010. Jaagsiekte sheep retrovirus transformation in Madin-Darby canine kidney epithelial cell three-dimensional culture. *J Virol,* 84**,** 5379-90.

JONSSON, S. R., HACHE, G., STENGLEIN, M. D., FAHRENKRUG, S. C., ANDRESDOTTIR, V. & HARRIS, R. S. 2006. Evolutionarily conserved and non-conserved retrovirus restriction activities of artiodactyl APOBEC3F proteins. *Nucleic Acids Res,* 34**,** 5683-94.

JOUVENET, N., NEIL, S. J., ZHADINA, M., ZANG, T., KRATOVAC, Z., LEE, Y., MCNATT, M., HATZIIOANNOU, T. & BIENIASZ, P. D. 2009. Broad-spectrum inhibition of retroviral and filoviral particle release by tetherin. *J Virol,* 83**,** 1837-44.

JUDE, B. A., POBEZINSKAYA, Y., BISHOP, J., PARKE, S., MEDZHITOV, R. M., CHERVONSKY, A. V. & GOLOVKINA, T. V. 2003. Subversion of the innate immune system by a retrovirus. *Nat Immunol,* 4**,** 573-8.

KAJASTE-RUDNITSKI, A., MARELLI, S. S., PULTRONE, C., PERTEL, T., UCHIL, P. D., MECHTI, N., MOTHES, W., POLI, G., LUBAN, J. & VICENZI, E. 2011. TRIM22 inhibits HIV-1 transcription independently of its E3 ubiquitin ligase activity, Tat, and NF-kappaB-responsive long terminal repeat elements. *J Virol,* 85**,** 5183-96.

KASSIOTIS, G. 2014. Endogenous retroviruses and the development of cancer. *J Immunol,* 192**,** 1343-9.

KATZ, E., DUBOIS-MARSHALL, S., SIMS, A. H., FARATIAN, D., LI, J., SMITH, E. S., QUINN, J. A., EDWARD, M., MEEHAN, R. R., EVANS, E. E., LANGDON, S. P. & HARRISON, D. J. 2010. A gene on the HER2 amplicon, C35, is an oncogene in breast cancer whose actions are prevented by inhibition of Syk. *Br J Cancer,* 103**,** 401-10.

KATZOURAKIS, A., TRISTEM, M., PYBUS, O. G. & GIFFORD, R. J. 2007. Discovery and analysis of the first endogenous lentivirus. *Proc Natl Acad Sci U S A,* 104**,** 6261-5.

KIERNAN, J. A. 2007. Indigogenic substrates for detection and localization of enzymes. *Biotech Histochem,* 82**,** 73-103.

KITAMURA, S., ODE, H., NAKASHIMA, M., IMAHASHI, M., NAGANAWA, Y., KUROSAWA, T., YOKOMAKU, Y., YAMANE, T., WATANABE, N., SUZUKI, A., SUGIURA, W. & IWATANI, Y. 2012. The APOBEC3C crystal structure and the interface for HIV-1 Vif binding. *Nat Struct Mol Biol,* 19**,** 1005-10.

KOBA, R., KOKAJI, C., FUJISAKI, G., OGUMA, K. & SENTSUI, H. 2013. Characterization of feline TRIM genes: molecular cloning, expression in tissues, and response to type I interferon. *Vet Immunol Immunopathol,* 153**,** 91-8.

KOITO, A. & IKEDA, T. 2013. Intrinsic immunity against retrotransposons by APOBEC cytidine deaminases. *Front Microbiol,* 4**,** 28.

KOLOKITHAS, A., ROSENKE, K., MALIK, F., HENDRICK, D., SWANSON, L., SANTIAGO, M. L., PORTIS, J. L., HASENKRUG, K. J. & EVANS, L. H. 2010. The glycosylated Gag protein of a murine leukemia virus inhibits the antiretroviral function of APOBEC3. *J Virol,* 84**,** 10933-6.

KONING, F. A., NEWMAN, E. N., KIM, E. Y., KUNSTMAN, K. J., WOLINSKY, S. M. & MALIM, M. H. 2009. Defining APOBEC3 expression patterns in human tissues and hematopoietic cell subsets. *J Virol,* 83**,** 9474-85.

KOZAK, M. 1987. At least six nucleotides preceding the AUG initiator codon enhance translation in mammalian cells. *J Mol Biol,* 196**,** 947-50.

KRALL, W. J., SKELTON, D. C., YU, X. J., RIVIERE, I., LEHN, P., MULLIGAN, R. C. & KOHN, D. B. 1996. Increased levels of spliced RNA account for augmented expression from the MFG retroviral vector in hematopoietic cells. *Gene Ther,* 3**,** 37-48.

KRUPP, A., MCCARTHY, K. R., OOMS, M., LETKO, M., MORGAN, J. S., SIMON, V. & JOHNSON, W. E. 2013. APOBEC3G polymorphism as a selective barrier to cross-species transmission and emergence of pathogenic SIV and AIDS in a primate host. *PLoS Pathog,* 9**,** e1003641.

LABONTE, J. A., BABCOCK, G. J., PATEL, T. & SODROSKI, J. 2002. Blockade of HIV-1 infection of New World monkey cells occurs primarily at the stage of virus entry. *J Exp Med,* 196**,** 431-45.

LAEMMLI, U. K. 1970. Cleavage of structural proteins during the assembly of the head of bacteriophage T4. *Nature,* 227**,** 680-5.

LAGUETTE, N., SOBHIAN, B., CASARTELLI, N., RINGEARD, M., CHABLE-BESSIA, C., SEGERAL, E., YATIM, A., EMILIANI, S., SCHWARTZ, O. & BENKIRANE, M. 2011. SAMHD1 is the dendritic- and myeloid-cell-specific HIV-1 restriction factor counteracted by Vpx. *Nature,* 474**,** 654-7.

LANGELIER, C. R., SANDRIN, V., ECKERT, D. M., CHRISTENSEN, D. E., CHANDRASEKARAN, V., ALAM, S. L., AIKEN, C., OLSEN, J. C., KAR, A. K., SODROSKI, J. G. & SUNDQUIST, W. I. 2008. Biochemical characterization of a recombinant TRIM5alpha protein that restricts human immunodeficiency virus type 1 replication. *J Virol,* 82**,** 11682-94.

LARUE, R. S., ANDRESDOTTIR, V., BLANCHARD, Y., CONTICELLO, S. G., DERSE, D., EMERMAN, M., GREENE, W. C., JONSSON, S. R., LANDAU, N. R., LOCHELT, M., MALIK, H. S., MALIM, M. H., MUNK, C., O'BRIEN, S. J., PATHAK, V. K., STREBEL, K., WAIN-HOBSON, S., YU, X. F., YUHKI, N. & HARRIS, R. S. 2009. Guidelines for naming nonprimate APOBEC3 genes and proteins. *J Virol,* 83**,** 494-7.

LARUE, R. S., JONSSON, S. R., SILVERSTEIN, K. A., LAJOIE, M., BERTRAND, D., EL-MABROUK, N., HOTZEL, I., ANDRESDOTTIR, V., SMITH, T. P. & HARRIS, R. S. 2008. The artiodactyl APOBEC3 innate immune repertoire

shows evidence for a multi-functional domain organization that existed in the ancestor of placental mammals. *BMC Mol Biol,* 9**,** 104.

LI, K., MARKOSYAN, R. M., ZHENG, Y. M., GOLFETTO, O., BUNGART, B., LI, M., DING, S., HE, Y., LIANG, C., LEE, J. C., GRATTON, E., COHEN, F. S. & LIU, S. L. 2013a. IFITM proteins restrict viral membrane hemifusion. *PLoS Pathog,* 9**,** e1003124.

LI, M., SHANDILYA, S. M., CARPENTER, M. A., RATHORE, A., BROWN, W. L., PERKINS, A. L., HARKI, D. A., SOLBERG, J., HOOK, D. J., PANDEY, K. K., PARNIAK, M. A., JOHNSON, J. R., KROGAN, N. J., SOMASUNDARAN, M., ALI, A., SCHIFFER, C. A. & HARRIS, R. S. 2012. First-in-class small molecule inhibitors of the single-strand DNA cytosine deaminase APOBEC3G. *ACS Chem Biol,* 7**,** 506-17.

LI, W. H., GU, Z., WANG, H. & NEKRUTENKO, A. 2001. Evolutionary analyses of the human genome. *Nature,* 409**,** 847-9.

LI, X., KIM, J., SONG, B., FINZI, A., PACHECO, B. & SODROSKI, J. 2013b. Virus-specific effects of TRIM5alpha(rh) RING domain functions on restriction of retroviruses. *J Virol,* 87**,** 7234-45.

LI, X. & SODROSKI, J. 2008. The TRIM5alpha B-box 2 domain promotes cooperative binding to the retroviral capsid by mediating higher-order self-association. *J Virol,* 82**,** 11495-502.

LINNERTH-PETRIK, N. M., WALSH, S. R., BOGNER, P. N., MORRISON, C. & WOOTTON, S. K. 2014. Jaagsiekte sheep retrovirus detected in human lung cancer tissue arrays. *BMC Res Notes,* 7**,** 160.

LIU, L., OLIVEIRA, N. M., CHENEY, K. M., PADE, C., DREJA, H., BERGIN, A. M., BORGDORFF, V., BEACH, D. H., BISHOP, C. L., DITTMAR, M. T. & MCKNIGHT, A. 2011. A whole genome screen for HIV restriction factors. *Retrovirology,* 8**,** 94.

LOGAN, A. C., NIGHTINGALE, S. J., HAAS, D. L., CHO, G. J., PEPPER, K. A. & KOHN, D. B. 2004. Factors influencing the titer and infectivity of lentiviral vectors. *Human Gene Therapy,* 15**,** 976-988.

LUKIC, Z., HAUSMANN, S., SEBASTIAN, S., RUCCI, J., SASTRI, J., ROBIA, S. L., LUBAN, J. & CAMPBELL, E. M. 2011. TRIM5alpha associates with proteasomal subunits in cells while in complex with HIV-1 virions. *Retrovirology,* 8**,** 93.

LUTRINGER-MAGNIN, D., GIRARD, N., CADRANEL, J., LEROUX, C., QUOIX, E., COTTIN, V., DEL SIGNORE, C., LEBITASY, M. P., CORDIER, G., VANHEMS, P. & MORNEX, J. F. 2012. Professional exposure to goats increases the risk of pneumonic-type lung adenocarcinoma: results of the IFCT-0504-Epidemio study. *PLoS One,* 7**,** e37889.

MACMILLAN, A. L., KOHLI, R. M. & ROSS, S. R. 2013. APOBEC3 inhibition of mouse mammary tumor virus infection: the role of cytidine deamination versus inhibition of reverse transcription. *J Virol,* 87**,** 4808-17.

MADIN, S. H. & DARBY, N. B., JR. 1958. Established kidney cell lines of normal adult bovine and ovine origin. *Proc Soc Exp Biol Med,* 98**,** 574-6.

MAEDA, N. & FAN, H. 2008. Signal transduction pathways utilized by enzootic nasal tumor virus (ENTV-1) envelope protein in transformation of rat epithelial cells resemble those used by jaagsiekte sheep retrovirus. *Virus Genes,* 36**,** 147-55.

MAEDA, N., FAN, H. & YOSHIKAI, Y. 2008. Oncogenesis by retroviruses: old and new paradigms. *Rev Med Virol,* 18**,** 387-405.

MAEDA, N., FU, W., ORTIN, A., DE LAS HERAS, M. & FAN, H. 2005. Roles of the Ras-MEK-mitogen-activated protein kinase and phosphatidylinositol 3-kinase-Akt-mTOR pathways in Jaagsiekte sheep retrovirus-induced transformation of rodent fibroblast and epithelial cell lines. *J Virol,* 79**,** 4440-50.

MAEDA, N., PALMARINI, M., MURGIA, C. & FAN, H. 2001. Direct transformation of rodent fibroblasts by jaagsiekte sheep retrovirus DNA. *Proc Natl Acad Sci U S A,* 98**,** 4449-54.

MAILLOT, B., LEVY, N., EILER, S., CRUCIFIX, C., GRANGER, F., RICHERT, L., DIDIER, P., GODET, J., PRADEAU-AUBRETON, K., EMILIANI, S., NAZABAL, A., LESBATS, P., PARISSI, V., MELY, Y., MORAS, D., SCHULTZ, P. & RUFF, M. 2013. Structural and functional role of INI1 and LEDGF in the HIV-1 preintegration complex. *PLoS One,* 8**,** e60734.

MALFAVON-BORJA, R., SAWYER, S. L., WU, L. I., EMERMAN, M. & MALIK, H. S. 2013. An evolutionary screen highlights canonical and noncanonical candidate antiviral genes within the primate TRIM gene family. *Genome Biol Evol,* 5**,** 2141-54.

MARIANI, R., CHEN, D., SCHROFELBAUER, B., NAVARRO, F., KONIG, R., BOLLMAN, B., MUNK, C., NYMARK-MCMAHON, H. & LANDAU, N. R. 2003. Species-specific exclusion of APOBEC3G from HIV-1 virions by Vif. *Cell,* 114**,** 21-31.

MARKOWITZ, D., GOFF, S. & BANK, A. 1988. A safe packaging line for gene transfer: separating viral genes on two different plasmids. *J Virol,* 62**,** 1120-4.

MARNO, K. M., OGUNKOLADE, B. W., PADE, C., OLIVEIRA, N. M., O'SULLIVAN, E. & MCKNIGHT, A. 2014. Novel restriction factor RNA-associated early-stage anti-viral factor (REAF) inhibits human and simian immunodeficiency viruses. *Retrovirology,* 11**,** 3.

MARTIN-SERRANO, J. & NEIL, S. J. 2011. Host factors involved in retroviral budding and release. *Nat Rev Microbiol,* 9**,** 519-31.

MARTINEAU, H. M., COUSENS, C., IMLACH, S., DAGLEISH, M. P. & GRIFFITHS, D. J. 2011. Jaagsiekte sheep retrovirus infects multiple cell types in the ovine lung. *J Virol,* 85**,** 3341-55.

MARTINEZ-SALAS, E. 1999. Internal ribosome entry site biology and its use in expression vectors. *Curr Opin Biotechnol,* 10**,** 458-64.

MBISA, J. L., BARR, R., THOMAS, J. A., VANDEGRAAFF, N., DORWEILER, I. J., SVAROVSKAIA, E. S., BROWN, W. L., MANSKY, L. M., GORELICK, R. J., HARRIS, R. S., ENGELMAN, A. & PATHAK, V. K. 2007. Human immunodeficiency virus type 1 cDNAs produced in the presence of APOBEC3G exhibit defects in plus-strand DNA transfer and integration. *J Virol,* 81**,** 7099-110.

MCCARTHY, K. R., SCHMIDT, A. G., KIRMAIER, A., WYAND, A. L., NEWMAN, R. M. & JOHNSON, W. E. 2013. Gain-of-sensitivity mutations in a Trim5-resistant primary isolate of pathogenic SIV identify two independent conserved determinants of Trim5alpha specificity. *PLoS Pathog,* 9**,** e1003352.

MCDONALD, D., VODICKA, M. A., LUCERO, G., SVITKINA, T. M., BORISY, G. G., EMERMAN, M. & HOPE, T. J. 2002. Visualization of the intracellular behavior of HIV in living cells. *J Cell Biol,* 159**,** 441-52.

MCEWAN, W. A., SCHALLER, T., YLINEN, L. M., HOSIE, M. J., TOWERS, G. J. & WILLETT, B. J. 2009. Truncation of TRIM5 in the Feliformia explains the absence of retroviral restriction in cells of the domestic cat. *J Virol,* 83**,** 8270-5.

MCGEE-ESTRADA, K. & FAN, H. 2007. Comparison of LTR enhancer elements in sheep beta retroviruses: insights into the basis for tissue-specific expression. *Virus Genes,* 35**,** 303-12.

MCNATT, M. W., ZANG, T. & BIENIASZ, P. D. 2013. Vpu binds directly to tetherin and displaces it from nascent virions. *PLoS Pathog,* 9**,** e1003299.

MERTZ, J. A., LOZANO, M. M. & DUDLEY, J. P. 2009. Rev and Rex proteins of human complex retroviruses function with the MMTV Rem-responsive element. *Retrovirology,* 6**,** 10.

MIKL, M. C., WATT, I. N., LU, M., REIK, W., DAVIES, S. L., NEUBERGER, M. S. & RADA, C. 2005. Mice deficient in APOBEC2 and APOBEC3. *Mol Cell Biol,* 25**,** 7270-7.

MILLER, A. D. 2003. Identification of Hyal2 as the cell-surface receptor for jaagsiekte sheep retrovirus and ovine nasal adenocarcinoma virus. *Curr Top Microbiol Immunol,* 275**,** 179-99.

MILLER, A. D. 2008. Hyaluronidase 2 and its intriguing role as a cell-entry receptor for oncogenic sheep retroviruses. *Semin Cancer Biol,* 18**,** 296-301.

MINGOZZI, F. & HIGH, K. A. 2013. Immune responses to AAV vectors: overcoming barriers to successful gene therapy. *Blood,* 122**,** 23-36.

MORGENSTERN, J. P. & LAND, H. 1990. Advanced mammalian gene transfer: high titre retroviral vectors with multiple drug selection markers and a complementary helper-free packaging cell line. *Nucleic Acids Res,* 18**,** 3587-96.

MORNEX, J. F., THIVOLET, F., DE LAS HERAS, M. & LEROUX, C. 2003. Pathology of human bronchioloalveolar carcinoma and its relationship to the ovine disease. *Curr Top Microbiol Immunol,* 275**,** 225-48.

MOROZOV, V. A., LAGAYE, S., LOWER, J. & LOWER, R. 2004. Detection and characterization of betaretroviral sequences, related to sheep Jaagsiekte virus, in Africans from Nigeria and Cameroon. *Virology,* 327**,** 162-8.

MORRISON, J. H., GUEVARA, R. B., MARCANO, A. C., SAENZ, D. T., FADEL, H. J., ROGSTAD, D. K. & POESCHLA, E. M. 2014. Feline immunodeficiency virus envelope glycoproteins antagonize tetherin through a distinctive mechanism that requires virion incorporation. *J Virol,* 88**,** 3255-72.

MÜHLEBACH, M. D., SCHÜLE, S., GERLACH, N., SCHWEIZER, M., BUCHHOLZ, C., HOHENADL,C., CHICHUTEK,K. 2010. Gammaretroviral and Lentiviral Vectors for Gene Delivery. *In:* KURTH, R. A. B., N. (ed.) *Retroviruses Molecular biology Genomics and Pathogenesis.* Berlin: Caister Anademic Press.

MURAMATSU, M., SANKARANAND, V. S., ANANT, S., SUGAI, M., KINOSHITA, K., DAVIDSON, N. O. & HONJO, T. 1999. Specific expression of activation-induced cytidine deaminase (AID), a novel member of the RNA-editing deaminase family in germinal center B cells. *J Biol Chem,* 274**,** 18470-6.

MURCIA, P. R., ARNAUD, F. & PALMARINI, M. 2007. The transdominant endogenous retrovirus enJS56A1 associates with and blocks intracellular trafficking of Jaagsiekte sheep retrovirus Gag. *J Virol,* 81**,** 1762-72.

MURGIA, C., CAPORALE, M., CEESAY, O., DI FRANCESCO, G., FERRI, N., VARASANO, V., DE LAS HERAS, M. & PALMARINI, M. 2011. Lung Adenocarcinoma Originates from Retrovirus Infection of Proliferating Type 2 Pneumocytes during Pulmonary Post-Natal Development or Tissue Repair. *PLoS Pathog,* 7**,** e1002014.

MURIAUX, D. & REIN, A. 2003. Encapsidation and transduction of cellular genes by retroviruses. *Front Biosci,* 8**,** d135-42.

NAIR, S., SANCHEZ-MARTINEZ, S., JI, X. & REIN, A. 2014. Biochemical and Biological Studies on Mouse APOBEC3. *J Virol*.

NARVAIZA, I., LINFESTY, D. C., GREENER, B. N., HAKATA, Y., PINTEL, D. J., LOGUE, E., LANDAU, N. R. & WEITZMAN, M. D. 2009. Deaminase-independent inhibition of parvoviruses by the APOBEC3A cytidine deaminase. *PLoS Pathog,* 5**,** e1000439.

NATHANS, R., CHU, C. Y., SERQUINA, A. K., LU, C. C., CAO, H. & RANA, T. M. 2009. Cellular microRNA and P bodies modulate host-HIV-1 interactions. *Mol Cell,* 34**,** 696-709.

NAVARATNAM, N., MORRISON, J. R., BHATTACHARYA, S., PATEL, D., FUNAHASHI, T., GIANNONI, F., TENG, B. B., DAVIDSON, N. O. & SCOTT, J. 1993. The p27 catalytic subunit of the apolipoprotein B mRNA editing enzyme is a cytidine deaminase. *J Biol Chem,* 268**,** 20709-12.

NAVARRO, F., BOLLMAN, B., CHEN, H., KONIG, R., YU, Q., CHILES, K. & LANDAU, N. R. 2005. Complementary function of the two catalytic domains of APOBEC3G. *Virology,* 333**,** 374-86.

NEAGU, M. R., ZIEGLER, P., PERTEL, T., STRAMBIO-DE-CASTILLIA, C., GRUTTER, C., MARTINETTI, G., MAZZUCCHELLI, L., GRUTTER, M., MANZ, M. G. & LUBAN, J. 2009. Potent inhibition of HIV-1 by TRIM5-cyclophilin fusion proteins engineered from human components. *J Clin Invest,* 119**,** 3035-47.

NEIL, S. J., ZANG, T. & BIENIASZ, P. D. 2008. Tetherin inhibits retrovirus release and is antagonized by HIV-1 Vpu. *Nature,* 451**,** 425-30.

NIK-ZAINAL, S., ALEXANDROV, L. B., WEDGE, D. C., VAN LOO, P., GREENMAN, C. D., RAINE, K., JONES, D., HINTON, J., MARSHALL, J., STEBBINGS, L. A., MENZIES, A., MARTIN, S., LEUNG, K., CHEN, L., LEROY, C., RAMAKRISHNA, M., RANCE, R., LAU, K. W., MUDIE, L. J., VARELA, I., MCBRIDE, D. J., BIGNELL, G. R., COOKE, S. L., SHLIEN, A., GAMBLE, J., WHITMORE, I., MADDISON, M., TARPEY, P. S., DAVIES, H. R., PAPAEMMANUIL, E., STEPHENS, P. J., MCLAREN, S., BUTLER, A. P., TEAGUE, J. W., JONSSON, G., GARBER, J. E., SILVER, D., MIRON, P., FATIMA, A., BOYAULT, S., LANGEROD, A., TUTT, A., MARTENS, J. W., APARICIO, S. A., BORG, A., SALOMON, A. V., THOMAS, G., BORRESEN-DALE, A. L., RICHARDSON, A. L., NEUBERGER, M. S., FUTREAL, P. A., CAMPBELL, P. J. & STRATTON, M. R. 2012. Mutational processes molding the genomes of 21 breast cancers. *Cell,* 149**,** 979-93.

NOWARSKI, R. & KOTLER, M. 2013. APOBEC3 Cytidine Deaminases in Double-Strand DNA Break Repair and Cancer Promotion. *Cancer Res,* 73**,** 3494-8.

OKEOMA, C. M., LOVSIN, N., PETERLIN, B. M. & ROSS, S. R. 2007. APOBEC3 inhibits mouse mammary tumour virus replication in vivo. *Nature,* 445**,** 927-30.

OKEOMA, C. M., LOW, A., BAILIS, W., FAN, H. Y., PETERLIN, B. M. & ROSS, S. R. 2009a. Induction of APOBEC3 in vivo causes increased restriction of retrovirus infection. *J Virol,* 83**,** 3486-95.

OKEOMA, C. M., PETERSEN, J. & ROSS, S. R. 2009b. Expression of murine APOBEC3 alleles in different mouse strains and their effect on mouse mammary tumor virus infection. *J Virol,* 83**,** 3029-38.

ORTIN, A., COUSENS, C., MINGUIJON, E., PASCUAL, Z., VILLARREAL, M. P., SHARP, J. M. & HERAS MDE, L. 2003. Characterization of enzootic nasal tumour virus of goats: complete sequence and tissue distribution. *J Gen Virol,* 84**,** 2245-52.

ORTIN, A., MINGUIJON, E., DEWAR, P., GARCIA, M., FERRER, L. M., PALMARINI, M., GONZALEZ, L., SHARP, J. M. & DE LAS HERAS, M. 1998. Lack of a specific immune response against a recombinant capsid protein of Jaagsiekte sheep retrovirus in sheep and goats naturally affected by enzootic nasal tumour or sheep pulmonary adenomatosis. *Vet Immunol Immunopathol,* 61**,** 229-37.

OVERBAUGH, J. & BANGHAM, C. R. 2001. Selection forces and constraints on retroviral sequence variation. *Science,* 292**,** 1106-9.

PAGES, J. C. & BRU, T. 2004. Toolbox for retrovectorologists. *J Gene Med,* 6 Suppl 1**,** S67-82.

PALMARINI, M., DATTA, S., OMID, R., MURGIA, C. & FAN, H. 2000a. The long terminal repeat of Jaagsiekte sheep retrovirus is preferentially active in differentiated epithelial cells of the lungs. *J Virol,* 74**,** 5776-87.

PALMARINI, M., DEWAR, P., DE LAS HERAS, M., INGLIS, N. F., DALZIEL, R. G. & SHARP, J. M. 1995. Epithelial tumour cells in the lungs of sheep with pulmonary adenomatosis are major sites of replication for Jaagsiekte retrovirus. *J Gen Virol,* 76 (Pt 11)**,** 2731-7.

PALMARINI, M. & FAN, H. 2001. Retrovirus-induced ovine pulmonary adenocarcinoma, an animal model for lung cancer. *J Natl Cancer Inst,* 93**,** 1603-14.

PALMARINI, M. & FAN, H. 2003. Molecular biology of jaagsiekte sheep retrovirus. *Curr Top Microbiol Immunol,* 275**,** 81-115.

PALMARINI, M., GRAY, C. A., CARPENTER, K., FAN, H., BAZER, F. W. & SPENCER, T. E. 2001a. Expression of endogenous betaretroviruses in the ovine uterus: effects of neonatal age, estrous cycle, pregnancy, and progesterone. *J Virol,* 75**,** 11319-27.

PALMARINI, M., HALLWIRTH, C., YORK, D., MURGIA, C., DE OLIVEIRA, T., SPENCER, T. & FAN, H. 2000b. Molecular cloning and functional analysis of three type D endogenous retroviruses of sheep reveal a different cell tropism from that of the highly related exogenous jaagsiekte sheep retrovirus. *J Virol,* 74**,** 8065-76.

PALMARINI, M., HOLLAND, M. J., COUSENS, C., DALZIEL, R. G. & SHARP, J. M. 1996. Jaagsiekte retrovirus establishes a disseminated infection of the lymphoid tissues of sheep affected by pulmonary adenomatosis. *J Gen Virol,* 77 (Pt 12)**,** 2991-8.

PALMARINI, M., MAEDA, N., MURGIA, C., DE-FRAJA, C., HOFACRE, A. & FAN, H. 2001b. A phosphatidylinositol 3-kinase docking site in the cytoplasmic tail of the Jaagsiekte sheep retrovirus transmembrane protein is essential for envelope-induced transformation of NIH 3T3 cells. *J Virol,* 75**,** 11002-9.

PALMARINI, M., MURGIA, C. & FAN, H. 2002. Spliced and prematurely polyadenylated Jaagsiekte sheep retrovirus-specific RNAs from infected or transfected cells. *Virology,* 294**,** 180-8.

PALMARINI, M., SHARP, J. M., DE LAS HERAS, M. & FAN, H. 1999a. Jaagsiekte sheep retrovirus is necessary and sufficient to induce a contagious lung cancer in sheep. *J Virol,* 73**,** 6964-72.

PALMARINI, M., SHARP, J. M., LEE, C. & FAN, H. 1999b. In vitro infection of ovine cell lines by Jaagsiekte sheep retrovirus. *J Virol,* 73**,** 10070-8.

PANGANIBAN, A. T. & TEMIN, H. M. 1983. The terminal nucleotides of retrovirus DNA are required for integration but not virus production. *Nature,* 306**,** 155-60.

PATTON, G. S., ERLWEIN, O. & MCCLURE, M. O. 2004. Cell-cycle dependence of foamy virus vectors. *J Gen Virol,* 85**,** 2925-30.

PEDERSEN, F. S. A. S., A.B. 2010. Pathogenesis of Oncoviral Infections. *In:* KURTH, R. A. B., N. (ed.) *Retroviruses Molecular biology Genomics and Pathogenesis.* Berlin: Caister Anademic Press.

PEREZ-CABALLERO, D., HATZIIOANNOU, T., YANG, A., COWAN, S. & BIENIASZ, P. D. 2005. Human tripartite motif 5alpha domains responsible for retrovirus restriction activity and specificity. *J Virol,* 79**,** 8969-78.

PERKOVIC, M., SCHMIDT, S., MARINO, D., RUSSELL, R. A., STAUCH, B., HOFMANN, H., KOPIETZ, F., KLOKE, B. P., ZIELONKA, J., STROVER, H., HERMLE, J., LINDEMANN, D., PATHAK, V. K., SCHNEIDER, G., LOCHELT, M., CICHUTEK, K. & MUNK, C. 2009. Species-specific inhibition of APOBEC3C by the prototype foamy virus protein bet. *J Biol Chem,* 284**,** 5819-26.

PERRON, M. J., STREMLAU, M., SONG, B., ULM, W., MULLIGAN, R. C. & SODROSKI, J. 2004. TRIM5alpha mediates the postentry block to N-tropic murine leukemia viruses in human cells. *Proc Natl Acad Sci U S A,* 101**,** 11827-32.

PERTEL, T., HAUSMANN, S., MORGER, D., ZUGER, S., GUERRA, J., LASCANO, J., REINHARD, C., SANTONI, F. A., UCHIL, P. D., CHATEL, L., BISIAUX, A., ALBERT, M. L., STRAMBIO-DE-CASTILLIA, C., MOTHES, W., PIZZATO, M., GRUTTER, M. G. & LUBAN, J. 2011. TRIM5 is an innate immune sensor for the retrovirus capsid lattice. *Nature,* 472**,** 361-5.

PETIT, V., GUETARD, D., RENARD, M., KERIEL, A., SITBON, M., WAIN-HOBSON, S. & VARTANIAN, J. P. 2009. Murine APOBEC1 is a powerful mutator of retroviral and cellular RNA in vitro and in vivo. *J Mol Biol,* 385**,** 65-78.

PHILBEY, A. W., COUSENS, C., BISHOP, J. V., GILL, C. A., DEMARTINI, J. C. & SHARP, J. M. 2006. Multiclonal pattern of Jaagsiekte sheep retrovirus integration sites in ovine pulmonary adenocarcinoma. *Virus Res,* 117**,** 254-63.

PICHLMAIR, A., DIEBOLD, S. S., GSCHMEISSNER, S., TAKEUCHI, Y., IKEDA, Y., COLLINS, M. K. & REIS E SOUSA, C. 2007. Tubulovesicular structures within vesicular stomatitis virus G protein-pseudotyped lentiviral vector preparations carry DNA and stimulate antiviral responses via Toll-like receptor 9. *J Virol,* 81**,** 539-47.

PLATT, J. A., KRAIPOWICH, N., VILLAFANE, F. & DEMARTINI, J. C. 2002. Alveolar type II cells expressing jaagsiekte sheep retrovirus capsid protein and surfactant proteins are the predominant neoplastic cell type in ovine pulmonary adenocarcinoma. *Vet Pathol,* 39**,** 341-52.

RAHM, N., GFELLER, D., SNOECK, J., MARTINEZ, R., MCLAREN, P. J., ORTIZ, M., CIUFFI, A. & TELENTI, A. 2013. Susceptibility and adaptation to human TRIM5alpha alleles at positive selected sites in HIV-1 capsid. *Virology,* 441**,** 162-70.

RAHM, N., YAP, M., SNOECK, J., ZOETE, V., MUNOZ, M., RADESPIEL, U., ZIMMERMANN, E., MICHIELIN, O., STOYE, J. P., CIUFFI, A. &

TELENTI, A. 2011. Unique spectrum of activity of prosimian TRIM5alpha against exogenous and endogenous retroviruses. *J Virol,* 85**,** 4173-83.

RAI, S. K., DEMARTINI, J. C. & MILLER, A. D. 2000. Retrovirus vectors bearing jaagsiekte sheep retrovirus env transduce human cells by using a new receptor localized to chromosome 3p21.3. *Journal of Virology,* 74**,** 4698-4704.

RAI, S. K., DUH, F. M., VIGDOROVICH, V., DANILKOVITCH-MIAGKOVA, A., LERMAN, M. I. & MILLER, A. D. 2001. Candidate tumor suppressor HYAL2 is a glycosylphosphatidylinositol (GPI)-anchored cell-surface receptor for jaagsiekte sheep retrovirus, the envelope protein of which mediates oncogenic transformation. *Proc Natl Acad Sci U S A,* 98**,** 4443-8.

RAJAN, A. 1987. Carcinoma of the mucosa of the ethmoid in domestic animals. *Ann Rech Vet,* 18**,** 13-7.

REYMOND, A., MERONI, G., FANTOZZI, A., MERLA, G., CAIRO, S., LUZI, L., RIGANELLI, D., ZANARIA, E., MESSALI, S., CAINARCA, S., GUFFANTI, A., MINUCCI, S., PELICCI, P. G. & BALLABIO, A. 2001. The tripartite motif family identifies cell compartments. *EMBO J,* 20**,** 2140-51.

RIHN, S. J., WILSON, S. J., LOMAN, N. J., ALIM, M., BAKKER, S. E., BHELLA, D., GIFFORD, R. J., RIXON, F. J. & BIENIASZ, P. D. 2013. Extreme genetic fragility of the HIV-1 capsid. *PLoS Pathog,* 9**,** e1003461.

ROCCA, S., SANNA, M. P., LEONI, A., COSSU, A., LISSIA, A., TANDA, F., SATTA, M. P. & PALMIERI, G. 2008. Presence of Jaagsiekte sheep retrovirus in tissue sections from human bronchioloalveolar carcinoma depends on patients' geographical origin. *Human Pathology,* 39**,** 303-304.

ROSADIO, R. H., LAIRMORE, M. D., RUSSELL, H. I. & DEMARTINI, J. C. 1988. Retrovirus-associated ovine pulmonary carcinoma (sheep pulmonary adenomatosis) and lymphoid interstitial pneumonia. I. Lesion development and age susceptibility. *Vet Pathol,* 25**,** 475-83.

ROSS, S. R. 1998. Mouse mammary tumor virus and its interaction with the immune system. *Immunol Res,* 17**,** 209-16.

ROSS, S. R. 2000. Using genetics to probe host-virus interactions; the mouse mammary tumor virus model. *Microbes and Infection,* 2**,** 1215-23.

ROSS, S. R. 2009. Are viruses inhibited by APOBEC3 molecules from their host species? *PLoS Pathog,* 5**,** e1000347.

ROSS, S. R. 2010. Mouse mammary tumor virus molecular biology and oncogenesis. *Viruses,* 2**,** 2000-12.

ROSS, S. R., SCHMIDT, J. W., KATZ, E., CAPPELLI, L., HULTINE, S., GIMOTTY, P. & MONROE, J. G. 2006. An immunoreceptor tyrosine activation motif in the mouse mammary tumor virus envelope protein plays a role in virus-induced mammary tumors. *J Virol,* 80**,** 9000-8.

SAITOU, N. & NEI, M. 1987. The neighbor-joining method: a new method for reconstructing phylogenetic trees. *Mol Biol Evol,* 4**,** 406-25.

SAKUMA, R., NOSER, J. A., OHMINE, S. & IKEDA, Y. 2007. Rhesus monkey TRIM5alpha restricts HIV-1 production through rapid degradation of viral Gag polyproteins. *Nat Med,* 13**,** 631-5.

SALVATORI, D., GONZALEZ, L., DEWAR, P., COUSENS, C., DE LAS HERAS, M., DALZIEL, R. G. & SHARP, J. M. 2004. Successful induction of ovine pulmonary adenocarcinoma in lambs of different ages and detection of viraemia during the preclinical period. *J Gen Virol,* 85**,** 3319-24.

SAWYER, S. L., WU, L. I., EMERMAN, M. & MALIK, H. S. 2005. Positive selection of primate TRIM5alpha identifies a critical species-specific retroviral restriction domain. *Proc Natl Acad Sci U S A,* 102**,** 2832-7.

SAYAH, D. M., SOKOLSKAJA, E., BERTHOUX, L. & LUBAN, J. 2004. Cyclophilin A retrotransposition into TRIM5 explains owl monkey resistance to HIV-1. *Nature,* 430**,** 569-73.

SCHOGGINS, J. W., WILSON, S. J., PANIS, M., MURPHY, M. Y., JONES, C. T., BIENIASZ, P. & RICE, C. M. 2011. A diverse range of gene products are effectors of the type I interferon antiviral response. *Nature,* 472**,** 481-5.

SHEEHY, A. M., GADDIS, N. C., CHOI, J. D. & MALIM, M. H. 2002. Isolation of a human gene that inhibits HIV-1 infection and is suppressed by the viral Vif protein. *Nature,* 418**,** 646-50.

SHIN, N. H., HARTIGAN-O'CONNOR, D., PFEIFFER, J. K. & TELESNITSKY, A. 2000. Replication of lengthened Moloney murine leukemia virus genomes is impaired at multiple stages. *J Virol,* 74**,** 2694-702.

SI, Z., VANDEGRAAFF, N., O'HUIGIN, C., SONG, B., YUAN, W., XU, C., PERRON, M., LI, X., MARASCO, W. A., ENGELMAN, A., DEAN, M. & SODROSKI, J. 2006. Evolution of a cytoplasmic tripartite motif (TRIM) protein in cows that restricts retroviral infection. *Proc Natl Acad Sci U S A,* 103**,** 7454-9.

SINGHAL, R., DENG, X., CHENCHIK, A. A. & KANDEL, E. S. 2011. Long-distance effects of insertional mutagenesis. *PLoS One,* 6**,** e15832.

SODROSKI, J. G. 2004. Innate intracellular immunity to retroviruses. *Harvey Lect,* 100**,** 143-53.

SONEOKA, Y., CANNON, P. M., RAMSDALE, E. E., GRIFFITHS, J. C., ROMANO, G., KINGSMAN, S. M. & KINGSMAN, A. J. 1995. A transient three-plasmid expression system for the production of high titer retroviral vectors. *Nucleic Acids Res,* 23**,** 628-33.

SPENCER, T. E., BLACK, S. G., ARNAUD, F. & PALMARINI, M. 2010. Endogenous retroviruses of sheep: a model system for understanding physiological adaptation to an evolving ruminant genome. *Soc Reprod Fertil Suppl,* 67**,** 95-104.

SPENCER, T. E., MURA, M., GRAY, C. A., GRIEBEL, P. J. & PALMARINI, M. 2003. Receptor usage and fetal expression of ovine endogenous betaretroviruses: implications for coevolution of endogenous and exogenous retroviruses. *J Virol,* 77**,** 749-53.

STABEL, J. R. & STABEL, T. J. 1995. Immortalization and characterization of bovine peritoneal macrophages transfected with SV40 plasmid DNA. *Vet Immunol Immunopathol,* 45**,** 211-20.

STAVROU, S., CRAWFORD, D., BLOUCH, K., BROWNE, E. P., KOHLI, R. M. & ROSS, S. R. 2014. Different modes of retrovirus restriction by human APOBEC3A and APOBEC3G in vivo. *PLoS Pathog,* 10**,** e1004145.

STAVROU, S., NITTA, T., KOTLA, S., HA, D., NAGASHIMA, K., REIN, A. R., FAN, H. & ROSS, S. R. 2013. Murine leukemia virus glycosylated Gag blocks apolipoprotein B editing complex 3 and cytosolic sensor access to the reverse transcription complex. *Proc Natl Acad Sci U S A,* 110**,** 9078-83.

STEHELIN, D., VARMUS, H. E., BISHOP, J. M. & VOGT, P. K. 1976. DNA related to the transforming gene(s) of avian sarcoma viruses is present in normal avian DNA. *Nature,* 260**,** 170-3.

STENGLEIN, M. D., BURNS, M. B., LI, M., LENGYEL, J. & HARRIS, R. S. 2010. APOBEC3 proteins mediate the clearance of foreign DNA from human cells. *Nat Struct Mol Biol,* 17**,** 222-9.

STENGLEIN, M. D. & HARRIS, R. S. 2006. APOBEC3B and APOBEC3F inhibit L1 retrotransposition by a DNA deamination-independent mechanism. *J Biol Chem,* 281**,** 16837-41.

STIELER, K. & FISCHER, N. 2010. Apobec 3G efficiently reduces infectivity of the human exogenous gammaretrovirus XMRV. *PLoS One,* 5**,** e11738.

STREMLAU, M., OWENS, C. M., PERRON, M. J., KIESSLING, M., AUTISSIER, P. & SODROSKI, J. 2004. The cytoplasmic body component TRIM5alpha restricts HIV-1 infection in Old World monkeys. *Nature,* 427**,** 848-53.

SUMMERS, C., BENITO, A., ORTIN, A., GARCIA DE JALON, J. A., GONZALEZ, L., NORVAL, M., SHARP, J. M. & DE LAS HERAS, M. 2012. The distribution of immune cells in the lungs of classical and atypical ovine pulmonary adenocarcinoma. *Vet Immunol Immunopathol,* 146**,** 1-7.

SUMMERS, C., DEWAR, P., VAN DER MOLEN, R., COUSENS, C., SALVATORI, D., SHARP, J. M., GRIFFITHS, D. J. & NORVAL, M. 2006. Jaagsiekte sheep retrovirus-specific immune responses induced by vaccination: a comparison of immunisation strategies. *Vaccine,* 24**,** 1821-9.

SUMMERS, C., NORVAL, M., DE LAS HERAS, M., GONZALEZ, L., SHARP, J. M. & WOODS, G. M. 2005. An influx of macrophages is the predominant local immune response in ovine pulmonary adenocarcinoma. *Vet Immunol Immunopathol,* 106**,** 285-94.

SUN, S., SCHILLER, J. H. & GAZDAR, A. F. 2007. Lung cancer in never smokers--a different disease. *Nat Rev Cancer,* 7**,** 778-90.

SUSPENE, R., AYNAUD, M. M., KOCH, S., PASDELOUP, D., LABETOULLE, M., GAERTNER, B., VARTANIAN, J. P., MEYERHANS, A. & WAIN-HOBSON, S. 2011. Genetic editing of herpes simplex virus 1 and Epstein-Barr herpesvirus genomes by human APOBEC3 cytidine deaminases in culture and in vivo. *J Virol,* 85**,** 7594-602.

SZE, A., BELGNAOUI, S. M., OLAGNIER, D., LIN, R., HISCOTT, J. & VAN GREVENYNGHE, J. 2013a. Host restriction factor SAMHD1 limits human T cell leukemia virus type 1 infection of monocytes via STING-mediated apoptosis. *Cell Host Microbe,* 14**,** 422-34.

SZE, A., OLAGNIER, D., LIN, R., VAN GREVENYNGHE, J. & HISCOTT, J. 2013b. SAMHD1 host restriction factor: a link with innate immune sensing of retrovirus infection. *J Mol Biol,* 425**,** 4981-94.

TAFLIN, C., FAVIER, B., CHARRON, D., GLOTZ, D. & MOONEY, N. 2013. Study of the allogeneic response induced by endothelial cells expressing HLA class II after lentiviral transduction. *Methods Mol Biol,* 960**,** 461-72.

TAKEDA, E., TSUJI-KAWAHARA, S., SAKAMOTO, M., LANGLOIS, M. A., NEUBERGER, M. S., RADA, C. & MIYAZAWA, M. 2008. Mouse APOBEC3 restricts friend leukemia virus infection and pathogenesis in vivo. *J Virol,* 82**,** 10998-1008.

TAREEN, S. U., SAWYER, S. L., MALIK, H. S. & EMERMAN, M. 2009. An expanded clade of rodent Trim5 genes. *Virology,* 385**,** 473-83.

TAYLOR, B. J., NIK-ZAINAL, S., WU, Y. L., STEBBINGS, L. A., RAINE, K., CAMPBELL, P. J., RADA, C., STRATTON, M. R. & NEUBERGER, M. S. 2013. DNA deaminases induce break-associated mutation showers with implication of APOBEC3B and 3A in breast cancer kataegis. *Elife,* 2**,** e00534.

THEODOROU, V., KIMM, M. A., BOER, M., WESSELS, L., THEELEN, W., JONKERS, J. & HILKENS, J. 2007. MMTV insertional mutagenesis identifies genes, gene families and pathways involved in mammary cancer. *Nat Genet,* 39**,** 759-69.

TURELLI, P., MANGEAT, B., JOST, S., VIANIN, S. & TRONO, D. 2004. Inhibition of hepatitis B virus replication by APOBEC3G. *Science,* 303**,** 1829.

TUSTIN, R. C. 1969. Ovine Jaagsiekte. *Journal of the South African Veterinary Medicine Association***,** 3-20.

UCHIL, P. D., QUINLAN, B. D., CHAN, W. T., LUNA, J. M. & MOTHES, W. 2008. TRIM E3 ligases interfere with early and late stages of the retroviral life cycle. *PLoS Pathog,* 4**,** e16.

UREN, A. G., KOOL, J., BERNS, A. & VAN LOHUIZEN, M. 2005. Retroviral insertional mutagenesis: past, present and future. *Oncogene,* 24**,** 7656-72.

VALCKE, H. S., BERNARD, N. F., BRUNEAU, J., ALARY, M., TSOUKAS, C. M. & ROGER, M. 2006. APOBEC3G genetic variants and their association with risk of HIV infection in highly exposed Caucasians. *AIDS,* 20**,** 1984-6.

VARELA, M., GOLDER, M., ARCHER, F., DE LAS HERAS, M., LEROUX, C. & PALMARINI, M. 2008. A large animal model to evaluate the effects of Hsp90 inhibitors for the treatment of lung adenocarcinoma. *Virology,* 371**,** 206-15.

VARTANIAN, J. P., GUETARD, D., HENRY, M. & WAIN-HOBSON, S. 2008. Evidence for editing of human papillomavirus DNA by APOBEC3 in benign and precancerous lesions. *Science,* 320**,** 230-3.

VASUDEVAN, A. A., SMITS, S. H., HOPPNER, A., HAUSSINGER, D., KOENIG, B. W. & MUNK, C. 2013. Structural features of antiviral DNA cytidine deaminases. *Biol Chem*.

VAUGHAN, A. E., HALBERT, C. L., WOOTTON, S. K. & MILLER, A. D. 2012. Lung cancer in mice induced by the jaagsiekte sheep retrovirus envelope protein is not maintained by rare cancer stem cells, but tumorigenicity does correlate with Wnt pathway activation. *Mol Cancer Res,* 10**,** 86-95.

VERSTEEG, G. A., RAJSBAUM, R., SANCHEZ-APARICIO, M. T., MAESTRE, A. M., VALDIVIEZO, J., SHI, M., INN, K. S., FERNANDEZ-SESMA, A., JUNG, J. & GARCIA-SASTRE, A. 2013. The E3-ligase TRIM family of proteins regulates signaling pathways triggered by innate immune pattern-recognition receptors. *Immunity,* 38**,** 384-98.

VOISSET, C., WEISS, R. A. & GRIFFITHS, D. J. 2008. Human RNA "rumor" viruses: the search for novel human retroviruses in chronic disease. *Microbiol Mol Biol Rev,* 72**,** 157-96, table of contents.

WALSH, S. R., LINNERTH-PETRIK, N. M., LAPORTE, A. N., MENZIES, P. I., FOSTER, R. A. & WOOTTON, S. K. 2010. Full-length genome sequence analysis of enzootic nasal tumor virus reveals an unusually high degree of genetic stability. *Virus Res,* 151**,** 74-87.

WANISCH, K. & YANEZ-MUNOZ, R. J. 2009. Integration-deficient lentiviral vectors: a slow coming of age. *Mol Ther,* 17**,** 1316-32.

WEIDNER, J. M., JIANG, D., PAN, X. B., CHANG, J., BLOCK, T. M. & GUO, J. T. 2010. Interferon-induced cell membrane proteins, IFITM3 and tetherin, inhibit vesicular stomatitis virus infection via distinct mechanisms. *J Virol*.

WOLF, D. & GOFF, S. P. 2007. TRIM28 mediates primer binding site-targeted silencing of murine leukemia virus in embryonic cells. *Cell,* 131**,** 46-57.

WOOTTON, S. K., HALBERT, C. L. & MILLER, A. D. 2005. Sheep retrovirus structural protein induces lung tumours. *Nature,* 434**,** 904-7.

WOOTTON, S. K., HALBERT, C. L. & MILLER, A. D. 2006a. Envelope proteins of Jaagsiekte sheep retrovirus and enzootic nasal tumor virus induce similar bronchioalveolar tumors in lungs of mice. *J Virol,* 80**,** 9322-5.

WOOTTON, S. K., METZGER, M. J., HUDKINS, K. L., ALPERS, C. E., YORK, D., DEMARTINI, J. C. & MILLER, A. D. 2006b. Lung cancer induced in mice by

the envelope protein of jaagsiekte sheep retrovirus (JSRV) closely resembles lung cancer in sheep infected with JSRV. *Retrovirology,* 3**,** 94.

XU, H., CHERTOVA, E., CHEN, J., OTT, D. E., ROSER, J. D., HU, W. S. & PATHAK, V. K. 2007. Stoichiometry of the antiviral protein APOBEC3G in HIV-1 virions. *Virology,* 360**,** 247-56.

YAP, M. W., NISOLE, S., LYNCH, C. & STOYE, J. P. 2004. Trim5alpha protein restricts both HIV-1 and murine leukemia virus. *Proc Natl Acad Sci U S A,* 101**,** 10786-91.

YORK, D. F., VIGNE, R., VERWOERD, D. W. & QUERAT, G. 1991. Isolation, identification, and partial cDNA cloning of genomic RNA of jaagsiekte retrovirus, the etiological agent of sheep pulmonary adenomatosis. *J Virol,* 65**,** 5061-7.

YOSHIDA, M., MIYOSHI, I. & HINUMA, Y. 1982. A retrovirus from human leukemia cell lines: its isolation, characterization, and implication in human adult T-cell leukemia (ATL). *Princess Takamatsu Symp,* 12**,** 285-94.

YOUSEM, S. A., FINKELSTEIN, S. D., SWALSKY, P. A., BAKKER, A. & OHORI, N. P. 2001. Absence of jaagsiekte sheep retrovirus DNA and RNA in bronchioloalveolar and conventional human pulmonary adenocarcinoma by PCR and RT-PCR analysis. *Human Pathology,* 32**,** 1039-42.

YU, X., YU, Y., LIU, B., LUO, K., KONG, W., MAO, P. & YU, X. F. 2003. Induction of APOBEC3G ubiquitination and degradation by an HIV-1 Vif-Cul5-SCF complex. *Science,* 302**,** 1056-60.

ZENNOU, V., PETIT, C., GUETARD, D., NERHBASS, U., MONTAGNIER, L. & CHARNEAU, P. 2000. HIV-1 genome nuclear import is mediated by a central DNA flap. *Cell,* 101**,** 173-85.

ZHU, P., CHERTOVA, E., BESS, J., JR., LIFSON, J. D., ARTHUR, L. O., LIU, J., TAYLOR, K. A. & ROUX, K. H. 2003. Electron tomography analysis of envelope glycoprotein trimers on HIV and simian immunodeficiency virus virions. *Proc Natl Acad Sci U S A,* 100**,** 15812-7.

ZIELONKA, J., BRAVO, I. G., MARINO, D., CONRAD, E., PERKOVIC, M., BATTENBERG, M., CICHUTEK, K. & MUNK, C. 2009. Restriction of equine infectious anemia virus by equine APOBEC3 cytidine deaminases. *J Virol,* 83**,** 7547-59.